

The Molecular Pathogenesis of Huntington's Disease

Dr Christopher Turner BSc (Hons) MB ChB (Hons) MRCP

Department of Clinical Neurosciences

Royal Free Campus

Institute of Neurology

University College London

University of London

A thesis submitted in fulfilment for the degree
of Doctor of Philosophy

July 2009

Declaration

I, Christopher Turner, confirm that the work presented in this thesis is my own. Where information has been derived from other sources, I confirm that this has been indicated in the thesis.

Signature:

Abstract

Huntington's Disease (HD) is caused by an expansion in the CAG repeats of the huntingtin gene. This thesis describes an Ecdysone cell model which expressed inducible wild type (WT) and mutant (MT) N-terminal huntingtin (htt) in HEK 293 cells and constitutive EYFP full length (FL) htt in SH-SY5Y cells.

WT and MT EYFP FL htt was diffusely localised to the cytoplasm whereas endogenous FL htt and N-terminal htt localised to the nucleus and cytoplasm suggesting that htt has a role both in the nucleus and cytoplasm and EYFP inhibited nuclear translocation. N-terminal htt partially colocalised with vesicular and mitochondrial markers suggesting that N-terminal htt may be involved in vesicle trafficking and mitochondrial function.

The decrease in mitochondrial complex IV activity in MT FL htt cells supported previous reports that a complex IV defect is an early event in the pathogenesis of HD. Normal mitochondrial respiratory chain activities in cells expressing N-terminal htt contrasted with some cells models demonstrating a complex II/III defect when highly expanded CAG repeats were expressed. This suggested that a detectable complex II/III defect is not an early feature in the pathogenesis of HD.

Muscle biopsies from HD patients revealed a relationship between clinical progression, CAGs and a decrease in complex II/III:CS ratio, consistent with the defect in HD brains and cell models and suggested that muscle may be a useful tissue to study the disease.

Decreased aconitase activity with MT FL htt expression and increased sensitivity to paraquat with MT N-terminal htt expression demonstrated that MT htt was associated with increased oxidative stress or compromised antioxidant defences.

There was evidence of proteasomal dysfunction in the MT FL htt clones and inhibition of the proteasome by lactacystin caused the formation of perinuclear "aggresome-like" inclusions in both WT and MT FL htt clones. These inclusions contained FL htt which suggested that the proteasome was necessary for processing of FL WT and MT htt.

Under normal conditions there was no evidence of cleavage of WT or MT FL htt, however following treatment with lactacystin, an additional 11 kDa N-terminal htt fragment was present in most MT FL htt clones representing a novel mutation-specific cleavage product which may play an important role in the toxicity of MT htt.

This thesis has demonstrated several defects in cellular function in the absence of gross cell death and htt inclusion formation. These findings expand on previous hypotheses in the pathogenesis of HD involving abnormal MT htt cleavage, oxidative stress, mitochondrial dysfunction and proteasomal inhibition.

Acknowledgements

Many thanks to:

Mark Cooper and Tony Schapira as my supervisors for their guidance and support

The laboratory at the Royal Free including

Mike, Jane Bradley, Michelle, Sion, Jane Workman, Ross, Jan-Willem and Mei.

Lesley Jones for antibodies, protocols and support

Tom Warner for providing guidance on the UHDRS

Chris Shaw for providing some of the HD muscle samples

To Barbara, Ann, Valerie, Elaine and Sarah for a friendly face and refreshments

and finally

Emma, Sophie and Toby for 10 years of patience and love.

In memory of Valerie Turner

Index

Page

Declaration	2
Abstract	3
Acknowledgements	5
Dedication	6
Table of Contents	7
List of Tables	9
List of Figures	10
Abbreviations	16

Table of Contents

18	CHAPTER 1
<u>Introduction.....18</u>	
90	CHAPTER 2
<u>Materials and methods.....90</u>	
125	CHAPTER 3
<u>An inducible N-terminal htt HEK 293 cell model.....125</u>	
182	CHAPTER 4
<u>A constitutive EYFP-tagged full-length htt182</u>	
<u>SH-SY5Y cell model.....182</u>	
229	CHAPTER 5
<u>Mitochondrial function in HD muscle.....229</u>	

<u>List of Tables</u>	Page
Table 1.1. Proteins sequestered in htt inclusions	47
Table 1.2. The major studies of oxidative phosphorylation in HD	61
Table 1.3. Summary of MRC activities in HD N-terminal cell models	65
Table 1.4. The Polyglutamine diseases: The clinical and pathological spectrum	74
Table 1.5. Stable (A) inducible and (B) constitutive htt-expressing cell models	79-80
Table 2.1. Anti-huntingtin antibodies	98
Table 2.2. (A) Primary antibodies to subcellular compartments in HEK 293 model	100
Table 2.2. (B) Primary antibodies to subcellular compartments in EYFP model	100
Table 2.3. Reagents used in proteasome function analysis	125
Table 3.1. HEK 293 clones: positive immunostaining with Ab675	132
Table 3.2. Predicted base pair lengths of PCR products	140
Table 3.3. Specific enzyme activities and CS ratios	162
Table 3.4. Pon A-induced differences in specific enzyme activities and CS ratios	162
Table 3.5. Specific aconitase activities	166
Table 3.6. Pon A-induced differences in specific aconitase activities	168
Table 3.7. Background % cell death	171
Table 3.8. Malonate-induced % cell death	173
Table 3.9. Cyanide-induced % cell death	176
Table 3.10. Paraquat-induced % cell death	179
Table 3.11. Lactacystin-induced % cell death	182
Table 4.1. WT, MT, pcDNA 3.1 and EYFPcon clones	188
Table 5.1. HD patient clinical details	234
Table 5.2. Mitochondrial CS ratios and enzyme specific activities for controls	240
Table 5.3. Mitochondrial CS ratios and enzyme specific activities for HD patients	241

Table 5.4. Summary of correlations between complex activities and clinical scores	244
Table 6.1. Summary of extra htt bands in EYFP clones with lactacystin	293

<u>List of Figures</u>	Page
Fig. 1.1. Structure of huntingtin with functional sites	27
Fig. 1.2. Proposed mechanism of protein aggregation in neurodegeneration	45
Fig. 1.3. The mitochondrial respiratory chain	57
Fig. 2.1. Epitopes of anti-huntingtin antibodies	97
Fig. 2.2.(A) Restriction map and multiple cloning site of EYFP-C1	102
Fig. 2.2.(B and C) WT and MT constructs in the SH-SY5Y cell model	102
Fig 2.3. The Ecdysone Expression System with huntingtin constructs	103
Fig. 3.1. A. Sequence Chromatograms of LJ21CAG plasmid	128
Fig. 3.1. B. Sequence Chromatograms of LJ57CAG plasmid	129
Fig. 3.2. IF of MT and WT clones developed with Ab675	131
Fig. 3.3. Western blots of WT (A and B), MT clones (C and D) and pIND0 (D) developed with Ab675	134
Fig. 3.4. Western blots of (A) WT and (B) MT clones developed with Ab675-protein loading	135
Fig. 3.5. Western blots of clones 21 2 c (WT) and 57 2 e (MT) developed with Ab675-protein loading and background expression	136
Fig. 3.6. Western blots of (A) WT and (B) MT clones developed with Ab675-endogenous and construct htt	137
Fig. 3.7. Subcloning of clone 21 1 h following 48 hours induction and stained with Ab675	139
Fig. 3.8. PCR amplification of clones 21 2 d, 57 2a e and pIND 0 with primers G49/50	141

Fig. 3.9. Dose-dependence of pon A induction for 48 hours in IF and and Western blot of clone 21 1 h developed with Ab675	143
Fig. 3.10. Dose-dependence of pon A induction for 48 hours in IF and and Western blot of clone 57 2a d developed with Ab675	144
Fig. 3.11. Dose-dependence of pon A induction for 48 hours in IF and and Western blot of clone 21 2 c developed with Ab675	145
Fig. 3.12. Dose-dependence of pon A induction for 48 hours in IF and and Western blot of of clone 57 2 e developed with Ab675	146
Fig. 3.13. (A) Immunofluorescence and (B) Western blot of time-dependence of pon A in clone 21 2 c developed with Ab675	147
Fig. 3.14. (A) Immunofluorescence and (B) Western blot of time-dependence of pon A in clone 57 2 e developed with Ab675	148
Fig. 3.15. Wild-type and mutant α -synuclein clones following induction with pon A and developed with an anti-HA antibody	150
Fig. 3.16. Subcellular co-localisation of (A) COX1 and (B) Golgi with Ab675 following pon A induction in WT clone (21 2 c).	152
Fig. 3.17. Subcellular co-localisation of (A) LAMP and (B) VAMP with Ab675 in WT clone (21 2 c)	153
Fig. 3.18. Subcellular co-localisation of (A) synaptophysin and (B) ubiquitin with Ab675 in WT clone (21 2 c)	154
Fig. 3.19. Subcellular co-localisation of (A) COX1 and (B) Golgi with Ab675 in MT clone (57 2 e)	155
Fig. 3.20. Subcellular co-localisation of (A) LAMP and (B) VAMP with Ab675 in MT clone (57 2 e)	156
Fig. 3.21. Subcellular co-localisation of (A) Synaptophysin and (B) Ubiquitin with Ab675 in MT clone (57 2 e)	157

Fig. 3.22. Cell Proliferation curves for pIND 0, 21 CAG and 57 CAG clones	159
Fig. 3.23. Cell Proliferation curves for pIND 0, 21 CAG and 57 CAG clones corrected for initial cell number	160
Fig. 3.24. Mitochondrial Respiratory Chain specific activities of 5 pIND 0, WT and MT clones	163
Fig. 3.25. Mitochondrial Respiratory Chain CS corrected ratios of 5 pIND 0, WT and MT clones	164
Fig. 3.26. (A) Pon A-induced change in mean specific enzyme activities	165
Fig. 3.26. (B) Pon A-induced change in mean CS ratios	165
Fig. 3.26. (C) Statistical comparisons using Student's t test	165
Fig. 3.27. (A) Mean specific aconitase activities for 5 pIND 0, 5 WT and 5 MT clones	167
Fig. 3.27. (B) Mean pon A-induced change in specific aconitase activities for 5 pIND 0, 5 WT and 5 MT clones	167
Fig. 3.28. (A) Mean background cell death in 4 pIND 0, 5 WT and 5 MT clones	170
Fig. 3.28. (B) Mean pon A-induced background cell death in 4 pIND 0, 5 Wt and 5 MT clones	170
Fig. 3.29. The effect of malonate (150mM) for 48 hours on mean % cell death in 5 pIND0, 5 WT and 5 MT clones	174
Fig. 3.30. The effect of cyanide (20mM) for 48 hours on mean % cell death in 5 pIND0, 5 WT and 5 MT clones	177
Fig. 3.31. The effect of paraquat (5mM) for 48 hours on mean % cell death in 5 pIND0, 5 WT and 5 MT clones	180
Fig. 3.32. The effect of lactacystin (7.5 μ M) for 48 hours on mean % cell death in 5 pIND0, 5 WT and MT clones	183

Fig. 4.1. Confocal microscopy of mitotic EYFP clones	187
Fig. 4.2. Western blots of EYFP clones probed with anti-EYFP	189
Fig. 4.3. Cycling WT (clone 23 1/1) and MT (clone 88 1/3) EYFP clones and control clone (pcDNA 3.1 1) developed with the anti-htt antibodies	192
Fig. 4.4. WT and MT htt EYFP clones and pcDNA 3.1 probed with (A) Ab7666, (B) Ab2168 (C) anti-EYFP and (D) Ab7667	194
Fig. 4.5. (A) cDNA and primer sites for 5' sequencing of construct	196
Fig. 4.5. (B) cDNA and primer sites for 3' sequencing of construct	196
Fig. 4.6. PCR amplification of 5' end of htt	197
Fig. 4.7. (A) PCR amplification of 5' end of the htt WT clone 23 7 7	198
Fig. 4.7. (B) PCR amplification of 5' end of the htt MT clone 88 1 1	199
Fig. 4.7. (C) PCR amplification of 3' end of the htt WT clone 23 3 3	200
Fig. 4.8. PCR amplification of 3' end of EYFP construct huntingtin	201
Fig. 4.9. Confocal microscopy of WT htt clones differentiated for 2, 7 and 14 days	204
Fig. 4.10. Confocal microscopy of MT htt clones differentiated for 2, 7 and 14 days	205
Fig. 4.11. Fluorescence microscopy of clones differentiated for 14 days	206
Fig. 4.12. WT clone 23 1 1 differentiated and developed with anti-htt antibodies	208
Fig. 4.13. MT clone 88 1 3 differentiated and developed with anti-htt antibodies	209
Fig. 4.14. pcDNA 3.1 1 differentiated and developed with anti-htt antibodies	210
Fig. 4.15. (A) Western blot of WT and MT clones after differentiation	211
Fig. 4.15. (B) Western blot of WT and MT clones after differentiation	211
Fig. 4.16. Western blot of four week differentiation of EYFP clones	213
Fig. 4.17. EYFP htt clones following treatment with 5 μ M lactacystin	215
Fig. 4.18. PcDNA 3.1 23 1 1 and 88 1 3 following treatment with 5 μ M lactacystin and staining with (A) anti-COX 1 and (B) anti-Golgi	217
Fig. 4.19. PcDNA 3.1 following lactacystin treatment	218

Fig. 4.20 (A) 23 1 1, (B) 88 1 3 and (C) pcDNA 3.1 1 treated with lactacystin and developed with anti-htt antibodies	219
Fig. 4.21. (A) 23 1 1, (B) 88 1 3 and (C) pcDNA3.1 1 differentiated and treated with lactacystin	221
Fig. 4.22. Western blots of lactacystin-treated clones developed with anti-EYFP	222
Fig. 4.23. PcDNA 3.1, 23 1 1 and 88 1 3 clones treated lactacystin and probed with (A) Ab675, (B) EM 48, (C) Ab2168 and (D) Ab7666 antibodies	224
Fig. 4.24. Treatment of pcDNA 3.1, WT and MT clones with lactacystin and probed with anti-EYFP	226
Fig. 4.25. (A) Mitochondrial CS ratios. (B) Mitochondrial enzyme specific activities (protein corrected). (C) Aconitase activities	228
Fig. 4.26. (A) PGP-like and chymotrypsin-like activity in EYFP clones	230
Fig. 4.26. (B) Trypsin-like activity in EYFP clones	230
Fig. 5.1. Age (A and B), CAG repeats (C and D) and repeat years (E and F) of HD patients versus cognitive and motor scores in UHDRS	235
Fig. 5.2. (A) Cognitive versus motor scores in UHDRS	237
Fig. 5.2. (B) Statistical results for comparison of age, repeats and repeat years with cognitive and motor subscales of UHDRS	237
Fig. 5.3. (A) Histochemical staining of muscle from HD patient 12 for succinate dehydrogenase and cytochrome oxidase	238
Fig. 5.3. (B) Inclusion Body Myositis (IBM) and HD muscle developed with anti-ubiquitin, Ab675 and haematoxylin	238
Fig. 5.3. (C) Ultrastructural detail of HD muscle from patient 10	238
Fig. 5.4. (A) Mitochondrial CS ratios and (B) complex specific activities for control and HD muscle samples. (C) Mann-Whitney (M-W) two-tailed comparison of controls and HD patients	242

- Fig. 5.5. Complex II/III CS ratios versus (A) cognitive, (B) patient age, 245
(C) repeat years, (D) disease duration, (E) functional checklist
and (F) independence
- Fig. 5.6. Complex II/III:CS ratios versus (A) motor subscale and (B) control 246
patient's age
- Fig. 6.1. The postulated mechanisms involved in the pathogenesis of HD 322

Abbreviations

ADP	Adenine diphosphate
ATP	Adenine triphosphate
BSA	Bromodeoxyuridine
BSA	Bovine serum albumin
CNS	Central nervous system
COX	Cytochrome oxidase
DAB	3'diaminobenzidine
ddH ₂ O	Double distilled water
DMEM	Dulbelco's modified Eagles medium
DMSO	Dimethylsulphoxide
DNA	Deoxyribonucleic acid
DRPLA	Dentatorubropallidolusian atrophy
DTNB	5-5'-dithiobis-nitrobenzoic acid
ϵ	Molar extinction coefficient
EDTA	Ehtylenediaminetetra acetic acid
FADH ₂	Flavin adenine dinucleotide
FL	Full length
G418	Geneticin sulphate
GABA	Gamma aminobutyric acid
GAPDH	Glyceraldehyde-3-phosphate dehydrogenase
GSH	Reduced glutathione
HA	Haemagglutinin
HD	Huntington's Disease
HEK	Human embryonic kidney

HRP	Horseradish peroxidase
HSV	Herpes simplex virus
Htt	Huntingtin
IF	Immunofluorescence
MPTP	1-methyl-4-phenyl-1,2,3,6-tetrahydropyridine
MRC	Mitochondrial respiratory chain
MRS	Magnetic resonance spectroscopy
MT	Mutant
MtDNA	Mitochondrial DNA
NADH	Nicotine adenine dinucleotide
NMDAN	methyl-D-aspartic acid
NOS	Nitric oxide synthase
3-NP	3-nitropropionic acid
PAGE	Polyacrylamide gel electrophoresis
PBS	Phosphate buffered saline
PCR	Polymerase chain reaction
PD	Parkinson's disease
PET	Positron emission tomography
PM	Post-mortem
Pon A	Ponasterone A
RNA	Ribonucleic acid
ROS	Reactive oxygen species
SBMA	Spinobulbar muscular atrophy
SCA	Spinocerebellar ataxia
SDH	Succinate dehydrogenase
SDS	Sodium dodecyl sulphate

SN	Substantia nigra
SOD	Superoxide dismutase
TBS	Tris buffered saline
TCA	Tricarboxylic acid cycle
Tris	Trishydroxymethylaminomethane
TUNEL	Terminal transferase-mediated deoxyuridine triphosphate-biotin nick-end labelling
UV	Ultraviolet
WT	Wild type

CHAPTER 1

Introduction

1.1. A brief history and future of Huntington's disease

In 1872 George Huntington described a movement disorder clinically characterised by early personality changes, chorea and dementia (Huntington 1872) and the disorder subsequently took his name, Huntington's disease (HD). Huntington documented HD as an autosomal dominant condition with complete penetrance and many of the clinical features. It was not until 1993 that a collaborative effort by the international scientific community resulted in the discovery of the causative gene, huntingtin (Huntington's Disease Collaborative Research Group, 1993). A cure for HD still remains elusive, but the molecular mechanisms that connect the mutant gene to the clinical phenotype are currently being described and enabling work to be extrapolated to the study of other neurodegenerative diseases. Treatment options for HD are close to clinical translation and the near future promises to herald the onset of a new generation of therapeutics in clinical neurosciences.

1.2. Clinical features

HD has an estimated prevalence in North America and Europe of 4-10 per 100,000 (Quarrell et al. 1988). The first clinical symptoms of HD are personality changes, mood disturbances and other psychiatric abnormalities. Involuntary choreiform movements develop in the fourth or fifth decades as part of a complex movement disorder. The choreiform movements can occur early or late in the disease and can affect the limbs, trunk, face, neck, and respiratory muscles. Parkinsonian features, in the form of bradykinesia and dystonia, become more prominent as the disease progresses. The associated eye movement disorder is often typical and includes slow and hypometric saccades, convergence paresis, and gaze impersistence. Orolingual dyspraxia is common.

The disease progresses over 10-20 years and is associated with cognitive decline and eventually dementia. Death usually occurs due to the complications of immobility and suicide is more common than in the general population (Kremer 2002).

A minority of cases present in childhood or adolescence (“juvenile” HD) with an akinetic-rigid form of the disease or “Westphal variant”, which is associated with early parkinsonism, seizures and a shorter life-expectancy (Bruyn 1968).

There is no treatment for the progressive neurodegenerative process underlying HD and management includes pharmacological symptomatic control of the movement disorder and psychiatric features, as well as non-pharmacological treatments, such as parenteral feeding and therapy services (Haskins et al. 2000).

1.3. Genetics of HD

The HD gene was discovered in 1993 by the Huntington’s Disease Collaborative Research Group (Huntington’s Disease Collaborative Research Group, 1993). The exon amplification of cosmids in the chromosome 4p16.3 interval yielded “interesting transcript 15” or “IT15” from a novel gene in which an expanded CAG repeat size within the predicted open reading frame was associated with HD. The gene was called *HD* and protein product were called “huntingtin” (htt) or HD. HD is a true autosomal dominant condition with homozygotes presenting with the same phenotype as heterozygotes (Wexler et al. 1987). However, more recent clinical and molecular studies have suggested that although homozygosity for the *HD* mutation does not influence the age of onset of symptoms, homozygosity is associated with a more aggressive disease course (Squitieri et al 2003, Maglione et al 2006). The *HD* gene lacks homology with any other known gene

apart from the CAG repeat tract in exon 1. There is significant sequence homology of htt across a wide variety of mammalian species suggesting a fundamental cellular function. The gene spans 180kb and contains 67 exons. The predicted open reading frame yields a protein containing 3144 amino acids with a predicted molecular mass of 348 kDa (Huntington's Disease Collaborative Research Group, 1993).

The normal htt CAG repeat length within exon 1 has been demonstrated to be between 9 and 35 although most normal individuals have between 17-20 repeats (Myers et al. 2004). Repeat lengths between 27 and 35 are uncommon and are not associated with HD but are meiotically unstable and can expand into the disease range of 36 and above especially when transmitted paternally. Most HD patients have between 40-50 repeats. In a study by Rubinsztein et al. (1996) of 178 HD patients world-wide, there were no HD patients with less than 36 repeats. Patients with between 36 and 39 repeats have an increasing risk of developing the disease with increased repeat length. The overlap suggests that there are other factors influencing phenotype expression other than CAG repeat length.

The CAG sequence is inherently unstable between generations causing a tendency for repeat lengths to increase. This underlies the phenomenon of genetic anticipation (Harper 2002 for a review). When inherited from the mother, the repeat increases or decreases by approximately 4 CAG repeats with a tendency for a slight increase to occur. When inherited from the father, there are much larger expansions, up to double the original size, and expansions occur more frequently than contractions. The molecular basis of this sex-difference is still uncertain but is postulated to derive from the large number of cell cycles the gametes undergo in men versus women.

The CAG repeat size correlates inversely with the age of onset and directly with the

severity of the phenotype and the neuropathological severity (Ross et al 1995, Brinkman et al 1997, Penney et al. 1997). However, within each individual the CAG repeat length poorly predicts the age of onset and only 70% of the variance in the age of onset in HD can be accounted for by the CAG repeat length (Imarisio et al. 2008). In spite of this variation, most patients with greater than 50 repeats develop the disease before the age of 30 and often present with the “Westphal variant” described above.

1.4. Neuropathology of HD

In the early stages of the disease, the brain can be macroscopically normal. As the clinical phenotype progresses, characteristic neuropathological features develop. There is a direct correlation between disease duration and brain weight (Vonsattel et al. 1985). The brain volume loss is severe in the basal ganglia with up to 60% reduction in mass in the caudate, putamen and globus pallidus. The neuronal loss and gliosis is most severe in the caudate nucleus with the medium γ -aminobutyric acid (GABA)ergic spiny neurons being the most affected within the caudate. These neurons project to the globus pallidus and receive glutaminergic input from the cortex and dopaminergic input from the substantia nigra. The larger cholinergic and aspiny NADPH-diaphorase interneurons are relatively spared. The putamen and cerebral cortex also demonstrate neuronal loss and gliosis and are less severely affected compared to the caudate nucleus. The cerebellum is only mildly affected (Vonsattel et al. 1998). The cause of such specific regional and sub-population neuronal loss and the absence of cell loss in other tissues remain uncertain. The formation, location and putative role of aggregates will be discussed in Section 1.7 and the location of htt in Section 1.5.

1.5. Huntingtin transcription, translation, functions and protein interactions

1.5.1. Htt transcription

In situ hybridization studies have demonstrated that htt mRNA is expressed widely in neuronal and non-neuronal tissues. Expression is highest in neurons, testes, ovaries and lung (Li, S-H et al 1993, Strong et al. 1993, Sharp et al. 1995 and Sapp et al. 1997). These studies demonstrated no qualitative difference in mRNA expression between different brain regions and neuronal subtypes. There was no correlation between transcript expression levels and neuropathology. There are two expressed mRNAs at 10kb and 13kb. The larger form appears to be expressed more in brain than the smaller form, although it is unclear whether this is responsible for the greater protein expression in brain. The expression of huntingtin mRNA is much lower in glia than neurons. (Dure et al. 1994).

1.5.2. Htt translation

The levels of htt protein expression have been reported using a panel of antibodies, which have been developed to internal sequences of htt in order to delineate the location of various htt fragments. Immunocytochemical studies in post-mortem tissue have demonstrated that htt is widely expressed in neurons throughout the normal brain (Gutekunst et al. 1995; DiFiglia et al. 1995) with the highest levels in the cortical pyramidal cells, striatal cells and cerebellar Purkinje cells.

The expression of htt is heterogeneous within each region of the brain. In the striatum, the neurons with the highest expression have been found in one study to be the same as those that are most vulnerable to neurodegeneration, whilst the relatively-spared interneurons express low levels of htt (Ferrante et al. 1997). A study in rats also found higher levels of

htt expression in cells of the striatum that would be most vulnerable in humans (Kosinski et al. 1997). These findings may partly explain the selective neuronal vulnerability within the striatum, although many neurons that express high levels in other brain regions e.g. cerebellum (Gutekunst et al. 1995) do not degenerate and so levels of htt expression represents only one factor contributing to selective regional cell death.

1.5.3. Subcellular localisation and physiological function of htt

Full-length (FL) wild-type (WT) htt has been consistently found in the cytoplasm (DiFiglia et al. 1995, Gutekunst et al. 1995) but there are several reports of FL WT htt in the nucleus (Bessert et al. 1995, De Rooij et al. 1996, Sapp et al. 1997 and Kegel et al. 2002) and in a perinuclear location (Sapp et al. 1997, Strehlow et al. 2007). Bessert et al. (1995) found nuclear and cytoplasmic localisation of WT htt in HEK 293 cells (one of the cell types used in this thesis). Htt is associated with various organelles within the cytoplasm including the nucleus, endocytic vesicles (clathrin-coated and non-coated), autophagic vesicles, mitochondria, endoplasmic reticulum and Golgi complex in the cell body, neurites, axons and synapses (DiFiglia et al. 1995, Velier et al. 1998, Hilditch-Maguire et al. 2000, Hoffner et al. 2002, Kegel et al. 2002, Panov et al. 2002, Li et al. 2003, Choo et al. 2004, Caviston et al. 2007, Strehlow et al. 2007, Rockabrand et al. 2007, and Atwal et al. 2007). The widespread subcellular localisation of htt throughout the cell has not facilitated a specific understanding of the function of htt although it does suggest that htt has a widespread cellular function.

Htt is a soluble protein of 3,144 amino acids and has many potential domains whose boundaries and activities are not fully understood. The primary amino acid sequence of htt also reveals little about its function, as there are only a few known sequence motifs

and no structural domains with defined functions. A diagrammatic representation of htt and the main functional regions are shown in Fig. 1.1. The first 17 aa of htt, prior to the polyglutamine stretch, have been associated with the nuclear pore protein “translocated promotor region “ (TPR). The removal of these 17aa results in accumulation of the protein in the nucleus (Cornett et al. 2005) suggesting that the first 17aa. are a nuclear export sequence (NES). Atwal et al. (2007) have suggested that the first 17aa. in htt are an amphipathic alpha helical membrane binding domain that is involved in targeting htt from the nucleus to the endoplasmic reticulum. A single point mutation in the first 17aa of htt, caused nuclear accumulation and increased cell death in a mouse striatal cell model of HD (N171-Q138). Several lysine residues within the first 17aa sequence compete for SUMOylation and ubiquitination which are post-translational modifications that could regulate the half-life, localisation and nuclear export of WT htt, as well as modifying the toxicity of MT htt (Kalchman et al 1996, Dohmen et al 2003 and Steffan et al 2004).

One of the most important parts of htt is the polyglutamine (polyQ) region which begins at the eighteenth amino acid. It is possible that the polyglutamine stretch is not essential for physiological function (Harjes et al 2003, Li, S.H. et al 2004 and Clabough et al 2006). A polyQ region is also present in many transcription factors (Yu et al 2002), which may represent one mechanism by which MT htt impairs transcriptional activity. Perutz et al. (1994) demonstrated that the polyQ region may form a polar zipper structure and suggested that its physiological function was to bind transcription factors that contain a polyQ (Perutz et al 1994). It has been shown that WT htt interacts with

Fig 1.1

several polyQ-containing proteins and that the polyQ tract is a key regulator of this interaction (Harjes et al. 2003, Goehler et al. 2004 and Li S.H et al. 2004).

In higher vertebrates, the polyQ region is followed by a polyproline (polyP) stretch,

which may keep htt in solution (Steffan et al. 2004). Downstream of the polyP region is a HEAT (huntingtin, elongation factor 3, the PR65/A subunit of protein phosphatase 2A and the lipid kinase Tor) repeat sequence. HEAT repeats are approximately 50aa long sequences that occur multiple times within a given protein and are involved in protein–protein interactions (Andrade et al. 1995, Neuwald et al 2000). HEAT repeat sequences are found in proteins that often play roles in intracellular transport (including nucleocytoplasmic shuttling), microtubule dynamics and chromosome segregation. Bioinformatics analysis has found 37 putative HEAT repeats in htt (MacDonald 2003). The number of functionally active HEAT repeats remains uncertain (Takano et al 2002), although there are probably three main clusters (Fig. 1.1.) (Andrade et al 1995).

Htt contains a functionally active C-terminal nuclear export signal (NES) sequence (Fig. 1.1.) which may also suggest that the protein is involved in transporting molecules from the nucleus to the cytoplasm (Xia et al. 2003). Hoffner et al (2002) demonstrated that htt associates with β -tubulin in a perinuclear and centrosomal distribution and the authors suggested that htt may regulate entry of proteins into the nucleus. The role of nuclear translocation of htt in HD is discussed further in Section 6.9.3.

Htt contains three protease cleavage consensus sites (Goldberg et al., 1996, Gafni et al. 2002 and 2004, Wellington 1998 and 2000, Lunkes et al 2002) (Fig. 1.1). Cleavage at these sites leads to fragments of WT and MT htt, although MT htt is more susceptible to proteolysis (Davies et al 1997, DiFiglia et al 1997, Kim 2001, Lunkes et al. 2002 and Wellington et al. 2002, Mende-Mueller et al. 2001). The processing of htt is discussed in more detail in Section 1.6.

Htt can undergo four types of post-translational modification. The N-terminal lysines K6,

K9 and K15 compete for sumoylation and ubiquitination (Steffan et al. 2004, Kalchman et al. 1996) and these post-translational modifications could regulate the half-life, localisation and nuclear export of WT htt as well as modifying the toxicity of the MT protein (Dohmen et al 2004, Steffan et al. 2004, Kalchman et al. 1996). Phosphorylation at serines 421 and 434 influences cleavage and toxicity, and is reduced in HD (Humbert et al. 2002, Warby et al. 2005, Luo et al. 2005). Htt is palmitoylated by its co-partner, huntingtin-interacting protein 14 (Hip-14, a palmitoyl transferase) at cysteine 214. Hip-14 regulates trafficking and function of htt as well as several other neuronal proteins (DiFiglia et al 1995, Huang et al. 2004, Yanai et al 2006). Htt containing expanded polyQ has been found to be a poorer Hip-14 substrate compared with WT htt and therefore differential palmitoylation may represent one mechanism by which MT htt is toxic (Yanai et al 2006).

Htt is phylogenetically conserved which suggests that it is an essential protein for cellular function. WT and MT htt are expressed during development (Ambrose et al. 1994) although expression in non-neuronal tissues is relatively down-regulated (Schmitt et al. 1995). The htt knock-out mouse model was generated independently and simultaneously by three groups (Duyao et al. 1995, Nasir et al. 1995, Zeitlin et al. 1995). All three models demonstrated that nullizygous mice die at embryonic days 6-10 suggesting that htt is vital for embryonic survival, although all three have different phenotypes. Nullizygous mice embryos can be rescued from lethality by WT extra-embryonic tissues suggesting that htt has a role in the development of extra-embryonic tissues (Dragatsis et al. 1998). Embryos with less than 50% normal htt die by E18.5 with extensive mid and hind-brain abnormalities suggesting that htt also has a role in gastrulation and neurogenesis (White et al. 1997). A chimeric study has demonstrated that following the injection of nullizygous embryonic stem (ES) cells into WT blastocysts, viable nullizygous neurons were found in

the brain although they were sparse in the cortex and striatum. This suggests that expression of htt is critical for region-specific survival and differentiation of neurons (Reiner et al. 2001 and 2003). However, the absence of htt does not kill cells in culture, suggesting that htt is not critical for post-embryonic cell survival (Metzler et al. 1999).

The cellular roles of htt remain poorly defined. This is mainly due to the large size of the protein, making it difficult to isolate and analyse, the lack of sequence homology with other proteins of known function, its ubiquitous localisation within the body and the cell, and its interactions with over 200 other proteins (see Harjes et al 2003 for review). In general, most evidence to date suggests that htt is a scaffold protein within the cell involved in controlling intracellular trafficking and signalling pathways. More specifically, it has anti-apoptotic effects (Rigamonti et al 2001), it is involved in transcriptional regulation, possibly involving its HEAT domain regions and nucleocytoplasmic shuttling of transcriptional regulatory proteins (Boutell et al. 1999, Truant et al 2007 and Section 1.8), and it may have a role in vesicle trafficking and axonal transport through its association with endosomal vesicles and trafficking proteins such as Hip1 and Hap1 (Li et al. 1995, DiFiglia et al. 1995, Gutekunst et al. 1995, Sharp et al. 1995, Colomer et al. 1997, Engelender et al. 1997, Velier et al. 1998, Hattula and Peranen 2000, Harjes et al 2003 and Section 1.9). Htt may also have a role in iron homeostasis (Hilditch-Maguire et al. 2000).

There is growing evidence that a reduction in WT htt may have a role in the pathogenesis of HD. Van Raamsdonk et al. (2005) generated a mouse model that expressed FL human htt with CAG repeats up to 128, with and without endogenous mouse htt. The authors found a slightly worse phenotype with worse motor dysfunction, hyperkinesia, testicular atrophy and slightly reduced lifespan in the mice lacking endogenous mouse htt but there

were no gross neuropathological differences. This suggested that replacement of WT htt will not be sufficient to treat HD and that MT htt can maintain its physiological function even with highly expanded CAG repeats.

1.5.4. Protein interactions with htt

Many protein/htt interactions have been described and most of these interactions are CAG repeat length-dependent. CREB-binding protein (CBP) is involved in transcriptional regulation and binds htt strongly in a direct repeat length-dependent manner (Kazantsev et al. 1999 and Section 1.8.1.). Huntingtin associated protein 1 (Hap-1) was one of the first proteins to be found to interact with htt and may also be involved in cellular trafficking in a repeat length-dependent manner (Li, X.J. et al. 1995 and Section 1.9.). Huntingtin interacting protein 1 (Hip-1) is involved in endocytosis and intracellular vesicular transport and binds htt in an inverse length-dependent manner (Kalchman et al. 1997, Wanker et al. 1997 and section 1.9.). Hip-1 has been demonstrated to have pro-apoptotic activity which can be modulated by htt (Hackam et al. 2000). The strength of the interaction between htt and Hip-1 is inversely proportional to the length of the polyglutamine repeat. It is postulated that sequestration of pro-apoptotic Hip-1 by WT htt prevents apoptosis that could occur when Hip-1 is released by MT htt (Hackam et al. 2000). Huntingtin interacting protein 2 (Hip-2) is a ubiquitin conjugating enzyme which ubiquitinates proteins for degradation by the 26S proteasome (Kalchman et al. 1996) although abnormal interactions between MT htt and Hip-2 have not been investigated. Gusella and MacDonald (1998), using a yeast two-hybrid interactor screen, identified 13 protein interactions with htt and three of these were WW domain proteins (HYP A,B and C). WW domains are 38-40 amino acid sequences involved in protein-protein interactions through the binding of polyproline regions such as the region following the polyQs in htt.

1.6. The molecular pathogenesis of HD: Processing of huntingtin

1.6.1. Processing of WT and MT htt in humans and cell and mouse models

There is compelling evidence that the first step in the pathogenesis of HD is the processing of FL htt to generate toxic N-terminal htt fragments, which accumulate not only in the nucleus but also in the cytoplasm, axons, dendrites and synapses. The selective neuronal loss in post-mortem HD brain and in HD mice may partially be explained by variations in regional processing, since N-terminal MT htt expressing transgenic and knock-in mouse models demonstrate more widespread aggregates than FL models (Davies et al. 1997, Schilling et al 1999 and Becher et al 1998). Transgenic or knock-in HD mice that express FL htt with expanded CAG repeats develop inclusions formed by N terminal fragments of MT htt (Reddy et al. 1998, Hodgson et al. 1999 and Wheeler 2000). Aggregates in HD post-mortem brains and in animal models contain epitopes for N-terminal (1-549 amino acids) but not internal or C-terminal antibodies (DiFiglia et al. 1997; Gutekunst et al. 1999; Sapp et al 1997 and Sieradzan et al. 1999) suggesting that processing occurs prior to aggregation. N-terminal fragments of MT htt have been detected in immunoblots of homogenates from HD brains (DiFiglia et al. 1997) and from transgenic mouse models expressing FL MT htt (Zhou et al. 2003 and Tanaka et al. 2006). N-terminal fragments of approximately 40kDa in length have been described in Western blots of the nuclear fraction of striatal lysates of post-mortem juvenile HD brain (DiFiglia et al. 1997). Similar fragments have been described in the nuclear fractions of striatal lysates of MT FL htt knock-in mice by Li, H. et al. (2000). Lunkes et al (2002) demonstrated that the pathologic htt fragments terminated between the polyglutamine domain (beginning at amino acid 19) and amino acids 115-129 in HD post-mortem brain

and HD cell models (all amino acid numbers, unless otherwise stated, are based on WT htt with 23Q/21CAGs). Sieradzan et al (1999) demonstrated that an antibody to an htt peptide encompassing amino acids 80-113 recognized nuclear and cytoplasmic aggregates of MT htt in human HD brain, localising the C terminus of the putative N-terminal htt fragment to this 33-amino acid region of htt. A recent study has demonstrated that pathologic inclusions in the brains of HD patients, the N171-82Q mouse model of HD and a HEK 293 transiently transfected N233-78Q cell model are composed of N-terminal fragments of htt that terminate at an epitope between amino acids 81-90 and 115-129 (Schilling et al 2007). This would produce a fragment containing the polyproline region, and would be N-terminal to the caspase/calpain cleavage sites (Fig 1.1). The authors also demonstrated that a transiently transfected HEK 293 cell model expressing an N-terminal WT htt fragment (N171-18Q) formed a fragment approximately 10kDa smaller than the MT construct fragment suggesting that WT htt may also be processed to N-terminal fragments. There is evidence suggesting WT htt processing may also follow an ischaemic insult to brain (Kim et al. 2003). In contrast to MT N-terminal htt fragments, which are considered to have a key role in the pathogenesis of HD, the role of potential WT htt processing remains to be elucidated.

In summary there is evidence of multiple potential cleavage sites in htt which could lead to the formation of an N-terminal htt fragment, but the precise size of the toxic N-terminal fragment has not consistently been described.

1.6.2. Htt processing by caspases and calpains

Caspases have an important role in apoptosis and some have a greater role in initiation and regulation of apoptosis e.g. caspases 8, 9 and 10, whereas others are involved in the molecular dismantling of cells e.g. 3, 6 and 7 (Vila et al. 2003 for review of apoptosis in

the context of neurodegeneration). Caspase cleavage sites in htt have been described for caspases 2, 3 and 6 (Wellington et al. 1998, 2000, 2002, Goldberg et al. 1996, Sun et al 2002). The caspase cleavage sites were located at amino acids 513 (caspase 3), 552 (caspase 3 and 2) and 586 (caspase 6) in htt (Fig. 1.1) and produced N-terminal htt fragments of 70, 75 and 80 kDa respectively. Caspase 3 can cleave both WT and MT htt and site-directed mutagenesis abolishes the cleavage (Wellington et al 2000). Caspase 3 is only expressed in cells already undergoing apoptosis and therefore cleavage of htt by caspase 3 is unlikely to be an initiating event in cell death in HD.

Calpains are a ubiquitously expressed family of calcium-dependent non-lysosomal cysteine proteases. Ischaemic brain injury caused increased calpain processing of WT htt into 55kDa fragments (Kim et al. 2003). Gafni et al. (2002) found that calpain-mediated cleavage of htt produced three N-terminal products of 62, 67 and 72 kDa. Subsequently, Gafni et al. (2004) described two putative calpain-cleavage sites in htt at amino acid residues 469 (corresponding to the 67kDa fragment) and 536 (corresponding to the 72kDa fragment) and preferential accumulation of these fragments in the nucleus (Fig. 1.1). The mutation of these cleavage sites produced less proteolysis, less aggregates and less toxicity in a cell culture model (Gafni et al. 2004) which suggested that calpain cleavage was an important event in the pathogenesis of HD.

1.6.3. Ubiquitin proteasome system (UPS) inhibition by htt

The ability of the proteasome to degrade htt and the failure of molecular chaperones to maintain the molecular conformation of htt are potentially important events in the molecular pathogenesis of HD (Gusella and MacDonald 1998, Bence et al. 2001, Jana et

al. 2001). Proteasomes are large protein complexes located in the nucleus and the cytoplasm of all eukaryotic cells (Voges et al. 1999). The main function of proteasomes is to regulate the concentration of proteins and degrade misfolded proteins by proteolytic degradation which yields peptides of seven to eight amino acids. Proteins are tagged for degradation by ubiquitin. The tagging reaction is catalyzed by ubiquitin ligases. Once a protein is tagged with a single ubiquitin molecule, this signals other ligases to attach additional ubiquitin molecules. The result is a polyubiquitin chain that is recognised and bound by the proteasome, allowing it to degrade the tagged protein (Ciechanover et al. 2000 and 2006 for review).

Several proteasome inhibitors have been described. Lactacystin was the first natural proteasomal inhibitor identified from *Streptomyces* and it inhibits the chymotryptic and tryptic activities of the proteasome by covalently binding to the N-terminal Thr1 of the $\beta 5$ proteasome subunit in the 20S catalytic core (Fenteany et al 1995; Groll et al 1997). Lactacystin inhibits the proteasome specifically without inhibiting other proteases *in vitro*, and it does not inhibit lysosomal protein degradation (Fenteany et al. 1998).

Seo, H. et al (2004) described a reduction in peptidyl-glutamyl peptide-hydrolyzing (PGPH) and chymotrypsin-like activities of the UPS in early and late-grade post-mortem HD cerebellum, cortex, substantia nigra and caudate/putamen. HD patient's skin fibroblasts demonstrated similar reductions in the UPS suggesting that MT htt caused a widespread inhibition of the UPS and that additional factors must be responsible for selective neuronal cell death. The authors found a specific increase in ubiquitin in late-grade caudate/putamen and a reduction in caudate/putamen BDNF levels and complex II/III activity. It was suggested that a composite of several metabolic abnormalities could explain the regional specific loss in HD. Subsequently, the same authors described a

reduction in all three proteasomal activities in primary striatal cells from an HD mouse model. These activities were significantly improved with transfection of a lentiviral vector expressing the proteasome activator subunit PA28 γ which also partially protected the cells from a proteasomal inhibitor (MG132), and quinolinic acid (an excitotoxic) but not a complex II mitochondrial inhibitor (3-NP) (Seo, H et al. 2007). Bence et al. (2001) demonstrated a failure of degradation of GFP in cells expressing N-terminal MT htt suggesting proteasomal inhibition by N-terminal htt. Jana et al. (2001) demonstrated that expanded polyglutamines, in an N-terminal htt inducible cell model, inhibited chymotrypsin-like activity in the cytosolic fractions. This was associated with reduced degradation of p53 and a transfer of proteasomal activity to aggregate-containing precipitated fractions. Bennet et al (2005) described inhibition of the UPS in cells co-expressing ubiquitin tagged with GFP and MT htt exon 1 in the absence of visible aggregates. Isolated polyglutamine aggregates in vitro do not inhibit the proteasome (Bennett et al 2005) but fibrillar species of MT htt purified from HD transgenic mice and HD post-mortem brain can decrease proteasome function (Diaz-Hernandez et al. 2006).

The 20S proteasomal subunit is sequestered in htt inclusions in the R6/1 mouse model, N-terminal htt expressing cell cultures (Cummings et al 1998, Jana et al. 2001, Waelter et al. 2001a, Wyttenbach et al. 2000) and post-mortem HD brain (DiFiglia et al 1997), which may underlie UPS inhibition and htt aggregate toxicity (Section 1.7).

SH-SY5Y cells stably expressing polyQ (19, 56, or 80Q) within GFP did not lead to proteasomal impairment (Ding et al 2002) and there was no evidence of decreased UPS activity in a knock-in mouse cell model of SCA7 (Bowman et al. 2005). These studies suggest that the protein context of the polyglutamine repeats may be important in polyglutamine-mediated UPS inhibition.

In contrast to decreased UPS function in HD, Diaz-Hernandez et al. (2003) found an increase in the chymotrypsin and trypsin activities of the proteasome in striatal and cortical, but not cerebellar, lysates from a conditional HD mouse model expressing exon with 1-94Q. This was attributed to an increase in the levels of the proteasome subunits LMP2 and LMP7 and the induction of the immunoproteasome. Increased proteasomal chymotrypsin-like activity has also been observed in brain lysates from the R6/2 model of HD compared with non-transgenic littermates (Bett et al 2006). However, this study found no change in overall 26S proteasome activity and showed that the nuclear proteasome activator PA28 was not involved in polyglutamine pathology. This is in contrast with data demonstrating the reversal of proteasome dysfunction in MT htt-expressing striatal neurons and rescue of cell death by PA28 overexpression (Seo et al 2007).

In conclusion, there is contrasting evidence relating the influence of MT htt upon UPS function in HD. This may in part be due to the different model systems (stable, inducible and transient cell models, transgenic mice and post-mortem HD brain), the variation in the sizes of the htt fragments used in the studies (isolated polyQ, compared to N-terminal and FL htt) and the different methodologies used to assess UPS function. Therefore, conclusive proof of UPS dysfunction in HD has yet to be verified.

1.6.4. UPS and degradation of htt

Htt aggregates are ubiquitinated in human post-mortem brain (DiFiglia 1997) and in HD transgenic mice (Mangiarini et al 1997) which suggests that they have been targeted for degradation by the proteasome. The ubiquitin-conjugating enzyme, E2 or huntingtin interacting protein-2 (Hip-2), has been found to equally bind to, and ubiquitinate, MT and

WT htt (Kalchman et al. 1996). This suggested that preferential labeling of MT htt for the proteasome was not a potential mechanism for the selective toxicity of MT compared to WT htt in this system. Parkin, an E3-ubiquitin ligase, co-localises with htt aggregates in HD mouse and human brains and overexpression of parkin enhances the clearance of the MT protein (Tsai et al 2003). These data suggest that htt may be a proteasome substrate. The HD94 conditional mouse model (Yamamoto et al. 2000), demonstrated that by switching off the MT htt transgene, there was reversal of neuropathology and neurological phenotype in the mice (Section 1.7.4 for further description). Martin-Aparicio et al. (2001) subsequently demonstrated the conditional formation of htt aggregates in a striatal culture model of HD94, and that the loss of aggregates on switching off the transgene was inhibited by lactacystin, suggesting that removal of htt aggregates is proteasome-dependent. Proteasome inhibition also increases MT htt aggregation and toxicity in other HD cell models (Wytttenbach et al 2000, Jana et al 2001, Waelter et al 2001a, Ravikumar et al. 2002).

Venkatraman et al. (2004) and Holmberg et al (2004) have demonstrated that eukaryotic proteasomes are incapable of digesting proteins of between 9 and 29 polyglutamine repeats and therefore these must be released from the proteasome for further hydrolysis. Bhutani et al (2007) described the very slow and inefficient degradation of polyglutamine tracts released from the proteasome by a puromycin-sensitive aminopeptidase. It is therefore unclear whether enhancing proteasome function to remove toxic MT htt species may actually increase the amount of polyglutamine tracts without a protein background which could potentially be more toxic. There is therefore no direct evidence of proteasome processing of htt.

1.6.5. Protein folding and htt

The folding of newly synthesized proteins and the refolding of misfolded proteins is performed by the sequential actions of several molecular chaperones. If the molecular chaperones fail, then the misfolded protein is often degraded by the proteasome (Fink 1999). Heat shock protein 40 and 70 (HSP 40 and 70) are the two main classes of molecular chaperones that coordinate folding and maintenance of proteins into a soluble conformation (Hartl and Hayer-Hartl 2002). If misfolded proteins are not degraded, this results in the accumulation of insoluble protein and aggregation can occur.

Following the generation of N-terminal htt fragments from FL MT htt, as described in Section 1.6.1., it is postulated that MT N-terminal htt misfolds and forms oligomers and subsequently aggregates. This is not a feature of WT htt. Htt interacts with both HSP 40 and 70 families of molecular chaperones, with both co-localising with aggregates in HD tissue and animal and cellular models (Sakahira et al. 2002). This sequestration may lead to an increase in protein misfolding and lead to a cascade of molecular events culminating in cell death (Hay et al. 2004). This may be a feature of other CAG repeat disease as the overexpression of HSP 40 and 70 in a *Drosophila* model of spinocerebellar ataxia type 3, rescued cells expressing truncated protein with 78 CAGs (Bonini 2002).

1.6.6. Autophagy and htt

Autophagy is a process involving the formation of double-membrane structures, called autophagosomes, around a portion of cytoplasm. These autophagosomes ultimately fuse with lysosomes, where their contents are degraded. MT htt has been shown to be degraded by autophagy (Ravikumar et al 2002). The strategy of up-regulating autophagy to increase clearance of MT protein has shown promise in cell, *Drosophila* and mouse

models of HD where the increase in clearance shows a preference for the MT form of the protein (Ravikumar et al 2004). Drugs which can be used to up-regulate autophagy, such as rapamycin, carbamazepine, sodium valproate, have been shown to work in animal and cell models expressing other aggregate-prone proteins that lead to human disease, including tau and MT α -synuclein (Berger et al 2006). Pharmacological enhancement of the autophagosome may represent a possible method of removal of aggregate-prone mutant proteins in several neurodegenerative diseases.

1.7. The molecular pathogenesis of HD: Aggregate formation

The formation of cytoplasmic and nuclear protein inclusions is a striking histological feature of HD post-mortem brains and all other known polyglutamine diseases, most HD transgenic mice and some HD cell models (DiFiglia et al 1997 Becher et al 1998, Davies et al 1997 Lunke et al 1998 and Section 1.11).

1.7.1. Distribution of aggregates in HD brain

N-terminal htt aggregates, with detectable epitopes between amino acids 1-549 (DiFiglia et al. 1997), are heterogeneously distributed throughout the HD brain. Aggregates are mostly found in the layers V and VI of the cerebral cortical grey matter. The insular and cingulate cortices contain more inclusions than the prefrontal, temporal association and pre-motor cortices (Gutkunst et al. 1999). The aggregates are uncommon and scattered widely in the striatum where neurodegeneration is most prominent, in contrast to the R6/2 mouse model (Sections 1.7.3 and 1.10.7.). Aggregates are rarely seen in the globus pallidus, hippocampus and cerebellum, but may be found in the thalamus, brainstem nuclei and substantia nigra (pars compacta) (Gutkunst et al. 1999).

At a subcellular level, the aggregates form in the nucleus, perikaryon and neuropil. Neuropil aggregates are the most common form (Gutkunst et al. 1999). They can be small round structures or long tubular forms that fill the axons for hundreds of microns (DiFiglia et al. 1997, Becher et al. 1998, Gutkunst et al. 1999). The nuclear aggregates are round to oval and are between 3-5 μ m in diameter. There is usually only one or occasionally two per nucleus. The perikaryal aggregates are smaller in size (0.3-1.5 μ m).

Ultrastructural studies have suggested that the aggregates are not membrane-bound but are made up of granular and filamentous material. The filaments have a width of approximately 10nm (DiFiglia et al. 1997, Gutkunst et al. 1999). The first possible description of aggregates probably came from an ultrastructural study of the neuronal nuclei in HD brains in 1979 but the significance of these filamentous inclusions was not fully appreciated at the time (Roizin et al. 1979).

1.7.2. Aggregates in early HD

There have been relatively few studies which have examined the distribution of aggregates in early HD (DiFiglia et al. 1997; Gutkunst et al. 1999). These studies demonstrated that there were neuropil aggregates in two presymptomatic HD patients in the cortex, especially in cortical layers V and VI. Aggregates in the dorsal striatum, where the earliest neurodegeneration occurs, were rare, apart from one report of aggregates in the tail of the caudate in a presymptomatic patient (Gomez-Tortosa et al. 2001).

1.7.3. Aggregates in mouse models

Neuronal nuclear aggregates were first described in the R6/2 mouse model (Davies et al. 1997). Aggregates have subsequently been described in many HD mouse models. Aggregate formation is most extensive in models which express truncated htt which contain highly expanded CAG repeats. The R6/2 model is a good example of this, where the transgene htt background consists of only exon 1 (90aa.) containing 148 CAG repeats. In the R6/2 mouse, by 8 weeks, most groups of neurons contain aggregates, but there is a sequence of progression of aggregate formation e.g. cortex and hippocampus before striatum in the R6/2 mouse (Morton et al. 2000). Aggregates have also been described in organs outside of the CNS including skeletal muscle, heart, liver, pancreas, kidneys, stomach, and adrenal glands (Sathasivam et al 1999, Orth et al 2003). The mice tend to develop striatal nuclear aggregates in contrast to the human disease where striatal aggregates are relatively sparse and more frequent in the cerebral cortex (Li et al. 2000). There appears to be a consistent sequence of events in the formation of nuclear inclusions in the mouse models. At first, using the EM48 antibody to detect expanded polyglutamines, there was diffuse nuclear staining followed by intense nuclear staining and the development of small puncta in the nucleus. The puncta then coalesce to form a single inclusion and the diffuse nuclear staining disappears. It is postulated that the early diffuse staining represents translocation of an N-terminal fragment of htt into the nucleus or even retention of FL htt and truncation to an N-terminal fragment within the nucleus.

At an ultrastructural level, the inclusions are granular and fibrillar structures which are not membrane-bound and they are similar to nuclear inclusions described in post-mortem HD brain (Roizin et al. 1979, Davies et al. 1997). The aggregates are associated with changes in the nuclear membrane and pores (Davies et al. 1997). The nuclear aggregates are ubiquitinated and are associated with a number of other proteins including, components of the proteasome, heat shock proteins (Jana et al. 2000), transcription

factors, e.g. CREB-binding protein (CBP) (Nucifora et al. 2001), Sin3b, and complexin II (Morton and Edwardson 2001).

There is evidence from a conditional transgenic model of HD that aggregates are involved in a dynamic process of formation and breakdown (Yamamoto et al. 2000). Turning off the transgene, resulted in not only resolution of the aggregates but also a dramatic improvement in the neurological phenotype, demonstrating that the aggregates are in a dynamic cycle of deposition and removal. Progression of the disease also required that the MT transgene was continuously expressed. These findings suggest that HD therapeutics may be able to benefit patients who already have developed an HD phenotype.

1.7.4. Mechanism of aggregate formation

Perutz et al. (1994) proposed that elongated polyglutamine chains can form stable hairpins when the number of polyglutamines exceeds 37 and that the hairpins associate to form aggregates. This was termed the “polar zipper” model of aggregation because antiparallel β -strands of polyglutamine were proposed to link together by hydrogen bonds. Subsequently, *in vitro* studies have confirmed that MT N-terminal htt can form fibrils (Georgalis et al. 1998). These *in vitro* htt fibrils, and htt aggregates in HD post-mortem brain, stain with Congo red and demonstrate green birefringence when examined under polarized light, suggesting that the fibrils/aggregates contain amyloid with a β -pleated sheet structure (Huang et al. 1998). Fig. 1.2. summarises the proposed mechanism of self-assembly of MT htt into aggregates. *In vitro* and transgenic studies have demonstrated that the more truncated the N-terminal fragment and the longer the CAG repeats, the faster aggregation occurs and the more widespread are the inclusions, although aggregation only occurs when there are greater than 37 glutamines (Cooper et al.

1998, Hackam et al. 1998, Kazantsev et al. 1999, Kim et al. 1999, Lunkes and Mandel 1998, Marsh et al. 2000, Martindale et al. 1998, Peters et al 1999).

Transglutaminases are a family of calcium-dependent enzymes that catalyse the formation of covalent ϵ -(γ -glutamyl)-lysine isopeptide bonds, resulting in the formation of insoluble cross-linked proteins (Greenberg et al. 1991). Aggregation of htt has also been proposed to occur by cross-linking of MT htt to itself or other lysyl residues by transglutaminases (Kahlem et al. 1996, 1998, Karpuj et al. 1999). Cystamine is primarily an inhibitor of the enzyme transglutaminase and several studies have variably demonstrated significant clinical and neuropathological improvements in the phenotype of mouse models following administration of cystamine (Karpuj et al. 2002, Dedeoglu et al. 2002, Lesort et al. 2003, Wang et al. 2005). These studies have contrasting results in that Karpuj et al (2002) and Lesort et al (2003) did not find a dramatic effect on aggregates in spite of clinical improvement and suggested that this may be due to an anti-caspase 3 effect of cystamine (Lesort et al 2003). In contrast, Dedeoglu et al (2002) Fig 1.2.

and Wang et al. (2005) found a reduction in aggregate formation which may have been due to the administration of cystamine *in utero* (Dedeoglu et al 2002).

1.7.5. Toxicity of aggregates

One of the biggest controversies in HD biology is the role of the htt aggregates in the pathogenesis of the disease. In HD post-mortem brains, the density of the inclusions in the cerebral cortex correlates with repeat length (Becher et al. 1997), although there is little correlation between inclusion burden and the areas of the brain most affected by neurodegeneration in HD (Gutekunst et al 1999). There are several *in vitro* cell models that have associated toxicity with N-terminal MT htt expression and aggregate formation (Carmichael et al. 2000, Lunkes 1998, Hackam et al. 1999 Waelter et al. 2001a) and there

is a strong correlation between the appearance of inclusions with cell dysfunction and death (Hackam 1998 and Lunkes et al 1998).

Several putative mechanisms of polyglutamine aggregate toxicity have been proposed. These mechanisms can be summarised as aggregates causing sequestration of vital cellular proteins (Table 1.1.) or direct aggregate cellular toxicity by non-specific interference in cellular trafficking (Section 1.9) or by obstruction of the ubiquitin-proteasomal system as has been demonstrated (Bence et al. 2001 and section 1.6.3.). These findings are in contrast to several *in vitro* cell models which have found that cell death and aggregate formation are independent processes and that aggregates may be protective (Kim et al. 1999 and Saudou et al. 1998). Bodner et al (2006) demonstrated decreased proteasome dysfunction and cell death in a cell model of HD following treatment with a small molecule, in spite of greater inclusion formation. In cell culture, MT htt expression was more protective in cells demonstrating aggregate formation than

Transcription factors (TBP/TFIID, CBP)	Steffan et al. 2000, Nucifora et al. 2001, Suhr et al 2001
Caspases (caspase 8)	Sanchez et al. 1999
Protein kinases (MEKK1)	Meriin et al. 2001
Components of the UPS (ubiquitin, 20S, 19S and 11S proteasome)	Cummings et al. 1998, Waelter et al. 2001a, Suhr et al 2001
α -synuclein	Charles et al. 2000, Waelter et al. 2001a
Components of the nuclear pore complex	Suhr et al. 2001
Cell cycle proteins (p53, mdm-2)	Suhr et al. 2001
Cytoskeletal proteins (actin)	Suhr et al. 2001
Molecular chaperones (HSP70 and 40, BiP/ GRP78)	Waelter et al. 2001a
RNA binding proteins (TIA-1)	Waelter et al. 2001a

Table 1.1. Proteins sequestered in htt inclusions

cells that did not form aggregates (Arrasate et al (2004). Saudou et al. (1998) transiently

transfected rat striatal and hippocampal neurons with plasmids expressing N-terminal human htt of 171 or 480aa. in length containing either 17Q or 68Q. They found that inclusions formed maximally in the striatal cultures at day 6 but significant apoptosis did not occur until day 9. Hippocampal neurons also formed inclusions but did not undergo apoptosis suggesting that MT htt induced-apoptosis was dependent on the cell type. AC-DEVD-CHO (a caspase inhibitor), growth factors (BDNF and CNTF) and the anti-apoptotic protein, BclX_L all rescued cells from apoptosis but did not prevent nuclear inclusion formation. This in itself did not prove that inclusions are protective, as apoptosis may have been activated by the inclusions and subsequently these agents rescued the cells by interfering with downstream execution of apoptosis. The authors then demonstrated the level of apoptosis was not related to the length of the htt construct. A dominant negative mutation in the ubiquitin-conjugating enzyme hCdc34p(CL→S) was expressed in the model and inhibited nuclear inclusion formation but produced greater cell death at day 6 compared to day 9 in the cells containing inclusions without the dominant negative mutation. These results suggested that nuclear localisation of htt is important in htt-induced cell death but that aggregate formation may be independent and possibly protective of cell death.

The overexpression of CA150, a transcription factor, in HD transgenic rats and knock-in mice rescued neuronal toxicity whilst increasing neuritic aggregates and had no effect on nuclear inclusions (Arango et al 2006). These findings suggested against htt aggregate-induced toxicity.

In summary, at the very least, the presence of htt inclusions demonstrates that there is abnormal processing or misfolding of the MT htt protein. The presence of nuclear and non-nuclear inclusions of various types in a wide range of neurodegenerative diseases

(Trojanowski and Lee 2000) suggests that insoluble protein deposits are a pivotal feature of neurodegeneration and that these diseases may have a common underlying pathogenic mechanism. The demonstration of inclusions in the brain of a mouse model with ectopic expression of polyglutamine in the hypoxanthine ribosyl transferase gene (hprt) and the subsequent development of a neurological phenotype (Ordway et al. 1997) further highlights the link between inclusions, neurodegeneration and polyglutamine repeats. However, based on current evidence, it is not certain whether inclusions are pathological, protective or an epiphenomenon.

1.8. The molecular pathogenesis of HD: Transcriptional regulation

An early observation in HD biology was that WT FL htt was mainly found in the cytoplasm, and only truncated MT N-terminal htt was found in the nucleus (Martindale et al 1998). This early observation suggested that the nucleus may be an important site of MT htt toxicity. Nuclear localisation of MT htt enhanced toxicity in HD cell models and transgenic mice (Saudou et al. 1998, Ross et al 2004 and Schilling et al. 2004). A number of transcriptional regulators contain glutamine-rich activating domains, which are important for the interaction between transcription factors and transcription regulators. Therefore, proteins containing polyglutamines may influence transcription factors and alter transcription (Perutz et al 1994, Gerber et al 1994).

In support of transcriptional dysregulation as an important mechanism in HD, in situ hybridization studies have demonstrated downregulation of several genes in HD post-mortem striatum, including substance P, enkephalin and D1 and 2 dopamine receptor mRNA (Augood et al. 1996, 1997), as well as cannabinoid receptors and NR1 and NR2B subunits of the NMDA receptor (Arzberger et al. 1997 and Richfield and Herkenham

1994). In situ hybridization studies in R6/2 transgenic mouse striatum have revealed that the D1 dopamine receptor, metabotropic glutamate receptor and A2a adenosine receptor mRNA were decreased by four weeks of age before neuronal loss was observed (Cha et al. 1998 and 1999). PET studies in asymptomatic HD mutation carriers have demonstrated decreased D1 and D2 receptor activities, and these abnormalities correlated with subtle cognitive deficits (Backman et al. 1997, Lawrence et al. 1998). This suggested that these changes may account for some of the early cognitive features observed in HD patients and that functional neuronal changes may occur before gross cell death and inclusion formation.

Changes in at least six transcriptional systems have been described in HD. These include the CREB system (Li and Li for a review 2004, Steffan JS. et al. 2000, Steffan et al. 2001 and Hockly et al. 2003), SP-1 (Dunah et al. 2002), TATA-binding protein (TBP) (Stevanin et al. 2003), repressor complexes containing nuclear corepressor protein and Sin3a (Boutell et al. 1999), neuron-restrictive silencer elements (NRSEs) (Zuccato et al. 2003) and PGC-1 α (Cui et al. 2006). These will be discussed below.

1.8.1. The cAMP-responsive element binding protein (CREB)

CREB proteins are transcription factors which bind to DNA sequences called cAMP response elements (CRE) (Mantamadiotis et al. 2002). The disruption of the CREB system in mice leads to an HD-like phenotype in which there is progressive neurodegeneration in the hippocampus and striatum (Mantamadiotis et al. 2002). The downregulation of CREB-regulated genes has also been detected in HD patients (Glass et al. 2000). The CREB-binding protein (CBP) is involved in controlling the activity of CREB proteins and has been found to be sequestered into aggregates in HD as well as other polyglutamine diseases (Li and Li 2004). Htt interacts with CBP via its

polyglutamine and acetyltransferase domains, which may explain why there is a reduction in CREB-mediated transcription and acetyltransferase activity in models of HD (Steffan et al. 2000). In cellular, fly and mouse models of HD, neurodegeneration can be partly ameliorated through the administration of histone deacetylase inhibitors which is associated with a reversal in the reduction of acetyltransferase activity (McCampbell et al. 2001, Steffan et al. 2001 and Hockly et al. 2003). Further data has challenged some of these findings. A double-transgenic mouse model of MT htt overexpression and the CRE- β galactosidase reporter construct suggested that CREB-regulated transcription was upregulated (Obrietan and Hoyt 2004).

1.8.2. Specificity protein-1 (Sp1)

MT htt has also been demonstrated to sequester another transcriptional regulator, Sp1, into aggregates and therefore disrupt Sp1-mediated transcription. MT htt also disrupts the specific interaction of Sp1 with co-activator TAF_{II}130. Of particular importance, an enhanced association between Sp1 and MT htt has been described in presymptomatic HD patients and the association of Sp1 with TAF_{II}130 was reduced in HD brain (Dunah et al. 2002). The interaction between Sp1 and htt also blocks the binding of Sp1 to its promoter region. The overexpression of both Sp1 and TAF_{II}130 has been demonstrated to overcome the inhibition of D2 receptor gene expression by MT htt (Dunah et al. 2002). In contrast, more recent studies by Qui et al. (2006) demonstrated an increase in Sp1 expression levels in different experimental models of HD, suggesting that suppression of Sp1 could be beneficial for HD pathology, while an increase in Sp1 levels may enhance MT htt toxicity.

1.8.3. TATA-binding protein (TBP)

TBP has also been found to localise to htt nuclear inclusions. Sp1 binds to and regulates molecules of the transcription machinery, such as transcription factor IID (TFIID) which is a multi-protein complex and contains TBP and multiple TAF_{II}s. An expansion of the polyglutamine region of TBP causes SCA17 which is an autosomal dominant ataxia with overlapping clinical features of HD (Stevanin et al. 2003).

1.8.4. Nuclear co-repressor protein and mSin3a

Yeast two-hybrid analysis has demonstrated that htt may also disrupt transcriptional repressors as well as promoters. Htt directly interacts with repressor complexes containing nuclear corepressor protein and mSin3a in a polyglutamine-dependent manner (Boutell et al. 1999). These are involved in repressing the transcriptional activation of nuclear receptors such as retinoic acid. One quarter of the genes with altered transcription in the R6/2 mouse were found to be under the control of retinoic acid (Luthi-Carter et al. 2000).

1.8.5. NRSE-regulated pathways

WT htt has been found to regulate the activity of genes that contain neuron-restrictive silencer elements (NRSEs) (Zuccato et al. 2003). Brain-derived neurotrophic factor (BDNF) is regulated by NRSE and WT htt binds cytosolic REST/NRSF complex, the transcription factor that binds to the NRSE in the promotor of BDNF, preventing it from entering the nucleus and inhibiting BDNF transcription. MT htt does not bind REST/NRSF effectively, which enables REST/NRSF to enter the nucleus and switch off BDNF transcription. BDNF has been found to be an important pro-survival factor of striatal neurons, which may explain not only the mechanism of cell death induced by MT

htt but also the regional specificity due to the loss of BDNF in the striatum from cortical neurons (Zuccato et al. 2001).

1.8.6. PGC-1 α

Transgenic mice lacking PGC-1 α , a transcriptional coactivator that regulates several genes involved in mitochondrial biogenesis and respiration, show defects in brown adipose tissue as well as a pattern of neurodegeneration similar to HD (Lin et al 2002, Leone et al 2005). MT htt may cause disruption of mitochondrial function by inhibiting expression of PGC-1 α and over expression of PGC-1 α reverses the effects of MT htt in cell models and HD transgenic mice (Cui et al. 2006). This suggests that inhibition of mitochondrial function by htt may occur at an early biosynthetic level.

1.9. The molecular pathogenesis of HD: Cellular transport

Htt purifies with vesicle fractions from human and rat brain (DiFiglia et al. 1995, Gutekunst et al. 1995, Sharp et al. 1995, Velier et al. 1998, Wood et al. 1996). Htt also associates with microtubules (Bhide et al. 1996, DiFiglia et al. 1995, Gutekunst et al 1995, Tukamoto et al 1997) and interacts with several proteins involved in retrograde transport (Colomer et al. 1997, Engelender et al. 1997, Hattula and Peranen 2000, Velier et al 1998). Polyglutamine tracts interact with neurofilament proteins (Nagai et al 1999). Following a crush injury to rat sciatic nerve, the accumulation of N-terminal and FL htt was demonstrated either side of the injury (Block-Galarza et al. 1997). These findings suggest that htt is involved in axonal transport and vesicle trafficking.

The role of htt in vesicle trafficking was therefore originally proposed on the basis of its

localisation to endocytic/endosomal vesicles in axons and synaptic terminals and from its interaction with a number of endocytic/trafficking proteins, including α -adaptin, Hip1, Hip14, Hap (huntingtin-associated protein) 1, Hap40, PACSIN1 (protein kinase C and casein kinase substrate in neurons-1) and SH3GL3 [SH3 (Src homology 3)-domain Grb2-like 3] (endophilin 3) (Harjes et al. 2003, Li and Li 2004).

The endocytic proteins, clathrin and dynamin have been found to colocalise with htt (Velier et al 1998, Kaltenbach et al 2007). Mutations in the huntingtin-interacting protein 1 (Hip-1) yeast homologue (S1a2p) have been associated with disrupted endocytosis (Raths et al. 1993). Hip-1 has been found to bind to clathrin, is localised to clathrin-coated vesicles and is probably involved in receptor-mediated endocytosis (Metzler et al. 2001, Waelter et al. 2001b). Hip-1 also directly interacts with Hap-1 (Waelter et al. 2001b). Htt interacts with SH3GL3, the human homologue of the mouse endophilin 3 gene which may be involved in endocytosis (Sittler et al. 1998). In spite of the associations with htt described above, a direct role of htt in endocytosis is still uncertain, as the effect of reducing htt levels on endocytosis has yet to be shown. There is some evidence that MT htt disrupts synaptic vesicular function. MT N-terminal htt binds synaptic vesicles and inhibits glutamate uptake *in vitro* (Li et al. 2000). Sun et al. (2001) described a reduced association between MT htt and post-synaptic density protein 95 (PSD-95). PSD-95 is involved in regulating the NMDA receptor and the GluR6 subunit of the kainate receptor. The weakening of the huntingtin/PSD-95 interaction may result in increased NMDA receptor signaling and excitotoxicity. It is also possible that this effect may underlie the association between a polymorphic marker in the GluR6 gene and the age of onset in HD (Rubinsztein et al. 1997).

The role of htt in axonal transport has been documented more extensively than

endocytosis, although the role of MT htt interrupting this process also remains unclear. Hap-1 was the first protein found to interact with htt (Li et al 1995). Hap-1 interacts with the p150 subunit of dynactin, and htt, p150 and Hap-1 all co-immunoprecipitate from rat brain homogenates (Engelender et al. 1997, Li et al. 1998). Dynactin interacts with the protein dynein and these are involved in the movement of vesicles along microtubules (Allan 1996). It has been proposed that Hap-1 and htt are involved in the formation of the dynein/dynactin complex during fast axonal transport. A reduction in endogenous htt or expression of MT htt inhibits movement of vesicles and mitochondria along neuronal projections (Trushina et al 2004, Caviston et al 2007) Defective retrograde transport can result in dystrophic neurite formation similar to those observed in HD brains (Sapp et al. 1999).

Vesicle associated membrane protein (VAMP) or synaptobrevin is a small integral membrane protein of secretory vesicles. VAMP is one of the SNARE proteins involved in formation of the SNARE complexes (see Duman et al 2003 for review of SNARE proteins). SNARE proteins are the key components of the molecular machinery that drives fusion of membranes in exocytosis and VAMP has been linked to neurite outgrowth (Martinez-Arca, et al 2000). Synaptophysin is a synaptic vesicle glycoprotein and is present in most neurons in the brain and spinal cord that participate in synaptic transmission. The precise function of the protein is unknown, although it interacts with VAMP (Gincel et al 2002). Direct evidence for the involvement of MT htt in disrupting axonal transport in vitro and in vivo, including mitochondrial trafficking, has been described by Trushina et al (2004).

1.10. The molecular pathogenesis of HD: Energetic defects in HD

1.10.1. The spectrum of mitochondrial function

Mitochondria are subcellular organelles in eukaryotic cells which have several roles in maintaining cellular homeostasis such as transient storage of intracellular calcium, fatty acid oxidation, the Krebs's cycle and iron metabolism (McBride et al. 2006 for review).

Mitochondria also have a key role in the regulation of apoptosis (Wang 2001 for review). Pro-apoptotic proteins cause mitochondrial swelling, through the formation of membrane pores, or by directly increasing the permeability of the mitochondrial membrane. This results in the release of apoptotic effector proteins, and the induction of apoptosis. Mitochondrial proteins known as SMACs (second mitochondria-derived activator of caspases) are released into the cytosol following an increase in mitochondrial membrane permeability. SMAC binds to inhibitor of apoptosis proteins (IAPs) and deactivates them, preventing the IAPs from inhibiting caspases. Cytochrome c is also released from mitochondria following the formation of the mitochondrial apoptosis-induced channel (MAC), in the outer mitochondrial membrane (Dejean et al 2006 for review). Once cytochrome c is released, it binds with Apaf-1 and ATP, which then bind to pro-caspase-9 to create a protein complex known as an "apoptosome". The apoptosome cleaves the pro-caspase 9, to its active form, caspase-9, which in turn activates the effector caspase-3 leading to cell death by apoptosis. One of the most important roles of mitochondria is to catalyse the phosphorylation of the majority of cellular adenosine diphosphate (ADP) to adenosine triphosphate (ATP). ATP is generated by oxidation of intermediates, such as NADH and FADH₂, via the process of oxidative phosphorylation (OXPHOS) within mitochondria (Fig. 1.3).

1.10.2. The mitochondrial respiratory chain

The mitochondrial respiratory chain consists of five multi-subunit protein complexes, which are located in the inner mitochondrial membrane, and two mobile electron carriers, cytochrome c and ubiquinone (Fig. 1.3). The respiratory chain generates a proton gradient across the inner mitochondrial membrane which drives ADP

Fig. 1.3.

phosphorylation by ATP synthase or complex V. The proton gradient is produced by the release of protons from complexes I, III and IV into the intermembranous space. The energy for this process is yielded from the transfer of electrons from NADH/FADH₂ through the protein complexes to the final electron acceptor, oxygen. Complex V couples the re-entry of protons into the mitochondrial matrix with the phosphorylation of ADP.

1.10.3. The mitochondrial hypothesis in neurodegeneration

Neurons require a high level of ATP production to maintain ionic homeostasis following the controlled flux of ions across the cell membrane during electrical signaling. Most of the ATP, utilised by Na⁺/K⁺ ATPase and Ca²⁺ ATPase in maintaining ionic homeostasis, is generated in mitochondria. The mitochondrial hypothesis in neurodegeneration postulates that defects in mitochondrial metabolism may lead to chronic mitochondrial dysfunction and eventually to depletion of cellular ATP. The entry into apoptosis may be linked to the competence of mitochondria to produce ATP and provide a mechanism by which chronic mitochondrial dysfunction could lead to neurodegeneration.

Mitochondrial dysfunction may be precipitated by exogenous and endogenous oxidative phosphorylation (OXPHOS) inhibitors or by mutations in nuclear or mitochondrial DNA-encoded proteins involved in OXPHOS or non-OXPHOS mitochondrial function

(Leonard et al. 2000a and b). This hypothesis is supported by evidence that disorders of mitochondrial function caused by mutations in mitochondrial proteins or the presence of mitochondrial inhibitors have a role in several neurodegenerative diseases.

1.10.4. Imaging energetic defects

PET studies are consistent with a defect in energy utilisation in HD striatum and cortex. Studies using ^{18}F -deoxyglucose positron emission tomography (PET) have demonstrated reductions in striatal and cortical but not thalamic or cerebellar regional utilisation of glucose in symptomatic HD patients (Kuhl et al. 1982, Leenders et al. 1986, Kuwert et al. 1990, Martin et al. 1992). Striatal reductions in utilisation of glucose have also been described in pre-symptomatic/chorea-free/"at risk" patients (Mazziotta et al. 1987, Grafton et al. 1990, Grafton et al. 1992, Kuwert et al. 1993).

Subsequently, nuclear magnetic resonance (NMR) spectroscopy has enabled more accurate determination of perfusion and metabolite changes in HD brains. ^1H NMR spectroscopy demonstrated elevated lactate levels in the occipital cortex (Jenkins et al. 1993), frontal cortex of symptomatic and some pre-symptomatic HD patients (Harms et al. 1997) and in the striatum of symptomatic and some pre-symptomatic HD patients (Jenkins et al. 1998). The levels of lactate correlated with the length of the CAG repeats and disease duration. The striatal levels of N-acetyl aspartate (NAA), a putative neuronal marker, was also reduced and choline (Ch), a putative glial marker, was elevated. This suggested that there was striatal neurodegeneration and gliosis in regions of elevated lactate formation and therefore a greater dependence on anaerobic metabolism (Jenkins et al. 1993, Davie et al. 1994, Martin et al. 1996, Sanchez-Pernaute, 1999). The absence of a reduction in the NAA/Ch ratio in pre-symptomatic HD patients in spite of an elevation in

lactate levels, suggested that defects in energy metabolism occurred before gross neuronal loss and before phenotypic expression (Harms et al. 1997). A widespread defect in energy metabolism in HD that is not confined to the nervous system has been demonstrated by a significant decrease in the phosphocreatine to inorganic phosphate ratio in symptomatic HD patient's skeletal muscle (Koroshetz et al. 1997, Lodi et al. 2000). Muscle ATP/(PCr + inorganic P) was significantly reduced in both symptomatic and pre-symptomatic HD patients. During recovery from exercise the maximum rate of ATP production (V_{\max}) in HD skeletal muscle was also reduced. The V_{\max} deficit divided by age also correlated with CAG repeat length. These results suggest that ^{31}P MRS of HD muscle may be utilised as a surrogate marker to study disease progression and response to therapy (Lodi et al. 2000). ^1H NMR spectroscopy of R6/2 mice brains has demonstrated a large reduction in NAA levels commencing at 6 weeks of age coincident with the onset of symptoms and the presence of intranuclear inclusions but in the absence of neuronal death (Jenkins et al. 2000). Further studies using the R6/2 mouse demonstrated that dietary supplementation with creatine enhanced brain creatine levels and reduced the reduction in NAA with time (Ferrante et al. 2000). Chronic systemic administration of 3-nitropropionic acid (3-NP), an irreversible inhibitor of succinate dehydrogenase (SDH) or complex II, reproduces most of the motor, cognitive and histopathological features of HD in primates, rodents and humans (Chyi et al 1999). Serial ^1H -NMR spectroscopy in 3-NP treated baboons (Dautry et al 1999) demonstrated a region-selective increase in lactate and progressive decrease in NAA, creatine and choline in the striatum in association with the formation of a lesion in the dorsolateral putamen on T2-weighted MRI. The selective decrease in NAA and creatine in the striatum suggested that there was preferential vulnerability of the striatum to impairment of mitochondrial function by 3-NP. It is postulated that the impairment of mitochondrial function in HD, especially complex II, may therefore cause selective neuronal loss within the basal ganglia in HD patients.

1.10.5. Mitochondrial respiratory chain function in HD tissues

The major studies of oxidative phosphorylation in HD are shown in Table 1.2. The more recent studies have demonstrated a consistent defect in mitochondrial complex II/III activity and to a lesser extent complex IV activity in regions associated with significant neurodegeneration. The abnormalities found in HD lymphoblasts and muscle suggested that a widespread peripheral, as well as CNS, mitochondrial respiratory chain defect occurs in HD.

Respiratory chain defect	Authors
↓ complex II	Stahl et al. 1974, Butterworth, 1975
↓ caudate cytochrome oxidase (COX) and cytochrome aa3 (complex IV subunit)	Brennan et al. 1985
↓ caudate complex II/III	Mann et al. 1990
↓ complex I in platelet mitochondria	Parker et al. 1990
↓ caudate complex II/III and IV	Gu et al. 1996, Tabrizi et al. 1999
↓ caudate and putamen complex II/III and putamen complex IV	Browne et al. 1997
↓ skeletal muscle complex I	Arenas et al. 1998
↑ apoptosis with cyanide (complex IV inhibitor) in HD lymphoblasts	Sawa et al. 1999

Table 1.2. The major studies of oxidative phosphorylation in HD

1.10.6. 3-nitropropionic acid (3-NP) and malonate: mitochondrial inhibitors

3-NP is a widely distributed plant and fungal neurotoxin that causes damage to the basal ganglia, hippocampus, spinal tracts and peripheral nerves in animals (Alexi et al. 1998). Reports from Northern China have suggested that 3-NP caused putaminal necrosis and delayed dystonia in children who have eaten mildewed sugar cane (Ludolph et al. 1991).

The accidental ingestion of 3-NP in humans caused nausea, vomiting, encephalopathy, coma and, if the patient survived, chorea and dystonia in the context of basal ganglia degeneration (Ludolph et al. 1991).

The intrastriatal administration of 3-NP to rats caused neuronal loss in the striatum (Beal et al. 1993a). This neuronal loss was ameliorated by decortication of the rats and suggested that the glutaminergic input from the corticostriatal pathway may be required to cause excitotoxic damage in 3-NP-mediated cell death (Beal et al. 1993a). NMDA receptor antagonists, such as MK-801, also block the toxic effects of 3-NP indicating that mitochondrial respiratory chain dysfunction and impaired energy metabolism may predispose to excitotoxic damage (Beal et al. 1993b). Malonate has also been injected intrastrially into rats to produce similar but milder lesions than were seen with 3-NP. These lesions were also reduced by glutamate antagonists suggesting an excitotoxic mechanism (Greene et al. 1995).

The chronic systemic administration of 3-NP in rats produced an animal model displaying lesions that closely resembled the neuropathological features of HD with selective loss of striatal medium spiny neurons. This suggested that the cell population that was most vulnerable in HD was sensitive to energy impairment (Beal et al. 1993a).

The systemic administration of 3-NP to primates caused spontaneous dystonia and dyskinesia accompanied by lesions in the caudate and putamen on MRI. The histopathology was similar to HD with depletion of calbindin-positive neurons, gliosis, sparing of NADPH-diaphorase neurons, and growth-related proliferative changes in dendrites of spiny neurons (Brouillet et al. 1995).

The addition of 3-NP to neuronal cell cultures resulted in a dose-dependent increase in neuronal death after 48 hours. Some neurons underwent rapid necrotic cell death while others exhibited a slow apoptotic cell death over 48 hours. The rapid necrosis was inhibited by MK-801, an allosteric inhibitor of the NMDA receptors, whereas the delayed mechanism was not inhibited (Pang et al. 1997) suggesting that 3-NP induced cell death was mediated by both excitotoxic and non-excitotoxic mechanisms.

1.10.7. Mitochondrial dysfunction and the R6/2 mouse

The R6/2 mouse exhibited progressive neurological disease from 2 months of age and both the light microscopic and ultrastructural pathology were very similar to those seen in HD brain. These neuropathological features occur approximately 4 weeks prior to a progressive movement disorder and muscle wasting, and 10 weeks before neuronal cell death in selected brain regions. This suggested that, in this model at least, neuronal dysfunction is responsible for the initial phenotype rather than cell death. A reduction in complex IV in the striatum and cerebral cortex of 12 week old R6/2 mice and a reduction in aconitase in the striatum have been described (Tabrizi et al. 2000). These changes were associated with increased immunostaining for inducible nitric oxide synthase (iNOS) and nitrotyrosine (a marker of increased peroxynitrate generation) in the mouse brains (Tabrizi et al. 2000). These results suggested that complex IV deficiency and elevated nitric oxide and superoxide radical generation precede neuronal death in the R6/2 mouse and may have contributed to subsequent neurodegeneration. An increase in the lesion size produced by 3-NP in the R6/2 mice and increased striatal 3,4-dihydroxybenzoic acid (a marker of ROS) also support a role for mitochondrial dysfunction and free radical damage in the R6/2 model (Bogdanov et al. 1998).

1.10.8. Mitochondrial respiratory chain dysfunction in cell models of HD

There have been four studies investigating mitochondrial respiratory chain activities in N-terminal htt cell models (Table 1.3). The first, by Wytttenbach et al. (2001), did not find any reduction in respiratory chain activities in an inducible PC12 “Tet-ON” cell model expressing exon 1 of htt with 21 and 72 CAGs for 18 hours. The MT clones did not demonstrate excess cell death at this time point but were found to have inclusions in 13% of cells. These findings were in contrast to Solans et al (2006) who described a reduced complex II/III:CS ratio, but not complex IV:CS ratio, 4-6 hours following induction of exon 1 of htt (90aa with respect to 21 CAGs) containing 101 CAGs in yeast. Aggregates formed in 50% of the cells 2 hours post-induction. The mitochondrial morphology and distribution were altered by the aggregates. The third model by Fukui et al. (2007) was a mifepristone-inducible model in human osteosarcoma 143B cells which expressed 25 or 103Q in exon 1 of htt. MT clones demonstrated a reduced complex II/III:CS ratio and reduced isolated complex III:CS ratio at day 3 post-induction. An increase in complex IV:CS ratio was also observed and complex I activity was not measured. The authors subsequently established a link between MT htt aggregation, reduced complex III activity, increased complex IV activity and reduced chymotrypsin-like activity of the proteasome, independently of free radical and ATP levels. They also found that complex III inhibitors, antimycin A (AA) and myxothiazol, selectively promoted the accumulation of htt aggregates. Inhibitors of other components of the respiratory chain did not have significant effects on the formation of htt aggregates and therefore the process was independent of the reduction in ATP. The fourth model used rat primary striatal cultures constitutively expressing the first 171aa of htt with 19Q or 82Q from a lentiviral vector (Benchoua et al. 2006). The authors described a reduction in complex II specific activity (corrected for protein) in the MT clones associated with a reduction in complex II levels

on Western blots by 6 weeks post-transfection. Cell death at 8 weeks was prevented by overexpression of complex II in the MT clones. Other complex activities were not investigated. The authors also described a downregulation of subunits of complex II in HD post-mortem striatum. These studies are summarised in Table 1.3. These models suggested that a reduction in complex II/III activity is a consistent abnormality following early expression of highly truncated and expanded MT htt (exon 1 with 82-103Q). The cell model by Wyttenbach et al. (2001) may not have demonstrated any abnormalities of mitochondrial function because of the relatively smaller polyQ and short induction time compared to the other three models (Table 1.3 and Section 6.4.3. for further discussion).

Study	Cell type	Induction	PolyQ (WT/MT)	Htt	Time/hrs	Complex CS ratios in MT clones
Wyttenbach et al. (2001)	PC12	Yes	23/74	Exon 1	18	No difference compared to WT
Solans et al. (2006)	Yeast	Yes	25/103	Exon 1	4-6	↓CxII/III CxIV normal
Fukui et al. (2007)	143B	Yes	25/103	Exon 1	72	↓CxII/III ↑Cx IV
Benchoua et al. (2006)	Primary rat striatal	No (Constitutive)	19/82	171aa	1008	↓CxII (specific activity)

Table 1.3. Summary of HD N-terminal cell models and MRC activities

1.10.9. Htt localisation to mitochondria

The direct association of htt with mitochondria was first described by Panov et al. (2002) who demonstrated by electron microscopy that N-terminal MT htt localised to mitochondria in the brain of an HD transgenic FL htt mouse model. Subsequently, in SH-SY5Y and clonal striatal cells established from HdhQ7 (WT) and HdhQ111 (MT)

homozygote mouse knock-in embryos, FL htt was present in the purified mitochondrial fraction and was associated with the outer membrane of mitochondria (Choo et al. 2004). Htt inclusions have been described in association with mitochondria in a rat transgenic model of HD (Petrasch-Parwez et al. 2007). The direct association of MT htt with mitochondria may have inhibited complex II/III activities in an N-terminal htt yeast cell model of HD (Solans et al. 2006). A further study suggested that MT htt disrupted the normal intracellular trafficking and distribution of mitochondria in primary cortical neurons (Chang et al. 2005). In the skeletal muscle of desmin-null mice, failure of locating mitochondria to the correct position within the cell impaired mitochondrial function (Milner et al. 2000). Solans et al. (2006) have proposed that misfolded or aggregated htt can disturb the network of actin cytoskeleton, which in turn leads to the alteration of mitochondrial distribution and an early reduction in complex II/III function. The role of the co-activator PGC-1 α in the pathogenesis of HD has provided an exciting link between abnormalities in mitochondrial biogenesis and respiration, with abnormalities in several transcription factors (McGill et al 2006 for review and Section 1.8.6).

1.10.10. The pathogenic role of free radicals in HD

Mitochondria form the majority of intracellular reactive oxygen species (ROS) which are constantly being produced as a byproduct of aerobic metabolism. Complex III and, to a lesser extent complex I, are major sites of generation of ROS (Beal et al. 1997). Mitochondrial production of free radicals increases when the electron transport chain is

inhibited or acquires mutations in mitochondrial DNA (Dykens et al. 1994, Dugan et al. 1995). An adaptive cellular response to increased free radicals is to up-regulate components of the anti-oxidant system such as superoxide dismutase (SOD) (Warner et al. 2004), catalase and reduced glutathione (GSH) (Bains et al. 1997). When these systems become overwhelmed and fail to control macromolecular oxidation, the system undergoes oxidative damage. Mitochondrial DNA (mtDNA) is especially susceptible to oxidative damage due to its location in the mitochondrial matrix next to the respiratory chain and its lack of histones (Browne et al. 1999). The paucity of mtDNA repair mechanisms was also suggested to predispose mtDNA to oxidative damage, although recent studies have suggested that mtDNA repair mechanisms are present (Larsen et al. 2005).

Several mechanisms by which oxidative stress may be produced in HD have been proposed. These include cellular energetic defects (section 1.10.4-8), nitric oxide dysregulation (section 1.10.11), excitotoxicity (section 1.10.11), an uncontrolled inflammatory response (Simmons et al. 2007), dopamine (Hattori et al. 1998, McLaughlin et al. 1998, Petersen et al. (2001) and heavy metal accumulation (Barzokis et al. 1999, Hilditch-Maguire et al 2000).

There is evidence in vivo and in vitro in HD of free radical damage to DNA (Butterworth et al. 1998, Ferrante et al. 1996, Browne et al. 1997, Alam et al. 2000), lipids (Tellez-Nagel et al. 1974, Ferrante et al. 1996, Greco et al. 2000, Ferrante et al. 1996, Perez-Severiano et al. 2000). and proteins (Ferrante et al. 1996, Browne et al. 1997, La Fontaine et al. 2000).

Aconitase is an iron-sulphur (FeS) containing enzyme that is involved in the Krebs's cycle and iron homeostasis. Aconitase activity is especially susceptible to inhibition by O_2^- and by the reaction product of O_2^- with NO , peroxynitrate ($ONOO^-$) (Hausladen, 1994, Gardner 1994, Patel 1996). Complexes II and III are also FeS-containing compounds and they are also susceptible to inhibition by free radicals. Aconitase deficiency has been found in HD caudate (92%), putamen (73%) and cortex (48%) but not cerebellum and this deficiency closely followed the pathology in HD (Tabrizi et al. 1999). The pattern of aconitase deficiency in HD is therefore consistent with ROS having a role in the pathogenesis of the disease.

1.10.11. Excitotoxicity and nitric oxide

Na^+/K^+ ATPase and Ca^{2+} ATPase are very active in neurons and are required to maintain the correct ionic gradients and membrane potential. Both of these ionic pumps utilise high levels of ATP. Mitochondrial oxidative phosphorylation produces most of the ATP in neurons. Impairment of respiratory chain function can cause a failure of maintenance of ionic gradients and partial depolarisation of the neuronal membrane. This has been shown to lead to a loss of the Mg^{2+} -dependent block of the NMDA Ca^{2+} channel and enable ambient levels of glutamate to activate the receptor (Beal 1992, Raymond 2003). This leads to elevated intracellular calcium and causes calcium entry into mitochondria which is linked with opening of the mitochondrial permeability transition pore and cell death (Rizzuto et al. 2001, Petersen et al. 1999). This unifying cellular mechanism, leading to apoptosis, has been called the "slow excitotoxic theory" (Albin and Greenamyre 1992, Beal 1992).

In support of an excitotoxic mechanism in HD, Seong et al (2005) have reported a relationship between the number of CAG repeats and mitochondrial ATP production. In striatal cells expressing htt, ATP production decreased as CAG repeats increased independently of whether the repeat number was in the WT or MT range. The decreased ATP/ADP ratio was linked to enhanced calcium influx through NMDA receptors. Impaired energy metabolism has been demonstrated to cause reduced ATP production, with a concomitant reduced mitochondrial membrane potential and a higher vulnerability to NMDA-mediated calcium influx and excitotoxicity (Novelli et al 1998, Fagni et al 1994). A potentiating effect of MT htt on NMDA receptor activity has been described as NMDA-evoked currents and NMDA-mediated calcium transients were significantly increased in striatal neurons from YAC72 transgenic mice compared with WT controls leading to increased excitotoxicity (Zeron et al 2002 and 2004). Further support for the excitotoxic hypothesis comes from evidence that the striatal injection of NMDA agonists, such as quinolinic acid, into rats and primates produced lesions that closely followed the neurochemical, neuropathological and behavioural changes seen in HD (Hantraye et al. 1990, Cull-Candy et al. 2001). Levine et al. (1999) have demonstrated increased sensitivity to NMDA receptor activation in HD mouse models. Zeron et al. (2001) demonstrated increased apoptosis in cell culture systems co-expressing glutamate receptor NR1A/NR2B with MT htt. Several components in the intracellular signaling pathways involved in excitotoxicity in HD have been found to be modulated by htt (Liu et al. 2000, Sun et al. 2001). MT htt may therefore directly increase the sensitivity of NMDA receptors to background levels of glutamate, causing greater calcium influx and excitotoxicity. Isolated mitochondria from HD mice demonstrated decreased membrane potential, depolarized at lower calcium loads compared with controls (Panov et al 2002) and were more sensitive to calcium-induced cytochrome c release (Choo et al 2004). These effects could be reproduced by incubating normal mitochondria with MT htt in

vitro and further support a role for MT htt inducing cell death by a possible excitotoxic mechanism. In spite of the evidence discussed above, there is limited data directly demonstrating excitotoxicity in HD apart from a study on HD post-mortem brain which showed that striatal neurons with high levels of NMDA receptor expression had increased degeneration (Albin et al. 1990).

Elevated intracellular calcium levels also cause an increase in activation of nitric oxide synthase and generation of nitric oxide (NO) and peroxynitrite. Tabrizi et al. (2000) demonstrated increased levels of inducible NOS immunostaining in 12 week old R6/2 mice (Section 1.10.7). The experimental data (Deckel 2001 for review) in HD patients and HD mice suggest that there is an overall reduction, and not an increase, in NOS activity and NO production in HD. Increased NOS activity in localised regions could still be occurring in the HD brain with a subsequent reduction following the death of neurons. Shin et al (2005) have further suggested a role for the impairment of glial uptake of glutamate in causing excitotoxicity in HD.

In summary, the slow progressive nature of HD could be explained by an excitotoxic mechanism involving a cycle of energy impairment and oxidative damage initiated by MT htt. The evidence for an excitotoxic mechanism in HD is mostly indirect and a definitive study demonstrating the proposed sequence of excitotoxic events has not been demonstrated.

1.10.12. Weight loss and HD

It has been a clinically observed but unexplained observation that HD patients suffer extreme weight loss in spite of an adequate calorific intake. Further studies have found that a higher BMI at presentation is associated with slower disease progression (Myers et

al. 1991). Weight loss was initially felt to be related to the severity of chorea but a subsequent study did not find a relationship between the severity of chorea and energy expenditure (Pratley et al. 2000). Patient's sedentary energy expenditure was proportionately related to the severity of the movement disorder, but total energy expenditure was the same as controls because HD patients tended not to take part in as much voluntary physical activity. It therefore remains uncertain whether the weight loss observed in HD is due to a generalised metabolic defect or other causes as yet to be elucidated.

1.10.13. Treatment of mitochondrial dysfunction in HD

Increasing brain levels of ubiquinone (co-enzyme Q₁₀) may ameliorate some of the energetic defects that have been demonstrated and theoretically delay neurodegeneration in HD. Ubiquinone has been demonstrated to protect cultured neurons against glutamate toxicity (Favitt et al. 1992). Ubiquinone has anti-oxidant properties (Favitt et al. 1992) and protects against malonate and 3-NP-induced striatal lesions in rats (Beal et al. 1994). The oral administration of 600mg/day of ubiquinone for 30 months significantly reduced occipital cortex lactate levels as measured by ¹H MRS in 18 symptomatic HD patients. The levels of lactate returned to pre-treatment values when ubiquinone was stopped and therefore this supported a treatment-related effect (Koroshetz et al. 1997). A randomised placebo-controlled trial of 300mg twice daily of ubiquinone and 200mg three times daily of remacemide (a noncompetitive N-Methyl-D-Aspartate (NMDA) receptor antagonist) has been performed (Huntington's Disease Study Group 2001). The primary measure of efficacy was the change in total functional capacity (TFC) of the UHDRS between baseline and following 30 months of treatment or placebo. Neither drug significantly altered the decline in TFC. There was a trend towards slower disease progression (13%

decline in TFC) with ubiquinone but remacemide had no clinical benefit. Unfortunately, the trial was designed to identify an approximate 35-40% slowing in functional decline and so smaller benefits would have been missed (Huntington's Disease Study Group 2001). A transgenic mouse model study with the R6/2 and N171-82Q mice, has demonstrated a significant benefit from remacemide and ubiquinone on the phenotype and pathology of the mice when treatment was commenced on day 21 following birth (Ferrante et al. 2002). There was an approximately 32 and 17% increase in survival in the R6/2 and N171-82Q mice respectively. Treatment of HD patients may therefore need to occur sooner and for longer before a clinical effect can be observed.

Creatine has been found to have a protective effect in the R6/2 mouse. Dietary creatine improved survival, slowed the development of brain atrophy and delayed degeneration of striatal neurons and the formation of intranuclear inclusions. The onset of diabetes was also delayed. NMR in these mice demonstrated delayed decreases in NAA and elevated brain creatine concentrations (Matthews et al. 1998, Ferrante et al. 2000). The mechanism causing improvement may involve increasing intracellular energy reserves in order to clear misfolded and/or aggregated MT htt. Subsequently, Tabrizi et al (2005) have described clinical benefit to some HD patients taking 10g creatine per day. The results of the CREST-HD trial (a large placebo-controlled double-blind study of 8g/day creatine in HD) is awaited.

In summary, there is substantial evidence from imaging, post-mortem, animal and in vitro studies of a metabolic defect in association with MT htt expression and a reduction in mitochondrial respiratory chain activity. The mechanism by which this occurs may involve direct inhibition of the mitochondria by MT htt or by an indirect effect from other pathological processes such as alter mitochondrial biogenesis, excess free radical production and excitotoxicity. The precise molecular mechanisms involved in causing the

metabolic disturbance in HD and the timing of this disturbance in relationship to cell dysfunction and death remain undetermined.

1.11. The molecular pathogenesis of HD: The polyglutamine diseases

The polyglutamine diseases include HD, spinal bulbar muscular atrophy (SBMA) (Lieberman and Fischbeck 2000, La Spada et al 1991), dentatorubralpallidoluysian atrophy (DRPLA) (Tsuji 2000) and seven of the spinocerebellar ataxias (SCAs). They are characterised by CAG triplet repeat expansions and typically cause a progressive neurological phenotype with onset in middle age (Table 1.4). All the polyglutamine diseases are autosomal dominant except for SBMA which is X-linked, and they all demonstrate anticipation. There is heterogeneity in the clinical phenotype and the molecular pathogenesis of these diseases but there are also many similar features which have given insights into unifying pathogenic mechanisms in the polyglutamine diseases.

All polyglutamine diseases demonstrate an inverse relationship between age of clinical onset and the CAG repeat length (Gusella and MacDonald 2000). The correlation is not absolute, and for any repeat length there is a wide variation in the age of onset suggesting other epigenetic and environmental factors are involved (MacDonald et al. 1999, Georgiou et al. 1999).

Disease	Protein	Normal Repeats	Mutant Repeats	Clinical Features	Neuropathology	Inclusions
HD	Huntingtin	6-39	36->200	Chorea, dementia	CS, CTX	N/C
SCA1	Ataxin 1	6-44	39-83	Ataxia, ophthalmoplegia, pyramidal signs	CBL, BSMN	N
SCA2	Ataxin 2	13-33	32->200	Ataxia, ophthalmoplegia, neuropathy	CBL, BSMN	N/C
SCA3	Ataxin 3	3-40	54-89	Ataxia, extra-pyramidal, amyotrophy	CBL, AHC, SN, STN, GP, BSMN	N
SCA6	CACNA1A	4-19	20-33	Ataxia	CBL	N/C
SCA7	Ataxin 7	4-35	37-306	Ataxia and macular dystrophy	CBL, retina	N
SCA12	PPP2R2B	<29	66-78	Tremor with ataxia	Unknown	Unknown
SCA17	TBP	25-44	43-63	Ataxia, psychiatric, extra-pyramidal	CS, CTX, THL and CBL	N
SBMA	Androgen Receptor	9-33	38-65	Amyotrophy, hypogonadism	AHC, BSMN, DRG	N
DRPLA	Atrophin 1	3-35	49-88	Ataxia, chorea, epilepsy, dementia	CS, CBL, CTX, STN, SN,	N

Table 1.4. The Polyglutamine diseases. N=nuclear, C=cytoplasmic. CS Corpus Striatum. SN Substantia Nigra. STN Subthalamic Nucleus. AHC Anterior Horn Cell. BSMN brainstem motor nuclei. DRG Dorsal Root Ganglia. GP Globus Pallidus. CTX Cerebral Cortex. CBL cerebellum THL thalamus.

Three of the ten polyglutamine diseases have protein products of known function. The androgen receptor in SBMA, the α_{1A} voltage-dependent calcium channel (CACNA1A) in

SCA6 and TATA-binding protein (TBP) in SCA 17. The protein products of the other polyglutamine diseases have unknown function and apart from the CAG repeat sequence have unrelated sequences.

The polyglutamine proteins are expressed in a wide variety of neuronal and peripheral tissues even though the pathology is often largely confined to the CNS. The protein products localise to the nucleus and cytoplasm, although TBP is found exclusively in the nucleus and CACNA1A and ataxin 2 are mainly found in the cytoplasm. The major sites of neuronal loss are summarised in Table 1.4. In common with HD, larger repeat numbers are associated with more widespread and overlapping neurodegeneration which suggests common pathogenic mechanisms. Ubiquitinated nuclear polyglutamine aggregates have been described in all polyglutamine diseases. The aggregates in HD, DRPLA, SBMA, SCA 2 and SCA 7 are associated with possible cleavage products but not in SCA 1 and 3 (Servadio et al. 1995 and Perez et al. 1999). SCA 17 can be phenotypically similar to HD with patients developing dementia, and involuntary movements, including chorea and dystonia (Wild et al. 2007 for review of HD phenocopies). The association of transcriptional changes related to TATA-binding protein (TBP) in HD and the CAG expansion within TBP in SCA 17 has suggested a possible molecular link to transcriptional dysregulation in neurodegeneration, as well as the clinical link with chorea and dementia. (Schaffer et al. 2004, for a review of polyglutamine diseases, see Chapter 14 in "Huntington's Disease" eds. Bates, Harper, Jones 3rd Ed).

1.12. The molecular pathogenesis of HD: "loss" or "gain" of htt function

HD is a dominantly inherited disease and haploinsufficiency or a “dominant negative” effect would result in a loss of function in WT htt (reviewed by Cattaneo et al. 2001). A more probable third mechanism suggests that a toxic gain of function of MT htt causes the majority of neuronal dysfunction and death in HD.

Haploinsufficiency occurs when a single copy of a gene produces insufficient protein to enable cellular function or survival. This appears unlikely in HD, as there are reports of loss of the relevant part of chromosome 4p without the development of HD (Ambrose et al. 1994). Nullizygous WT HD mice are embryonic lethal but heterozygous WT HD mice do not show any signs of HD which suggests that haploinsufficiency does not a significant contribution on neurodegeneration in HD.

A “dominant negative” effect occurs when a MT protein affects the normal function of the WT protein in a deleterious manner for the cell. The sequestration of WT htt into aggregates resulting in a reduction in WT htt and its physiological effects may occur although there is little experimental evidence for this happening *in vitro* or *in vivo* (Section 1.7.5). BDNF is an important neuronal survival factor generated in the cortical neurons and released into the striatum (Canals et al. 2001). Zuccato et al. (2001) demonstrated up-regulation of brain-derived neurotrophic factor (BDNF) in cortical neurons mediated by WT htt. When FL MT htt was expressed in conditionally immortalized CNS cell lines, there was reduced BDNF expression. A mouse model carrying a transgene of FL MT htt (72CAGs) also demonstrated a 50% reduction in cortical BDNF and similar results were observed in HD post-mortem brain (Zuccato et al. 2001 and Section 1.8.5.). The expression of MT htt therefore appears to inhibit the pro-survival effects of WT htt on BDNF expression.

Most current evidence suggests a toxic gain of function for MT htt based on evidence in transgenic mice and cellular models that polyglutamine stretches alone (Ikeda et al. 1996), with N-terminal MT htt (Mangiarini et al. 1996) or in an unrelated protein (Ordway et al. 1997) cause neurodegeneration. This suggests that the protein context of MT polyQ may alter the specific sites and rate of neurodegeneration but loss of function of the protein context of MT polyQ is not the main determinant of triggering neurodegeneration.

The possibility remains that a combination of haploinsufficiency, a dominant negative effect and a toxic gain of function of htt, may contribute to neuronal cell loss in HD.

1.13. Cellular models of Huntington's Disease

There have been two main types of cellular models of Huntington's disease. The first, and more commonly used, are transiently transfected cell lines. The advantages of these models are that the cells have not been exposed to previous ectopic protein and the process of cloning a stably transfected cell line can be avoided. Transient transfections also enable the use of primary cultures and enable high levels of protein expression to be achieved. There is often a lack of consistency in the proportion of the cells transfected and variable levels of expression. This makes controlling for expression difficult when whole populations of cells are investigated.

The second type of model involves the stable transfection of htt constructs. This has the advantage that prolonged exposure of htt can be investigated and repeated transfections are not needed. There is also greater predictability of construct expression levels. Inducible stable transfections add another level of control of expression but require an

inducing agent which can often be toxic. Constitutive stable transfections do not require an inducing agent but cells are continually exposed to construct expression throughout cloning and passage which may select against those cells most vulnerable to the construct. Therefore there is no ideal cell model and the type of model chosen depends on the issue being investigated.

1.13.1. Stably transfected cell models

Table 1.5 A and B. summarises the known stably-transfected (A) inducible and (B) constitutively expressing htt cell models.

Inducible HD cell models

The first stably transfected cell model of HD was published by Lunkes and Mandel (1998) using a mouse/rat neuroblastoma/glioma hybrid cell line (NG108-15). It was an inducible cell model expressing 15, 73 and 116 CAG repeats in FL, N-terminal 502 aa and 80 aa. human htt (size of htt excluding CAG repeats). The model used a tetracycline-inducible promoter but the authors did not comment on whether they saw background breakthrough expression prior to induction. The authors demonstrated the formation of nuclear and cytoplasmic inclusions which formed faster with greater truncation of htt and increased CAG repeat length. They also demonstrated a positive correlation between apoptosis and inclusion load and cell death by day 6 post-induction with 80aa, day 12 with 502 aa. and day 16 with FL htt. The formation of an approximately 98kDa fragment by day 10 following induction was consistent with

Table 1.5A

Table 1.5B

cleavage at the proposed caspase 3 site. This study confirmed that truncated htt and longer polyQ form inclusions more rapidly and that the appearance of inclusions coincided with

cell death but did not prove that the inclusions were the cause of cell death.

The second stably transfected model used an inducible Ecdysone/pIND system in a mouse N2a cell line with exon 1 of human htt containing 16, 60 or 150 CAG repeats (Wang et al 1999, Jana et al. 2001). Following two days induction with ponasterone A (1 μ M) and simultaneous differentiation with dbcAMP, approximately 7% of 60Q cells and 85% of 150Q cells demonstrated cytoplasmic aggregates. The rate of aggregate formation and cell death was proportional to the length of the CAG repeat. The proteasomal 20S core catalytic component was redistributed to polyglutamine-containing aggregates in 65% of 150 CAG cells. The proteasomal inhibitor, lactacystin, dramatically increased the rate of aggregate formation with 60 glutamine repeats, but had very little influence on aggregate formation with 150 glutamine repeats. WT and MT htt were degraded by the proteasome, but the rate of degradation was inversely proportional to the CAG repeat length. The shift of the proteasomal components to the aggregates, as well as the comparatively slower degradation of htt with longer polyglutamines, decreased the availability of the proteasome for degrading other key target proteins, such as p53. This altered proteasomal function was associated with disrupted mitochondrial membrane potential, released cytochrome c from mitochondria into the cytosol and activated caspase-9- and caspase-3-like proteases. These results suggested that the impaired proteasomal function was an important step in the pathogenesis of HD. Wang et al. (1999) used the same model as Jana et al (2001) and found increased cell death in 60 and 150Q cells after 4 days induction with evidence of apoptosis and caspase activation suggesting that apoptosis may occur in HD.

The third stably transfected inducible cell model was in HEK 293 cells using the Tet-“off” system and CMV promotor (Waelter et al. 2001a). The authors’ constructs contained human htt exon 1 with 20, 51 or 83Q. The 51Q and 83Q clones formed

aggresome-like perinuclear inclusions following withdrawal of doxycycline for 3 days. These structures contained aggregated, ubiquitinated htt exon 1 protein. Inclusion bodies with truncated htt protein were detected by anti-HD1 antibody (raised to the first 222 aa. of htt) and formed at centrosomes. The inhibition of proteasome activity by lactacystin resulted in a two-fold increase in the amount of ubiquitinated, SDS-resistant aggregates, indicating that inclusion bodies accumulated when the capacity of the ubiquitin–proteasome system to degrade aggregation-prone htt protein was exhausted or inhibited. Immunofluorescence and electron microscopy with immunogold labeling revealed that the 20S, 19S, and 11S subunits of the 26S proteasome, the molecular chaperones BiP/GRP78, Hsp70, and Hsp40, as well as the RNA-binding protein TIA-1, the potential chaperone 14–3–3, and α -synuclein colocalised with the perinuclear inclusions (Waelter et al. 2001a). Inclusion body formation was associated with cell toxicity and dramatic ultrastructural changes such as indentations and disruption of the nuclear envelope. Concentrations of mitochondria around the inclusions and cytoplasmic vacuolation were also observed.

These findings supported the hypothesis that the ATP-dependent ubiquitin–proteasome system is involved in the accumulation of htt inclusions and other proteins and that the accumulations form in a perinuclear localisation similar to collections of mutant cystic fibrosis transmembrane conductance regulator (CFTR) protein observed in cystic fibrosis. Wigley et al. (1999) have demonstrated that the centrosome, or a closely associated structure, may play a functional role in the degradation of misfolded proteins in mammalian cells. Using immunofluorescence microscopy, they identified a specific structure in the centrosomal region in which components of the 26S proteasome, as well as ubiquitin and heat shock proteins, were concentrated under basal conditions. These perinuclear collections have been named “aggresomes” (Johnston et al.1998) and may be

part of a generalised response of the cell following failure of misfolded/damaged proteins.

Wytttenbach et al (2001) published the fourth inducible htt cell model using differentiated and mitotic PC12 cells with Tet-“On” system expressing exon 1 of human htt containing 23,43, 53 and 74Q. Components of the UPS and HSP40/70 were described in association with htt inclusions which formed in the nucleus in differentiated cells. Using the TUNEL method to assess apoptosis, they found 7% cell death in the 53Q and 15-20% cell death in 74Q after 6 days post-induction. Cell death was reduced with the broad caspase inhibitor zVAD-fmk in mitotic cells in spite of similar levels of inclusions. The 53 and 74Q clones demonstrated greater cell loss at day 6 post-differentiation than in mitotic cells. There was also loss of neurite outgrowth in 74Q cells post-differentiation. There was no effect of MT htt on mitochondrial respiratory chain activities, but there was impaired CRE mediated transcription after 18 hours of induction.

Sipione et al. (2002) and Seo et al. (2007) used a primary rat striatal Tet”On” cell model expressing 548aa of htt with 26,67, 105 and 118Q. Sipione et al. (2002) found no htt aggregates or cell death by 36 hours post-induction. Gene expression profiles demonstrated changes in cell signalling, transcription, lipid metabolism and vesicle trafficking genes within 12 hours of MT htt induction. The findings of Seo et al. (2007) using the same model are described in Section 1.6.3.

Sugars et al. (2004) developed a PC12 Tet”On” cell model expressing exon 1 or FL htt with 17/136Q which developed nuclear and cytoplasmic htt inclusions. The main findings were of a down regulation of CRE and RARE (retinoic acid responsive element)-regulated genes and up regulation of NF-κB pathways in the MT exon 1 htt model and a down-regulation of the CRE pathway in the FL model. There was also a reduction in htt

inclusions and cell death with co-expression of CREB in the models. This study confirmed the role of transcriptional dysregulation in HD and suggested that reversal of the transcriptional abnormalities is a potential therapeutic strategy.

The models developed by Benchoua et al. (2006), Solans et al (2006), and Fukui et al. (2007) investigated the role of mitochondrial dysfunction in HD cell models and are discussed in detail in Section 1.10.8.

Constitutive HD cell models

The first published stably transfected constitutive HD cell model used the rat PC12 cell line with a CMV promoter, producing constitutive expression of human htt exon 1, and either 20 or 150 CAGs (Li, S.H. et al. 1999). One of the main findings was that the 20Q cells expressed htt diffusely in the cytoplasm in contrast to the 150Q cells which demonstrated diffuse staining in the nucleus. Less than 3% of the 150Q cells demonstrated nuclear aggregates and the authors suggested this may have been due to cell division preventing aggregate formation. The 150Q model also demonstrated poor neurite development in response differentiation with nerve growth factor (NGF) and was more susceptible to staurosporine-induced apoptosis than the 20Q model. Differential display PCR and expression studies showed that cells expressing 150Q had altered expression of multiple genes including a reduction in TrkA/NGF and p75NTR (subunits of the NGF receptor) and Hap-1. This suggested that the lack of response to NGF may have been due to reduced NGF receptor expression and impaired intra-neuronal transport which has been linked with Hap-1 (Section 1.9.). Their conclusion was that nuclear MT htt induced multiple cellular defects by interfering with gene expression even in the absence of aggregation (Li, S-H. et al 1999).

Chun et al (2001 and 2002) characterised a constitutively expressing 63aa htt model with 18/82Q in SH-SY5Y cells. The authors described that tissue transglutaminase was not involved in htt aggregate formation and that caspase 3 activity was increased but not associated with htt aggregates.

Benchoua et al. (2006) described a constitutive cell model which investigated the role of mitochondrial function in HD and is described in more detail in Section 1.10.8.

Ye et al. (2008) characterised a differentiated N2a cell model constitutively expressing exon 1 htt with 20/150Q. 150Q cells had decreased viability and were more susceptible to apoptotic stimulation in the absence of inclusion formation. The 150Q cells also had poor neuritic out growth following differentiation.

1.13.2. Transiently transfected cell models

Several transiently-transfected models have demonstrated time and CAG repeat length-dependent formation of htt inclusions (Cooper et al. 1998, Saudou et al. 1998, Kim et al. 1999). They have also demonstrated that nuclear localisation of MT htt caused an increase in cell toxicity (Saudou et al. 1998 Cooper et al. 1998), increased susceptibility to apoptosis (Cooper et al. 1998, Kim et al. 1999) and activation of caspase 8 (Sanchez et al. 1999). The protective effect of WT htt (Ho et al 2001) and caspase inhibitors (Kim et al 1999, Wellington et al. 2000) on cell death has also been described. The co-expression of the NMDA glutamate receptor subtype NR2B with N-terminal MT htt (138Q in exon 1) in HEK 293 cells produced greater cell death in response to NMDA (Zeron et al. 2001) suggesting a possible excitotoxic mechanism for cell death in HD.

1.14. The investigation of the molecular pathogenesis of HD

There are several important issues in the molecular pathogenesis of HD that remain poorly understood. Some of these issues, and the questions that still surround them, will be summarised as they formed the main areas of investigation in the current thesis.

1.14.1. CAG repeat size

The size of the CAG repeat in HD is associated with an earlier onset of disease, more severe neuropathological findings, imaging abnormalities and clinical phenotype (Brinkman et al 1997, Penney et al. 1997, Jenkins et al. 1998). The CAG repeat length accounts for between 47-73% of the variance in the age of onset of symptoms (Brinkman et al 1997, Squitieri et al. 2000). There is less evidence for a relationship between the rate of progression of disease and psychiatric features, although psychiatric features correlate within each affected family (Brandt et al. 1996, Weigell-Weber et al. 1996, Tsuang, D. et al. 1998). Foroud et al. (1995), Siemers et al (1996) and Jason et al (1997) have found a correlation between CAG repeat length with subtle cognitive and motor dysfunction in presymptomatic HD patients suggesting that CAG repeat length may determine early clinical features before gross motor symptoms develop. It is well established that the greater the number of CAG repeats, the more likely MT htt is to aggregate in non-cell and cell-based *in vitro* models and in transgenic mouse models (Section 1.7). The molecular basis for the pathogenic threshold of CAG repeat number and the molecular effects of a pathological number of CAG repeats on the processing and function of MT htt remain are less well understood.

1.14.2. Full length versus N-terminal htt: processing of htt

One of the most important aspects of the molecular pathogenesis of HD is the potential role of processing of FL-htt to a toxic N-terminal fragment (Section 1.6). Htt inclusions have only been found to contain N-terminal htt epitopes in mouse models, including the R6/2 mouse (Mangiarini et al. 1996), and in HD post-mortem brain (DiFiglia et al. 1997). There is some evidence that the UPS, caspases/calpains as well as other proteases are involved in processing htt to an N-terminal fragment (Section 1.6.). The exact size of the toxic N-terminal fragment in HD remains uncertain. WT htt may also undergo N-terminal truncation which raises the questions as to how the effects of N terminal WT and MT htt differ, are the N-terminal fragments identical in length except for the CAG repeats and is the N-terminal MT fragment the toxic molecule in HD?

1.14.3. Sub-cellular localisation of htt and htt aggregates

The sub-cellular localisation of WT and MT htt has been described predominantly in the cytoplasm but also in the nucleus and in a perinuclear distribution (Section 1.5.3.). MT htt N-terminal aggregates form mostly in the neuropil and cytoplasm, and less often in the nucleus in HD brain (Section 1.7.1), in comparison to HD mice, such as the R6/2, and inducible cell models of HD (Table 1.5), in which nuclear aggregates are common (Section 1.7.3). The transfer of N-terminal or FL-MT htt into the nucleus may represent an important step in the development of MT htt toxicity. The relative contribution of nuclear and cytoplasmic htt aggregates to the pathogenesis of HD is unknown (Martindale et al 1998, Hackam et al. 1999). In cell culture models, nuclear localization of htt is associated with greater toxicity (Peters et al. 1999, Saudou et al. 1998). MT htt localised to the nucleus may disrupt the function and/or transport of transcription factors (Nucifora

et al. 2001) and alter the normal transcriptional profile of neurons (Luthi-Carter et al. 2000, and 2002). In addition, in most other polyglutamine diseases, the predominant pathological finding is of MT protein and inclusions only in the nucleus, suggesting that nuclear localisation may be important in the pathogenesis of triplet repeat disorders (Section 1.11 and Gusella et al. 2000). Schilling et al. (2004) described a transgenic mouse model with the first 171 aa. of htt containing 82 CAG repeats with a nuclear localising signal (NLS). MT htt was only detected in the nucleus and the neurological phenotype of the mouse was similar to a mouse model without the NLS. This suggested that cytoplasmic MT htt was not necessary for toxicity. Several in vitro cell models of HD have demonstrated that by blocking the nuclear accumulation of MT htt by fusing it with a nuclear export signal (NES), neurotoxicity is significantly reduced which further supports the importance of subcellular location of MT htt for toxicity (Saudou et al. 1998, Peters et al. 1999, Benn et al. 2005). Subsequently, Steffan et al. (2004) and Rockabrand et al. (2007) demonstrated that the first 17aa of htt act as a strong cytoplasmic retention signal, controlled the mitochondrial localisation of htt and promoted the association of htt with the endoplasmic reticulum (ER) and Golgi. It is postulated that loss of the nuclear export signal (NES) function of the first 17aa. by an expanded polyglutamine tract may cause accumulation of nuclear htt and toxicity.

In contrast, nuclear localisation of MT htt may be an epiphenomena of expanded CAG repeats and not necessarily the main toxic event in HD. Cytoplasmic aggregates are described in other polyglutamines disease such as micro-aggregates in SCA2 (Huynh et al. 2002) and equal numbers of nuclear and cytoplasmic aggregates in SCA6 (Ishikawa et al 2001). Several studies have demonstrated that cytoplasmic MT htt can inhibit synaptic function and glutamate release, disrupt the axonal transport of protein and vesicles, and impair mitochondrial and proteasome function (Li, J.Y. et al 2003, Li, H et al 2003,

Bence et al. 2001, and Petrasch-Parwez et al. 2007). The relative roles of cytoplasmic compared to nuclear toxicity of MT htt therefore remains to be fully investigated.

1.14.4. Energetic defects in HD

Energetic defects have been described in HD, before the gene was cloned, using ¹⁸F-deoxyglucose PET (Section 1.10.4). Subsequently, defects in mitochondrial respiratory chain function have been described in HD post-mortem brain, as well as in animal and cell models of HD (Section 1.10.5-7). The association of htt with mitochondria has recently been described. A direct role for MT htt in causing mitochondrial dysfunction through direct inhibition of the MRC, loss of calcium homeostasis, free radical generation and impaired mitochondrial biogenesis and trafficking have been postulated but the precise mechanism by which MT htt causes mitochondrial impairment remains elusive (Section 6.9.2 and 1.10.8-12). The timing of mitochondrial dysfunction in the cascade of events leading to neurodegeneration is also poorly understood. The impairment of mitochondrial function during neurodegeneration is probably inevitable at some point in cell degeneration, but whether it is a primary initiating event or a secondary, albeit possibly still important, downstream secondary mechanism requires investigation.

1.14.5. Proteasome dysfunction and chaperones

The proteasome and molecular chaperone systems in cells are integral to the metabolism of folded and misfolded proteins. An imbalance in this system can lead to the accumulation of potentially toxic proteins (Section 1.6.3-4). There is some evidence that MT htt may directly impair proteasome function, or sequester components of the proteasome system within htt aggregates causing impairment of proteasome function. An

alternative hypothesis states that MT htt undergoes proteasomal degradation leading to the production of toxic N-terminal htt fragments (Section 1.6.3-4), although there is little evidence for this mechanism.

1.14.6. Aims of investigation

This thesis aims to examine the molecular mechanisms involved in the pathogenesis of HD using two distinct in vitro cell models and HD muscle tissue. The cell models enabled the investigation of the processing of WT and MT htt in non-neuronal mitotic and neuronal mitotic and post-mitotic cells. Subsequently, the cell models enabled the investigation of the relationship of CAG repeat length, size of htt, cell background and length of expression of MT htt, to mitochondrial function, proteasomal function, inclusion formation, htt localisation, free radical production and sensitivity to mitochondrial, free radical and proteasomal toxins. As a parallel study, mitochondrial function in HD muscle biopsies was assessed and related to clinical parameters including the Unified Huntington Disease Rating Scale (UHDRS) and CAG repeat length.

CHAPTER 2

Materials and methods

2.1. Materials

2.1.1. Tissue culture and human tissue handling equipment

ICN-Flow Automatic CO₂ Incubator model 320 (ICN-Flow, Ltd, High Wycombe, Bucks, UK); Gelair (ICN Flow) for tissue culture; Class I ICN Flow Hood.

2.1.2. Centrifuges

All centrifugation steps used; Beckman GPR bench-top centrifuge with GH-3.7 swing-out rotor (Beckman Ltd., High Wycombe, Bucks, UK), Kontron T-124 high speed centrifuge with 8.24 (8x50 ml) fixed angle rotor (Kontron Instruments, Watford, Herts, UK), Biofuge 13 with 18x1.5ml fixed angle rotor (Heraeus, Germany), Fresco Microcentrifuge (Heraeus).

2.1.3. Molecular biology apparatus

Hybaid mini hybridization oven (Hybaid Ltd., Middlesex, UK), Perkin-Elmer 2400 thermal cycler (Perkin-Elmer, Warrington, Cheshire, UK), Infors-HT orbital shaker (Infors Ltd., Crewe, UK), G25 Incubator-shaker (New Brunswick Scientific Co. Inc. Edison, NJ, USA).

2.1.4. Electrophoresis apparatus

BioRad 200/2.0 constant voltage power packs (BioRad Lab. Ltd., Hemel Hempstead, Herts, UK), BRL horizontal system for agarose gel electrophoresis (Bethesda Research

Lab., Life Tech Inc. Gaithersburg, MD, USA), the NuPAGE electrophoresis systems using the pre-cast 4-12% acrylamide Bis-Tris and 3-8% acrylamide Tris-acetate Novex gels were used for polyacrylamide gel electrophoresis (Invitrogen Ltd., Paisley, UK), UV transilluminator (GRI Ltd., Dunmow, Essex, UK) and Polaroid camera.

2.1.5. Cell and tissue homogenisers

Uni-form 5ml and 10ml glass/Teflon homogenizer (Jencons Ltd., Leighton Buzzard, Bedfordshire, UK), 5ml glass homogenizer and Glass-Col stirrer (CamLam Ltd., Cambridge, UK)

2.1.6. Spectrophotometers

Hitachi U-3210 (Hitachi Scientific Instruments, Wokingham, Berks, UK) and Kontron Uvikon 940 (Kontron Instruments, Watford, Herts, UK) split beam spectrophotometers.

2.1.7. Microscopy and photography

All microscopy for immunohistochemistry, immunocytochemistry and immunofluorescence was performed using the Zeiss axiophot microscope (Carl Zeiss Microscope Division, Oberkochen, Germany) with Kodak T64 film for light microscopy and Kodak Ektachrome 400 for fluorescence microscopy. All confocal microscopy was performed using the MRC 600 microscope (BioRad Microscience division, Herts, UK).

2.1.8. Chemicals

Unless otherwise stated all chemicals were purchased from Sigma, Poole, Dorset, UK or Merck Ltd. Dagenham, Essex, UK.

2.2. Cell culture

2.2.1. Cell culture materials

All chemicals and plates were from Life Technologies (Paisley, UK) except DMSO and pyruvate which were from Sigma Chemical Co. (Poole, UK) and 100mm plates which were from NUNC (Roskilde, Denmark)..

2.2.2. Cells and growth conditions

2.2.2.1. EcR HEK 293 cell line (Invitrogen, UK)

The EcR HEK 293 cell line are transformed human kidney epithelial cells which have been stably transfected with the pVgRxR plasmid (Invitrogen, UK) which renders them zeocin-resistant at a zeocin concentration of 400 μ g/ml. HEK 293 cells were grown in standard growth medium which consisted of Dulbecco's modified Eagles medium (DMEM) containing high (4.5g/litre) or low concentrations of glucose (1g/litre). Glutamine (5mM), penicillin 50units/ml, streptomycin 50mg/l, 10% v/v fetal calf serum, 0.2mM uridine, and 1mM sodium pyruvate were added.

2.2.2.2. SH-SY5Y cells

These were obtained from the European Collection of Cell Cultures (ECACC) ECACC No. 94030304. The cells were originally made from a sub-clone of a human bone marrow biopsy-derived line SK-N-SH (ECACC No. 86012802). The SH-SY5Y cells have a neuroblastoma morphology and can convert glutamate to GABA (glutamic acid decarboxylase), tyrosine to dopamine (tyrosine hydroxylase) and dopamine to noradrenaline (dopamine- β -hydroxylase) (Biedler et al. 1978). SH-SY5Y cells were grown in DMEM/F12 50/50 mix containing glutamine (5mM), penicillin 50units/ml, streptomycin 50mg/l, 10% v/v fetal calf serum, 0.2mM uridine, and 1mM sodium pyruvate.

2.2.3. Cell culture maintenance and harvesting

Cells were grown on 100mm cell culture dishes (NUNC, Denmark). Standard growth medium was changed every 48-72 hours. Cells were harvested, when approximately 80% confluent, by first washing in phosphate buffered saline (PBS, Sigma UK, consisting of 137mM NaCl, 2.7mM KCl, 10mM Na₂HPO₄ and 1.8mM KH₂PO₄ pH 7.4) before 1ml of trypsin (4% v/v in Versene) was added for 2 minutes (SH-SY5Y) or 30-60 seconds (HEK293) at 37°C until the cells were easily dislodged by gentle tapping of the plate. The trypsin was inactivated by the addition of 9mls of fresh growth medium. The cells were split 1:2-1:8 onto fresh plates.

2.2.4. Cell freezing and defrosting

A 90% confluent plate of cells was harvested and centrifuged at 350g for 10mins at room temperature. The pellet was resuspended in sterile freezing medium. For all cell lines freezing medium consisted of 90% growth medium and 10% DMSO filter sterilized. All cells were frozen in 1.5ml cryotubes and put in sealed polystyrene boxes at -80°C overnight, before transfer to liquid nitrogen for long term storage.

Frozen cells were defrosted by rapidly thawing the vial at 37°C. The vial contents were transferred to 20mls of pre-warmed growth medium in a 100mm plastic culture dish and incubated overnight at 37°C. The plate was gently washed with 10 mls of PBS and replaced with 8 mls of standard growth medium the following day.

2.2.5. Immunofluorescence staining

Cells were harvested and grown on 22mm sterile glass coverslips in a well from a 6-well plate and allowed to adhere to the coverslips overnight. The cells were washed three times in PBS, fixed in 4% paraformaldehyde and permeabilised in methanol at -20°C for 15 minutes. The coverslips were washed three times in PBS and then incubated in 10% goat serum in PBS at 37°C in a humidified chamber for 1 hour. They were drained and then incubated with 100µl of PBS-diluted primary antibody overnight at 4°C. This was followed by three washes in PBS before being incubated for 1 hour at 37°C in 1 in 1000 in PBS goat anti-mouse IgG Alexa 488 (FITC linked) for mouse monoclonal primary antibodies or goat anti-rabbit IgG Alexa 568 (rhodamine linked), for rabbit polyclonal primary antibodies. The coverslips were washed three times in PBS and mounted on glass slides in Citifluor/PBS/glycerol (Agar. Stansted, UK) with 1µg/ml of DAPI (Sigma) to counterstain the nuclei. A control was set up during each experiment which was processed identically except the cells were incubated in PBS only and not primary

antibody. Double immunofluorescence was performed on the HEK 293 cells using the protocol for single IF except two primary antibodies from different species were used. A rabbit polyclonal antibody to huntingtin, “675”, and a mouse monoclonal antibody, to various subcellular compartments, were combined. The secondary antibodies were also a combination of goat anti-rabbit IgG Alexa 488 (FITC linked) and goat anti-mouse IgG Alexa 568 (rhodamine linked) at a dilution of 1 in 1000.

2.2.6. Primary antibodies.

2.2.6.1. Huntingtin antibodies

There are many antibodies to various portions of the huntingtin protein (Wilkinson et al 1999). Fig. 2.1 illustrates the antibodies, and their epitopes, that were used during the study. Table 2.1 shows the dilutions the antibodies were used in IF and Western blotting. The primary antibody, “675” used was a kind donation by Dr Lesley Jones, University of Cardiff, Wales. It is a polyclonal primary antibody and was raised to the first 9 amino acids of huntingtin.

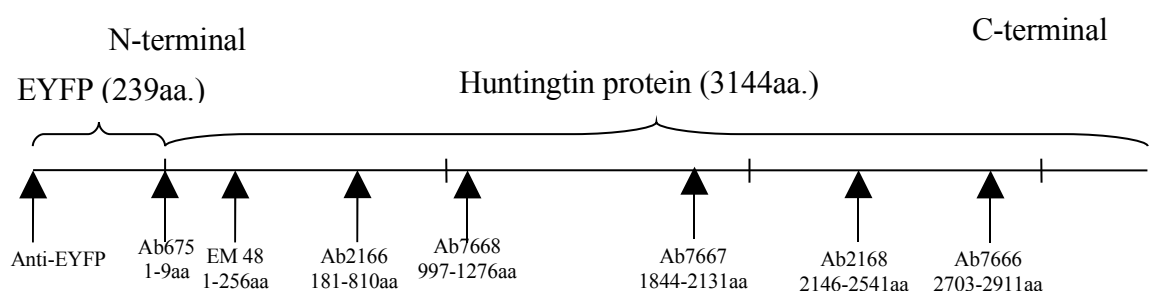


Fig. 2.1. Schematic representation of epitopes of anti-huntingtin antibodies

Table 2.1.

2.2.6.2. Other primary antibodies

Primary antibodies used in co-localisation studies in the HEK 293 model are listed in Table 2.2a. and those used in co-localisation studies in the SH-SY5Y model are listed in Table 2.2b. All antibodies were used overnight at 4°C at the dilutions shown and developed with the Alexa 568 (red) linked secondary antibody.

2.2.7. Differentiation of SH-SY5Y cells

Cells were plated out at 1×10^5 /well in a 6-well plate containing a sterile glass coverslip for immunofluorescence or 6.5×10^5 /10cm plate for Western blots. The surface area of a 10cm plate was calculated as 6.5 times greater than a 6-well plate. The cells were left to adhere overnight and the following morning, the medium was replaced and all trans-retinoic acid (Sigma) was added to a final concentration of 30µM. The medium and retinoic acid were replaced every 48 hours for prolonged experiments.

2.3. Plasmid transfections

All transfections were performed with Escort transfection reagent (Sigma). Cells were plated out at 50% confluence on 6-well plates. The DNA transfection mixture was prepared with 230µl of unsupplemented DMEM, 5µg plasmid DNA and 15µl Escort reagent and mixed by gentle tapping of the vial. This was then incubated for 15 minutes at room temperature and then added to 2mls of pre-warmed standard growth medium. 0.7mls of the Escort/DNA mixture was then added to the each well and incubated at 37°C for 6 hours. Following this the Escort/DNA mixture was aspirated and replaced with growth medium.

Table 2.2.

2.3.1. EYFP-C1 plasmid

The pEYFP-C1 (Clontech, San Jose, CA, USA) encodes an enhanced yellow-green variant of the *Aequorea victoria* green fluorescent protein (GFP). It is maximally excited at 513nm and the emission spectrum has a peak at 527nm, to give a green-yellow fluorescence. The EYFP sequence lies at the 5' end of a multiple cloning site (MCS) and therefore expressed proteins will have an N-terminal EYFP tag. The EYFP sequence is preceded by a CMV_{IE} ("immediate early") promoter and the plasmid contains a neomycin resistance gene for selection purposes. The EYFP-C1 plasmid was a very generous donation by Dr. Lesley Jones, University of Cardiff, Wales. The full-length htt cDNA with a 23 and a 88 CAG repeat was first cloned into pRc/CMV by Dr Jones and then into EYFP-C1 within the MCS at the *EcoR I* and *Sma I* sites (Fig. 2.2.).

2.3.2. pIND plasmid and the Ecdysone-Inducible Expression Kit

The plasmid, pIND, was used as a part of the Ecdysone-Inducible Expression Kit (Invitrogen, San Diego, CA, USA). This is designed for mammalian gene transcription based on the ability of the insect hormone 20-OH Ecdysone to activate gene expression via the Ecdysone receptor. The system uses a heterodimer of the Ecdysone receptor (VgEcR) and the retinoid X receptor (RXR) that binds a modified ecdysone response element (EcRE) in the presence of ecdysone or a synthetic analogue such as ponasterone A (pon A) (Fig. 2.3.). Binding of the heterodimer to the EcRE activates transcription. Mammalian cells are not responsive to ecdysone and do not contain the ecdysone receptor leading to very low or absent basal levels of expression (No et al. 1996). HEK 293 EcR cells, which already has the pVgRXR plasmid stably integrated, was purchased from Invitrogen (San Diego, USA). This plasmid contains the zeocin

Fig. 2.2.

Fig.2.3.

resistance gene for selection purposes. The pIND plasmids were a generous donation from Dr Lesley Jones (University of Cardiff, UK). These plasmids contain the EcRE, a

multiple cloning site and the neomycin resistance gene for selection with antibiotic G418. An N-terminal huntingtin construct, containing 21 or 57 CAG repeats, was cloned into the multiple cloning site of pIND by Dr Jones. Construct expression was induced by the addition of pon A to the growth medium. Pon A was bought as aliquots of 250µg lyophilized powder (Invitrogen) and stored at -20°C. Prior to use, the lyophilizate was solubilised in 500µl of DMSO and excess was stored at 4°C to prevent freeze/thaw cycles.

2.3.3. Isolation of stably transfected clones

Titration experiments demonstrated HEK293 cells died within 1 week when treated with 400µg/ml of Zeocin. In similar titration experiments EcR HEK293 cells (containing the Zeocin resistance gene) and SH-SY5Y cells died within one week at 250µg/ml for G418. For isolation of stably transfected clones, the cells were harvested from the 6 well plates 24 hours post-transfection and split 1:4 into 100mm plates. Cell with stable vector expression were selected with 8 mls of standard growth medium containing 400µg/ml of Zeocin and 250µg/ml of G418 for the HEK 293 cells or 250µg/ml of G418 only for the SH-SY5Y cells. The development of individual clones was monitored using phase-contrast microscopy and circles were drawn below the clones on the under surface of the plate. When clones had formed at between 4 and 6 weeks, they were harvested by aspirating off the medium from a plate, washing and aspirating the plate in PBS and then gently scraping a clone, using a yellow (200µl.) pipette tip, until the cells were loosened from the plate. The loosened cells were gently aspirated into the pipette tip using a 200µl pipette and transferred directly into fresh medium. This was repeated for between 4 and 10 clones per plate and each clone was then labeled and grown up separately. Cells from harvested clones were grown up in 100mm plates and then processed for freezing (Section 2.2.4.) and immunofluorescence (Section 2.2.5.).

2.4. DNA methods

2.4.1. DNA extraction

DNA was extracted from one cell pellet from a 80% confluent 100mm plate using the Nucleon DNA extraction kit (Scotlab, UK) according to the manufacturers' instructions. The extracted DNA was dissolved and stored in TE (Appendix 1.4)

2.4.2. Estimation of DNA purity and concentration

5 μ l of DNA solution was added to 995 μ l of 100% ethanol in a 1ml silica cuvette and mixed by inverting with parafilm. The solution was scanned by measuring the absorbance pattern between 310nm and 210nm. The DNA concentration (μ g/ μ l) was calculated assuming a 1mg/ml DNA solution had an absorbance of 20 at 260nm. The purity was accepted when the A_{260}/A_{280} ration was greater than 1.7.

2.4.3. Polymerase chain reaction (PCR)

DNA primers were obtained from MWG-Biotech (Milton Keynes, UK) (Section 2.4.7 for primers). ReddyMix PCR Master Mix (x2) was obtained from ABgene (Epsom, UK). This contained 1.25 units Taq DNA polymerase, 75mM Tris-HCl (pH8.8 at 25°C), 20mM (NH₄)₂SO₄, 1.5mM MgCl₂, 0.01% (v/v) Tween 20, 0.2mM each of dATP, dCTP, dGTP, and dTTP and precipitant and red dye for electrophoresis. The standard reaction mixture (25 μ l) contained 12.5 μ l of PCR Master Mix, forward and reverse primers (25 picomoles of each), DNA (50ng to 5 μ g) and made up to 25 μ l with autoclaved double-distilled water.

The reaction was performed in a 0.3ml thin-walled PCR tube in a Perkin-Elmer 24000 thermal cycler. All PCR reactions performed with CAG repeats included 10% DMSO (Sigma).

The standard reaction conditions for HEK 293 cells using G49 and G50 primers can be found in Appendix 1.1. The standard conditions for sequencing the 5' junction between EYFP sequence and the 5' end of full-length huntingtin sequence in SHSY5Y cells, using the EYFPfor and RS2 can be found in Appendix 1.2. The standard conditions for sequencing the 3' junction between EYFP-C1 plasmid and the 3' end of full-length huntingtin sequence in SHSY5Y cells, using the R2 and F3 can be found in Appendix 1.3.

These conditions were adjusted according to the nature of the template and the primers and specific details can be found in the relevant chapters.

2.4.4. Clean-up of PCR products

PCR products were purified using the Qiaquick PCR clean-up kit (Qiagen, West Sussex, UK) according to manufacture's instructions. The cleaned-up DNA products were stored in Tris-EDTA (pH8.0) at -20°C (see Appendix).

2.4.5. Detection of DNA products

All PCR reaction products were separated on agarose gels using the BRL horizontal system for agarose gel electrophoresis (Bethesda Res. Lab, Life Technologies Inc) 1.5% (w/v) agarose gels (Sigma) were prepared in 1xTAE Buffer (Appendix 1.4.) containing

1µg/ml ethidium bromide. 5µl of PCR product was loaded carefully into each lane and 1µg of 2-log ladder (New England Biolabs, Beverly, MA) or Benchtop 1kb DNA ladder (Promega, Southampton, UK) were used as markers. Electrophoresis was performed in 1X TAE buffer at 100V for 1-3 hours. The sample was visualized using a UV transilluminator and photographed with a black and white Polaroid film.

2.4.6. Sequencing of PCR products

DNA sequencing was outsourced to MWG Biotech (Milton Keynes, UK).

2.4.7. Primers used in sequencing and PCR reactions

Primers used with EYFP-C1 plasmids

	5'	3'	Primer binding site
5' EYFP			
EYFP-F	CATGGTCCTGCTGGAGTTCGTG		EYFP 1266-1287
RS1-F	ATGGCGACCCTGGAAAAGCTGATGAA		
	GGCCTTCGAGTCCCTCAAGTCCTC		Htt 316-366
RS2-R	GGTCGGTGCAGCGGCTCCTCAG (exonic)		
	/GTGAGTTT(intronic)		Htt 563-574(exonic)

EL2-R	ATGCCCAGAAGTTTCTGAAA	Htt 682-701
3'EYFP		
F1	TTCTGTCCAACCAGCAGCCAT	Htt 9323-9343
F2	TGAACATTCACAGCCAGCAGC	Htt 8783-8803
F3	AGGTGGACGTGAACCTTTTCT	Htt 9575-9595
R1	CCTCTACAAATGTGGTATGGCTG	EYFP MCS
R2	GATCAGTTATCTAGATCCGGTGG	EYFP MCS
R3	CACAAGGGCACAGACTTCCAA	3' UTR of htt

Primers used with pIND plasmids

G49 (Ecdysone Forward priming site) 5'-CTCTGAATACTTTCAACAAGTTAC-3'

G50 (BGH Reverse priming site) 5'-TAGAAGGCACAGTCGAGG-3'

2.4.8. Analysis of sequences

“Edit Seq” and “Seqman 2” software packages by DNASTAR, Inc. (Madison, USA) were used to analyse the DNA sequences.

2.5. Enzyme Analyses

All assays were performed at 30°C in a final volume of 1ml. Each enzyme was assayed in triplicate and values accepted if they were within 15% of each other.

2.5.1. Citrate Synthase (CS)

Respiratory chain activities were expressed as CS (a mitochondrial matrix protein) ratios to correct for variations in the purity of mitochondrial preparations or to correct for the mitochondrial mass in tissue homogenates. The assay is based on the method of Coore et al. (1971). The enzyme catalyses the condensation of acetyl-CoA and oxaloacetate to form citrate, producing CoA whose free thiol group combines with 5-5'-dithiobisnitrobenzoic acid (DTNB), resulting in an increase in absorbance at 412nm.

Two cuvettes were set up containing: final concentrations of 100mM of Tris-HCl buffer pH8.0, 200µM Acetyl-CoA, 200µM DTNB, 0.1% (v/v) Triton-X-100 and sample, and the reaction was initiated by adding 10µl of 10mM oxaloacetate to the test cuvette only to make a final volume of 1ml in both cuvettes. The increase in absorbance at 412nm was measured during the reaction. Citrate synthase activity was calculated using the molar extinction coefficient of 13.6×10^3 for the DTNB-CoA-SH complex and activity expressed as nmol/min/mg protein.

2.5.1.1 Preparation of Acetyl CoA

Acetyl CoA was prepared by the method of Ochoa (1955) from free Coenzyme A and acetic anhydride. Briefly, 1ml of dd H₂O was added to 10mg of enzyme CoA and 100µl of 1M potassium hydrogen carbonate. The eppendorf was vortexed briefly, put on ice to

cool down to approximately 0°C for 5 mins and 1µl of acetic anhydride was added to the first eppendorf. The contents were vortexed immediately and the eppendorf put back on ice to cool down for 3 minutes as the reaction is exothermic. The cycle of adding 1µl of acetic anhydride/eppendorf, vortexing and cooling was repeated a further 3 times until a total volume of 4µl of acetic anhydride had been added per eppendorf. The tube was left on ice for a further 15 mins to enable the reaction to attain completion. The pH was checked using pH strips to ensure that the reaction was complete, as indicated by a pH value within the range of 6.3 to 6.5. The acetyl CoA was used within a few months and was stored at -20°C.

2.5.2. NADH-CoQ1 oxidoreductase (complex I activity)

The assay is based on the method of Ragan et al. (1987) and measures the rotenone sensitive CoQ₁ dependent oxidation of NADH at 340nm. The CoQ₁ was a generous gift from the Eisai Chemical Co., Japan. A dilution of the stock CoQ₁ was made in ethanol and the absorbance of the CoQ₁ at 275nm noted. An excess of sodium borohydride was added to the reference cuvette to completely reduce the quinone to quinol and the absorbance change was used to calculate the CoQ₁ concentration using the molar extinction coefficient of 2.25×10^3 (Redfearn et al. 1967). Two identical cuvettes were set up containing (final concentrations) 20mM potassium phosphate buffer pH 7.2 with 8.2mM MgCl₂, 150µM NADH, 1mM KCN, 2.5mg/ml BSA and 50µM CoQ₁. 10µl of ethanol was added to the reference cuvette and 10µl of rotenone, to a final concentration of 10µM of rotenone, was added to the sample cuvette and double-distilled water was added to make the volume up to 1ml minus the sample volume. The cuvettes were mixed by three inversions using parafilm and zeroed in the spectrophotometer. The reaction was initiated by adding the sample to both cuvettes followed by further mixing with parafilm.

The rate of NADH oxidation was monitored by the change in the absorbance at 340nm. The linear rate for the first 2-3 minutes was taken as the rotenone sensitive component of the reaction. The molar extinction coefficient of NADH is 6.22×10^3 , but the oxidation of the quinone to a quinol causes an increase in absorbance at 340nm and therefore the corrected value of 6.81×10^3 was used for the calculation of complex I activity. Enzyme activity was expressed as nmol/min/mg of protein and also as a ratio with citrate synthase (CS).

2.5.3. Succinate cytochrome c oxidoreductase (complex II/III)

This assay determines the activity of both complex II and III and is based on the method of King (1967). It detects the antimycin A sensitive, succinate dependent reduction of cytochrome c at 550nm. Two identical cuvettes were set up containing (final concentrations) 0.1M potassium phosphate buffer pH 7.4, 0.3mM potassium EDTA (K_2 -EDTA), 0.1mM cytochrome c. Two separate eppendorfs were set up containing 1mM KCN, 20mM succinate and sample, and these were incubated at 30°C for two minutes to fully activate the enzyme. This was then added to the cuvettes to initiate the reaction. The change in absorbance was measured at 550nm. After 10 minutes 20µM antimycin A was added. The antimycin A-sensitive complex II/III activity was calculated using the molar extinction coefficient of cytochrome c of 19.2×10^3 . Activity was expressed as nmol/min/mg and as a CS ratio.

2.5.4. Cytochrome c oxidase (complex IV)

This assay is based on the method of Wharton and colleagues (Wharton et al 1967) which monitors the oxidation of the reduced cytochrome c at 550nm.

2.5.4.1 Preparation of reduced cytochrome c

In brief, 100 ml of 1% solution of cytochrome c (horse heart) was made up in 10mM potassium phosphate buffer. This was reduced by adding an excess of ascorbate (13mg), gently mixed and checked that it was fully reduced at 550nm. This was performed by adding 50 μ l of the cytochrome c solution to each of the two cuvettes containing 950 μ l of 10mM potassium phosphate buffer. To the sample cuvette 10 μ l of freshly made ascorbate solution and the change in absorbance was noted. If the change was positive, i.e. the cytochrome c could be further reduced by the addition of ascorbate, then the cytochrome c solution was reduced further. If the cytochrome c was fully reduced, then the sample was dialysed to remove excess ascorbate using size 1 dialysis tubing (Medicell International Ltd., London) and dialysing against 5L of 10mM potassium phosphate buffer pH 7.0 at 4^oC overnight. To check that excess ascorbate did not remain, oxidised cytochrome c was added to the dialysed reduced sample and if no change in the absorbance occurred, then the ascorbate was removed.

2.5.4.2 Calculation of the concentration of reduced cytochrome c

Two identical cuvettes were made up with 100 μ l of 100mM potassium phosphate buffer pH7.0, 850 μ l of ddH₂O and 50 μ l of reduced cytochrome c. To the reference cuvette was added 10 μ l of 0.1M potassium ferric cyanide to oxidize the reduced cytochrome c. The change in absorbance was noted and the concentration calculated by the following equation with 50 μ M of cytochrome c producing an absorbance of 0.96, $(0.96/\text{absorbance}) \times 50 = \text{volume of stock reduced cytochrome c required for a } 50\mu\text{M solution in final 1ml reaction.}$

2.5.4.3 Assay

Two identical cuvettes were set up containing 10mM potassium phosphate buffer pH7.0 and 50 μ M reduced cytochrome c. 10 μ l of 100mM potassium ferric cyanide was added to the reference cuvette to oxidise the cytochrome c. The reaction was commenced by the addition of sample to the test cuvette and monitored at 550nm.

2.5.4.4 Calculation of the pseudo first-order rate constant (k)

This was performed by the extrapolation of the absorbance back to time=0 secs. and the calculation of the change in absorbance at time points 1,2 and 3 minutes. The non-enzyme rate of absorbance was calculated and subtracted from the sample absorbance values. K/min/ml was therefore calculated by: $\ln 0.96 - \ln(0.96 - \text{change in absorbance at time } t) \times 1000 / \text{sample volume}(\mu\text{l}) \times \text{dilution factor}$, where 0.96 represents the absorbance of cytochrome c when fully reduced. The k/ml values for four time points (0,1,2,3 mins) were plotted against time and the gradient of the line calculated using linear regression analysis to obtain complex IV activity (k/min/ml). The final results were expressed as k/min/mg protein and as a CS ratio.

2.5.5. Aconitase

This assay measures the activity of aconitase which catalyses the isomerisation of citrate to isocitrate which in turn forms α -ketoglutarate with the reduction of NADP to NADPH. The rate of formation of NADPH can be measured at 340nm. Two identical cuvettes were

set up containing: 50mM Tris-HCl pH7.4, 0.4mM NADP, 5mM sodium citrate, 0.6mM MgCl₂, 1% (v/v) Triton X-100 and 2 units of isocitrate dehydrogenase. The sample was added to the test cuvette only. Both cuvettes were incubated at 30°C for 30 minutes pre-incubation and the absorbance change at 340nm was measured for 15 minutes and aconitase activity was calculated using the molar extinction coefficient for NADP ($\epsilon=6.22 \times 10^3$).

2.6. Preparation of mitochondrial-enriched fractions (MEFs)

MEFs were prepared from 20 confluent 10cm plates of cells based on the method by Ragan et al (1987). Harvested cells were washed three times in PBS and the resultant pellets frozen overnight at -70°C. The pellets were thawed and resuspended in 2 ml of ice-cold homogenisation buffer (Appendix 1.4). Each sample was homogenized on ice using a Potter homogenizer for 20 strokes at 1000rpm, and then spun at 1500g for 10 minutes 4°C. The resultant post-nuclear supernatant (PNS) was collected in a fresh tube on ice. Homogenisation of the residual pellet and centrifugation was repeated a further 2 times. The combined PNS was further centrifuged for 10minutes and any residual pellet discarded. The final PNS was further centrifuged at 10,000g for 12 minutes at 4°C on a Kontron Centrikon T-124 centrifuge which resulted in a brownish pellet (MEF). This pellet was resuspended in 200-800µl of ice-cold homogenisation buffer, snap frozen in liquid nitrogen and stored at -70°C for up to 6 days before assaying. To assay complexes I, II/III and IV samples were freeze-thawed in liquid nitrogen three times before assaying to maximize the mitochondrial enzyme activities.

2.7. Preparation of muscle homogenates

Samples were stored at -70°C and immediately homogenized in ice-cold homogenization buffer using a glass/glass homogenizer. The samples were freeze-thawed in liquid nitrogen as described above and assayed within one hour.

2.8. Protein Assays

All protein assays were performed using the Pierce BCA Protein Assay Reagent Kit (Rockford, IL). This system uses the reaction of protein with Cu^{2+} which is then detected by the reagent bicinchoninic acid (BCA). The purple reaction product of BCA and Cu^{2+} is water soluble and exhibits a strong absorbance at 562nm. For each assay a set of protein standards was made using dilutions of bovine serum albumin (BSA) in the sample diluent and these were used to create a standard curve. The “enhanced protocol” was used which required incubation at 60°C for 30 minutes and subsequent immediate cooling of the samples on ice to stop the reaction before measuring the absorbance of the samples at 562nm. Each assay was performed in triplicate and calibrated relative to a control assay of diluent and reaction mixture only.

2.9. Protein extraction from cells and preparation for electrophoresis

2.9.1. Preparation of cell pellet

One confluent plate of cells was washed in PBS and the cells were harvested using a cell scraper. The pellet was washed twice in PBS and resuspended in 0.4-0.8ml of dissociation buffer and protease inhibitors (Appendix 1.4). The sample was needle-sheared using a 19G needle and 1ml syringe to break up the genomic DNA and reduce its viscosity. The sample was stored at -70°C until needed. A protein assay, using the BCA protocol as described above, was performed on all samples to adjust for protein loading during electrophoresis.

2.9.2. Cell pellet solubilisation

The NuPAGE Bis-Tris and Tris-acetate systems (Invitrogen, Life Technologies) were used to solubilise the samples. In summary, 30 μl of each sample was made up from:

- 1) 7.5 μl of NuPAGE LDS Sample Buffer (x4)
- 2) 3 μl of NuPAGE Reducing Agent (x10)
- 3) Sample (between 5 and 50 μg of protein per lane)
- 4) Made up to 30 μl with ddH₂O

The samples were vortexed briefly to enable mixing, heated at 70°C for 10 minutes and then centrifuged for 10 secs at 6000g to concentrate any insoluble material at the bottom of the eppendorf, before the supernatant was loaded.

2.9.3. Concentration of protein extracts

The long-term differentiation of some SH-SY5Y samples made it impractical to harvest the small residual number of cells on many plates into concentrated extracts. The

centricon YM-3 centrifugal filter devices (Millipore, Bedford, MA, USA) were used to concentrate samples with the loss of proteins below 25kDa.

2.10. SDS-PAGE of protein extracts

The NuPAGE Bis-Tris and Tris-acetate systems (Invitrogen, Life Technologies) were used to separate proteins. For large proteins (>100kDa) the Tris-acetate system was used with a 3-8% pre-cast polyacrylamide gel and the Bis-Tris system was used for smaller proteins (<100kDa) with a 4-12% pre-cast polyacrylamide gel. These gels did not contain SDS but were used for denaturing gel electrophoresis in conjunction with the recommended denaturing SDS running and sample buffers. For constituents of individual buffers see (Appendix 1.4). Between 5 and 50 μ g of protein was loaded per well as well as a pre-stained molecular weight marker, MultiMark Multi-Colored Standard, which covers between myosin (approximately 189kDa) and insulin (approximately 3kDa). The gel was run at 150V for between 2 and 3 hours for the Tris-acetate gels and at 200V for 35 minutes (MES buffer) or 50 minutes (MOPS buffer) for Tris-Bis gels.

2.11. Western Blotting

A polyvinylidene difluoride (PVDF) membrane (Millipore, Bedford, MA, USA) was briefly (approximately 30 seconds) wetted in methanol. NuPAGE transfer buffer was made up fresh and 1 ml of NuPAGE antioxidant was added. The blot pads, filter paper and the PVDF membrane were soaked for 5 minutes in the transfer buffer, making sure not to allow the membrane to dry. The pre-cast gel was carefully separated. The gel was transferred onto a transfer buffer-soaked piece of blotting paper and then placed face-up onto two soaked blot pads. The PVDF was carefully placed onto the gel and covered with

a further layer of soaked filter paper and two more layers of blot pads. The PVDF was upper most towards the anode. The whole blot module was slid into the lower buffer chamber of the blot tank and topped up with transfer buffer to just cover the pads, filter paper, membrane and gel. The outer chamber was filled with ddH₂O. The transfer was performed using 30V constant supply for 1 hour.

2.12. Staining of PVDF membrane for protein extracts

Adequate loading and separation of protein was confirmed by immersing the membrane for 1 minute in Ponceau S solution (Sigma), which contains 0.1% Ponceau S (w/v) and 5% acetic acid (w/v). Ponceau S binds to positively charged amino groups and also non-covalently to non-polar regions of the protein. To remove the Ponceau S, the membrane was gently washed with PBS until all the stain was removed and prior to blocking in 10% low fat milk (Marvel™) in PBS for 2 hours at room temperature. After two 10 minute washes in PBS at room temperature, the membrane was incubated for 2 hours at room temperature in primary antibody made up in 0.3% Tween/PBS (v/v) (PBS-T), and left on a shaker. After 3 further washes for 10 minutes in PBS-T, the membrane was incubated in the appropriate secondary antibody (HRP conjugated) diluted in PBS-T for 1 hour at room temperature. The membrane was then washed 3 times in PBS-T for 10 minutes per wash followed by two 10 minute washes in PBS alone. The membrane was developed for 1 minute in 1:1 volumes of chemiluminescence oxidizing reagent and enhanced luminal reagent (Renaissance kit, Dupont NEN, Boston, MA, USA). The membrane was exposed to ECL film (Amersham) for times varying from 10 seconds to 6 minutes, depending on the strength of the signal.

2.13. Assessment of cell proliferation

The Cell titer 96 Aqueous Non-Radioactive One Solution Cell Proliferation assay (Promega) was used to assess the cell growth in the HEK 293 cell model. The Cell Titer 96 assay is a colorimetric method for determining the number of viable cells in proliferation assays. The assay uses a Cell titer 96 Aqueous One Solution Reagent which contains a novel tetrazolium compound 3-(4,5-dimethylthiazol-2-yl)-5-(3-carboxymethoxyphenyl)-2-(4-sulfophenyl)-2H-tetrazolium (MTS) and an electron coupling reagent, phenazine ethosulfate (PES). MTS is reduced, probably due to the production of NADH/NADPH by metabolically active cells, into a formazan product that is soluble in tissue culture medium. The absorbance of the formazan product at 490nm was measured directly from 96 well plates without additional processing. The quantity of formazan product, as measured by the amount of 490nm absorbance, is directly proportional to the number of living cells in culture. Cells were harvested and plated out in triplicate into 96 well plates, at a density that had been optimized during pilot experiments, and allowed to adhere for three hours in an incubator. The medium was then aspirated and replaced with 50µl of the appropriate growth medium. To standardize for background reactivity, blank wells in triplicate were set up on every plate which contained only standard growth medium and no cells. The samples were incubated for 0,1,2,3,4 and 5 days and the medium was carefully changed after every 48 hours because of a drop in pon A activity to 30% by 72 hours as stated by the manufacturers guidelines (Invitrogen). At each time-point, 10µl of MPS compound was added to each well using a multi-channel pipette and incubated at 37°C for 2 hours. The samples were immediately measured using a BioRad plate reader with a 500nm filter.

2.14. LDH cytotoxicity detection assay

2.14.1. Background

The CytoTox 96 Non-Radioactive Cytotoxicity Assay was used to assess cell death in the HEK 293 model. The assay quantitatively measures lactate dehydrogenase (LDH). Plasma membrane damage and cell death is associated with the release of LDH into the culture supernatant and LDH activity is measured with a 30 minute coupled colourimetric enzymatic assay which results in the conversion of a tetrazolium salt (INT) into a red formazan product. The chemical reaction on which this assay is based is divided into two steps. In the first step, NAD^+ is reduced to NADH/H^+ by the LDH catalysed conversion of lactate to pyruvate. In the second step, the catalyst (diaphorase) uses NADH to reduce the tetrazolium salt, INT, to form formazan (red) which shows maximum absorption at 492nm. The amount of colour formed is proportional to the number of cells with disrupted or damaged cell membranes and was measured using the BioRad 96-well plate reader with a 500nm filter.

2.14.2. Plating of cells

Cells were plated out at 2×10^5 /well into 12-well plates at approximately 1700 hours. They were then left to settle and adhere to the plate overnight. At 0900 hours the next morning, the medium was carefully aspirated and replaced with 1ml. of growth medium containing low glucose (1g/L.) with either 5 μ l of DMSO or 5 μ l of 1mM pon A (final concentration of 5 μ M). After 48 hours incubation, the medium was carefully aspirated and replaced with medium containing pon A or DMSO together with the appropriate toxin. A well with low glucose medium and DMSO was also incubated at this stage to be used as a “medium” control.

2.14.3. The LDH assay

Cell death was expressed as the percentage of LDH activity in the medium versus the total LDH activity in an equivalent well treated with 100 μ l of 10% Triton-X100 (final concentration 1%). The cultures were examined visually and the approximate percentage of cell death was assessed so that an appropriate dilution could be made to ensure that the LDH content of any sample was within a linear activity range at the end-point of the reaction. Medium was carefully removed with a 1 ml pipette and placed into a 1.6ml microcentrifuge tube. The sample was centrifuged at 6000rpm for 5 minutes to pellet out any residual cell remnants that may have been aspirated into the pipette which could interfere with the assay. The supernatant was diluted depending of the level of cell death assessed prior to harvesting. To ensure the LDH activity was linear, each sample was assessed four times with 4 different volumes and the samples were made up to a total of 50 μ l with double-distilled water. Typically, the medium controls were used neat with 20, 30, 40 and 50 μ l of sample, and the toxin-treated medium samples were also used neat with 15, 20, 25 and 30 μ l of sample. In general, the triton X100-treated cells required greater dilution and were diluted 1 in 4 with double-distilled water and 15, 20, 25 and 30 μ l. Three water blank controls were also plated out. Once the plate had been completed, a multi-channel pipette was used to add 50 μ l of the reaction mixture to each well over approximately 20 seconds. The 96-well reaction plate was then incubated for 30mins at R/T in the dark and the absorbance was measured immediately.

2.15. HD muscle analysis

2.15.1. Histochemical methods

2.15.1.1. COX Staining

HD muscle sections were incubated for 1 hour at 37°C in COX activity dye solution prepared as follows: 1ml of 0.5 M sodium phosphate buffer made up to pH 7.4, 5mg of DAB, 10mg horse heart oxidized cytochrome c, 10µl of PBS/catalase (2mg/ml) and 9ml ddH₂O. Sections were then washed in PBS and the nuclei were counterstained with Mayer's haematoxylin, washed for 10 minutes in water and then gradually dehydrated in 70%, 95% and 100% alcohol. The sections were cleared in xylene and mounted in DPX (Agar Scientific Ltd. Cambridge, UK) which is a colourless synthetic resin mounting medium.

2.15.1.2. Succinate dehydrogenase (SDH) staining

Muscle sections were washed in PBS and then incubated for 1 hour at 37°C in SDH dye solution prepared as follows: 5ml 0.2M sodium succinate, 5ml 0.2M potassium phosphate buffer, 10mg nitroblue tetrazolium. Sections were then washed in PBS and counterstained with haematoxylin before dehydrating, clearing and mounting in DPX as described above.

2.15.2. Immunocytochemistry

Immunocytochemistry on muscle was kindly performed by Jane Workman (Royal Free Hospital, London, UK) using standard protocols. The avidin-biotin-complex (ABC) method with horseradish peroxidase (HRP) was used. Peroxidase was demonstrated using 3'diaminobenzidine (DAB, Sigma) chromagen. Frozen sections were cut at 7µm on a

CM1900 Leica cryostat and mounted on poly-L-lysine-coated slides. The sections were air-dried for 30 minutes at room temperature, fixed in acetone for 10 minutes and then air-dried for another 30 minutes. The sections were stored at -20°C. To stain the sections, they were blocked by incubation with 10% v/v normal goat serum (DAKO)/ PBS for 60 minutes at room temperature in a humidified chamber. Sections were drained and the primary antibody was applied and incubated further in a humidified chamber at 4°C overnight. The following antibodies were used; a polyclonal antibody to the first 9 amino acids of huntingtin, 675, (kind gift from Dr L Jones, Cardiff), diluted 1 in 1000, incubated) and a monoclonal antibody to ubiquitin (Chemicon, 1 in 300). The sections were washed in PBS and incubated with biotinylated secondary antibody for 60mins at room temperature. The sections were then washed three times and the ABC (DAKO) added to the sections for 60 minutes at room temperature. The DAB substrate (Sigma) was prepared by dissolving 2.5mg of DAB in 5ml PBS and 50µl of 0.3% H₂O₂ was added. Sections were then drained and washed and the DAB substrate added. The sections were developed until a brown chromagen had formed and washed in running H₂O. Sections were dehydrated, cleared and mounted in DPX as described above.

2.15.3. Electron microscopy

Electron microscopy was kindly performed by Dr. David Landon at the Institute of Neurology, London.

2.16. Proteasome function

The four clones from WT, MT and pc DNA 3.1 were grown, harvested and washed twice in PBS before freezing down at -80°C. The assay: cells were re-suspended in ‘assay buffer’ (50mM Tris-Cl pH: 7.4) and freeze-thawed three times. Aliquots of the cell suspension were put into wells of a 96-well plate and doubling dilutions made (1:1, 1:2, 1:4 and 1:8) so each sample had 4 points for each proteasomal activity. Data was only taken for those points whose activity appeared to decrease in proportion to the dilution of the sample. Proteasomal function in whole cell suspensions was assessed by measuring the rate of proteolysis of proteasomal fluorogenic substrates. The substrates are polypeptides coupled to the fluorophore 7-amino-4-methylcoumarin (AMC) and proteolytic cleavage results in the release of AMC with an increase in fluorescence over time which was measured on a Synergy plate reader (Ex: 380nm, Em: 460nm). The substrates used are described in Table 2.3. The substrates were reconstituted in DMSO and stored in the dark at -20°C following reconstitution. Protein was estimated by BCA method and activities expressed as nmols/min/mg after relating the fluorescence to a standard curve of free 7-amino, 4-methyl coumarin. The proteasome assays were kindly performed by Dr Mike Cleeter, UCL.

<u>Substrate</u>	<u>Supplier</u>	<u>Proteolytic target</u>	<u>Sequence</u>	<u>Excitation</u>	<u>Emission</u>
II	Calbiochem	Trypsin-like	Z-Leu-Leu-Glu-AMC	380nm	460nm
III	539141 Calbiochem	Chymotrypsin-like	Suc-Leu-Leu-Val-Tyr-AMC	380nm	460nm
VI	539142 Calbiochem	Post acidic	Z-Ala-Arg-Arg-AMC · HCl	360-380nm	430-460nm
	539149				

Table 2.3. Reagents used in proteasome function analysis.

2.17. Statistical methods

Statistical analysis in the HEK 293 and SH-SY5Y cell models was performed using the Student's t test. Statistical analyses were performed using the unpaired two-tailed Mann-Whitney U test and the Spearman correlation test for the analysis and correlation of mitochondrial enzyme activities and clinical parameters in HD muscle where a normal distribution could not be assumed.

CHAPTER 3

Results

An inducible N-terminal htt

HEK 293 cell model

3.1. Plasmid sequencing

The plasmids LJ21CAG and LJ57CAG were a kind gift from Dr Lesley Jones, University of Cardiff and were plasmids pIND (Invitrogen) containing an N-terminal fragment of huntingtin with either 21 or 57 CAG repeats. Prior to transfection, PCR amplification with the G49/G50 primers was performed and the PCR products sequenced commercially by MWG Biotech (Milton Keynes, UK) (Section 2.4.3. for PCR method, 2.4.6 and 2.4.7. for sequencing of plasmids and the Figs.3.1. A and B for sequence chromatograms of plasmids). The constructs were correctly inserted into the Nhe-1 (5' end of construct) and Xba-1 (3' end of construct) multiple cloning sites (MCS) of pIND. There were two ATG start codons (out of frame with one another) within close proximity at the start of the htt sequence although the first ATG was immediately followed by a TAG stop codon and would therefore not transcribe and the second ATG was correctly followed by the htt sequence. The second ATG also had a strong Kozac consensus sequence with an A at position -3 and a G at position +4. There were 57 CAGs in the mutant (MT) sequence and 21 CAGs in the wild-type (WT) htt sequence. A base change (T to a C) in the 3' end of both constructs was identified, converting a leucine to a proline at amino acid 165 of the htt sequence. The stop codon was 6 codons 3' to the end of the htt sequence and included 5 additional codons of the pIND 0 sequence at the Xba-1 restriction site. The analysis of the sequences suggested that the WT construct would produce a protein of 176aa including the first 171aa of htt with 23 polyglutamines, and an additional 5aa (serine, arginine, glycine, proline and valine) from the pIND sequence. Similarly, the MT construct would produce the same protein except with 59 polyglutamines.

Fig. 3.1 A

Fig. 3.1 B

3.2. Plasmid transfections and cloning

EcR293 cells were transfected with 5 μ g of both the MT (LJ57CAG) and WT (LJ21CAG) htt constructs in pIND using the Escort (Sigma) lipofection method in 6-well plates (Section 2.3.2.). Twenty-four hours post-transfection, stable clones were selected by adding Zeocin (400 μ g/ml medium) and G418 (250 μ g/ml medium) to the medium and the cells were transferred to 10 cm plates. Three weeks after transfection 13 WT and 15 MT clones were cloned and transferred to a 10cm plate and allowed to divide. EcR293 cells were also transfected with an “empty” pIND plasmid without any construct and called “pIND 0”. These were cloned by the same method as cells containing a construct.

3.3. Construct expression

3.3.1. Immunofluorescence (IF) of clones using the “675” anti-N-terminal htt antibody

Once the clones had divided sufficiently to split the plates (approximately 10 days), cells were plated on coverslips, allowed to adhere overnight and pre-treated for 48 hours with 5 μ M ponasterone A (pon A) to induce construct expression. Immunofluorescence (IF) was performed on the 13 WT and 15 MT harvested clones as described in Section 2.2.5 using the 675 primary antibody to N-terminal huntingtin. Fig. 3.2. shows 2 representative WT clones, 21 2 c and 2d, and 2 representative mutant clones, 57 1g and 2e, with and without 5 μ M pon A treatment for 48 hours. All clones demonstrated punctate cytoplasmic staining with and without pon A induction (dotted arrow in Fig. 3.2). This represented endogenous htt or non-specific staining. Induction with pon A produced a greater degree of cytoplasmic staining as well as dense nuclear staining in

Fig. 3.2.

between 30-70% of cells in both WT and MT clones (solid arrow Fig. 3.2). There were no discernable differences in the pattern of staining between WT and MT clones and there

were no obvious inclusions. In general, all cells, with and without pon A, tended to clump together and there were few individual cells in spite of being plated out as single cells. Clumping of cells is a natural characteristic of HEK293 cells and due to the effects of DMSO.

Positive clones to be taken forward to the next level of selection were defined by those which demonstrated greater than 50% of the cells with strong Ab675 cross-reactivity following pon A induction and where there was a distinct difference in the intensity and pattern of staining between induced and non-induced clones. Seven WT and five MT clones (Table 3.1) were found to follow these criteria and each clone was expanded and frozen down for storage as described in Section 2.2.4. The clones were named after the number of CAG repeats (21 or 57), the plate from which they were cloned (1, 2 or 2a) and the number of the clone taken from the plate (a to j).

Wild-type	Mutant
21 1 d	57 1 f
21 1 h	57 1 g
21 1 j	57 2 e
21 2 a	57 2a d
21 2 b	57 2a e
21 2 c	
21 2 d	

Table 3.1. HEK 293 clones with positive immunostaining confirmed with 675.

3.3.2. Western Blots of HEK 293 transfected cells

To confirm the expression of the construct and to assess the size of the protein product, 7 WT and 5 MT clones were processed for Western Blot analysis as described in Section 2.9-11. Fig. 3.3. A-D demonstrates the Western blots of all clones following induction with 5 μ M pon A (“pon +”) or only the DMSO vector (“pon –”) for 48 hours. In the

absence of pon A, there were a number of minor bands. Exposure to pon A generated a protein product that cross-reacted with the Ab675 at approximate molecular weights of 29.5 kDa (WT) and 36kDa (MT) in all the clones treated (Fig. 3.3 A-D). The predicted sizes of the constructs, based on sequencing, were 19.5 kDa (WT) and 23.5 kDa (MT). There was no evidence of smaller cleaved products post-induction with pon A and non-specific bands were equal in induced and non-induced clones. Two representative pIND 0 clones (1 and 2) showed non-specific bands (Fig. 3.3D). One of these bands ran at a similar level to the MT N-terminal htt (arrow) but was equal in ponA treated and untreated clones. Fig. 3.4. demonstrates Western blots of clones 21 2 c and d (A) as well as 57 2a d and e (B) developed with Ab675. All clones produced a strong band at a size greater than 188kDa which suggested it was endogenous htt. Fig. 3.4 also demonstrates that for protein loading of 3, 10 and 30 μ g, there was a proportionate increase in band intensity. Fig. 3.5 demonstrates that there was no evidence of breakthrough expression within the clones that were not treated with pon A, even with high levels of protein loading (120 μ g) and when the ECL film was heavily exposed. Construct expression was clearly seen with pon A exposure (arrows). Fig. 3.6 demonstrates all 7 WT and 5 MT clones on Western blots developed with Ab675 and shows the relation of construct htt to endogenous htt. There was no evidence of aggregate formation such as larger bands or product staining within the wells. The relative intensities of the bands of construct N-terminal htt were similar although there

Fig 3.3.

Fig 3.4

Fig 3.5

Fig 3.6

was a difference of approximately one to three-fold in expression levels between the WT clones e.g. 21 2c versus 21 1 j, and the expression of 57 2ad was slightly less than the other MT clones (Figs. 3.3 and 3.6). There also tended to be similar band strength with construct versus endogenous htt expression with a trend to greater expression levels of the construct (Figs. 3.6).

3.4. Subcloning of WT and MT clones

The immunofluorescence of the cloned cells suggested that there was a wide variation of staining within the cells of each clone. Most clones had some cells which were stained very strongly positive and others which were similar to untransfected cells with punctate cytoplasmic staining only. This could have been due to a mixed population of cells being cloned or due to differences within transfected cells, for instance, at various stages in the cell cycle. To elucidate this further, subcloning of all 7 WT and 5 MT clones was undertaken which involved plating out a low concentration (approximately 1×10^4 cells/10cm plate) of well-triturated cells from each clone. These were grown to form subclones. After approximately 2 weeks, between 3 and 6 subclones were harvested from each plate, induced with $5 \mu\text{M}$ pon A for 48 hours and immunofluorescence with antibody 675 was performed. Fig. 3.7. demonstrates the immunofluorescence of a representative parent clone (21 1 h) with its subclones 1-3. It was found that there was no difference in the subcloned cells from the parent clones suggesting that the variable expression levels within each clone was a property of the cells, possibly due to variable induction, and not due to the clones containing cells with and without transfected construct.

Fig. 3.7

3.5. Sequencing of clones

To establish the sequence of the stably integrated cDNA constructs, DNA was extracted from the seven WT and five MT clones and PCR amplification was performed using G49 and G50 primers (Section 2.4.7 for details of primers). Fig. 3.8 demonstrates the PCR products, run on a 2% agarose gel, from two representative clones, 21 2 d (WT), 57 2a e (MT), and pIND 0. The predicted band size was calculated to be 626bp (21 2 d), 734bp

(57 2a e) and 192bp (pIND0) using the G49/50 primers, which approximately matched the band lengths of the PCR products observed in Fig. 3.8. In order to clarify the size of the PCR products, the distance from the well to each band in the DNA ladder was measured and plotted against the natural log of the known band length in the markers (Appendix 1.5.) to produce a standard curve. The distance from the loading wells to the PCR product bands was also measured and the base-pair length of the products was extrapolated from the standard curve in Appendix 1.5. Table 3.2. below shows the extrapolated base pair lengths which were 209bp (pIND0), 618bp (21 2 d) and 726 (58 2a e). The PCR products were commercially sequenced by MWG Biotech. (Milton Keynes, UK). The correct integration of the construct was confirmed in all clones (data not shown) and the sequence was identical to the chromatograms for the LJ21CAG and LJ57CAG transfecting plasmids (Figs. 3.1 A and B).

PCR product	Distance from well (mm)	ln base pair	Extrapolated base pairs	Predicted base pairs
pIND0	108	5.34	209	192
21 CAG	80	6.42	618	626
57 CAG	76	6.58	726	734

Table 3.2. Predicted base pair length of PCR products

Fig 3.8

3.6. Influence of pon A concentration and time on expression

The response of the clones to varying doses and times of exposure to pon A was studied in 2 representative WT (21 1 h and 2 c) and 2 MT (57 2a d and 2 e) clones. The clones were plated out on glass coverslips for immunofluorescence and a 10cm plate for Western analysis as described previously, and developed using the primary anti-huntingtin antibody, 675. The cells were induced with doses of pon A at 0, 1, 2, 5, 10, 20 μ M for 48 hours. The immunofluorescence of MT clone 57 2ad and WT clone 21 1 h, showed increasing intensity of fluorescence staining with increasing doses of pon A up to 20 μ M

(Figs. 3.9a and 3.10a). The Western blots of 58 2a d and 21 1 h also demonstrated an increasing intensity of the predicted 36kDa (MT) and 29.5kDa (WT) bands up to 20 μ M (Figs. 3.9b and 3.10b). A similar pattern of positive immunofluorescence occurred with all doses of pon A between 1 and 20 μ M with clones 21 2 c and 57 2 e (Figs. 3.11a and 3.12a). The Western blot also demonstrated a predicted band at 29.5kDa (21 2 c) and 36 kDa (57 2 e), that was equal in intensity at all concentrations of pon A (Figs. 3.11b and 3.12b). The optimum expression, i.e. the maximum induction with the smallest dose of pon A and solvent, DMSO, for the clones was 5 μ M for 48 hours.

In order to determine the effects of the length of exposure to pon A on expression, the 2 WT and 2 MT clones (21 1 h and 2 c, 57 2a d and 2 e) used in the dose-dependence studies described above, were cultured for immunofluorescence and Western analysis for 2 weeks. The medium was replaced (with and without 5 μ M pon A) every 48 hours. Data from Invitrogen (Paisley, UK) indicates that pon A retains 70% activity at 48 hours and this decreases to 30% at 72 hours. Figs. 3.13 and 3.14 demonstrate the immunofluorescence and Western blots developed with Ab675 of representative WT

Fig. 3.9

Fig. 3.10

Fig. 3.11.

Fig. 3.12

Fig. 3.13.

Fig 3.14.

(21 2 c) and MT (58 2 e) clones. The immunofluorescence showed that by day 12 the intensity and number of positive cells was reducing in all clones and that by day 18 there was less than approximately 10% intensely positive staining cells. This was mirrored in the Western blots where there was a more obvious earlier reduction in intensity of the predicted bands by day 4 and by day 18 the Western blot was similar to untreated cells i.e. DMSO only.

3.7. Time-dependent expression of alpha-synuclein

A similar Ecdysone-based model using EcR HEK 293 cells transfected with pIND containing alpha-synuclein with the A53T point mutation has been described (Tabrizi et al 2000). To investigate whether the time-dependent effects of pon A were similar in this model, and therefore due to the model system rather than an effect of the construct, a time-dependent experiment was performed similar to the one described above using the A53T alpha-synuclein HEK 293 model. Fig. 3.15. demonstrates the Western blots which were developed with an anti-haemagglutinin (HA) antibody to a tag at the C-terminus of the construct. It shows that expression of the predicted construct was stable up to 12 days of pon A induction and that there was a slight reduction in the intensity of the band with time of the wild-type alpha-synuclein versus the mutant which appeared to continue to express similar levels up to day 12.

3.8. Subcellular localisation studies

A panel of primary antibodies to components of subcellular organelles (Table. 2.2 A) and the anti-N-terminal huntingtin antibody, Ab675, were used to perform double immunofluorescence on one WT (21 2 c) and one MT (57 2 e) clone, in order to localise Fig. 3.15.

subcellular expression of the construct (Section 2.2.5. for method). These clones were treated with and without 5 μ M pon A for 48 hours prior to processing for immunofluorescence. Fluorescence was detected using a confocal microscope and Figs. 3.16-3.18 demonstrate the pattern of staining observed in the WT clone (21 2 c) and Figs. 3.19-3.21 in the representative MT clone (57 2 e). Confocal microscopy confirmed that the central staining with Ab675 in the pon A-treated cells was nuclear and not dense cytoplasmic staining as viewed from conventional immunofluorescence (Solid arrows in Figs. 3.16-3.21). The COX 1 staining was cytoplasmic and punctate and accumulated in the indentation formed by the typical kidney-shaped nucleus of HEK 293 cells (Dotted

arrow in Figs. 3.16a and 3.19a). There was no difference in distribution or intensity of the COX 1 staining in the pon A-treated and untreated cells. The yellow arrows in Figs. 3.16a and 3.19a demonstrate that there was partial co-localisation between COX 1 and Ab675 staining in MT and WT clones especially in a perinuclear distribution. The Golgi staining also tended to accumulate in the nuclear indentation of the cells in the cytoplasm but there were no clear differences between the MT and WT treated and untreated cells and no evidence of co-localisation (Figs. 3.16b and 3.19b).

Anti-LAMP antibody labels lysosomes and produced a fine granular cytoplasmic stain that was similar to the 675 stain but there was no evidence of co-localisation in treated or untreated cells (Figs. 3.17a and 3.20a). Figs. 3.17b and 3.20b demonstrate that vesicle-associated membrane protein (VAMP) staining was punctate and cytoplasmic and colocalised with 675. Fig. 3.18a demonstrates that synaptophysin had a weak cytoplasmic punctate staining with and without pon A in the WT clone but had intense staining in some cells in pon A treated MT clones (Fig. 3.21a). In some pon A treated cells, there was punctate staining with synaptophysin which weakly colocalised with

Fig 3.16.

Fig. 3.17.

Fig 3.18.

Fig. 3.19.

Fig 3.20

Fig. 3.21.

punctate 675 staining (Dotted arrows in Figs. 3.18a and 3.21a). There was very weak cytoplasmic synaptophysin staining of untreated cells. The association of WT and MT htt with VAMP and synaptophysin was unlikely to be non-specific as demonstrated in Figs. 3.16 a and b and Fig. 3.17 a as well as Figs. 3.19a and b and Fig. 3.20a, where there was no co-localisation with LAMP or Golgi network antibodies. Figs. 3.18b and 3.21b demonstrate that ubiquitin staining was very weak in both pon A treated and untreated cells and there was no evidence of ubiquitin positive inclusion formation.

3.9. Cell Proliferation

Cell proliferation was studied using the Aqueous One Cyt96 Cell Proliferation Assay (Promega) as described in Section 2.13. A pilot experiment was performed to determine the length of incubation in the MTS solution before the absorbance was measured and the optimum number of cells to plate at the start of the experiment so that there was an exponential increase in cell number that was within the limits of detection at both extremes of the plate reader. The data from these pilot studies is not shown but suggested that the plates were optimally read two hours after incubation with MTS. The optimum concentration of cells was 500/well. Subsequently, five WT (21 1 h, 2a 2b, 2c, and 2 d), five MT (57 1f, 1g, 2ad, 2ae, and 2e) and 5 pIND 0 (1-5) clones were analysed and the mean absorbance of the WT, MT and pIND 0 clones was plotted against time. Fig. 3.22. demonstrates that DMSO alone did not inhibit cell growth but pon A inhibited cell growth in all clones equally as can be seen in Fig. 3.22 C compared with 3.22 A and B, and also in 3.22 D, E, and F comparing the diamond points (pon A) versus the DMSO (square) and cells only (triangle). There was also an apparent reduction in cell growth with the MT versus WT and WT versus pIND 0 clones as can be seen in Figs. 3.22 A-C. When the graphs were adjusted for starting cell numbers and the rate of cell

Fig 3.22.

Fig. 3.23.

growth expressed as a percentage of the initial cell count versus time (Fig. 3.23.) there was no gross difference in the rate of growth between pIND 0, WT and MT clones (Fig. 3.23 A, B and C). It was confirmed that there was a reduction in cell growth caused by 5 μ M pon A (Fig. 3.23 D, E and F) which was similar in pIND0, 21 CAG and 57 CAG clones and therefore independent of N-terminal htt expression and CAG repeats.

3.10. Mitochondrial function

Mitochondrial function was measured in five WT (21 1 h, 2 a 2 b, 2 c, and 2 d), five MT (57 1f, 1g, 2a d, 2a e, and 2 e) and five pIND 0 (1-5) clones with and without 5 μ M pon A

induction for 48 hours as described in Section 2.5. All assays were performed blinded. Table 3.3. and Figs. 3.24. and 3.25. show the enzyme specific activities and the ratio of these activities to citrate synthase (CS) enzyme specific activity or “CS ratio” with and without pon A induction. There was a significant reduction of 9% in complex II/III CS ratios in the untreated versus treated MT clones ($p=0.05$) (Fig. 3.25). There were no other significant differences between the treated and untreated clones in all cell types. For each of the 5 pIND 0, WT and MT clones, the pon A treated activities and ratios were subtracted from the untreated values to obtain the difference in activity related to pon A (Figs 3.26a and b and Table 3.4). There was no significant difference in either the CS ratios or the specific activities between WT, MT and pIND0 clones (Fig. 3.26c). There was a trend for lower specific activities in WT and MT clones for complexes II/III and IV versus pIND 0 (Fig. 3.26a) but this did not reach statistical significance and was not present when CS-corrected for total mitochondrial numbers (Fig. 3.26b).

Enzyme/Clone	pIND 0	pIND 0	WT	WT	MT	MT
Pon A	+	-	+	-	+	-
I	80.0	70.3	104.0	90.5	73.4	70.6
(nmols/mg/min)	± 11.3	± 8.2	± 19.0	± 19.0	± 10.0	± 9.2
II/III (nmols/mg/min)	260	259	271	301	223	256
	± 34	± 29	± 26	± 53	± 17	± 26
IV (nmols/mg/min)	7.90	7.71	8.86	9.19	7.62	8.68
	± 0.58	± 0.47	± 1.06	± 1.33	± 0.91	± 0.83
CS x 10	814	898	919	992	779	984
(nmols/mg/min)	± 46	± 88	± 89	± 110	± 58	± 80
I (CS ratio)	0.101	0.082	0.120	0.092	0.119	0.091
	± 0.018	± 0.014	± 0.026	± 0.016	± 0.057	± 0.046
II/III (CS ratio)	0.317	0.288	0.297	0.299	0.286	0.260
	± 0.029	± 0.014	± 0.018	± 0.028	± 0.010	± 0.006
IVx10 ⁻² (CS ratio)	0.972	0.877	0.978	0.923	0.966	0.885
	± 0.047	± 0.062	± 0.115	± 0.010	± 0.088	± 0.046

Table 3.3 Specific enzyme activities and CS ratios for WT, MT and pIND 0 clones \pm SEM

(Figs. 3.24 and 3.25.).

Enzyme	pIND 0	Wild-type	Mutant
I (nmols/mg/min)	9.67 \pm 6.36	14.0 \pm 15.3	2.77 \pm 4.69
II/III (nmols/mg/min)	1.55 \pm 23.6	-30.2 \pm 36.4	-30.7 \pm 14.3
IV (nmols/mg/min)	1.84 \pm 7.83	-3.36 \pm 10.5	-10.06 \pm 6.25
CS x 10 (nmols/mg/min)	-8.45 \pm 8.21	-7.31 \pm 9.65	-20.5 \pm 8.42
I (CS ratio)	0.019 \pm 0.007	0.027 \pm 0.012	0.028 \pm 0.01
II/III (CS ratio)	0.028 \pm 0.023	-0.002 \pm 0.020	0.026 \pm 0.011
IV x 10 ⁻² (CS ratio)	0.085 \pm 0.036	0.055 \pm 0.042	0.081 \pm 0.048

Table 3.4. Mean pon A-induced differences in specific enzyme activities and CS ratios

(pon A+ minus pon A-) for WT, MT and pIND 0 clones \pm SEM (Fig. 3.26.).

Fig. 3.24.

Fig. 3.25.

Fig. 3.26.

3.11. Aconitase function

Aconitase can be used as an indirect measure of free radical damage especially by peroxynitrite. Aconitase activity was measured in five WT (21 1 h, 2a 2b, 2c, and 2 d), five MT (57 1f, 1g, 2ad, 2ae, and 2e) and 5 pIND 0 (1-5) clones using the technique described in Section 2.5.5. following induction with and without 5 μ M pon A for 48 hours. Fig. 3.27a. and Table 3.5. demonstrate the mean specific aconitase activities in pon A treated and untreated clones. There was no significant difference between the activities in treated and untreated MT, WT or pIND 0 clones (Fig. 3.27a).

Cell Type	Mean specific aconitase activity (nmols/mg/	Mean specific aconitase activity (nmols/mg/
	min) \pm SEM	min) \pm SEM
Pon A	+	-
pIND 0	9.30 \pm 1.16	7.49 \pm 0.68
WT	10.1 \pm 1.3	8.43 \pm 0.30
MT	7.81 \pm 0.81	6.38 \pm 0.76

Table 3.5. Mean specific aconitase activities for 5 WT, 5 MT and 5 pIND 0 clones \pm SEM (Fig. 3.27a).

Fig. 3.27b and Table 3.6. demonstrate the mean pon A-induced difference in specific aconitase activities between treated and untreated clones i.e. pon A–DMSO treated

clones. Table 3.6. demonstrates that there was a trend for lower activities in the WT than pIND 0 and in the MT versus WT but there was no significant differences (Fig. 3.27b). There was also an increase in aconitase activity in pIND 0, WT and MT clones treated with pon A. This may have been caused by an induction of aconitase activity by pon A.

Fig 3.27.

Cell Type	Mean ponA-induced difference in specific activity (nmols/mg/min)
pIND 0	1.82±1.34
21 CAG	1.67±1.40
58 CAG	1.43±0.460

Table 3.6. Mean pon A-induced difference in specific aconitase activities for 5 WT, 5 MT and 5 pIND 0 clones ± SEM (Fig. 3.27b).

3.12. Toxicity of construct expression and in response to cellular toxins

Cell death was analysed using the lactate dehydrogenase (LDH) release assay to express the released LDH activity as a percentage of the total LDH activity within cells grown under identical conditions as described previously in Section 2.14.3. The five WT (21 1 h, 2a 2b, 2c, and 2 d), five MT (57 1f, 1g, 2ad, 2ae, and 2e) and 5 pIND 0 (1-5) clones were used for these experiments and were grown in low glucose (1g/L) growth medium in order to metabolically stress the cells and maximize the impact of any mitochondrial dysfunction. Initial pilot experiments were performed to determine the optimum concentration of cells to add to the 12-well plates. Cells from three representative clones (pIND 0 1, 21 2 c and 57 2 e) were plated at 1×10^4 , 5×10^4 , 1×10^5 , 2×10^5 and 5×10^5 per well at approximately 5pm and allowed to settle overnight. The next morning, the cells were treated with and without 5µM pon A. After 48 hours the medium was aspirated and replaced with the fresh medium with and without 5µM pon A. The cells were observed by phase-contrast microscopy every day and an estimation was made of the density of cells.

It was found that after 48 hours, a concentration of cells at 2×10^5 /well produced approximately 30-50% confluency with pon A and 40-70% without pon A in pIND 0 WT and MT clones.

3.12.1. Background cell death

Prior to adding toxins to the clones, the background cell death was assessed. The five MT, five WT and pIND 1-4 clones were plated into 12-well plates at 2×10^5 /well left overnight, and 1 ml. of fresh medium with and without $5 \mu\text{M}$ pon A was added the following morning. The medium was carefully aspirated after 48 hours and replaced with 1ml of fresh medium with and without $5 \mu\text{M}$ pon A. A separate well with medium only and no cells was also incubated for the next 48 hours to use as control medium. After 96 hours following induction, an LDH assay was performed as described in Section 2.14.3. Fig. 3.28 A and Table 3.7. demonstrate that there was a mean pon A-associated cell death of $-1.63\% \pm 0.406$ ($p=0.0024$) in the pIND 0 clones, $2.85\% \pm 0.711$ ($p=0.058$) in the WT clones and $-0.0491\% \pm 0.364$ ($p=0.95$) in the MT clones. The negative percentages means that there was an excess cell death in the DMSO-treated clones versus the ponA-treated clones. Fig. 3.28 B and Table 3.7. demonstrate the mean percentage pon A-induced cell death for pIND 0, WT and MT clones. There was a significant reduction in pon A-induced cell death in pIND 0 versus WT clones ($p=0.0014$) and versus MT clones ($p=0.023$) (Fig. 3.28 B). There was also a significant reduction in cell death in MT versus WT clones ($p=0.0067$) (Fig. 3.28 B). Table 3.7. also demonstrates that the percentage cell death associated with or without pon A treatment was greater in the WT (1.59-9.58%) and MT (2.97-5.84%) than the pIND 0 clones (0.39-2.9%).

Fig. 3.28.

	% Cell Death Pon A +	% Cell Death Pon A -	Pon A-induced cell death (pon A + minus pon A -)	Mean % cell death±SEM
pIND 0 1	1.08	1.57	-0.49	
pIND 0 2	0.67	2.90	-2.22	-1.63± 0.41
pIND 0 3	0.53	2.15	-1.62	
pIND 0 4	0.39	2.59	-2.20	
Mean	0.67	2.30	-1.63	
21 1 h	2.59	1.59	1.00	
21 2 a	4.81	1.77	3.03	
21 2 b	9.58	4.29	5.29	2.85± 0.71
21 2 c	4.51	2.52	2.00	
21 2 d	6.59	3.68	2.90	
Mean	5.62	2.77	2.85	
57 1 f	5.35	4.34	1.01	
57 1 g	2.97	3.15	-0.18	
57 2a d	3.37	3.51	-0.14	-0.05± 0.36
57 2a e	4.62	5.84	-1.22	
57 2 e	5.36	5.07	0.29	
Mean	4.33	4.38	-0.05	

Table 3.7. Background % cell death in 4 pIND 0, 5 WT and 5 MT clones with and without 5µM pon A for 96 hours.

3.12.2. Toxin-induced cell death

The relative toxicity of four toxins (malonate, cyanide, paraquat and lactacystin) to the five WT (21 1 h, 2a 2b, 2c, and 2 d), five MT (57 1f, 1g, 2ad, 2ae, and 2e) and 5 pIND 0 (1-5) clones following 48 hours induction with and without 5µM pon A was investigated. The concentration of toxin to use in subsequent experiments was determined by plating pIND 0 1 clone at 2×10^5 per well in 12-well plates and, allowing the cells to settle overnight. The cells were then treated for two days with growth medium and DMSO (5µL/ml of medium) and the medium was carefully aspirated and replaced with fresh medium containing a broad range of toxin doses (see below for details on individual

toxins). Cell death was visually assessed using phase-contrast microscopy after 48 hour toxin exposure and the concentration which produced approximately 30-50% cell death was taken as a dose around which to base a subsequent toxicity curve. This range was taken, because of concerns that the combination of pon A and a toxic would produce rapid and early cell death. For each toxin a similar experiment was then repeated, except with clones pIND 0 1, 21 2 c and 57 2 e, and rather than visually assessing the degree of toxicity after 48 hours the samples were processed for the LDH assay.

3.12.3. Toxicity experiments

3.12.3.1. Malonate

Malonate is a reversible inhibitor of complex II of the mitochondrial respiratory chain. A toxicity curve (data not shown) using malonate at doses between 0 and 200mM suggested that 150mM of malonate produced between 20-40% cell death at 48 hours in the three clones. Five WT (21 1 h, 2a 2b, 2c, and 2 d), five MT (57 1f, 1g, 2ad, 2ae, and 2e) and 5 pIND 0 (1-5) clones were induced with and without 5 μ M pon A for 48 hours and subsequently a further 48 hours with 150mM malonate. An LDH assay was performed on all clones as described in Section 2.14.3. and performed a total of four times. Table 3.8. demonstrates the combined results from these 4 experiments. The mean % cell death for each clone with (column 2 Table 3.8.) and without ponA (column 3 Table 3.8.) induction and the mean % pon A-induced cell death (pon A –DMSO) for each clone (columns 4 Table 3.8.) were calculated. Fig. 3.29 A demonstrates that there was a significant increase in the cell death between treated and untreated pIND 0, WT and MT clones (pIND 0 $p=0.0007$, WT $p=0.0337$, MT $p=0.0018$). Fig. 3.29 B demonstrates that there was a trend

for greater toxicity in MT versus WT versus pIND 0 clones but that this was not significant.

Clone	Mean % Cell death pon A	Mean % Cell death DMSO	Pon A-induced % cell death (pon A – DMSO)	Mean pon A-induced % cell death±SEM
pIND 0 1	31.8	15.9	15.9	
pIND 0 2	31.3	11.8	19.5	
pIND 0 3	25.7	16.9	8.78	12.3±2.84
pIND 0 4	32.3	18.1	14.1	
pIND 0 5	26.5	23.2	3.37	
21 1 h	55.1	32.2	23.0	
21 2 a	25.3	14.4	10.9	
21 2 b	33.1	24.3	8.74	15.5±2.95
21 2 c	35.1	13.0	22.1	
21 2 d	34.4	21.6	12.8	
58 1 f	40.9	22.5	18.5	
58 1 g	32.0	15.1	16.9	
58 2a d	35.0	17.2	17.8	17.5±3.08
58 2a e	49.8	23.0	26.8	
58 2 e	33.8	26.3	7.46	

Table 3.8. Malonate-induced % cell death in 5 pIND 0, 5 WT and 5 MT clones with and without 5µM pon A for 96 hours and malonate (150mM) for 48 hours.

Fig. 3.29.

3.12.3.2. Cyanide

Cyanide is an irreversible inhibitor of complex IV of the mitochondrial respiratory chain. A toxicity curve using cyanide at doses between 0 and 50mM suggested that 20mM cyanide produced approximately 40-80% cell death. Five WT (21 1 h, 2a 2b, 2c, and 2 d), five MT (57 1f, 1g, 2ad, 2ae, and 2e) and 5 pIND 0 (1-5) clones were induced with and without 5 μ M pon A for 48 hours and subsequently a further 48 hours with 20mM cyanide. An LDH assay was performed on all clones as described in Section 2.14.3. and performed a total of four times. Table 3.9. demonstrates the combined results from these 4 experiments. The mean % cell death for each clone with (column 2 Table 3.9.) and

Clone	Mean % Cell death pon A	Mean % Cell death DMSO	Pon A-induced % cell death (pon A – DMSO)	Mean pon A-induced % cell death±SEM
pIND 0 1	43.5	60.9	-17.3	
pIND 0 2	46.8	60.1	-13.4	
pIND 0 3	42.7	59.3	-16.6	-16.2±1.41
pIND 0 4	34.3	54.9	-20.6	
pIND 0 5	43.0	55.9	-12.9	
21 1 h	43.8	59.1	-15.3	
21 2 a	34.6	66.7	-32.2	
21 2 b	43.9	69.7	-25.8	-21.0±3.42
21 2 c	32.2	48.5	-16.4	
21 2 d	38.2	53.4	-15.3	
57 1 f	48.1	78.3	-30.1	
57 1 g	47.9	79.6	-31.8	
57 2a d	46.1	65.5	-19.4	-27.9±4.59
57 2a e	24.8	66.6	-41.8	
57 2 e	46.35	62.6	7.46	

without ponA (column 3 Table 3.9.) induction and the mean % pon A-induced cell death (pon A –DMSO) for each clone (column 4 Table 3.9.) were calculated. Fig. 3.30 A demonstrates that there was a significant reduction in cell death with cyanide in all pon A treated clones (pIND 0 p=0.0001, WT p=0.0019, MT p=0.0012). Fig. 3.30 B demonstrates that there was a significant (p=0.0406) reduction in cell death in MT cells versus pIND 0 clones.

Table 3.9. Cyanide-induced % cell death in 5 pIND 0, 5 WT and 5 MT clones with and without 5µM pon A for 96 hours and cyanide (20mM) for 48 hours.

Fig. 3.30.

3.12.3.3. Paraquat

Paraquat is an intracellular generator of the free radical, superoxide. A toxicity curve using paraquat at doses between 0 and 5 mM suggested that 5mM of paraquat produced approximately 20-50% cell death. Five WT (21 1 h, 2a 2b, 2c, and 2 d), five MT (57 1f, 1g, 2ad, 2ae, and 2e) and 5 pIND 0 (1-5) clones were induced with and without 5 μ M pon A for 48 hours and subsequently for a further 48 hours with 5 mM paraquat. An LDH assay was performed on all clones as described in Section 2.14.3. and performed a total of seven times. Table 3.10. demonstrates the combined results from these 7 experiments. The mean % cell death for each clone with (column 2 Table 3.10.) and without ponA (column 3 Table 3.10.) induction and the mean % pon A-induced cell death (pon A – DMSO) for each clone (columns 4 Table 3.10.) were calculated. Fig. 3.31 A demonstrates that there was a significant increase in cell death with paraquat in pIND 0 and MT pon A treated clones (pIND 0 $p=0.0015$ and MT $p=0.0375$) but not in WT clones ($p=0.2486$). Fig. 3.31 B demonstrates that paraquat produced a significant increase in cell death in MT (23.5% \pm 3.68) versus pIND 0 (11.7% \pm 1.83) clones ($p=0.0350$). There was also a trend for WT (16.0% \pm 4.65) clones to also demonstrate increased cell death but this was not significant ($p=0.429$).

Clone	Mean % Cell death pon A	Mean % Cell death DMSO	Pon A-induced % cell death (pon A – DMSO)	Mean pon A-induced % cell death±SEM
pIND 0 1	37.9	22.6	15.3	
pIND 0 2	30.4	22.7	7.75	
pIND 0 3	30.4	21.4	8.98	11.7±1.83
pIND 0 4	42.7	25.8	16.9	
pIND 0 5	33.2	23.6	9.68	
21 1 h	80.2	80.9	-0.670	
21 2 a	60.68	33.2	27.3	
21 2 b	60.5	41.1	19.43	16.0±4.65
21 2 c	37.7	18.3	19.4	
21 2 d	71.6	57.1	14.5	
57 1 f	75.6	48.8	26.8	
57 1 g	69.8	36.4	33.4	
57 2a d	68.5	43.3	25.2	23.5±3.68
57 2a e	55.2	34.2	21.0	
57 2 e	30.7	19.5	11.1	

Table 3.10. Paraquat-induced % cell death in 5 pIND 0, 5 WT and 5 MT clones with and without 5µM pon A for 96 hours and paraquat (5mM) for 48 hours.

Fig 3.31

3.12.3.4. Lactacystin

Lactacystin is a proteasomal inhibitor. A toxicity curve using lactacystin at doses between 0 and 10 μ M suggested that with 7.5 μ M of lactacystin produced approximately 20-50% cell death. Five WT (21 1 h, 2a 2b, 2c, and 2 d), five MT (57 1 f, 1 g, 2a d, 2a e, and 2 e) and 5 pIND 0 (1-5) clones were induced with and without 5 μ M pon A for 48 hours and subsequently for a further 48 hours with 7.5 μ M paraquat. An LDH assay was performed on all clones as described in Section 2.14.3. and performed a total of seven times. Table 3.11. demonstrates the combined results from these 7 experiments. The mean % cell death for each clone with (column 2 Table 3.11.) and without ponA (column 3 Table 3.11.) induction and the mean % pon A-induced cell death (pon A –DMSO) for each clone (columns 4 Table 3.11.) were calculated. Fig. 3.32 A demonstrates that there was no significant change in cell death with lactacystin in all pon A treated versus untreated clones (pIND 0 p=0.894, WT p=0.0544 and MT p=0.747). Fig. 3.32 B demonstrates that lactacystin treatment showed a significant increase in cell death in MT (1.57 \pm 1.22%) clones versus WT (-5.62% \pm 1.63) (p=0.0097) and a significant decrease between in cell death in WT (-5.62% \pm 1.63) versus pIND 0 (-0.138% \pm 0.352) (p=0.030). There was trend for slightly greater cell death in MT versus pIND 0 but this was not significant (p=0.252).

Clone	Mean % Cell death pon A	Mean % Cell death DMSO	Pon A-induced % cell death (pon A – DMSO)	Mean pon A-induced % cell death±SEM
pIND 0 1	20.7	21.4	-0.715	
pIND 0 2	18.9	18.7	0.196	
pIND 0 3	19.8	19.0	0.793	-0.138±0.352
pIND 0 4	20.2	20.0	0.201	
pIND 0 5	17.0	18.1	-1.16	
21 1 h	22.6	33.8	-11.2	
21 2 a	18.7	20.2	-1.50	
21 2 b	21.5	25.2	-3.65	-5.62±1.63
21 2 c	18.9	23.9	-5.00	
21 2 d	22.7	29.6	-6.82	
57 1 f	33.1	28.9	4.28	
57 1 g	29.3	25.0	4.25	
57 2a d	27.24	27.6	-0.37	1.57±1.22
57 2a e	20.9	19.4	1.52	
57 2 e	11.8	13.6	-1.85	

Table 3.11. Lactacystin-induced % cell death in 5 pIND 0, 5 WT and 5 MT clones with and without 5µM pon A for 96 hours and lactacystin (7.5µM) for 48 hours.

Fig. 3.32

CHAPTER 4

Results

A constitutive EYFP-tagged

full-length htt

SH-SY5Y cell model

4.1. Plasmids

The pEYFP-C1 (Clontech, San Jose, CA, USA) encodes an enhanced yellow fluorescent protein (EYFP) 5' to the multiple cloning site. The EYFP-C1 plasmids were a kind donation by Dr. Lesley Jones, University of Cardiff, UK. Details of the donated plasmids are in Section 2.3.1. and Fig. 2.2. pcDNA 3.1 (Invitrogen, UK) is a 5.4kb vector derived from pcDNA3 and is designed for high-level transient or stable expression in mammalian hosts. It also contains a multiple cloning site and a neomycin resistance gene.

4.2. Transfections

SH-SY5Y cells were transfected with the EYFP-C1 containing 88 CAGs in FL htt (MT), 23 CAGs in FL htt (WT), and EYFP-C1 without any insert (EYFPcon). Clones were grown and harvested as described in section 2.3.3. using G418 at 250µg/ml of medium for selection (Clontech). Thirty WT clones and thirty MT clones were taken forward for further analysis. Four EYFP-C1 clones with no construct were also investigated and were labeled "EYFPcon". SH-SY5Y cells transfected with the pcDNA 3.1 plasmid and contained no construct were used as a cloned control cell line with G418 selection.

4.3. Expression of constructs on fluorescence microscopy

Cells from each cell line were processed for fluorescence microscopy as described in section 2.2.5. The clones were named such that they were either "23" or "88" representing the WT and MT number of CAG repeats, the next number represented the plate that the clone was taken from and the final number was the number of the clone from the plate. Figs. 4.1A and B demonstrate clones 23 1 1, 23 3 3, 23 6 7 and 23 7 2 and 88 1 3, 88 2 8,

88 2 9, and 88 2 11 on fluorescence microscopy using the FITC filter, which gave a bright green homogenous cytoplasmic fluorescence from all the WT and MT cells. Cells without fluorescence were rare in the clones that were selected. Fig. 4.1. C demonstrates a representative positive EYFP control clone, EYFPcon 2 2, without any construct, which displayed intense homogeneous nuclear (Arrows in fig. 4.1. C) and cytoplasmic fluorescence, and a typical pcDNA3.1 control clone (pcDNA3.1 1) which demonstrated background fluorescence only. The nuclear translocation of the EYFP tag in EYFPcon clones, which was absent in the WT and MT EYFP clones, was considered to render the EYFPcon clones inappropriate as controls. PcDNA3.1 clones were therefore used as control cells. Table 4.1. lists the clones isolated based on positive fluorescence. The clones 23 1 1, 23 3 3, 23 6 7, 23 7 2, 23 7 7, 23 7 8 and 23 7 10 and 88 1 3, 88 2 8, 88 2 9, 88 2 11, 88 3 1, 88 3 3, 88 3 10 and 88 3 11 demonstrated greater than 99% of cells with EYFP fluorescence and were taken forward to Western blot analysis. There was no evidence of inclusion formation on fluorescence microscopy of the EYFP tag in any of the WT or MT clones. The MT clones took longer to reach confluence suggesting they grew slightly slower than the WT although this was not quantified experimentally. There were otherwise no clear differences between the WT and MT clones on fluorescence microscopy and no difference in the cellular morphology between the WT, MT, EYFPcon or pcDNA 3.1 clones. The MT and WT clones expressed similar intensities of EYFP fluorescence as assessed qualitatively on fluorescence microscopy.

Fig. 4.1.

Wild-type clones	Mutant clones	pcDNA 3.1	EYFPcon
23 1 1	88 1 3	pc DNA 3.1 1	EYFPcon 1 2
23 3 3	88 2 8	pc DNA 3.1 2	EYFPcon 2 2
23 6 7	88 2 9	pc DNA 3.1 3	EYFPcon 3 1
23 7 2	88 2 11	pc DNA 3 .1 4	EYFPcon 3 2
23 7 7	88 3 1		
23 7 8	88 3 3		

23 7 10	88 3 10		
	88 3 11		

Table 4.1. WT, MT, pcDNA 3.1 and EYFPcon clones.

4.4. Western blots of EYFP clones

The 7 WT and 8 MT clones were prepared for Western Blot analysis as described in Section 2.9. The tris-acetate pre-cast gels (Invitrogen) were used because of the large size of the htt product (370kDa for WT htt EYFP and 377 kDa for MT EYFP) and the gels were run for three hours. The blots were probed with anti-EYFP antibody (1 in 1000) (Clontech). All WT and MT clones expressed cross-reactive bands to anti-EYFP (Fig. 4.2A and B). A single band at approximately 370kDa was apparent in the WT clones and there was no evidence of additional bands or material in the wells. The strongest expressing clones were 23 1 1, 6 7, 7 7 and 7 10. Clone 7 8 had the lowest levels of expression on Western blot. Of the 8 MT clones, four (88 1 3, 2 8, 2 9 and 2 11) expressed a single band at the predicted size of 377kDa (solid arrow in Fig. 4.2B), two (88 3 3 and 3 10) expressed an intense band at 335kDa. (dashed arrow in Fig. 4.2B) and a faint band at 377kDa.(not seen in Fig. 4.2B)and two (88 3 1 and 3 11) expressed bands at 377kDa and 335 kDa. The anti-EYFP antibody did not detect any construct expression from clone pcDNA 3.1 1. All MT clones demonstrated similar levels of construct expression although clone 88 1 3 was consistently stronger.

Fig. 4.2.

To compare the relative mobility of the WT and MT EYFP expressed proteins with endogenous htt, 3 clones were separated in two groups on the same gel, and one half was probed with anti-EYFP and the other half with Ab675 (Fig. 4.2C). The WT htt EYFP band (red arrow in Fig. 4.2C) migrated slightly further than the MT htt EYFP band (black arrow in Fig. 4.2C) and both migrated slightly less than the Ab675 cross-reactive bands of endogenous htt (dotted arrow in Fig. 4.2C). The additional EYFP band identified in some of the MT clones, migrated the fastest (dashed arrow in Fig. 4.2C). Neither WT nor MT

EYFP htt were recognised by Ab675 (dotted arrow in Fig. 4.2C). Ab675 recognises the first 9 amino acids of htt and the anti-EYFP antibody recognized the N-terminal EYFP tag. The absence of cross-reactivity of WT and MT htt EYFP with Ab675 could therefore have been caused by blocking of the binding site by the EYFP N-terminal tag.

To clarify the relative mobilities of the htt species, four MT clones and four WT clones that did not express an additional band, were separated and probed with anti-EYFP and Ab675 simultaneously (Fig. 4.2D). The WT and MT htt EYFP clones demonstrated a construct htt band (red arrow for WT and black arrow for MT in Fig. 4.2D) and an endogenous htt band (dotted arrow in Fig. 4.2D). The representative pcDNA3.1 clone demonstrated only an endogenous htt band (dotted arrow in Fig. 4.2D). The difference in size between the WT and MT htt EYFP bands is also demonstrated and would be compatible with the predicted 7.1 kDa difference between WT and MT constructs.

4.5. Anti-huntingtin antibodies and immunofluorescence

The anti-huntingtin antibodies and their respective epitopes can be found in Fig. 2.1. and Table 2.1. In order to characterise the location of different sized fragments of htt in both WT and MT htt EYPC clones, mitotic cells from clones 23 1 1 and 88 1 3, as representative WT and MT clones, were developed with the panel of htt antibodies. The immunofluorescence is shown in Fig. 4.3. All htt antibodies showed diffuse cytoplasmic co-localisation with the EYFP fluorescent tag in WT and MT clones. Antibody 7667 consistently demonstrated uniform punctate nuclear staining in the WT clones which was more prominent than in MT cells (solid arrows in Fig. 4.3). This also occurred in the other WT and MT clones (data not shown). There were occasional rare cytoplasmic inclusions

noted only in the MT cell lines, as seen with antibody 2168 in Fig. 4.3 (round stippled arrow).

Pc DNA 3.1 clones demonstrated cytoplasmic staining that was less intense and more punctate than the htt transfected clones with all antibodies. Antibodies EM48, Ab2166 and Ab2168 stained much less intensely than Ab7668, Ab7667, and Ab7666. There was punctate nuclear staining with antibody Ab7667 similar, but more intense, than the EYFP htt-transfected cells and a less intense nuclear pattern with Ab7668 (Fig. 4.3 solid arrow). There was also a collection of punctate staining in a perinuclear location with Ab7667 and Ab7668 antibodies which was more difficult to observe in EYFP htt-transfected clones, possibly due to strong cytoplasmic staining (Fig. 4.3 stippled square arrows). Ab7666 demonstrated a diffuse cytoplasmic staining in controls similar to WT and MT clones.

4.6. Characterisation of the anti-EYFP cross-reactive bands in MT clones

The additional bands in some MT htt EYFP clones were further characterised on Western blotting using anti-huntingtin antibodies to define which epitopes were cross-reactive.

The most C-terminal anti-htt antibody, Ab7666 (2703-2911aa), did not detect

Fig. 4.3.

the additional lower molecular weight band in clones 88 3 1, 3 3, 3 10 and 3 11 (Fig. 4.4. A) but did recognize both endogenous htt (dotted arrow) and WT (red arrow) and MT (black arrow) htt bands. Ab2168 (2146-2541aa) and Ab7667 (1844-2131aa) detected endogenous htt (round stippled arrow) as well as the expected (black arrow) and additional (square stippled arrow) MT htt bands (Fig. 4.4. B and C). This suggests that the additional band had lost the most C-terminal epitope of Ab7666 (aa2703-2911) but had

retained the epitope recognised by Ab2168 (aa2146-2541). The additional band was therefore a truncated form of htt with the C-terminal between aa 2541 and 2703.

The WT htt band would be predicted to migrate at 370kDa, the MT htt band at approximately 377kDa and endogenous htt at 348kDa. The additional band in some of the MT clones would therefore be predicted to be approximately 335kDa with loss of approximately 320aa at the C-terminus.

Fig. 4.4.

4.7. Sequencing of 5' and 3' ends of the inserted cDNA in each clone

DNA from WT htt clones 1 1, 3 3, 6 7, 7 2, 7 7, 7 8 and 7 10 and MT htt clones 1 3, 2 8, 2 9 and 2 11 was PCR amplified using the EYFP-F (sequencing from base -111) and RS2-R (reverse sequencing from base+282) primers (Section 2.4.7. for sequence of primers) to sequence the 5' junction between EYFP plasmid and the construct (Fig. 4.5A). The

products were run on an agarose gel as described in section 2.4.5. The predicted products, based on the correct insertion of the constructs at the restriction sites, were 393 base-pairs for WT clones and 588 base-pairs for MT clones. Fig. 4.6. demonstrates an approximately 400bp product from all the WT clones and an approximately 600bp product from all the MT clones. The PCR products were purified with Qiagen PCR clean-up kit and commercially sequenced by MWG biotech (Milton Keynes, UK). The WT constructs were found to be correctly sequenced and in frame for all clones. The MT constructs were also correctly sequenced and in frame for all clones. The sequencing of the CAG repeats could not precisely confirm the number of repeats in the MT clones as the sequencing reaction terminated in both directions before sequencing the whole of the repeat region. The PCR product size was still compatible with 88 CAG repeats and the sequencing reliably demonstrated over 75 CAGs i.e. MT range, in each clone (Fig. 4.7.A and B for sample sequence chromatograms).

DNA from WT htt clones 23 1 1, 3 3, 6 7, 7 2, 7 7, 7 8 and 7 10 and MT htt clones 88 1 3, 2 8, 2 9 and 2 11 were PCR amplified using the using the R2 and F3 primers to sequence the 5' junction between EYFP plasmid and the construct (Fig. 4.5B). The predicted 900bp PCR product was observed with all WT clones (Fig. 4.8A) and six out of eight of the MT clones (Fig. 4.8B) as well as from the parent WT and MT EYFP-C1 plasmids (Fig. 4.8C). Clones 88 3 3 and 3 10 did not demonstrate a 900bp band and this

Fig. 4.5.

Fig. 4.6.

Fig. 4.7. A.

Fig. 4.7. B.

Fig. 4.7. C.

Fig. 4.8.

would be consistent with the relative absence of a FL MT htt band on Western blotting and suggests that these clones contained 3' truncated cDNA. The R2/F3 PCR products were purified with Qiagen PCR clean-up kit and commercially sequenced by MWG biotech (Milton Keynes, UK). The correct 3' sequence and frame were found in all clones (Fig. 4.7C demonstrated sequence chromatograms for a representative WT clone, 23 3 3).

4.8. Selection of clones

Clones 23 1 1, 3 3, 6 7 and 7 2 and 88 1 3, 2 8, 2 9, and 2 11 were chosen as representative clones for WT and MT cell lines to perform subsequent detailed experiments. These clones demonstrated positive EYFP immunofluorescence, a predicted band on Western Blot analysis and the correct sequence at 5' and 3' ends of the integrated constructs. Clones 88 3 1, 3 3, 3 10 and 3 11 were not taken forward because of the uncertainty of the additional band on Western blotting which was probably due to a 3' truncated species of MT htt EYFP cDNA.

4.9. Differentiation of EYFP clones

4.9.1. Growth characteristics and IF of differentiated SH-SY5Y clones

Four MT, WT and pcDNA 3.1 clones were differentiated for 2, 7 and 14 days and processed for EYFP fluorescence microscopy as described in section 2.2.7. The WT clones demonstrated processes by day 2 and continued to develop complex networks of

processes by day 14 (stippled arrows in Fig. 4.9.). One WT clone (23 1 1) consistently demonstrated uniform nuclear fluorescence in approximately 50% of cells up to day 14 differentiation (solid arrows Fig. 4.9.). The other WT clones, especially 23 6 7, demonstrated inconsistent nuclear fluorescence (solid arrows Fig. 4.9). The MT htt clones demonstrated formation of processes by day 7 which were still present at day 14 (solid arrows Fig.4.10.). The MT clones formed shorter and thicker processes (stippled arrows Fig. 4.10.). There was an absence of nuclear fluorescence at all stages of differentiation in all MT clones. There was no evidence of inclusion formation in any of the clones within the two week study period of differentiation. The WT clones readily differentiated by day 2 compared to day 7 in the MT clones (Figs. 4.9 and 4.10). The WT clones (Fig. 4.11 A) also developed more interconnecting and complex networks of processes than the MT clones (Fig. 4.11B). The control clone pcDNA 3.1 1 differentiated by day 2 with complex networks of processes similar to WT clones (figures not shown) in the absence of fluorescence.

Fig 4.9.

Fig. 4.10.

Fig. 4.11.

4.9.2. Immunofluorescence and Western blots in differentiated clones

To investigate the effects of differentiation on processing of WT and MT EYFP htt and endogenous htt, the representative MT (88 1 3) and WT (23 1 1) clones and control cells (pcDNA3.1 1) were differentiated for two weeks with retinoic acid and then developed with the panel of anti-htt antibodies using the protocols previously described in sections 2.2.5, 2.2.6.1 and 2.2.7. Figs. 4.12-14 show the patterns of staining demonstrated with

anti-htt antibodies. These were similar to mitotic clones except for the following considerations. Firstly, antibody 7666 demonstrated a granular cytoplasmic pattern of staining (solid arrows in Figs. 4.12-14) with evidence of perinuclear accumulation in pcDNA 3.1, WT and MT clones (yellow arrows in figures 4.12-14) unlike in mitotic cells where there was greater uniformity of cytoplasmic staining and without perinuclear accumulation. Secondly, there was an increase in nuclear punctate staining with Ab7667 in differentiated versus cycling MT clones (Fig. 4.3 versus 4.13). This was also observed, to a lesser degree, in the WT clones (Fig. 4.3 versus 4.12).

To further investigate the effects of differentiation on processing of WT and MT EYFP htt and endogenous htt, the representative MT (881 3) and WT (23 1 1) clones and control cells (pcDNA3.1 1) were differentiated for three days with retinoic acid and processed for Western blotting and developed with anti-huntingtin antibodies. Fig. 4.15. A. demonstrates that following two weeks differentiation of 23 1 1 and 88 1 3 clones, there was a marked reduction in the intensity of the cross-reactivity of Ab675 (endogenous htt) and anti-EYFP (EYFP htt) on Western blots compared to mitotic 88 1 3 and pcDNA 3.1 cells with equal protein loading. Fig. 4.15. B. demonstrates the full Western blot of mitotic and 2 week differentiated 23 1 1, 88 1 3 and pcDNA 3.1 1 clones probed with Ab675 and anti-EYFP in parallel. There was no evidence of signal

Fig. 4.12.

Fig. 4.13.

Fig. 4.14.

Fig.4.15.

within the loading well with either Ab675 or anti EYFP in any of the clones which suggested that aggregates were not formed. Anti-EYFP probing demonstrated that there was loss of a 60 kDa band (red arrow) and a 100kDa band (round stippled arrow) in all the differentiated clones including pcDNA 3.1 1, suggesting that this was a non-specific change in cross-reactivity to anti-EYFP following differentiation. In the three differentiated clones tested (23 1 1, 88 1 3 and pcDNA 3.1 1) there was a gain of a band at 63kDa (yellow arrow in Fig.4.15.B) which was non-specific as it was present with

pcDNA 3.1 1. Ab675 demonstrated a reduction in endogenous htt expression in differentiated 23 1 1 and 88 1 3 (square stippled arrow Fig. 4.15. B) but not in differentiated pcDNA 3.1 1 clones and mitotic 88 1 3 cells, suggesting a reduction in endogenous htt expression in MT and WT EYFP clones following differentiation. To investigate the effects of more prolonged differentiation on inclusion formation and htt processing, 23 1 1, 88 1 3 and pcDNA 3.1 1 clones were differentiated for four weeks and a Western blot performed and probed with EM48, which preferentially recognises expanded polyglutamine tracts, and anti-EYFP in parallel on the same blot (Fig. 4.16). By 4 weeks differentiation, there was still ongoing WT and MT EYFP htt expression as recognised by anti-EYFP cross-reactivity (Fig. 4.16. red arrow). The intensity of the cross-reactivity to anti-EYFP, was less in the differentiated clones versus the mitotic 88 1 3 clone which was similar to that seen at 2 weeks differentiation. An additional band of approximately 90kDa was observed in the four week differentiated 23 1 1 clone with anti-EYFP (Fig. 4.16 yellow arrow) that was not observed at two weeks differentiation. This may have represented an N-terminal truncated species of WT EYFP htt that formed during differentiation. The EM48 antibody poorly recognised WT and MT EYFP htt expression (Fig. 4.16. dotted arrow on left of figure). Cross-reactivity to EM 48 at a position consistent with endogenous huntingtin was observed in all the differentiated clones greater than in the mitotic 88 1 3 clone (Fig. 4.16. blue arrow).

Fig. 4.16.

4.10. Treatment with lactacystin

4.10.1. Inclusion formation within mitotic WT and MT htt EYFP clones

Lactacystin causes UPS inhibition and therefore reduces the degradation of ubiquitinated protein. In order to investigate the effects of lactacystin on inclusion formation, WT and MT EYFP htt, as well as pcDNA 3.1, clones were plated out onto coverslips at 4×10^5 /well

of a 6-well plate and left to attach overnight. The cells were treated with 5 μ M lactacystin for 24 hours, and processed for fluorescence microscopy as previously described in Section 2.2.5. All 4 WT and MT htt EYFP clones treated with 5 μ M lactacystin demonstrated brilliant green perinuclear inclusions with EYFP fluorescence (Fig. 4.17. white arrows) which indented the nuclear membrane. The inclusions were not present in pcDNA 3.1 or untransfected SH-SY5Y cells (Fig. 4.17C). The inclusions were qualitatively more frequent in the WT clones than the MT clones and there was also qualitatively greater and earlier cell death in the MT clones and therefore fewer live cells at 24 hours. The Ab7667 antibody recognised the inclusions (Fig. 4.17. A and B yellow arrows) and this was confirmed by merging the two images to form yellow-green fluorescence (Fig. 4.17. A and B stippled arrows).

4.10.2. Subcellular localisation of inclusions

Four WT and four MT clones were plated out at 2x10⁵/well onto coverslips in a 6-well plate, left overnight to adhere, and treated for 24 hours with 5 μ M lactacystin and processed for immunofluorescence using the primary antibodies to localise subcellular compartments as shown in Table 2.2B.

Fig. 4.17.

The perinuclear inclusions co-localised to regions of strong COX 1 fluorescence (Fig. 4.18. A) but not to Golgi complex (Fig. 4.18. B). Subcellular compartment staining for pcDNA 3.1 is demonstrated in Fig. 4.19. except for ubiquitin which poorly stained. There was evidence of perinuclear COX 1 accumulation in the lactacystin-treated pcDNA 3.1 cells (Fig. 4.19 arrow). The cross-reactivity to ubiquitin, VMAT-1 and 2 and LAMP antibodies, following lactacystin treatment, did not demonstrate any co-localisation with EYFP in WT or MT htt EYFP clones (data not shown).

4.10.3. Inclusions and anti-htt antibodies in mitotic and differentiated cells

In order to investigate whether truncated htt products were present in the lactacystin-induced inclusions, the three representative clones (23 1 1, 88 1 3 and pcDNA 3.1 1) were treated with 5.0 μ M lactacystin for up to 24 hours and developed with EM 48, Ab2166, Ab7668, Ab7667, Ab2168 and Ab7666 anti-htt antibodies. If co-localisation of an anti-htt antibody with EYFP inclusion fluorescence was absent then this would suggest truncation of htt. Fig.4.20. A (23 1 1) and B (88 1 3) demonstrate that all of the anti-huntingtin antibodies positively stained the perinuclear inclusions in MT and WT clones following lactacystin treatment, except for Ab7666 which consistently poorly stained the edges of the inclusions (Fig.4.20.A and B arrows). This suggested that htt truncation between Ab2168 (aa2146-2541) and Ab7666 (aa2703-2911) may have occurred in WT and MT clones. The most intense staining of the inclusions occurred with antibodies EM48, Ab2166 and Ab2168 supplied by the same manufacturer (Fig.4.20.A and B) suggesting that the intensity of inclusion fluorescence was, at least in part, determined by the source of the anti-huntingtin antibody as the htt epitopes recognised by these antibodies were evenly distributed along the whole protein.

Fig. 4.18.

Fig. 4.19.

Fig. 4.20.

Lactacystin-treated pcDNA 3.1 clones demonstrated a pattern of staining with anti-huntingtin antibodies that was similar to that seen in untreated pc DNA 3.1 cells (Fig. 4.20C). The staining was absent with EM48 and relatively weak with antibodies Ab2166 and Ab2168. The htt staining was stronger with more punctate cytoplasmic granules using Ab7666, Ab7667 and Ab7668. This was consistent with earlier observations that the EM48, Ab2166 and Ab2168 recognised ectopically expressed htt better than endogenous htt on immunofluorescence.

Htt inclusions have been found to form more readily in differentiated cells in comparison to mitotic cells and following treatment with lactacystin. The influence of differentiation on inclusion formation following treatment with lactacystin, was therefore investigated. A representative WT (23 1 1) and MT (88 1 3) clone and control cells (pcDNA3.1 1) were differentiated for 48 hours with retinoic acid. Fresh medium containing retinoic acid and lactacystin was then added to the cells for 24 hours. The cells were developed with the panel of anti-htt antibodies. The staining pattern was similar to cycling cells treated with 5 μ M lactacystin for 24 hours alone (Fig. 4.21A (23 1 1), 4.21B (88 1 3) and 4.21C (pcDNA 3.1 1)).

4.10.4. Western blots of clones treated with lactacystin

To investigate the formation of htt cleavage products, the representative WT (23 1 1) and MT (88 1 3) clones and control cells (pcDNA3.1 1) were treated with lactacystin at 0, 1 or 5 μ M for 24 hours. A Western blot was performed and developed with anti-EYFP. The WT clone treated with 1 and 5 μ M lactacystin demonstrated an additional band at approximately 44kDa (Fig. 4.22A and B solid arrow) and 34kDa (Fig. 4.22A and B red arrow). These bands may have been faintly present in untreated 23 1 1 cells

Fig 4.21.

Fig. 4.22.

but were absent from MT and control cells. There was also a loss of a band in the 23 1 1 clones at approximately 60kDa (Fig. 4.22 A and B stippled arrow). To investigate whether these changes persisted with more prolonged lactacystin treatment, the representative clones were treated with 0 and 1 μ M lactacystin for 4 days with a change in the medium and fresh lactacystin added after 48 hours. There was no evidence of the additional 44kDa and 34kDa bands observed with only 24 hours lactacystin treatment in

the 23 1 1 clone (Fig. 4.22C). There was a 52kDa band ((Fig. 4.22C arrow) which was present in WT, MT and pc DNA 3.1 following treatment with 1 μ M lactacystin.

4.10.5. Western blots of lactacystin-treated clones using anti-htt antibodies

To investigate the processing of htt into smaller fragments following proteasome inhibition, clones 23 1 1, 88 1 3 and pcDNA 3.1 were treated with lactacystin for 24hrs at 0, 1 and 5 μ M, separated and then probed with Ab675, EM 48, Ab2168 and Ab7666 (Fig. 4.23).

In Fig. 4.23. A, antibody Ab675 demonstrated a band at greater than 209kDa consistent with endogenous huntingtin expression (see arrow in Fig. 4.23. A). There was a reduction in the intensity of the endogenous htt band in all three clones with increasing lactacystin concentration which was more pronounced with the 88 1 3 than 23 1 1 or pcDNA 3.1, eventhough other bands were of similar intensity suggesting that endogenous htt levels were reduced by lactacystin. There were no evidence of extra bands when 23 1 1 and 88 1 3 were compared with pcDNA 3.1.

In Fig. 4.23. B, EM 48 did not demonstrate any staining for endogenous htt in any of the clones. Clones 23 1 1 and 88 1 3 demonstrated a band at greater than 209kDa consistent
Fig 4.23.

with EYFP htt expression (red arrow). The intensity of this band reduced with increasing lactacystin concentration in the 88 1 3 clone but not the 23 1 1 clone. This suggests that lactacystin inhibition may have caused increased non-UPS degradation of MT htt, increased aggregation of MT htt or there was a reduction in cell construct expression.

In Figs. 4.23. C and D, antibodies Ab2168 and Ab7666 demonstrated a low intensity band in all three clones at greater than 185kDa (arrows) which represented endogenous htt. When probed with Ab2168, clones 23 1 1 and 88 1 3 both demonstrated strong bands (Figs. 4.23. C red arrow) of equal intensity at all lactacystin concentrations which migrated less than endogenous htt which represented EYFP htt expression. When probed with Ab7666, a band present at approximately 80kDa. (Figs. 4.23. D stippled arrow) demonstrated reduced intensity in all clones with increasing lactacystin concentration. This may have represented a UPS-cleaved htt fragment.

4.10.6. Western blots of lactacystin-treated clones developed with anti-EYFP

To investigate whether the changes on Western blotting following lactacystin treatment, occurred in other clones, the four MT and WT clones were treated for 24 hours with 5 μ M lactacystin, a Western blot performed and probed with anti-EYFP. The Western blot is shown in Fig. 4.24. and demonstrated an additional band at 44kDa in clone 23 1 1 (red arrow) as seen on previous Western blots (see Fig. 4.22. A). An additional band at 111kDa was also observed in clone 23 6 7 (black arrow). There was also an extra band at 36 kDa in 88 2 8, 88 2 9 and 88 2 11 clones (stippled arrows), which suggested processing of FL MT htt in 3 out of 4 clones to form an N-terminal fragment. This coincided with a reduction in the levels of EYFP MT htt

Fig. 4.24.

(Fig. 4.24. A. blue arrow). This suggested that lactacystin caused a reduced in MT EYFP htt expression by one of several mechanisms, including toxicity to strongly expressing cells leaving a population of proliferating poorly expressing cells or due to aggregate formation although there was no excess of stain in the well of MT versus WT clones to suggest aggregates (Fig. 4.24. A). A further explanation was that MT htt was processed

by a non-UPS system such as autophagy, which was activated by lactacystin inhibition of the UPS.

4.11. Mitochondrial function in mitotic clones

The mitochondrial function in four WT, four MT and four pcDNA3.1 clones was tested using the standard protocols as described in section 2.5. Fig. 4.25. A demonstrates that there was a significant ($p < 0.05$) reduction in the CS corrected complex IV activity in the MT clones compared to WT and pcDNA3.1 clones. Fig. 4.25. B demonstrates that there were also similar changes in the protein corrected values but in addition there was a significant reduction in the complex IV activities in WT versus pcDNA 3.1.

4.12. Aconitase activity in mitotic clones

Aconitase function in four WT, four MT, four EYFPcon and four pcDNA3.1 clones was tested using the standard protocols as described in section 2.5.5. Fig. 4.25. C demonstrates that there was a significant reduction in aconitase activity in the MT cells compared to WT clones ($p < 0.01$) and pcDNA3.1 ($p < 0.05$).

Fig. 4.25.

4.13. Proteasome function in mitotic clones

The activity of proteasome function was assessed as per protocol (Section 2.16) to investigate proteasomal dysfunction in response to WT and MT EYFP htt expression. Activities were not corrected for epoxymycin. Epoxymycin has been found to inhibit

chymotrypsin activity 100%, PGP-like activity to 70% and not inhibit trypsin-like activity in SH-SY5Y cells (personal communication Dr Mike Cleeter, Royal Free, UK).

Fig. 4.26. compares the means of the 4 control, 4 WT and 4 MT clones for the 3 proteasome activities. Fig. 4.26. A demonstrates that there was no significant difference between the clones in chymotrypsin-like and PGP-like activities. Fig. 4.26. B demonstrates that the 'trypsin-like' activity was reduced in the MT clones compared to the WT ($p < 0.0001$) and controls ($p = 0.0161$) as well as being reduced in the controls versus the WT clones ($p = 0.0361$). These results represented total activity in the cells and it can not be excluded that non-proteasomal activity was included in the findings.

Fig. 4.26.

CHAPTER 5

Results

Mitochondrial function in

HD muscle

5.1. HD patient and control muscle selection

A database of 43 patients with HD at the Royal Free Hospital, London, UK was used to select potential patients with a view to undertaking a research muscle biopsy. Ethical approval had been obtained from the local research ethics committee and patients and their general practitioners were sent information sheets regarding the study after initial interest had been expressed following contact by telephone. There were no inclusion/exclusion criteria for the study apart from a genetically confirmed diagnosis of HD and an absence of other neuromuscular disorders which could affect the biopsy such as co-existing polymyositis or diabetes mellitus. Patients with all levels of disability were deemed acceptable. Twelve HD patients underwent consented open muscle biopsy of the left vastus lateralis. The majority of the sample was flash frozen in isopentane cooled in liquid nitrogen and stored at -80°C and the rest was processed for ultrastructural studies. Twelve age and sex-matched controls were picked from the muscle bank at the Royal Free Hospital, London, UK. The 'control' biopsies were taken as a diagnostic procedure from patients with non-specific muscle symptoms, and showed no clinical evidence of a mitochondrial or neurodegenerative disease. The control patients consented to the use of their muscle for research and this was also approved by the local research ethics committee. Previous detailed histochemical analysis of these control samples did not reveal any abnormalities.

5.2. Genetic and clinical assessment of HD patients

All HD patients had been genotyped and the number of CAG repeats quantified by the department of Neurogenetics at the Institute of Neurology, London, UK or at the Kennedy-Galton Centre, Harrow, UK. The HD patients were also assessed clinically with

the modified Unified Huntington's Disease Rating Scale (UHDRS) scale as well as basic clinical data such as the time between biopsy and subjective onset of symptoms. The UHDRS can be found in Appendix 1.6. (Huntington Study Group, 1996). In summary, the Motor subscale was scored out of 124 with increasing scores representing increasing disease severity. The Cognitive subscale was the total score of the combination of a verbal fluency test, symbol digit modality test, and Stroop interference test with higher scores representing better cognitive function. The Behavioural subscale was out of a total of 80 with increasing scores representing worse behaviour. The Functional checklist was scored between 25 and 50 with a score of 25 representing no effect on daily function and a score of 50 representing full functional dependence of the patient. The Independence subscale was a percentage score with 100% representing full independence and 10% representing total bed care and tube feeding. The Functional Capacity was scored from 0 to 13 with higher scores representing higher functional dependence.

5.3. Clinical data of HD patients

Table 5.1. shows the Unified Huntington's Disease Rating Scale (UHDRS) for each of the 12 HD patients and other clinical parameters. The patients were taken from a wide spectrum of disease severities ranging from asymptomatic, with respect to the motor score, in two patients (patients 2 and 3), to severely affected and unable to perform the cognitive tests in one patient (patient 7). Figs. 5.1. A and B demonstrate that there was a significant positive correlation between motor scores and age ($r=0.698$, $p=0.014$) and a significant negative correlation between cognitive scores and age ($r=-0.597$, $p=0.043$). Figs. 5.1. C and D demonstrate that there was no correlation between cognitive ($p=0.49$) or motor scores ($p=0.26$) with CAG repeat length. To allow for the role of increased

Table 5.1.

Fig. 5.1.

disease duration upon the clinical score, the cognitive and motor subscales of the UHDRS were related to the product of the age of the patient and the number of CAG repeats. This was called the “CAG repeat years”. This produced a highly more significant positive correlation for the motor score ($r=0.823$, $p=0.0016$) and negative correlation for the cognitive score ($r=-0.727$, $p=0.0096$) than age alone as demonstrated in Figs. 5.1. E and F. Fig. 5.2. A shows that there was also a significant negative correlation between the motor and cognitive scores ($r=-0.799$, $p=0.0029$) in HD patients. The statistical results are summarised in Fig. 5.2. B.

5.4. Histochemistry, immunocytochemistry and electron microscopy

Muscle histology was performed on frozen sections for all 12 patients. The histochemical stains for SDH and COX revealed no discernable abnormalities in any controls or patients except patient 12, who was one of the more severely affected patients. Fig. 5.3. A demonstrates that there was an excess of SDH positive and COX negative fibres on histochemistry in the muscle biopsy of patient 12 which is suggestive of a mitochondrial respiratory chain defect. Immunocytochemical analysis kindly performed by Dr Jenny Morton (Cambridge, UK) on two of the more severely affected patients, 9 and 11, using an antibody to ubiquitin was suggestive of perinuclear inclusions but was not conclusive (images not shown). Fig. 5.3. B demonstrates that immunocytochemical studies using anti-ubiquitin and 675 antibodies did not suggest any inclusion formation although there was inconsistent nuclear staining by 675 (white arrows) which was also seen in control sections. The tissue preparation and antibody protocol was checked by the demonstration of an ubiquitin-positive inclusion in a sample of inclusion body myositis (IBM) muscle as a positive control using the same protocol (black arrow in Fig. 5.3. B).

Fig. 5.2.

Fig.5.3.

In patient number 10, who was also severely affected, ultrastructural studies suggested that there were nuclear accumulations of electron dense material (Fig. 5.3. C) consistent with intranuclear inclusion formation.

5.5. Spectrophotometric analyses

The spectrophotometric analyses of aconitase, citrate synthase and complexes I, II/III and IV activities were performed on muscle homogenates in all 12 HD patients and the age-matched controls as previously described (Sections 2.1.5, 2.5. and 2.7.). All assays were performed blinded and the enzyme activities were expressed as nmols/min/mg except complex IV which was expressed as the first order rate constant, K (/min/mg), and as a citrate synthase ratio. Protein was determined by the BCA protein assay using bovine serum albumin as the standard as already described (Section 2.8.). Statistical analyses were performed using the unpaired two-tailed Mann-Whitney U test and the Spearman correlation test.

5.5.1. Mitochondrial activities in HD muscle

The results of specific enzyme activities and CS corrected ratios for the control and HD patients are shown in Tables 5.2. and 5.3. When expressed as a specific activity or as a ratio with citrate synthase activity, complexes I, II/III and IV were not statistically different in the HD patients from the control group (Fig. 5.4. summarises statistical comparisons).

Table 5.2.

Table 5.3.

Fig. 5.4.

5.5.2. Correlations of clinical data and mitochondrial activities

The patients represented a diverse group with respect to their age, disease duration and clinical status at analysis (Table 5.1.). In order to assess whether mitochondrial function may relate to disease progression, complex I, II/III and IV citrate synthase ratios and specific activities were correlated with patient age, disease duration and various clinical scores within the UHDRS (Table 5.4.). The significant correlations related to complex II/III:CS ratios apart from repeat years versus complex II/III specific activity which was significantly negatively correlated ($r=-0.587$, $p=0.0489$). Figs. 5.5. A-D demonstrate that complex II/III:CS ratios correlated positively with the cognitive subscale of the UHDRS ($r=0.676$, $p=0.0185$), and negatively with the age of the patient ($r=-0.647$, $p=0.0257$), disease duration ($r=-0.681$, $p=0.0170$) and with repeat years ($r=-0.631$, $p=0.323$). Figs. 5.5. E-F show that of the four subscales of the UHDRS that measure behavioural and functional change, there was a significant negative correlation between the functional checklist ($r=-0.656$, $p=0.0238$), and positive correlation between the independence scale ($r=0.593$, $p=0.0457$) with complex II/III:CS. The statistical data is summarised in Fig. 5.5. Fig. 5.6. A shows that there was a trend for the motor subscale to be negatively correlated with II/III:CS ratio but it did not reach significance ($r=-0.454$, $p=0.140$). Fig. 5.6. B demonstrates that complex II/III:CS did not decline with increasing age in the control patients ($r=-0.0876$, $p=0.783$).

Table 5.4.

Fig. 5.5.

Fig. 5.6.

Chapter 6

Discussion

6.1. The molecular pathogenesis of HD

It was not until the linkage of the abnormal gene to chromosome 4 in 1983 and the subsequent cloning of the HD gene in 1993, that research into the molecular mechanisms of HD started to develop rapidly. Whilst this has led to a progressive understanding of several important issues in the pathogenesis of HD, many issues are still unresolved. It is clear that truncated forms of htt with more highly expanded CAG repeats cause greater toxicity in cellular and animal models of HD (Section 6.7) but the mechanism by which a toxic fragment is formed remains uncharacterised. The primary molecular pathogenic event(s) caused by MT htt has also still to be clarified and the role of htt aggregates, UPS dysfunction, mitochondrial inhibition, excess free radicals, transcriptional dysregulation and impairment of vesicular transport all remain possible mechanisms mediating MT htt toxicity. Only by further understanding the pathogenic mechanisms will effective targets for future treatments for HD be possible.

This thesis generated two different cell models to investigate the proposed molecular mechanisms in the pathogenesis of HD. Following their characterisation, these models were used to study the influence of the size of htt, number of CAG repeats, localisation of htt, the effects of differentiation, processing of htt, mitochondrial function, generation of excess free radicals, the role of the proteasome and htt inclusions on the pathogenesis of HD. These will be discussed alongside results from the analysis of mitochondrial function in HD muscle.

6.2. Characterisation of the Ecdysone HEK293 N-terminal htt cell model

The original aim was to generate cell lines with inducible N-terminal htt expression in SH-SY5Y cells. The Ecdysone inducible expression system has been used to a limited degree in the literature (No et al. 1996, Wang et al 1999, Dela Cruz et al. 2000, Jana et al. 2001, Downey et al. 2005) but generally has been shown to express construct proteins without background expression and in an inducer concentration-dependent manner. The inducer, pon A, has not been shown to have significant toxicity. Previous work in the laboratory had been unsuccessful in generating SH-SY5Y cells expressing a functional pVgRxR and these were not available commercially or in the literature. Consequently the model was generated in HEK 293 cells. These are human kidney epithelial cells used widely for transfection studies. While they do not express the phenotype of the cells predominantly affected in HD, they are suitable for investigating the expression of specific proteins upon generic cellular functions. The construct chosen was a kind gift from Dr Lesley Jones (University of Cardiff) and included the first 171 aa. of htt with 21 CAGs in the WT construct and the first 207aa. of htt with 57 CAGs in the MT construct.

6.2.1. Isolation of clonal HEK293 lines expressing N terminal htt

Following transfection, 13 WT and 15 MT htt clones were isolated and 7 WT and 5 MT clones were taken for further analysis. Cells within each clone demonstrated different levels of expression of WT and MT N-terminal htt. Some cells had cytoplasmic punctate Ab675 immunoreactivity similar to untransfected clones, whereas other cells demonstrated strong uniform nuclear and cytoplasmic immunoreactivity. This intra-clonal variability was not due to variable construct transfection between cells because subcloning experiments had demonstrated similar intra-clonal variation of N-terminal htt

expression within the subclones (Fig.3.7). It was also not due to the Ecdysone system, as evidenced by uniform expression throughout all cells in the alpha-synuclein model (Fig. 3.15). There is consistent reporting of variability in intra-clonal htt immunoreactivity in stably-transfected htt expressing in vitro cell models in the literature, although it is often not commented on in the published text but is present in the published photos of expressing clones. This variability has occurred with various cell types including NG105-15, N2a and PC12 cell lines, with various detection systems, including antibodies to htt, fluorescent tags and antibodies to non-fluorescent markers, in inducible and constitutive expression systems, and in WT and MT N-terminal htt clones (Lunkes et al. 1998, Li et al 1999, Wyttenbach et al. 2001, van Roon-Mom et al. 2008 and Ye et al 2008). The size of the htt construct expressed may have had a role as the FL htt cell model described by Sugars et al (2004) demonstrated uniform expression in all cells. This suggested that the variable expression may have been due to the effects of N-terminal htt itself, possibly by WT and MT N-terminal htt affecting transcription within expression systems (see Section 1.8 for discussion of transcription in HD).

6.2.2. Sequencing of constructs

Sequencing the plasmids and DNA from the 7 WT and 5 MT htt HEK 293 clones revealed sequences in keeping with that predicted for htt except a 3'end base-mutation resulting in a leucine to proline switch at aa.165 (relative to 21 CAG). Leucine and proline are both neutral non-polar amino acids and therefore any molecular consequences would be minimised. There was an additional 5aa (serine, arginine, glycine, proline and valine) at the C-terminal end of the WT and MT N-terminal constructs. These additional sequences were small and given the C-terminal location were not considered to exert a significant biological effect although this could not be ruled out (Fig 3.1. A and B).

6.2.3. Background construct expression

One advantage of the Ecdysone model was that pon A-induced expression occurred reliably without background expression of the construct in all the clones that were investigated, even at very high protein loading (120 μ g) on Western blot (Fig. 3.5). This is essential in an inducible system in order to study the early molecular effects of N-terminal htt expression and the lack of influence of htt expression upon the selection of clones. Tetracycline-based systems e.g. T-Rex (Invitrogen), have been associated with significant background breakthrough expression in the absence of doxycycline (Forster et al. 1999, Waelter et al 2001). To address these problems, the "second-generation reverse tet-off," or "rtTA2S-M2" (Urlinger et al. 2000), has been developed, which shows a greater trans-activation potential and a lowered affinity for the target gene promoter in the absence of doxycycline. RtTA2S-M2 has been shown to be successful in transgenic animals and hepatoma cell lines at reducing breakthrough expression (Koponen et al. 2003, Goldring 2006). This system potentially has the benefits of the tetracycline-inducible systems, such as high expression levels and a water-soluble inducer, without the disadvantage of breakthrough construct expression.

6.2.4. Levels of endogenous and construct htt expression

WT and MT htt clones expressed similar levels of endogenous htt on Western blots when corrected for protein loading and probed with Ab675 (Fig.3.6). This enabled comparison of relative expression levels of WT and MT htt constructs between the clones. The levels of construct htt expression were up to 3 times greater than endogenous htt in the WT htt clones and there was a wide range of expression levels amongst all the WT clones. The

MT htt clones expressed approximately twice as much construct htt as endogenous htt and levels were more consistent between clones than in the WT clones. No et al. (1996) found up to four times greater expression levels of reporter genes, β -galactocidase and luciferase, using the Ecdysone system in mammalian cells, which was within the limits found in the current HEK 293 htt model. The greater expression levels of construct htt compared to endogenous htt may have accelerated the toxicity of MT N-terminal htt in comparison to physiological levels. This enabled shorter experiments to be performed to demonstrate toxicity although may have confounded direct comparison with in vivo pathogenic mechanisms.

6.2.5. Time and concentration of pon A-dependence of expression

The clones exhibited a different response to pon A. In two clones (one WT and one MT clone) htt expression levels related to pon A concentration while in another 2 clones (one WT and one MT clone) expression was unrelated to pon A concentration. The levels of construct htt expression could therefore not be reliably controlled by varying pon A concentration (Figs. 3.9-3.12). The variable effect of pon A induction between clones was not related to type of protein expressed and may have been explained by variations in the population of HEK 293 cells or due to differential effects of random construct insertion within the host genome. There is no other published data to support these explanations. These studies were performed on 2 WT and 2 MT clones and testing further WT and MT clones may have clarified the response to pon A. A dose-dependent effect of the inducer on construct expression has been described in the Ecdysone system by Wang et al (1999) who made a stable inducible model of HD in N2a cells expressing exon 1 of htt using Muristerone A (an analogue of ponasterone A) as the inducer. The authors did not comment on whether this was consistent in all WT and MT clones.

There was stable expression of WT and MT N-terminal htt over 48 hours in 2 WT and 2 MT clones. By day 4 there was a reduction in WT and MT N-terminal htt expression on Western blotting (Figs 3.13-3.14) which did not enable the analysis of the effects of construct expression over a prolonged timeframe. This was not a feature of the HEK293 htt model itself, as a similar model expressing a mutant α -synuclein (A53T) construct, did not demonstrate a reduction in expression with time following 12 days of pon A induction (Fig. 3.15). A time and concentration-dependent expression of metabotropic glutamate receptors in HEK 293 cells using the Ecdysone system has also been described (Downey et al. 2005). These studies suggest that the reduction in construct htt expression over time was due to N-terminal htt expression and not the Ecdysone expression system or cellular background. One explanation is that WT and MT N-terminal htt may have affected transcription (Section 1.8), causing down regulation of one of the components within the Ecdysone system, although one would expect this to be self-limiting as construct expression would then be turned off and transcription would commence again once N-terminal htt levels had reduced. An alternative explanation for the reduction in htt expression after 8 days, was that some cells in each clone did not express the construct. The sub-cloning studies demonstrated similar intra-clonal variation in expression of construct htt in parent and sub-clones, which would argue against this.

6.2.6. Influence of pon A

There is increasing evidence of mitochondrial dysfunction in the pathogenesis of HD (Section 1.10.) and therefore a mammalian expression system which uses an inducing

agent that does not cause mitochondrial toxicity was important, especially if mitochondrial function was to be assessed. Pon A did not affect mitochondrial function as demonstrated by the absence of significant differences between pon A (dissolved in DMSO) and DMSO-treated pIND 0 clones (Figs. 3.24-3.26). This is in contrast to other inducible systems, such as tetracycline-based systems e.g. T-Rex (Invitrogen), which is associated with tetracycline-induced mitochondrial toxicity by inhibition of the mitochondrial 30S ribosome. This inhibits mitochondrial protein synthesis and can cause cell dysfunction and death (Riesbeck et al. 1990, McKee et al 2006). One of the disadvantages of using pon A was that it was soluble in an organic solvent. Previous studies in the laboratory have demonstrated that alcohol was toxic to cells and therefore DMSO was used. DMSO caused the HEK 293 cells to form clumps which made immunocytochemistry of single cells more difficult. The effects of pon A and DMSO on cell growth and cell death are discussed in Section 6.2.9.

6.2.7. Length of expressed htt N-terminal fragment and CAG repeat size

N-terminal fragments of MT htt are more toxic and form aggregates more quickly than FL-MT htt in transgenic HD mice and in vitro cell models of HD (Mangiarini et al 1996, Jana et al. 2001). It was therefore felt to be appropriate to express N-terminal htt in an inducible system in order to investigate the early molecular changes associated with WT and MT N-terminal htt expression. There has been only one study which has described physiological WT N-terminal htt in normal post-mortem human brain (Kim et al. 2001). There has been no evidence from previous stably transfected cell models of N-terminal WT htt toxicity (Lunkes and Mandel 1998, Li, SH. et al. 1999 and Jana et al. 2001). WT N-terminal htt may not exist in vivo but it was still felt to be an appropriate control for MT N-terminal htt in the HEK293 model. The MT N-terminal fragment used in the HEK

293 model consisted of approximately the first 3½ exons of htt (212aa. MT htt with 57 CAGs or 176 aa. WT htt with 21 CAGs (Figs. 3.1 A and B). Most studies expressing N-terminal htt in HD cell models and transgenic HD mice have used exon 1 (90aa.) of MT htt with at least 80 CAG repeats (Table 1.5 tabulates the details of published HD cell models). Smaller N-terminal htt fragments and larger CAG repeats have been demonstrated to cause the greatest toxicity and increased htt inclusions in cell models and transgenic HD mice (Davies et al. 1997, Lunkes et al. 1998, Section 6.8). The relatively large N-terminal fragment and low MT CAG repeat number used in the current study was felt to more accurately recapitulate the early pathological environment in HD cells similar to patients with severe HD who often have CAG repeats in excess of 50 (Telenius et al. 1993). CAG repeat lengths over 80 are uncommon in HD patients and may cause different molecular changes compared to most patients with HD who have between 40 and 50 CAG repeats. At the same time, potential toxicity of MT htt was accelerated by moderate N-terminal truncation, in order to enable molecular studies to be performed within a viable timeframe.

The N-terminal fragment used in the HEK 293 model contained the polyproline-rich region of htt, which is putatively involved in protein–protein interactions (Cubellis et al. 2005). Neither the putative caspase/calpain cleavage sites nor the HEAT repeat sequences were included in the N-terminal htt fragment used in this model (Fig. 1.1 for diagram of htt). This potentially enabled N-terminal fragment toxicity to occur in a background of htt protein, but without the need for extensive processing of the FL-htt.

6.2.8. Western blots and poly Q proteins

The Western blots of WT and MT htt expression suggested a discrepancy between the predicted bands (19.5 kDa for WT htt and 23.5 kDa for MT htt) and the bands seen on the

Western blots (29.5 kDa for WT htt and 36kDa for MT htt). The proportional increase in predicted size is approximately 50% in WT and MT clones. This can be either explained by the expression of constructs beyond the predicted stop codon or that these proteins did not migrate as predicted because of their primary structure. N-terminal htt contains polyQ sequences which has been demonstrated to slow the movement of the protein through the gel (Schilling et al 2007). The N-terminal htt constructs migrated similarly in Western blots in all WT and MT clones. This would have been unlikely if the random plasmid integration site in the host cell had caused the stop codon to be disrupted leading to variable alterations in the size of the protein product. The similar proportional increase in size of both WT and MT bands would also argue against translation beyond the predicted stop codon which would have caused a similar increase in construct size in both WT and MT clones.

6.2.9. Cell proliferation and death

Pon A is an insect steroid hormone involved in regulating metamorphosis, especially in molting (Nakanishi et al. 1992). It is reported that pon A is “inert to mammalian physiology and does not exert any pleiotropic effects” (A.G.Scientific Inc. San Diego, CA, USA). Within the current study, pon A caused a reduction in cell proliferation in all clones independent of construct expression (Figs. 3.22 and 3.23). This response to pon A has not been previously described. The ecdysone receptor (VgEcR) forms a heterodimeric complex with the retinoid X receptor (RXR) to form pVGRXR (Fig.2.3). Therefore, endogenous retinoic acid receptors forming a heterodimeric complex with upregulated levels of construct RXR, or with pVgRXR, could bind to promoter regions of endogenous retinoic acid-responsive genes. Pon A may subsequently induce transcription of

endogenous genes other than the exogenous construct. This could result in inhibition of cell growth or induction of apoptosis (Dela Cruz et al. 2000, Gianni et al. 2000).

The background levels of cell death were higher in both WT and MT htt clones than pIND 0, in the absence of pon A induction (Fig. 3.28. and Table 3.7.). In the absence of htt expression, this suggested that the chromosomal integration of WT or MT htt pIND constructs was more toxic to cells than if pIND contained no construct ie. pIND 0. This raises the possibility of toxicity of triplet repeats at a pre-transcriptional level. There is no published data on the role of CAG repeat toxicity at a pre-transcriptional level, but one could speculate that an altered repeat sequence within a chromosome may interfere with transcription as proposed in facioscapulohumeral dystrophy (FSHD) where contraction of a non-coding repeat sequence is postulated to interfere with distant transcription (Tawil et al. 2006).

There was a small, but significant decrease in cell death in the pIND0 clones when treated with pon A (Fig. 3.28. and Table 3.7.) which was not present in the WT and MT clones. There was no evidence of pon A-induced toxicity in MT clones which suggested that over 96 hours, N-terminal MT htt containing 57 CAG repeats, was not toxic.

These findings contrast with those of Wytttenbach et al (2001), who used positive TUNEL staining as a marker of cell death in a “Tet-ON” PC12 cell model of HD, and described in cells expressing exon 1 of htt, 15-20% cell death with 74Q and 8% in 53Q cells following 6 days of induction. Wang et al (1999) published an Ecdysone differentiated N2a cell model expressing exon 1 with 16, 60 or 150Q. By day 3 post-induction and differentiation, there was increased cell death in the 150Q cells and after 4 days in the 60Q cells. Lunkes et al (1998) described increased cell death, using Hoechst dye analysis,

by day 6 with 80aa of N-terminal htt, by day 13 with 502aa of N-terminal htt and day 16 in FL htt with 73Q in a differentiated NG105-15 “TetON” cell model. These three studies suggest that the combination of a shorter N-terminal fragment, increased polyQ, differentiation compared to mitotic cells, and longer induction times were sufficient to induce cell death with N-terminal htt. The critical role of a short N-terminal htt fragment in causing cell death was supported by a primary rat striatal “TetON” inducible model expressing the first 548 aa of htt and 26, 67, 105 or 118Q (Sipione et al. 2002). The authors found no cell death or aggregates by 36 hours post-induction suggesting that highly expanded polyQ is not sufficient to cause early cell death and that a longer N-terminal fragment probably delayed MT htt toxicity and would be compatible with the relatively large N-terminal htt fragment in the current HEK 293 model.

6.3. Characterisation of the EYFP SH-SY5Y FL htt cell model

6.3.1. SH-SY5Y cells as a background neuronal phenotype

The SH-SY5Y cells were selected as a background neuronal phenotype that could be differentiated into post-mitotic cells with neuronal characteristics (Biedler et al. 1978). Post-mitotic cells potentially had the advantage of modelling an important parameter from the in vivo setting, as mitotic cells in HD tend not to be affected. SH-SY5Y cells have adrenergic and glutaminergic systems but not GABAergic or serotonergic systems (Ross et al 1981). Experiments involving induction of excitotoxicity could therefore have been performed although this was not eventually undertaken in the current thesis.

There has been only one other published HD cell model which used SH-SY5Y cells (Chun et al 2002 and Table 1.5.). The authors demonstrated that a small N-terminal 63aa.

fragment of htt containing 82Q formed cytoplasmic, and occasional nuclear, htt inclusions with a background cytoplasmic htt construct expression. The authors did not attempt to differentiate the SH-SY5Y cells. Further discussion on the differentiation of SH-SY5Y cells can be found in Section 6.10.

6.3.2. EYFP huntingtin-length of htt fragment and CAG repeat size

The main aim of the SH-SY5Y model was to recapitulate the earliest molecular effects of MT htt expression, in particular the processing of FL htt into potentially toxic N-terminal fragments. Previous constitutive htt cell models have only expressed small N-terminal fragments up to 171aa in length (Section 1.13.1 and Table 1.5). In order to prevent acute toxicity, as has been observed in other htt cell models expressing 148 CAGs (Table 1.5), the CAG repeat length used was 88 CAGs. The discussion of the impact of FL htt and 88 CAG repeats on cellular function is discussed later.

6.3.3. EYFP-C1 as a constitutive expression system

One of the main advantages of choosing the EYFP-C1 mammalian system (Clontech) was that induction of protein expression was not required and therefore the potentially toxic effects of an inducing agent could be avoided. EYFP htt could also be monitored directly with fluorescence microscopy and using anti-EYFP antibody on Western blots without cross-reactivity with endogenous htt. One of the main disadvantages of the system was potential toxicity of EYFP htt during cloning, which would have selected against cells sensitive to EYFP htt. There was no evidence for this occurring as cells were readily cloned, although there remained the possibility that the clones selected for subsequent

experiments expressed EYFP htt at sufficiently low levels to remain non-toxic and that stronger expressing clones died at an earlier stage before cloning took place.

6.3.4. Levels of expression of EYFP htt on Western blots

All MT clones expressed similar levels of EYFP MT htt. Expression of EYFP htt in the WT clones were more varied, with the lowest levels in 23 7 2 and 7 8 being approximately three times less than 23 6 7 (Fig.4.2). For mitochondrial respiratory chain enzyme activities and proteasomal function assays clones 23 6 7, 7 2 and 7 8 were therefore not used to standardise for expression levels. The levels of expression of EYFP htt were approximately four times greater than endogenous htt on Western blots in both WT and MT EYFP clones (Fig 4.4). Increased expression levels were expected with the CMV_{IE} promoter although there is little data from other constitutively expressing htt cell models regarding this.

6.3.5. Control cells containing EYFP-C1 plasmid

The EYFP CON clones, which contained the EYFP-C1 plasmid without a construct, were found to have nuclear and cytoplasmic fluorescence. Nuclear and cytoplasmic fluorescence has been described with EYFP expression and with other fluorescent tags, such as EGFP, and it is due to passive diffusion of EYFP into the nucleus at high concentrations (Clontech, UK). The WT and MT FL htt blocked this passive process as evidenced by the purely cytoplasmic fluorescence in mitotic EYFP WT and MT htt clones. This has been described in other constitutive cell models of HD including Ye et al (2008) in an N2a model using EGFP-tagged exon 1 of htt with 20 and 120Q (Table 1.5). The EYFP CON clones were therefore not used as a control and SH-SY5Y cells stably

transfected with the plasmid pcDNA3.1 were felt to control for the cloning process and integration of a plasmid into the host cell genome.

6.4. Mitochondrial dysfunction in HD

6.4.1. The spectrum of mitochondrial dysfunction in HD

Mitochondrial respiratory chain dysfunction is a consistent feature in HD. Most importantly, there is evidence of mitochondrial respiratory chain (MRC) dysfunction in the striatum of post-mortem HD brain and in HD skeletal muscle (Gu et al. 1996, Browne et al. 1997 and Arenas 1998), as well as in the striatum and cortex of the R6/2 mouse (Tabrizi et al. 2000). ¹H MRS has demonstrated increased lactate in symptomatic and some presymptomatic HD striatum and cortex (Jenkins et al 1993 and 1998, Harms et al. 1997) suggesting an early *in vivo* energetic defect.

6.4.2. Mitochondrial function in HD skeletal muscle

Htt expression in skeletal muscle

Htt expression is not restricted to the CNS and has been documented in skeletal muscle and myoblast cultures from the R6/2 transgenic mouse model of HD (Sathasivam et al. 1999, Orth et al. 2003). Studies on human post-mortem normal and HD skeletal muscle have detected htt mRNA by in situ hybridisation studies (Li S-H et al 1993), cytoplasmic htt immunoreactivity (Hoogeveen et al. 1993) and htt inclusions in HD differentiated myotubes (Ciammola et al. 2006). The presence of htt inclusions in post-mortem HD skeletal muscle has not been published.

The advantages of studying skeletal muscle in HD

Brain has several limitations in the study of the pathogenesis of HD. The relative paucity of HD post-mortem material is a problem which will hopefully be improved by the development of HD “brain banks”. HD brain tissue is usually taken from post-mortems where there has been a delay between the death of the patient and the fixation of the brain. This can cause degeneration of the brain and consequently impair biochemical and histological analyses. Most HD post-mortem brains are end-stage in the disease process and this makes analysis of the progression of pathological changes difficult. In contrast, skeletal muscle represents a tissue that can be relatively easily biopsied at various stages of the disease and has the potential to be used to study molecular defects, such as mitochondrial dysfunction. HD patients lose muscle bulk disproportionately to their level of activity and calorific intake which suggests that muscle may be primarily involved in HD (Section 1.10.12). This suggests that HD skeletal muscle is an important tissue to study.

MRC activities and age in HD muscle

A specific respiratory chain defect in HD muscle was not found in the 12 muscle biopsies from the HD patients. Further analysis suggested that there was a relation between HD muscle MRC activities with various clinical parameters in the HD patients. Mitochondrial function has been demonstrated to decrease with age in many tissues (Coggan et al 1992, Trifunovic et al. 2004). Skeletal muscle mitochondrial respiratory chain activity has been shown to decline with increasing age over a wide age range (Coggan et al 1992). The controls in our study did not demonstrate a reduction in mitochondrial respiratory chain

activity with age. This probably reflected the relatively narrow age range of the control group (47.9 ± 11.8 years). However, over a similar age range (46.7 ± 11.1 years), there was a significant negative correlation between age and complex II/III:CS ratios in the HD group (Fig. 5.6.). The specificity of the complex II/III:CS changes observed with age in HD but not the control samples mitigated against a non-specific age-related effect which would be expected to include complexes I and IV, and suggested that MT htt either directly affected skeletal muscle complex II/III activity or was a secondary consequence of disease progression unrelated to htt expression e.g. progressive immobility. Immobility was not formally assessed but the most severely clinically affected patient, number 7 (Table. 5.1.), was still ambulant with support suggesting that MT htt may have had a direct effect on mitochondrial function unrelated to patient inactivity.

“Repeat years”-a possible marker of disease activity

Age and CAG repeat size are the main known risk factors for the progression of HD (Brinkman et al 1997). The age of the patient and the size of the CAG repeat were therefore incorporated to reflect severity of disease by correlating the product of age and CAG repeats, or “repeat years”, with clinical parameters. The cognitive and motor subscales of the UHDRS correlated substantially more significantly with repeat years than age alone. CAG repeats did not correlate with these clinical scales (Figs. 5.1. and 5.2.). This suggested that repeat years may be a better objective predictor of disease activity than age although the exact mathematical relationship between age, CAG repeats and disease status has yet to be determined.

Clinical parameters and MRC activities

The correlations of complex II/III:CS ratios with repeat years, disease duration, the cognitive subscale and two measures of functional status in the UHDRS, in the absence of age-related changes in the control samples, also suggested that decreasing complex II/III:CS ratios were associated with a worsening clinical phenotype and increasing CAG repeats (Figs. 5.8 and 5.10). Neuropsychological impairment in HD has been shown to occur at least two years prior to the manifestation of the motor features (Paulsen et al. 2001). Complex II/III:CS ratio positively correlated with the cognitive subscale and showed a trend, albeit not significant, to negatively correlate with the motor subscale (Fig. 5.5. and Table 5.4.). This suggested that mitochondrial dysfunction may be a sensitive indicator of early HD neuropathology and possibly underlie the cause of early neuronal dysfunction. It also indicated that worsening cognitive function may be a sensitive clinical indicator of underlying mitochondrial dysfunction within HD muscle.

Mechanisms of complex II/III dysfunction in HD skeletal muscle

If a progressive reduction in complex II/III activity occurred in HD patient's muscle, it could cause a sequence of biochemical events that may induce cellular damage, as is proposed for HD striatum (Tabrizi et al. 1999, Jackson et al. 2006). It may also explain the muscle wasting that occurs in HD patients independently of nutritional intake (Section 1.10.12). An excitotoxic mechanism in HD brain has been suggested to lead to an increase in nitric oxide which inhibits complex IV and subsequently complex II/III via free radical production (Tabrizi et al. 1999). There are few studies investigating the role of excitotoxicity in human muscle. Peripheral NMDA receptors in muscle, possibly on afferent fibre nerve terminals but also on muscle fibre membrane, are increasingly implicated in causing muscle pain (Cairns et al. 2003 and 2008). There is no data to suggest that classical neuronal excitotoxicity occurs in muscle, although a slow excess of

calcium influx through sarcolemmal NMDA receptors or from the sarcoplasmic reticulum, following acetylcholine stimulation of sarcolemmal nicotinic receptors, could possibly modulate a similar mechanism of cellular excitotoxicity within muscle fibres as in neurons.

Complex II/III inhibition in HD muscle may occur by alternate mechanisms to excitotoxicity and free radicals as has been increasingly described in HD brain. These mechanisms include MT htt aggregates impairing mitochondrial distribution and trafficking (Chang et al 2006, Solans et al. 2006, Orr et al. 2008) a direct effect of htt on mitochondrial function and the proteasome (Fukui et al 2007), and altered mitochondrial biogenesis (McGill et al 2006). These mechanisms and their role in HD are discussed in more detail in Sections 6.4.3 and 6.9.2.

Mitochondrial dysfunction in HD muscle

In contrast to Arenas et al. (1998), who found a complex I defect in HD muscle compared to age-matched controls, a specific respiratory chain defect in HD muscle was not found in the 12 muscle biopsies from the HD patients. This difference may partly be explained by the number of patients in the respective studies; Arenas et al. (1998) examined 3 muscle biopsies compared to 12 biopsies (Section 5.5.1). There was also a broad range of clinical severities within the HD patients in this study (Table 5.1) which may have caused a greater variability in the levels of mitochondrial function. The patients in the Arenas study had larger CAG repeats (mean 67 compared to a mean of 44 in this study) and longer disease duration (mean 14 years compared to 3.7 years in this study). Arenas et al. (1998) comment that all their patients were ambulatory and showed no evidence of muscle wasting which was unusual for patients with such high CAG repeats and long

disease duration. In the current study, patient 7 (46 CAG repeats and symptoms for 10 years) and patient 11 (44 CAG repeats and symptoms for 8 years) were ambulatory over short distances and were the most severely clinically affected. Therefore, the differences in mitochondrial complex activity between the two studies may be partially accounted for by increased disease duration and CAG repeat length causing more severe disease in the Arenas patients. Apart from one study by Parker et al. (1990), who described a complex I defect in HD platelet mitochondria, there have been no other reports of complex I defects in HD. The absence of the reproduction of a complex I defect and the small number of HD patient muscle biopsies analysed in the study by Arenas et al (1998) would suggest that a complex I defect is unlikely to have an important role in the pathogenesis of HD.

There have been few other studies apart from Arenas et al (1998) which have investigated bioenergetics in HD skeletal muscle. Using imaging techniques, energetic defects have been found in HD muscle using ^{31}P and ^1H MRS (Koroshetz et al. 1997, Lodi et al. 2000). In contrast, respiratory chain function in R6/2 mouse muscle at 12 weeks was normal in a single study by Tabrizi et al. (2000) which suggested against significant mitochondrial dysfunction in R6/2 mice skeletal muscle even when the brain was affected. However, gene expression profiles in the R6/2 mouse and HD muscle have demonstrated a transition from fast-twitch to slow-twitch muscle fibre types which also suggested a disturbance in energy metabolism in HD muscle before gross pathological features or respiratory chain dysfunction (Strand et al. 2005). Therefore, in spite of an absence of a major defect of mitochondrial function, there is evidence that the bioenergetics in HD muscle are not normal. The widespread association of a reduction in complex II/III activity with several clinical parameters in this study supports the hypotheses that either mitochondrial dysfunction is directly associated with clinical progression caused by MT htt, or that it is a direct consequence of another underlying metabolic disturbance due to

MT htt which secondarily is associated with worsening mitochondrial dysfunction. Irrespective of whether mitochondrial dysfunction was primary or secondary to MT htt, improving mitochondrial function may still have a molecular, and subsequently clinical, benefit.

6.4.3. Mitochondrial function in N-terminal and FL htt cell models

6.4.3.1. Mitochondrial function in the HEK 293 N-terminal htt model

The main advantage of the HEK 293 model in studying MRC activities was that cells naïve to MT N-terminal htt could be exposed to MT htt in order to assess if there was an early effect on MRC function. The expression of WT or MT N terminal htt for 48 hours in HEK 293 cells did not decrease MRC activities (Figs. 3.24.-3.26.). When MRC activities were compared between MT and WT N-terminal htt clones in four other stably transfected HD cell models, one found no change (Wytenbach et al 2001), two found a decrease in complex II/III activity in MT clones (Solans et al 2006 and Fukui et al. 2007) and one found a decrease in complex II activity in MT clones (Benchoua et al. 2006). Fukui et al. (2007) also demonstrated an increase in the activity of complex IV in the MT clones. The details of these cell models can be found in Table 1.5.

The influence of size of CAG repeat/N-terminal htt

The size of the CAG repeats and the N-terminal htt fragment in MT htt have been found to be important determinants of MT htt toxicity in HD cell models and transgenic mice. The normal MRC activities in the MT htt clones of the HEK 293 model may have been determined by the relatively large N-terminal htt fragment (171aa) and short number of

MT htt CAG repeats (59Q). The three models that demonstrated a defect in MRC activities expressed MT N-terminal htt with 82Q (Benchoua et al. 2006) and 103Q (Fukui et al 2007 and Solans et al 2006). This is in comparison to 74Q in Wyttenbach et al (2001) and 59Q in the current HEK 293 model where there was no MRC defect. This suggested that the MT CAG repeat size needed to be greater than 74Q to cause MRC dysfunction in N-terminal HD cell models. Furthermore, Solans et al (2006) and Fukui et al. (2007) expressed exon 1 of htt and Benchoua et al. (2006) expressed a longer 171aa N-terminal htt fragment and found MRC defects in comparison to Wyttenbach et al (2000) who expressed exon 1 of htt without finding an MRC defect. This suggested that small differences size in the size of the N-terminal htt fragment did not grossly influence MRC activities, whereas the size of the CAG repeat was a more important factor in determining MRC dysfunction.

The influence of the level of construct expression

The influence of levels of MT htt expression on toxicity in HD cell models and transgenic mice has not been studied in depth. However, the neurons vulnerable to neurodegeneration in HD post-mortem striatum have the highest levels of htt expression whilst the relatively-spared interneurons express low levels of htt (Ferrante et al. 1997). The level of MT htt expression has also been found to be important in determining the rate of aggregation of MT N-terminal htt in vitro. In the HEK 293 model, the level of N-terminal htt expression was up to 3 times greater than endogenous htt in the WT clones and 2 times greater in the MT clones. The level of expression of construct htt was not discussed in Wyttenbach et al (2001), Solans et al. (2006), Fukui et al (2007) or Benchoua et al. (2006) and it is therefore difficult to comment on the role of htt expression levels on mitochondrial toxicity in cell models. Benchoua et al. (2006) used a lentiviral vector

system containing the phosphoglycerate kinase (PGK) promoter which is associated with high levels of constitutive construct expression. One HD cell model which found an MRC defect (Fukui et al 2007) and two models which did not find an MRC defect (Wytenbach et al 2001 and the current HEK 293 model) used a CMV promoter and therefore similar levels of construct expression would have been expected. Therefore it would appear unlikely that differences in the levels of MT htt expression would explain the presence of an MRC defect.

The influence of cell background

HD has a striking predilection for affecting medium spiny neurones in the striatum more than any other cell type. Cell models with a neuronal background would therefore be expected to recapitulate the features in HD brain better than non-neuronal models. The four cell models described by Wytenbach et al (2001), Solans et al. (2006), Fukui et al (2007) or Benchoua et al. (2006) and the HEK293 model used different cell types making direct comparisons related to cellular background difficult. Benchoua et al. (2006) used a primary striatal model which would theoretically provide a cellular background that more closely modelled HD striatum and potentially would produce earlier mitochondrial dysfunction than non-striatal cell lines.

The influence of method of analysis of MRC function

The same spectrophotometric methods were used to assess mitochondrial respiratory chain complex activities in the current thesis as in Wytenbach et al. (2001), Solans et al. (2006) and Fukui et al.(2007). Solans et al. (2006) and Fukui et al.(2007) did not comment on why complex I activities were not assessed and Fukui et al.(2007) measured

complex II and III activities separately after finding a II/III defect using a combined complex II/III assay. Benchoua et al. (2006) used whole cell homogenates and not mitochondrial fractions to only assess complex II activity and used an iodonitrotetrazolium (INT) based spectrophotometric assay. They also adjusted activity to protein which does not compensate for the total mitochondria present in the preparation in contrast to comparison of citrate synthase (CS) ratios. These methodological factors may have significantly contributed to the finding of a complex II defect in MT clones by Benchoua et al. (2006) and make direct comparison with the other studies more difficult. For the studies performed by Wytttenbach et al. (2001), Solans et al. (2006) and Fukui et al.(2007) direct comparisons could be made because the same spectrophotometric methods were used.

The influence of experimental method of assessment of MRC activities

In the studies by Wytttenbach et al. (2001), Solans et al. (2006) and Fukui et al.(2007). Solans et al. (2006) and Fukui et al.(2007), a change in mitochondrial enzyme activity was calculated by comparing induced clones i.e. MT compared to WT. However, this thesis went on to compare the difference between induced and the uninduced pINDO, WT and MT clones because this comparison would control for the effect of the inducing agent, pon A, on mitochondrial function. The effects of the inducing agents, mifepristone (Fukui et al 2007) and galactose (Solans et al 2006) on respiratory chain activities is unknown, but the mitochondrial toxicity of tetracyclines (Wytttenbach et al. 2001) is well established (Section 6.2). The effects of the inducing agents have therefore not been controlled for in the cells models used by Wytttenbach et al. (2001), Solans et al. (2006) and Fukui et al.(2007) and this raises uncertainty about the validity of the reductions in complex II/III where it was described.

The influence of duration of induction of N-terminal htt

The construct expression induction time used in the cell models may have influenced mitochondrial function. Mitochondrial function was assessed at 48 hours and 18 hours post-induction in the models with normal mitochondrial function (the HEK 293 cell model and Wyttenbach et al. 2001). In the models with reductions in complex II/III activities, there were longer induction/expression times in 2 of the 3 cell models. Fukui et al (2007) assessed at 72 hours, Benchoua et al. (2006) at 6 weeks post-transfection of primary striatal cultures and Solans et al (2006) at 10 hours. The duration of exposure to N-terminal htt did not appear to have a major influence on MRC function, although the shorter duration of MT htt expression in the current HEK 293 model and Wyttenbach et al. (2001) can not be excluded as a potential factor influencing MRC function.

The influence of htt inclusions

MT htt intracellular inclusions in association with an MRC defect was described in three out of the four N-terminal htt cell models discussed above (Solans et al. 2006, Fukui et al. 2007 and Solans et al. 2006). The presence of inclusions in the Wyttenbach model (Wyttenbach et al. 2001) in the absence of MRC defects suggested that inclusions alone may not be sufficient to cause impaired respiratory chain function. The induction of MT htt occurred for only 18 hours prior to assessment of MRC function in the Wyttenbach model and therefore an MRC defect may have occurred at a later time point. The

HEK293 model did not demonstrate htt inclusions or an MRC defect and therefore htt inclusions may have been, at least in part, associated with MRC dysfunction. The role of htt inclusions in the pathogenesis of HD is discussed further in Section 6.8.

6.4.3.2. Mitochondrial function in the SH-SY5Y EYFP FL htt model

The constitutively expressing SH-SY5Y EYFP model enabled the investigation of MRC function in response to FL MT htt expression on a neuronal background without the need for an inducing agent. The potential disadvantage was that the SH-SY5Y cells had been exposed to constitutively expressing FL MT htt and this could have selected against cells that were more severely affected by MT htt toxicity. The brains of HD patients develop normally, as far as we understand, and the neurons within HD brains have been exposed to FL MT htt for many cell cycles during development. The SH-SY5Y model therefore recapitulated some of the features within neurons during the maturation of the HD brain. Therefore, the assessment of MRC function in the SH-SY5Y cells would enable the investigation of potential early defects in mitochondrial function in response to MT FL htt.

Complex IV defects were associated with prolonged exposure to htt

The SH-SY5Y cell model expressing FL MT htt exhibited a significant reduction in the complex IV:CS ratio and complex IV enzyme specific activities compared to WT htt and pcDNA3.1 control clones (Fig. 4.25). MRC activities in constitutive FL htt models have not been previously assessed in the literature. Complex IV defects have been described in post-mortem HD striatum (Gu et al. 1996, Browne et al. 1997 and Tabrizi et al. 1999) and in the striatum and cortex of the R6/2 mouse (Tabrizi et al. 2000). Tabrizi et al. (2000)

also found a mild, but non-significant defect in complex IV activity in R6/2 mouse skeletal muscle. In contrast, several inducible N-terminal htt cell models (Table 1.5), including Wytttenbach et al (2001), Solans et al. (2006) and the HEK 293 model from the current thesis, have found complex IV activities to be normal. Fukui et al. (2007) found increased complex IV activities in response to MT N-terminal htt expression in their cell model.

One explanation for the contrast in normal or increased complex IV activities in the N-terminal htt models (Solans et al. 2006, Wytttenbach et al. 2001, Fukui et al. 2007 and the HEK 293 model) with the reduced complex IV activities in the EYFP model, R6/2 mouse and human post-mortem brain, was that MT N-terminal htt may have inhibited complex IV but not for sufficiently long enough to produce a measurable reduction in activity in the N-terminal htt cell models. The maximum length of N-terminal htt expression was for 72 hours (Fukui et al. 2007). In contrast, prolonged expression of either N-terminal (exon 1 in the R6/2 mouse) or FL MT htt (HD post-mortem brain and the EYFP model) was associated with complex IV inhibition. It therefore appeared that the duration of MT htt expression was related to a complex IV defect rather than the size of the htt fragment. This delayed effect on complex IV activity by MT htt is in agreement with the hypothesis that following a reduction in complex IV activity, electron transfer is decreased leading to reduced oxidative phosphorylation and subsequently reduced intracellular ATP levels. As a secondary effect of impaired oxidative phosphorylation, increased superoxide is generated. As ATP levels reduce, neurons become increasingly vulnerable to glutamate-induced excitotoxicity or the “slow excitotoxicity” hypothesis (Novelli, A et al. 1998 and Tabrizi et al. 2000). This subsequently leads to further free radical generation, calcium dysregulation and inhibition of mitochondrial respiratory chain enzyme activities sensitive to free radicals, such as complex II/III, and aconitase. A secondary and delayed

reduction in complex II/III activity has been described following inhibition of an astrocytoma cell line with cyanide, a complex IV inhibitor (Hargreaves et al 2007). Consequently, complex IV inhibition could be involved as a primary event with complex II/III inhibition occurring later in the pathogenesis of HD. This would be consistent with the findings of complex IV inhibition, and not complex II/III, in the EYFP htt model and the R6/2 mouse, where exposure to MT htt would occur over weeks, whereas in HD brain, MT htt exposure occurs over decades in most patients enabling both complex II/III and complex IV defects to occur.

Complex II/III defects and cytoplasmic htt inclusions

The complex II/III defects in some of the N-terminal htt cell models (Solans et al. 1996, Fukui et al. 2007 and Benchoua et al. 2006) contrast with the FL htt EYFP and R6/2 models. The smaller N-terminal htt fragments, and/or the highly expanded CAG repeats used in these N-terminal models, may have by-passed the proposed early mechanism of complex IV inhibition, excitotoxicity and free radical generation. The mechanism by which this would occur is speculative but one possible explanation would be the location of the htt inclusions within the cells. The cell model by Wyttenbach et al. (2001) formed mostly nuclear, and not cytoplasmic, htt inclusions by 18 hours post-induction when complex activities were normal. This is in comparison to the cell models by Solans et al. (1996), Fukui et al. (2007) and Benchoua et al. (2006) which demonstrated cytoplasmic and nuclear inclusions at the time of assessment of mitochondrial function and demonstrated complex II/III defects. The presence of cytoplasmic htt inclusions may therefore have caused complex II/III defects by a direct effect on cytoplasmic mitochondria. This would also explain the findings in the R6/2 mouse which forms extensive mostly intranuclear htt inclusions and does not demonstrate a complex II/III

defect. It would also support the findings in the human post-mortem HD brain where there are neuropil/cytoplasmic and nuclear inclusions associated with complex II/III and IV defects. The mechanism by which cytoplasmic htt inclusion formation could cause complex II/III defects may include inhibition of proteasomal function (Fukui et al. 2007 and Section 6.6), inhibition of mitochondrial trafficking (Solans et al 2006 and section 6.9.1), or by the rapid development of cytoplasmic inclusions which directly distort and affect mitochondrial function (Solans et al. 2006). The direct role of htt and htt aggregates in the inhibition of mitochondrial function in HD is discussed further in Sections 6.8. and 6.9.2.

Summary: Mitochondrial dysfunction in HD

The reduction in complex II and/or III MRC activities in three HD N-terminal cell models (Solans et al. 2006, Fukui et al.2007 and Benchoua et al. 2006) appears to be strongly determined by the size of the expressed polyQ (greater than 74Q). This defect mirrors the findings in human HD post-mortem brain (Mann et al. 1990, Gu et al. 1996, Browne et al. 1997, and Tabrizi et al. 1999) and in HD muscle in this study. The R6/2 mouse, the N-terminal cell models with shorter polyQs (HEK 293 model in this thesis and the PC12 model (Wytttenbach et al. 2001)), and the EYFP FL htt model did not demonstrate a complex II/III defect. This may be partly explained by predominant cytoplasmic htt aggregates in systems demonstrating a complex II/III defect.

The reduction in complex IV activity in the EYFP FL MT htt model mirrored the changes in mitochondrial function seen in the R6/2 mouse and HD post-mortem brain and may reflect an early defect in mitochondrial complex activities better than the acute toxicity of N-terminal cell models. N-terminal htt probably still has a significant role in the

development of mitochondrial dysfunction as evidenced by the consistent defect in complex II/III function in three N-terminal htt cell models which mirrored the major defect in late-stage human HD brain. However, the findings in the EYFP model are likely to reflect the earliest molecular changes in the HD brain and model the early disease process better than expression of N-terminal htt which may model molecular changes at the later stages of the disease. It is postulated that over many years, a complex II/III defect develops in the HD brain and muscle, possibly as a result of increased accumulation of toxic N-terminal MT htt fragments. This would be in agreement with the findings in HD muscle where several clinical parameters of progression of disease were associated with a defect in complex II/III. Therefore, the toxic effect of FL MT htt may cause a reduction in complex IV as an early event in a molecular pathogenic cascade leading to a complex II/III defect, neurodegeneration and the HD clinical phenotype.

6.4.4. Mitochondrial toxins in htt cell models

The toxic inhibition of the MRC was a useful method to study the competence of cells expressing WT or MT N-terminal htt when metabolically stressed. If MT N-terminal htt caused a mild reduction in MRC function or affected another metabolic process that was dependent on ATP production, the MT cells should have been more sensitive to the mitochondrial toxin than WT cells.

There was a trend towards a non-significant increase in cell death in response to complex II inhibition by malonate in cells expressing MT N-terminal htt (Fig.3.29B). Antimycin A (a complex III inhibitor) has been described to cause increased aggregate formation, decreased proteasomal function and increased cell death in 143B (human osteosarcoma) cells expressing exon1-103Q htt (Fukui et al. 2007). If the major effect of N-terminal htt

is to inhibit complex II/III function as postulated in section 6.4.3., then further inhibition of complex II/III would be toxic to cells by causing a further reduction in ATP production.

In contrast to these findings, MT N-terminal htt expression was associated with a decrease in vulnerability to CN toxicity (Fig.3.30B). This suggested that the toxic effect of cyanide was partly ameliorated by MT N-terminal htt expression. However, one would expect that malonate, antimycin A and cyanide would inhibit the mitochondrial respiratory chain and cause a reduction in the phosphorylation of ADP which would cause cell death/dysfunction. The contrasting findings with malonate, antimycin A and cyanide in the HEK 293 cell model, Fukui et al (2006) and Sawa et al (1999) would suggest that the mechanism causing cell death is not entirely mediated by a reduction in cellular ATP production. One explanation for the contrast in response to mitochondrial toxins would relate to the duration of MT FL or N-terminal htt expression. An increase in apoptosis in HD lymphoblasts in response to cyanide has been described (Sawa et al. 1999). MRC function was not measured in the HD lymphoblasts but it was speculated that chronic exposure to MT FL htt in HD lymphoblasts would produce a reduction in complex IV activities and in turn cause a greater sensitivity to cyanide (Sawa et al 1999). However in cells exposed acutely to cyanide and MT N-terminal htt, where there is no evidence of a complex IV defect in cell models, an increase in cyanide-induced toxicity would not be expected. If this hypothesis were correct, one would predict that the EYFP MT FL htt model would demonstrate increased sensitivity to cyanide toxicity similar to HD lymphoblasts (Sawa et al 1999).

The protective effect of MT N-terminal htt on CN toxicity is difficult to explain. MT N-terminal htt could inhibit a process that is essential for mediating cyanide toxicity.

Alternatively, MT N-terminal htt may prevent binding of cyanide to the cytochrome aa3 subunit of complex IV and therefore reduce cyanide toxicity. There has been growing evidence of the association of N-terminal MT htt with mitochondria (Choo et al 2004 and Section 6.9.2.) although there is no published data to support the association of N-terminal htt with the components of the mitochondrial respiratory chain. A further alternative explanation would suggest that MT N-terminal htt protects against cyanide-mediated toxicity of iron-containing proteins outside of the mitochondrial respiratory chain, such as aconitase. This has not been investigated in the literature. A final explanation comes from the finding of increased complex IV activity associated with 143B (human osteosarcoma) cells expressing exon 1-103Q htt (Fukui et al. 2007). This would suggest that MT N-terminal htt may increase complex IV activity and therefore cause relative protection of MT compared to WT N-terminal htt expressing cells against complex IV inhibition.

There was a trend for increasing toxicity with malonate and reducing toxicity with cyanide in MT compared to WT compared to pIND0 cells in the HEK 293 cell model. WT N-terminal htt therefore caused a similar, but reduced, effect as MT N-terminal htt in response to cyanide and malonate. This suggested that N-terminal htt may independently have a toxic/protective effect unrelated to the size of the CAG repeats. WT N-terminal htt has been described in post-mortem brain (Kim et al. 2001) although the potential toxicity of WT N-terminal htt has not been investigated.

In summary, the greater cell death with malonate treatment and the reduction in cell death with cyanide treatment in cells expressing MT N-terminal htt expression supports the hypothesis that MT N-terminal causes a reduction in complex II/III function and bypassed the postulated initial reduction in complex IV activity to cause cell death. The protective

effect of MT N-terminal htt expression with cyanide treatment may have been caused by an increase in complex IV activity which has been described in one N-terminal htt expressing cell model (Fukui et al. 2007) but not in the current HEK 293 model. The potential mechanisms by which MT htt may affect mitochondrial function are discussed further in Section 6.9.2.

6.5. Oxidative Stress in cell models of HD

Aconitase activity as a marker of excess free radicals

Aconitase activity has been found to be extremely sensitive to superoxide and peroxynitrate and has been used as a marker of free radical damage (Hausladen, 1994, Gardner 1994, Patel 1996). Aconitase activity was reduced in the SH-SY5Y cells expressing MT FL htt but was normal in the WT FL htt expressing clones. This implied that FL MT htt caused decreased antioxidant defences and/or excess free radical production (Fig 4.25C). The reduction in aconitase and complex IV activity in the EYFP MT FL htt clones mirrored the defects in aconitase and mitochondrial function seen in the HD post-mortem striatum and cortex (Tabrizi et al. 1999) and in the R6/2 mouse striatum (Tabrizi et al. 2000). The reduction in aconitase and complex IV activities in the FL htt EYFP model contrasted with the normal aconitase activity in the WT and MT N-terminal htt HEK 293 models which suggested an absence of significant oxidative stress in response to N-terminal MT htt expression.

The inhibition of aconitase by FL htt but not N-terminal htt in the SH-SY5Y and HEK293 models suggested that FL htt may cause greater free radical production than N-terminal htt. This is unlikely to be due to the size of the htt fragment alone as the R6/2 mouse

expresses exon 1 htt and caused decreased aconitase activity in the striatum (Tabrizi et al. 2000). The duration that MT htt was expressed in the cells may be important and reduced aconitase activity may be caused by a progressive accumulation of excess free radicals over time. This could be investigated by assessing aconitase function in the SH-SY5Y model at increasing passages of the cells.

It remains unclear whether an increase in free radicals in HD results from MT htt-induced mitochondrial inhibition or whether MT htt-associated excess free radical production subsequently caused mitochondrial dysfunction. This has not been addressed in other FL htt cell models in the literature and could be investigated by adding antioxidants to the MT FL htt EYFP cells and measuring mitochondrial and aconitase activity. If mitochondrial dysfunction was an effect of MT htt expression upstream of free radical production, then potentially complex IV inhibition would be observed and associated with normal aconitase activity.

Paraquat toxicity in the HEK 293 model

Paraquat is an intracellular generator of free radicals, especially superoxide, which can rapidly react with NO to form peroxynitrate. In order to determine if N-terminal htt expression compromised the endogenous antioxidant system in the HEK 293 model, the clones were treated with paraquat. An increase in cell death in response to paraquat was seen in the MT N-terminal HEK 293 clones (Fig.3.31B). This supported the hypothesis that MT N-terminal htt expression compromised the antioxidant defences of the cells either by increasing production of free radicals and/or decreasing antioxidant defences. It also suggested that increased oxidative stress occurs within 48 hours of MT N-terminal htt expression, and that this is not sufficient to inhibit aconitase function. One explanation

suggests that early anti-oxidant compensatory mechanisms, such as increased glutathione or SOD, may prevent aconitase dysfunction. There is support for this in the inducible N-terminal htt model published by Wyttenbach et al (2001) in which van Roon-Mom et al. (2008) found an early up-regulation of genes in the anti-oxidant Nrf2-ARE pathway. Further support comes from the study by Choo et al (2005), who found similar levels of glutathione in the striatum and cortex of R6/2 mice compared to WT littermates, but found increased levels of glutathione in mitochondria isolated from the cortex and striatum. This suggested that compensatory mechanisms occurred specifically in mitochondria in response to a local excess of free radical generation that may not be detected when looking at whole brain tissue. Paraquat, as a source of free radicals and oxidative stress, has not been used extensively in the study of HD. Snider et al. (2003) found no difference in the effect of paraquat on cultured mouse cortical neurons from WT (HdhQ20) compared to MT (HdhQ111) transgenic mice but only used doses up to 100 μ M for 24 hours.

Mechanisms of free radical toxicity in HD

The generation of excess free radicals and the presence of oxidised end-products in HD post-mortem tissue and HD animal and cell models has been well described (Section 1.10.10). The molecular mechanisms of excess free radical production in HD and the role of free radicals either as a primary toxic effect of MT htt or a secondary consequence of MT htt-induced neuronal dysfunction, are poorly understood (Stack et al 2008). Fukui et al. (2007) found that complex III inhibition, by antimycin A, in their inducible N-terminal htt model (Table 1.5) promoted MT htt aggregation and cell death by proteasome inhibition independently of free radical production and ATP depletion. This suggested that oxidative stress or bioenergetic defects did not have a primary role in causing

neuronal cell death. The mechanism by which complex III inhibition may cause proteasomal dysfunction without excess free radical production and/or ATP depletion is uncertain. Puranam et al. (2006) have described the action of purified 62Q-GST on isolated mitochondria. The authors failed to demonstrate a direct effect of 62Q-GST on respiratory chain complex activities but did find increased free radicals and impaired mitochondrial respiration. The authors concluded that polyQ inhibited mitochondrial respiration by the generation of free radicals but the authors did not comment on the origin of the free radicals or the mechanism of impaired mitochondrial respiration. It therefore appears that isolated polyQ can generate free radicals independently of inhibiting the mitochondrial respiratory chain suggesting oxidative stress may be a primary event. In support for the primary pathogenic role of free radicals in HD, Solans et al. (2006) published an inducible N-terminal htt yeast model (Table 1.5) which demonstrated an increase in free radical production 5 hours post-induction of MT N-terminal htt and a partial reversal of the observed reduction in mitochondrial complex II activity by resveratrol. Resveratrol is a compound commonly found in plants and activates SIRT1 and PGC-1 α (peroxisome proliferators-activated receptor coactivator 1 α) which leads to improved mitochondrial biogenesis and anti-oxidant defenses (Lagouge et al 2006). This suggested that in the Solans et al (2006) model, complex II inhibition is preceded by free radical generation and that PGC-1 α may be inhibited by MT htt. A protective effect of PGC-1 α overexpression on paraquat toxicity in a neuronal cell line has been described (St-Pierre et al. 2006). The authors implicated the role of PGC-1 α in inducing mitochondrial and anti-oxidant defence genes suggesting that the impairment in the activity of PGC-1 α may be one mechanism by which MT htt mediates its pathogenic effect. Cui et al. (2006), in an HD striatal cell model and HD transgenic mice, have described MT htt-induced disruption of mitochondrial function by inhibition of the transcription of PGC-1 α and overexpression of PGC-1 α reversed the effects of MT htt.

This provides a possible common link between MT htt-induced transcriptional dysregulation, excess free radicals and mitochondrial dysfunction in HD.

In summary, the precise role of free radicals in the pathogenesis of HD remains unclear although there is increasing evidence from the current and previous studies that excess free radical production and increased sensitivity to free radicals is an early event which may be linked to transcriptional dysregulation of mitochondrial and anti-oxidant proteins by MT htt. In spite of this uncertainty, there is growing evidence from HD cell models, animal models of HD and small clinical studies (Stack et al 2008) that treatment with antioxidants e.g. high dose vitamin E and creatine, and respiratory chain components, e.g. ubiquinone, may reduce some of the pathogenic effects of MT htt *in vivo*. Clinical trials, such as CREST-E and CARE, are already investigating the treatment of HD patients with antioxidants, including creatine, and ubiquinone (Huntington Study Group).

6.6. The Ubiquitin-Proteasomal System (UPS) in HD

The UPS has been implicated in several neurodegenerative diseases (Ardley et al. 2005). The UPS may contribute to the pathogenesis of neurodegeneration due to inhibition of proteasomal function by toxic soluble or aggregated proteins, such as MT N-terminal htt and MT htt aggregates (Section 1.6.3.). The UPS may degrade proteins into toxic fragments, such as FL htt into N-terminal fragments, although there is little direct evidence for this (Section 1.6.4.). The proteasome may also have a protective role in removing toxic MT htt N-terminal fragments. Therefore, not only would proteasome inhibition theoretically impair general cellular function but would also cause an accumulation of toxic N-terminal htt fragments (Section 1.6.4.).

Proteasomal inhibition by MT htt

FL htt expression was associated with a decrease in the trypsin-like activity of the proteasome but trypsin-like activity was increased in the clones expressing WT FL htt (Fig. 4.26). This suggested that FL MT htt inhibited and FL WT htt enhanced proteasome function. An isolated reduction in trypsin-like activity by MT htt has not been described previously in HD and may represent an early event in proteasome dysfunction. The inhibition of the three proteasomal enzyme activities has been found in early and late-grade post-mortem HD cerebellum, cortex, substantia nigra and caudate/putamen, HD skin fibroblasts and in a primary striatal cell model expressing a 548aa. N-terminal fragment of htt with 105Q (Seo, H. et al 2004 and 2007). The more widespread decrease in proteasomal activities with the Seo et al (2007) model was possibly due to the longer poly Q and a shorter MT N-terminal htt fragment expressed. In the HD post-mortem brain and fibroblast studies the longer duration of exposure of the proteasome to FL MT htt, or its cleavage products, over many years may have also caused a more widespread reduction in proteasome activity. The mechanism by which MT FL htt or its cleavage products causes proteasomal dysfunction is uncertain. One possible mechanism would be free radical inhibition of the proteasome (Goswami et al 2007). Bulteau et al. (2001) described oxidative modification of the 20S proteasome and a reduction in all three proteolytic activities of the proteasome following reperfusion of ischaemic cardiac tissue. This suggested that proteasome function can be directly impaired by free radical modification. A study on proteasome function in rat livers found that the treatment of the proteasome with 4-hydroxy-2-nonenal, a major lipid peroxidation product, specifically inactivated trypsin-like activity and this effect was prevented by the addition of HSP 90 (Conconi et al 2004) which suggested that free radicals and/or lipid peroxidation may cause impaired trypsin-like activity. The reduced aconitase activity in the MT htt EYFP

clones would suggest excess free radical production and would support a role for free radicals in causing the isolated reduction in trypsin-like activity in the EYFP MT FL htt model. The free radical modification of proteasome components has not been investigated in HD.

MT htt aggregates are associated with many proteins in post-mortem brains and in HD transgenic mice (Section 1.7.5.). The accumulation of proteasomal components in the aggregates is an alternative possible mechanism by which MT htt could cause proteasomal dysfunction. The sequestration of the 20S proteasomal subunit into htt inclusions has been demonstrated in the R6/1 mouse model and N-terminal htt expressing cell culture systems (Waelter et al. 2001a, Wyttenbach et al. 2000). The EYFP model did not demonstrate spontaneous inclusions but did demonstrate a reduction in trypsin-like activity suggesting that htt aggregates were not necessary to mediate proteasomal dysfunction. This is in agreement with Seo et al. (2007) who found proteasomal dysfunction in the absence of htt inclusions at day three post-induction in their striatal cell model of HD.

The direct interference of MT htt with proteasome function may represent a further possible mechanism by which MT htt causes proteasomal dysfunction. In two studies, degradation of MT htt exon 1 by the proteasome was decreased. In the first, HEK 293 cells transiently expressed GFP-labeled exon 1 htt with 103Q (Bence et al. 2001), whilst in the second, N2a cells expressed exon 1 htt with 150Q in an inducible model of HD (Jana et al. 2001) (Table 1.5). The inhibition of proteasomal degradation of MT exon 1 htt occurred in a polyQ repeat length-dependent manner, with higher polyQs causing greater proteasomal dysfunction. These models did not investigate individual enzyme activities of the proteasome or whether degradation of other proteins was more broadly inhibited by

MT htt. The mechanism by which MT htt degradation by the proteasome is reduced remains uncertain, although it could have been caused by an indirect effect of MT htt on proteasome function, such as free radical generation, as opposed to MT htt directly inhibiting proteasome function.

In contrast to the EYFP model, an N-terminal inducible cell model (exon 1-Q103 htt) (Fukui et al. (2007) and Table 1.5) demonstrated reduced chymotrypsin-like activity of the proteasome following treatment with the complex III inhibitor, antimycin A, which was not prevented by antioxidants. The authors did not comment on proteasome function in their model without antimycin A. This suggested that complex III inhibition can synergistically cause proteasomal dysfunction with MT N-terminal htt expression and this process was independent of excess free radical production. The molecular mechanism linking the proteasome, complex III and htt is unknown and how this relates to the finding in the EYFP FL htt and HD post-mortem brain is uncertain but suggests that N-terminal MT htt can cause proteasomal dysfunction in the presence of mitochondrial inhibition. In vivo mitochondrial inhibition, potentially caused by FL htt, could potentiate the subsequent proteasomal inhibition by FL MT htt or its cleavage products.

The increased trypsin-like activity in the WT EYFP clones was a novel finding. There has been no link to proteasomal physiological function and htt, although WT htt has been linked to transcriptional regulation (Li and Li for a review 2004) which may afford one mechanism by which WT htt increased proteasomal function.

Sensitivity to lactacystin in the HEK293 model

Lactacystin specifically inhibits the chymotryptic and tryptic activities of the proteasome by covalently binding to the 20S catalytic core (Fenteany et al 1995; Groll et al 1997). The treatment of the HEK 293 N-terminal htt model with a mildly toxic dose of lactacystin allowed the assessment of the sensitivity of cells to WT and MT N-terminal htt in the context of proteasomal inhibition. If N-terminal htt impaired proteasomal function then an increase in cell death would have been expected. HEK 293 expressing WT N-terminal htt exhibited less cell death, whereas MT N-terminal htt expression increased lactacystin-induced cell death (Fig.3.32). A reduction in cell death by FL endogenous WT htt following expression of N-terminal MT htt has been described in cellular and transgenic models (Ho et al. 2001, Leavitt et al. 2001, Van Raamsdonk et al 2005). The HEK 293 model demonstrated an apparent protective effect of WT N-terminal htt in comparison to FL WT htt. In conjunction with the finding of increased trypsin-like activity in the EYFP WT FL htt clones, this suggested that WT htt may have a physiological role in controlling proteasome function. The protective effect appeared to be specific to proteasomal inhibition, as the toxicity of malonate and paraquat, were not improved with WT N-terminal htt expression. The potential mechanisms by which this protective effect occurred included ameliorating the downstream toxic molecular effects of proteasome inhibition, a direct effect on lactacystin rendering it less toxic, or a direct effect on the proteasome by N-terminal WT htt to inhibit the binding of lactacystin. There is no published data to support these hypotheses.

The increase in lactacystin-induced cell death was specific for N-terminal MT htt expression and suggested that either MT N-terminal htt was more toxic when it was not degraded by the proteasome or that inhibition of the proteasome affected other cellular processes, which rendered N-terminal MT htt more toxic. Cells expressing N-terminal MT htt have previously been demonstrated to be more vulnerable to lactacystin (Jana et al

2001, Table 1.5) which was suggested to relate to increased aggregate formation. The presence of htt aggregates in the HEK 293 model following treatment with lactacystin was not investigated in the current thesis and would be important question to answer in future work but was investigated in the FL htt EYFP model and is discussed below. Proteasome inhibitors have anti-tumour activity in cell culture and induce apoptosis by disrupting the regulated degradation of cell cycle proteins (Adams et al. 1999). Enhanced cell death with N-terminal MT htt expression would suggest that N-terminal MT htt may potentiate the lactacystin-induced apoptotic mechanism. There is limited evidence that apoptosis occurs in HD but there is evidence of upregulation of proapoptotic proteins (Hickey et al 2003). Future work would focus on assessing the frequency of apoptosis and htt inclusion formation following lactacystin treatment in the HEK 293 cells and the effects of lactacystin on apoptotic pathways in the context of WT and MT N-terminal htt expression.

Inclusion formation in response to lactacystin

Htt inclusions are an important feature of HD neuropathology and have variably been detected in HD transgenic animal and cell models (Section 1.7. and Table 1.5). Htt inclusions were not a feature of the cell models studied in this thesis (Section 6.8). However, EYFP fluorescent perinuclear inclusions formed in both mitotic and differentiated WT and MT FL htt clones treated with lactacystin but not in mitotic or differentiated untreated clones (Fig. 4.17). Similar inclusion formation following treatment with lactacystin has been described in an inducible Tet-“Off” HEK 293 cell model expressing exon 1 (51 or 83Q) (Waelter et al 2001a). The WT htt expressing cells (20Q) did not form inclusions following lactacystin treatment. The cells expressing 83Q htt formed inclusions more quickly than the 51Q htt which suggested that inclusion

formation was dependent on the size of the CAG repeats. The inclusions formed predominantly in a perinuclear distribution and occasionally in the nucleus. Mitochondria accumulated around the margins of the inclusions and the inclusions deformed and indented the nuclear membrane. The inclusions formed in the EYFP model displayed many properties similar to the inclusions in the Waelter et al. (2001a) model and were "aggresome-like" (Johnston et al. 1998). One of the most striking differences between the EYFP model and the model by Waelter et al (2001a), was that Waelter et al (2001a) found htt inclusions in the absence of lactacystin in the 51Q and 83Q MT clones, as has been described in other inducible and constitutive cell models (Table 1.5). This may be partially explained by the shorter htt fragment expressed in other cell models, in comparison to FL htt expressed in the EYFP model. FL htt delays the onset of inclusion pathology in FL htt knock-in HD mice (Shelbourne et al. 1999), transgenic HD mice (Reddy et al. 1998) and human post-mortem HD brains (Vonsattel et al 1985) in comparison to transgenic HD mice expressing N-terminal htt fragments (Mangiarini et al 1996) which rapidly form inclusions. Two inducible cell models expressing FL MT htt have demonstrated htt aggregate formation (Lunkes et al 1998, Sugars et al. 2004, Table 1.5). In comparison to the EYFP FL htt model described here, the models by Lunkes et al (1998) and Sugars et al. (2004) expressed 116Q and 136Q in comparison to the EYFP MT htt model which expressed MT htt with 90Q. Therefore, longer polyglutamines were associated with inclusion pathology without the requirement for proteasomal inhibition.

Similar inclusions were observed in lactacystin-treated WT htt as well as MT htt EYFP clones, in contrast to Waelter et al (2001a) and other cell models (Table 1.5). This suggested that both EYFP WT and MT htt were processed by the trypsin and chymotrypsin-like activities i.e. lactacystin sensitive, of the proteasome. It also suggested that inclusions may form from WT htt if the proteasome is inhibited sufficiently. Whether

the inclusions consisted of soluble htt or aggregated forms of htt was not investigated. Inclusion pathology from FL or N-terminal WT htt has not been previously described in other HD cell or animal models.

One explanation for the formation of inclusions in the WT htt EYFP clones was that rather than forming aggregates consisting of cross-linked N-terminal fragments in β -pleated sheets, which was proposed for MT htt in HD (Perutz et al 1994, DiFiglia et al 1997), the aggresome-like bodies represented accumulations of unprocessed FL WT and MT htt in response to failure of degradation by the proteasome. Nevertheless, this demonstrated that degradation of FL WT or MT htt involves proteasomal processing. This is supported by Martin-Aparicio et al. (2001) who found that proteasomal inhibition prevented the removal of htt aggregates from a conditional transgenic mouse model of HD.

The EYFP inclusions were immunostained by all htt antibodies used in the present study except for the most C-terminal antibody, Ab7666, which mostly stained the periphery of the inclusions but not the core (Fig. 4.20). This suggested that the inclusions did not consist predominantly of N-terminal htt products, as has been demonstrated for inclusions in HD post-mortem brain, HD mice and other cell models (DiFiglia et al 1997 and Davies et al. 1997). It did suggest that EYFP accumulations were mostly unprocessed FL WT and MT htt as suggested by the recognition of epitopes along the length of htt. The slightly reduced Ab7666 staining suggested that the C-terminus may have been processed by non-proteasomal pathways or that the epitope recognised by Ab7666 was hidden within the inclusion. This further suggested that processing of FL htt is dependent on the trypsin and chymotrypsin-like activities of the proteasome.

It was noted that there was a tendency for more EYFP WT htt cells to contain inclusions in comparison to MT cells. There were also more WT than MT cells in culture following lactacystin treatment suggesting that MT clones died faster or that WT cells grew more quickly. Waelter et al (2001a) also noted increased cell death in MT clones following lactacystin treatment (Table 1.5). This suggested that the perinuclear inclusions or proteins that were not degraded by the proteasome were more toxic in the MT than the WT EYFP clones.

In summary, the data from the EYFP model and other cell and animal models has suggested that the proteasome is involved in the processing and removal of FL WT and MT htt. The formation of “aggresome-like” inclusions in response to lactacystin in the WT and MT clones may represent a pathophysiological response of the cell to unprocessed EYFP htt. This has been described in other cell systems (Johnston et al 1998) although aggresome-like inclusions have not been described following WT htt expression and may represent a novel insight into the physiological processing of WT htt by lactacystin sensitive-proteasomal mechanisms.

6.7. Processing of htt

The first step in the pathogenesis of HD may involve abnormal processing of FL MT htt to generate toxic N-terminal MT htt fragments (Section 1.6.). The size of these fragments is still uncertain. The EYFP FL htt model enabled the assessment of processing of htt using antibodies to epitopes across FL htt and the treatment of the cells with lactacystin allowed the possibility of greater detection of fragments that may have been degraded by the proteasome.

There was no evidence of htt cleavage products in EYFP WT or MT FL htt clones without lactacystin treatment. Following lactacystin treatment of the EYFP FL htt WT clone 23 1 1 for 24 hours, additional htt bands at 44kDa and 34kDa were detected (Fig. 4.22 and Table 6.1). The EYFP insertion is approximately 25kDa, and therefore these N-terminal fragments would be predicted to be 19 and 9kDa respectively (approximately 173 and 82 amino acids). The 82aa fragment would therefore terminate just short of the C-terminal end of the polyglutamine stretch (exon 1 is 92 aa with 23 CAGs), and the 173 aa fragment at the start of exon 4.

WT/MT EYFP clones	Size (kDa) on blot	Estimated amino acids of N- terminal htt fragment	Similar bands in literature
1 WT clone (23 1 1)	44 and 34	173 and 82	Schilling et al. (2007) Lunkes et al (2002)
1 WT clone (23 6 7)	111	782	
3 MT clones (88 2 8, 2 9 and 2 11)	36	100	Sieradzan et al (1999), Lunkes et al (2002), Schilling et al (2007)

Table 6.1. Summary of extra htt bands in EYFP model following lactacystin treatment for 24 hours. Note that the size of the band on the blot included the EYFP protein (25kDa.)

Schilling et al (2007) used a panel of 4 anti-htt antibodies within the first 171aa of htt to estimate the size of these fragments and described two bands of 45kD and 35 kDa in the MT (82Q) cells with a similar 10kDa difference between the two bands as seen in their WT cells. The two bands observed in the current study migrated slightly less than those seen by Schilling et al. (2007) in their WT clones (44 and 34 kDa compared to 27 and 17kDa). This was partly due to the EYFP tag in the EYFP clones and therefore the predicted sizes of the fragments would be smaller at 19 and 9kDa. It was also possibly

due to differences in conditions within the gels used and due to difficulties in accurately estimating the size of proteins containing polyglutamines. An alternative explanation is that the extra bands in the EYFP model were different from the bands Schilling et al. (2007) observed. The extra htt bands recognised by Schilling et al. (2007) and in the current thesis are also similar in length to those seen by Lunkes et al (2002) between 18 and 129aa of htt in MT htt expressing cells (Table 6.1).

The presence of the 44 and 34KDa extra htt bands only with lactacystin, in the current study, suggested that the bands were possibly present at a low level and proteasome inhibition was required for accumulation of these cleavage products. It also suggested that the proteins forming these additional bands were processed by the proteasome. The absence of these bands in other WT EYFP clones may have been due to variation between clones in expression levels, the variation in the integration site of the construct within the host SH-SY5Y cells and the variable phenotype within the population of SH-SY5Y cells. There are no other reports apart from Schilling et al (2007) and the current thesis of processing of WT htt and therefore it remained possible that processing of WT htt was not a physiological event and was an artefact of both models.

There was an additional band at 111kDa in WT clone 23 6 7 following 24 hours treatment with 5 μ M lactacystin (Fig.4.24). This would represent an N-terminal fragment at approximately 782aa within the second proposed HEAT sequence (Fig.1.1). A fragment of this size has not been described and could represent abnormal transcription/translation of the integrated construct or physiological cleavage of WT htt.

Three out of the four EYFP MT htt clones demonstrated an additional band at 36kDa following treatment with lactacystin for 24 hours, representing an htt fragment of 11kDa

(approximately 100aa). The CAG repeat sequence in htt starts at aa18 and therefore this fragment would approximately terminate at the C-terminal end of the polyglutamines encoded by the 88 CAGs. An N-terminal fragment terminating within the region of the termination of the polyglutamine repeats has not been described previously and may represent a novel cleavage product. A MT htt cleavage product of 100aa would be more in keeping in size with the htt fragments described by Sieradzan et al (1999), Lunkes et al (2002) and Schilling et al (2007) between aa.18 and 129, than the caspase/calpain cleavage sites between aa.469-586 (Sun et al 2002, Wellington et al. 1998 and 2002, Gafni et al. 2004).

Cleavage within or close to the C-terminus of the polyglutamine stretch may represent one mechanism that distinguishes processing of MT and WT htt, causing an abnormal toxic MT N-terminal htt fragment to be cleaved. It is postulated that the expanded polyglutamine region alters the confirmation of FL htt at the boundary between the polyglutamine sequence and the polyproline region and this enables an otherwise unspecified protease to abnormally cleave htt to an N-terminal MT htt fragment.

The extra htt band in three out of four of the EYFP MT clones were only observed following treatment with lactacystin and therefore were probably cleavage products formed at a level too low to detect on Western blots in cells with an uninhibited proteasome. This would suggest that the extra bands were, at least partially, degraded by the chymotrypsin and trypsin-like activities of the proteasome i.e. lactacystin-sensitive components, and highlights the importance of the proteasome in the processing of htt. It also suggested that the extra bands were not formed by proteasomal processing mitigating against a significant role of the proteasome in formation of potentially toxic N-terminal htt fragments.

Apart from the extra bands described above, no further extra bands were observed in N-terminal or FL htt cell models. If processing of MT htt has a significant role in the pathogenesis of HD, greater evidence of differences in processing of MT htt in comparison to WT htt may have been expected. One explanation would be that processing was occurring but at levels too low to detect on the Western blots. Another possibility was that mitotic cells do not accumulate N-terminal MT htt fragments as efficiently as post-mitotic differentiated cells in vivo. The MT clone (88 1 3) was the only MT clone to be differentiated for 4 weeks and was the only MT clone which did not demonstrate an extra 36kDa band with lactacystin. It is possible that differentiation of the three MT EYFP clones which did demonstrate an extra band with lactacystin may have demonstrated an extra band without lactacystin treatment and this would be important future work to be performed.

The formation of EYFP htt inclusions occurred in all WT and MT EYFP clones and therefore was independent of the formation of the extra band in three out of four of the MT clones. This suggested that abnormal processing of htt was not necessary for the EYFP inclusions to form. There was also no qualitative differences in the rate of cell death, rate of inclusion formation or the morphology between the MT EYFP clone that did not express an extra band from the three that did express an extra 36kDa band although this would need to be investigated quantitatively.

Whether processing of FL htt to N-terminal htt fragments is necessary for initiating neurodegeneration in HD remains a complex and unanswered question. There are several lines of evidence which suggest that processing of FL MT htt occurs but the role of MT N-terminal fragments remains unclear. Firstly, transgenic mice that express only N-

terminal portions of MT htt develop inclusions and other neuropathological features more quickly than transgenic mice that express FL htt (Davies et al. 1997, Schilling et al 1999 and Becher et al 1998). This is suggestive but not conclusive of the requirement for FL htt processing in HD. FL htt may be toxic in its own right but less toxic than N-terminal htt. Secondly, the HD transgenic mice expressing only N-terminal htt develop a phenotype with some similar clinical and pathological features to HD (Davies et al. 1997, Schilling et al 1999 and Becher et al 1998). However, ectopically expressed CAG repeats cause intranuclear inclusions and a late-onset neurological phenotype in the mouse (Ordway et al. 1997) which suggests toxicity is conferred as much by the expanded CAG repeats as it is by the protein context. Thirdly, the inclusions formed in FL htt HD transgenic mice are formed by N-terminal fragments of MT htt (Reddy et al. 1998, Hodgson et al. 1999 and Wheeler 2000), suggesting that processing of FL htt was necessary for htt inclusion formation but not necessarily for mediating MT htt toxicity. Lastly, nuclear and cytoplasmic neuronal inclusions in HD post-mortem brain, have been found to be immunoreactive with antibodies directed against N-terminal but not C-terminal regions of htt (DiFiglia et al. 1997, Gutekunst et al. 1999, and Sieradzan et al. 1999) and N-terminal fragments of MT htt have been detected in immunoblots of homogenates from HD brains and HD mice (DiFiglia et al. 1997, Zhou et al. 2003 and Tanaka et al. 2006). These studies are strongly compelling for the existence of processing of FL MT htt, but do not prove that N-terminal htt is the toxic molecule in HD.

The FL EYFP model also suggested that there were differences in processing between WT and MT FL htt. The extra N-terminal MT htt band in three of four MT EYFP clones did not appear to cause gross toxic effects on the cells although detailed investigation would be needed to clarify this further. The possibility of FL WT htt processing and the role of WT N-terminal fragments in the function of htt also remain uninvestigated.

Schilling et al (2007) demonstrated that a transiently transfected HEK 293 cell model expressing N171-18Q formed smaller WT N-terminal htt non-toxic fragments between 90 and 115aa which suggested that WT htt may also be cleaved physiologically. It is postulated that processing of WT htt may be necessary for its nuclear translocation and its potential function in nuclear-cytoplasmic trafficking. This may explain why WT htt has been detected in the nucleus (Bessert et al. 1995) and how abnormally processed MT N-terminal htt may form nuclear inclusions as it abnormally accumulates in the nucleus.

6.8. Huntingtin Inclusions

Cytoplasmic and nuclear inclusions are a striking histological feature of HD post-mortem brains, HD transgenic mice and some HD cell models (Becher et al 1998, Davies et al 1997 Lunkes et al 1998). Intracellular inclusions have also been described in organs other than the brain such as R6/2 mouse skeletal muscle (Sathasivam et al. 1999, Orth et al. 2003) and in differentiated HD myotubes (Ciammola et al 2006). The precise role of htt inclusions in the pathogenesis of HD may be pathological, protective or an epiphenomenon (Davies et al 1997, Becher et al. 1998, Hackam 1998 and Lunkes et al 1998, Hackam 1998, Gutekunst et al 1999, Arrasate et al 2004, Arango et al 2006, Bodner et al 2006 and Section 1.7.).

HD cell models

There was no evidence of intranuclear or cytoplasmic htt inclusions in mitotic or differentiating SH-SY5Y cells constitutively expressing WT or MT FL htt, or in the inducible HEK293 WT and MT N-terminal htt cell model. Most inducible HD cell models in the literature have developed htt inclusions. These models expressed short N-

terminal fragments, such as exon 1 (90aa) (Wang et al 1999, Jana et al. 2001, Waelter et al 2001, Wyttenbach et al 2001, Solans et al 2006 and Fukui et al. 2007) and with up to 150 CAG repeats (Jana et al. 2001). Many of these models were also differentiated (Lunkes et al. 1998, Wang et al 1999, Jana et al. 2001, Wyttenbach et al 2001) and expressed N-terminal htt for up to 18 days (Lunkes et al. 1998). Table 1.5 summarises the characteristics of the inducible cell models and the location of the htt inclusions. The HEK 293 cell model described in the current thesis expressed MT N-terminal htt with a relatively short CAG repeat length (57 CAGs), the product was expressed for only 48 hours in mitotic cells and the N-terminal htt fragment was relatively long (176aa in WT). Benchoua et al. (2006) described a HD cell model expressing an 171aa htt N-terminal fragment with 82 CAGs in a rat primary striatal model, compared to 57 CAGs in 176aa N-terminal fragment in the current HEK 293 model. Benchoua et al. (2006) found htt aggregate pathology. This suggested that the size of the CAG repeat was possibly an important factor in determining htt aggregate formation, as discussed above, although it may have also been due to the neuronal primary striatal cells in the Benchoua et al. (2006) model, which may be expected to form htt inclusions more readily because of a neuronal background. The main factors which therefore influence formation of htt inclusions in inducible HD cell models include the length of N-terminal fragment, size of CAG repeat, duration of N-terminal htt expression, cell type and differentiation.

There are no constitutively expressing FL htt cell models for direct comparison with the EYFP model. The inducible model described by Lunkes et al. (1998) expressed MT FL htt with 73 CAG repeats in NG105-15 cells. The cells were differentiated and formed predominantly cytoplasmic inclusions which suggested that differentiation may be important in the formation of inclusions from FL MT htt. The inducible model described by Sugars et al (2004) expressed MT FL htt with 136 CAG repeats and formed htt

inclusions which also suggested that highly expanded CAGs could cause inclusion formation even on the background of FL htt (Table 1.5). In summary, highly expanded CAG repeats and/or post-mitotic cells appear to be important determinants of htt inclusion formation from FL MT htt. One would therefore have expected the EYFP MT htt model to form inclusions spontaneously following two weeks differentiation. The absence of inclusions in this model may have been secondary to the EYFP tag at the N-terminal end of FL htt which could have inhibited N-terminal htt fragment aggregation due to the size of the EYFP tag (25kDa).

Another explanation for the absence of inclusions in the EYFP FL htt model was secondary to constitutive expression. The cell models by Li et al. (1999) and Ye et al. (2008) constitutively expressed MT htt (exon 1-150Q) in PC12 and differentiated N2a cells respectively, and neither formed htt inclusions. Htt inclusions did not form in either model in spite of the small N-terminal fragment and high CAG repeat length. Chun et al (2001 and 2002) constitutively expressed 63 aa of htt with 82 CAGs and found infrequent inclusions. This suggested that aggregate formation was less common in constitutively expressing cell models than inducible cell models, possibly due to the toxicity in cells forming aggregates during cloning. Several other models lacking inclusion formation have been published. Sipione et al. (2002) and Seo et al. (2007) investigated ST14A (rat embryonic striatum) cells expressing N-terminal 548-amino-acid htt fragments with 26, 67, 105 or 118Q under the control of a doxycycline-regulated promoter. They found early changes in gene transcription within 24 hours of induction of MT N-terminal htt in the absence of inclusions. This suggested that a relatively long N-terminal fragment can inhibit aggregate formation in inducible cell models even when the fragment contains 118Q. The absence of inclusion formation in HD models has also been described in HD mouse models. Shelbourne et al. (1999) have described an HD knock-in mouse model

with 72-80 CAGs which demonstrated behavioural changes without gross neuronal cell loss or inclusions. These studies further support the hypothesis that neuronal dysfunction can occur without inclusion formation.

HD muscle

In the present thesis, immunocytochemistry with Ab675 or anti-ubiquitin antibody did not detect htt positive inclusions in any of the 12 HD muscle biopsies. This was confirmed with the absence of intranuclear inclusions on ultrastructural analysis with the exception of a severely affected 56 year old patient with a disease duration of 6 years and with the highest motor score in the UHDRS (76) and the third lowest cognitive score (126). This patient's muscle ultrastructural studies demonstrated electron dense intranuclear inclusions which suggested that inclusions possibly form in the later stages of HD in muscle. Clinically, these inclusions are unlikely to be useful to monitor the disease although they do confirm that abnormal MT htt processing does occur outside of the CNS and that similar pathological molecular mechanisms may exist in muscle. Htt mRNA expression in skeletal muscle (Li S-H et al 1993), cytoplasmic htt in HD muscle fibres (Hoogeveen et al. 1993) and htt inclusion formation in myotubes from HD skeletal muscle (Ciammola et al 2006) have been described . However, there has been no description of htt inclusion formation in skeletal muscle in the literature and this is the first description of possible htt inclusions in skeletal muscle from post-mortem tissue. The lack of inclusions detected in HD muscle may partially reflect that some of the patients were asymptomatic or only mildly symptomatic. Cortical neuropil threads and occasional cortical intracellular inclusions have been described in presymptomatic HD brain but prominent htt inclusion formation is not a common early feature in post-mortem HD brain (DiFiglia et al. 1997; Gutekunst et al. 1999, Gomez-Tortosa et al. 2001). The lack of

inclusions may also reflect that muscle is not a severely affected tissue in comparison to the brain as demonstrated by the normal routine muscle histology in the majority of severely affected HD patients. The molecular processes that relatively spare skeletal muscle from MT htt-associated pathology will potentially be important for our understanding of the mechanisms underlying predominantly neuronal degeneration in HD.

The early lack of inclusions in the HD brain and skeletal muscle can be compared to HD mice where htt aggregate pathology has been described most extensively in mouse transgenic models expressing truncated N-terminal fragments of htt with highly expanded CAG repeats, such as the R6/2 mouse (Davies et al 1997). HD transgenic mice show a more restricted distribution or absence of inclusions in FL htt mouse models (Reddy et al. 1998 and Shelbourne et al 1999) which suggests that FL htt slows the process of htt inclusion formation. In the HD mouse models, the aggregate pathology often occurs before the onset of a severe clinical phenotype (Davies et al. 1997, Reddy et al. 1998 and Lin et al 2001) and readily occurs in organs outside the CNS, such as skeletal muscle (Sathasivam et al 1999). These findings would suggest that aggregate formation occurs before the onset of gross clinical dysfunction. However, in some HD mouse models, such as the R6/2 mouse, where aggregate pathology starts at 4 weeks in the cortex, subtle cognitive and motor dysfunction has been detected at 3.5 and 5 weeks respectively, which suggests that early neuronal dysfunction may occur in transgenic HD mice before severe aggregate pathology and the method of clinical detection of a neurological phenotype may determine the temporal relationship of phenotype to aggregate formation (Carter et al 1999).

In summary, the formation of htt aggregates appears dependent on truncation of FL htt to a small N-terminal fragment. When the N-terminal fragment contains a highly-expanded CAG repeat, htt inclusions form more rapidly. The differentiation of cells may also influence aggregate formation. In vitro studies have demonstrated that the threshold for htt aggregation is between 32 and 37 polyglutamines when expressed in exon 1 of htt (Scherzinger et al 1999). The precise influence of the size of the N-terminal htt fragment and the mitotic state of cells on aggregate formation is not clear from the literature. The hypothesis generated by Perutz et al. (1994) for the formation of htt inclusions in the “polar zipper” model of htt inclusion formation did explain the important influence of CAG repeat size on the rate of aggregate formation. One explanation would suggest that more highly expanded CAGs would be more likely to form stable triplet repeat “hairpin loops” which would more easily aggregate due to greater availability of hydrogen bonds between the CAG repeats. Another explanation would suggest that small N-terminal fragments could cause less steric hindrance to hairpin loops binding to other hairpin loops which would enable htt aggregates to form more easily. Finally, post-mitotic cells could enable a cellular environment where accumulating protein aggregates would be less likely to be removed during mitosis and promote aggregate formation. There is no data in the literature to support these hypotheses and would provide areas of future work.

The mechanism of aggregate formation is fascinating however the question remains as to whether inclusions are pathological, an epiphenomenon, or protective. Inclusion formation was not a feature of the current HEK 293 and EYFP cell models or in most of the HD muscle biopsies. The absence of inclusions is similar to other constitutively expressing cell models (Li et al. 1999 and Ye et al. 2008), in some inducible cell models (Sipione et al. 2002 and Seo et al. 2007) and in some HD transgenic mice (Shelbourne et al 1999). These models and the current HEK 293 and EYFP cell models and HD muscle,

have demonstrated MT htt-associated mitochondrial dysfunction (EYFP models and HD muscle), excess free radical production (EYFP model), decreased neuritic outgrowth on differentiation (Li et al. 1999, Ye et al. 2008, EYFP model), increased cell death (Li et al. 1999, Ye et al. 2008), widespread abnormalities in cellular transcription, including proteins involved in cell signalling, vesicle trafficking and lipid metabolism (Sipione et al. 2002), behavioural abnormalities in HD mice (Shelbourne et al 1999), synaptic plasticity (Usdin et al 1999) and reduced proteasome function (Seo et al. 2007, EYFP model). These molecular changes occurred in the absence of htt aggregates. This would support the role of cellular dysfunction occurring before gross htt aggregate pathology. The lack of correlation between inclusion formation and cell death has also been described in several animal and cell models of HD (Saudou et al. 1998, Kim et al. 1999, Arrasate et al 2004, Arango et al 2006). Based on the cell models and HD skeletal muscle investigated in the current thesis, it is postulated that htt aggregates are not responsible for the early pathological changes in HD and that MT htt exerts its toxic effect by non-htt aggregate-related mechanisms.

6.9. Subcellular localisation of htt

The location of htt may be an important determinant of its function (Section 1.5.3). Most studies have used anti-huntingtin antibodies to the N-terminus of htt and therefore it is difficult to determine whether cleaved N-terminal fragments or FL htt were detected. Endogenous htt has been mostly found in the cytoplasm (DiFiglia et al. 1995, Gutekunst et al. 1995) but there are several reports of FL and N-terminal htt in the nucleus (Bessert et al. 1995, De Rooij et al. 1996 and Sapp et al. 1997) and in a perinuclear location (Sapp et al. 1997). Bessert et al. (1995) also described nuclear localisation of WT FL htt in HEK 293 cells which were the cells used in the N-terminal htt model in this study. The

predominantly cytoplasmic location of FL htt is not limited to one sub-cellular compartment. FL WT htt has been described in association with the plasma membrane, endocytic and autophagic vesicles, endosomal compartments, endoplasmic reticulum, Golgi apparatus, mitochondria and microtubules (Atwal et al. 2007, Rockabrand et al. 2007, Strehlow et al 2007). The widespread distribution of htt does not help in defining its physiological function but alterations in the subcellular distribution following MT htt expression may provide information as to the pathological role of expanded CAGs.

6.9.1. Co-localisation of htt with vesicular markers

The HEK 293 model in the current thesis demonstrated that WT and MT N-terminal htt partially co-localised with VAMP and synaptophysin suggesting that htt was associated with vesicles. There was no evidence of co-localisation with the Golgi complex or lysosomal markers. The association of N-terminal WT and MT htt with synaptophysin is in agreement with previous studies (Wood et al. 1996 and Gutekunst et al. 1998) although the association of VAMP and htt has not been described. These results suggested that VAMP/synaptophysin-associated vesicles may be involved in trafficking of N-terminal htt or that N-terminal htt may have a physiological function in vesicle trafficking. The presence of intensely staining cells for synaptophysin in some of the pon A-treated MT N-terminal htt HEK 293 cells suggested that N-terminal MT htt may cause increased expression of synaptophysin, possibly as a compensatory mechanism following failure of vesicular function, or MT N-terminal htt may have caused an accumulation of vesicles (Figs. 3.17, 3.18, 3.20 and 3.21). There is no previous literature suggesting accumulation of synaptophysin in HD. However, there is evidence that expression of MT N-terminal htt inhibits movement of vesicles and mitochondria along neuronal projections (Trushina et al 2004, McGuire et al 2006, Caviston et al 2007) suggesting that vesicular transport is

impaired in HD. In addition to its role in the transcriptional regulation of BDNF, htt is essential for efficient axonal transport of vesicles containing BDNF (Gauthier et al 2004). Therefore, failure of vesicular function may represent one mechanism by which MT htt causes neuronal dysfunction and cell death.

6.9.2. Mitochondrial association with huntingtin

There is recent evidence of the association of soluble htt and htt aggregates with mitochondria (Panov et al. 2002, Choo et al. 2004, Petrasch-Parwez et al. 2007 and Section 1.10.9). MT htt may directly inhibit the mitochondrial respiratory chain although there is no data to support this hypothesis. Other pathological roles by MT htt on mitochondrial function include impaired mitochondrial trafficking and distribution (Chang et al. 2005, Solans et al. 2006, Orr et al. 2008), altered mitochondrial biogenesis (McGill et al 2006 for review), induction of apoptosis (Sawa et al 2003) and impaired transient calcium storage (discussed in Section 1.10.).

The association of htt with mitochondria was investigated using subcellular localisation studies in the HEK 293 and SH-SY5Y cell models. There was a partial association of mitochondria with N-terminal MT and WT htt in the HEK 293 cell model. In some of the MT N-terminal htt clones, the association occurred as a perinuclear “aggresome-like” inclusion. This suggested that N-terminal htt associated with mitochondria. Panov et al. (2002) first demonstrated, by electron microscope, that MT N-terminal htt localised to mitochondria in the brain of a HD transgenic model. Subsequently, Choo et al.(2004) showed that both WT and MT FL htt were associated with the outer membrane of mitochondria isolated from WT and MT mouse striatal cells. The direct association of N-terminal MT htt with the mitochondria was suggested to affect the respiratory complex

activities of mitochondria (Solans et al 2006). In contrast, a recent study found no effect on the mitochondrial respiratory chain activities of MT polyQ protein on isolated mitochondria, although the poly Qs were not expressed in a htt background (Puranam et al 2006). The current HEK 293 cell model would support recent evidence linking the association of N-terminal htt with mitochondria although the role of the association is less clear and needs further investigation.

Mitochondria co-localised with the perinuclear EYFP inclusions in the lactacystin-treated EYFP WT and MT FL htt clones. The pcDNA3.1. clones also demonstrated a perinuclear accumulation of COX1 staining suggesting that the formation of an “aggresome-like” perinuclear body was a consequence of proteasomal inhibition, rather than a specific accumulation of EYFP htt. However, the association of mitochondria with MT FL htt within the aggresome-like inclusions may represent one of the mechanisms that inhibits mitochondrial function in HD. It is postulated that MT htt may impair proteasomal function and secondarily this leads to the formation of aggresome-like inclusions which could alter trafficking and the function of mitochondria. Impaired mitochondrial trafficking by MT htt has been described (Trushina et al 2004, Chang et al. 2006). In the skeletal muscle of desmin-null mice, failure of locating mitochondria to the correct position within the cell impaired mitochondrial function (Milner et al. 2000). Solans et al. (2006), in an inducible N-terminal htt cell model, found that misfolded or aggregated htt could disturb the network of actin cytoskeleton, which could impair mitochondrial distribution and function. Therefore, there is evidence for the association of FL and N-terminal WT and MT htt as well as htt inclusions with mitochondria but how and if htt affects mitochondrial function directly remains to be fully elucidated.

6.9.3. Nuclear and perinuclear localisation of htt

The nuclear localisation of htt and htt aggregates has been considered to be an important step in the pathogenesis of HD (Sections 1.6.1, 1.7.1 and 6.1.3). Nuclear WT htt may have a physiological role, but nuclear translocation of MT htt to the nucleus may be an important step in causing cell dysfunction/death by aggregate formation or inhibition of transcription.

Following the pon A induction of N-terminal htt expression, the nuclear localisation of both WT and MT N-terminal htt in the HEK 293 model was observed in all clones. Fluorescence microscopy demonstrated nuclear staining as intense fluorescence in the centre of the cell (Fig. 3.2). Confocal microscopy confirmed that the nuclei of both WT and MT N-terminal htt clones contained several punctate areas of staining with Ab675 (Fig. 3.16. A and 3.19. A). There was also less intense positive nuclear staining in uninduced WT and MT N-terminal htt clones (Fig. 3.16A) in support of the presence of physiological nuclear htt in HEK 293 cells.

The first 17 aa of htt, N terminal to the polyglutamine stretch, have been suggested to be vital in exporting htt out of the nucleus as a nuclear export signal (NES) (Cornett et al. 2005, Atwal et al. 2007) The C-terminus may also contain an NES and possibly a nuclear localisation signal (NLS) (Xia et al 2003 and Fig. 1.1). The current study would be consistent with a NLS in the first 171aa of htt or that truncation of htt to 171aa. was associated with the loss of a nuclear export signal (NES) such as that described in the C-terminal region of htt by Xia et al (2003 and Fig. 1.1.). The inducible cell model by Lunkes et al (1998) described nuclear localisation of FL htt with 116 polyQ and not with 73 or 15 (Table 1.5). This also occurred more quickly with an N-terminal fragment of 80aa compared to 502aa. Nuclear localisation did not occur with WT htt. This study

demonstrated that nuclear htt immunostaining increased with shorter N-terminal fragments of htt and with longer CAG repeats and suggested that similar factors leading to inclusion formation were also associated with translocation of MT htt to the nucleus. Most other inducible cell models of HD expressing exon 1 of htt have described nuclear and cytoplasmic localisation of htt (Wang et al 1999, Jana et al. 2001, Wyttenbach et al 2001 and Fukui et al. 2007). The constitutive N-terminal htt models have suggested that MT N-terminal htt also localised to the nucleus (Li et al. 1999, Chun et al. 2001, 2002) when the N-terminal htt fragment was exon 1 or 63aa (Table 1.5b). This is in contrast to Sugars et al. (2004) who expressed FL htt and Sipione et al. (2002) and Seo et al. (2007) who expressed 548aa of htt in inducible HD cell models. These authors described cytoplasmic htt expression only, in spite of nuclear inclusions forming in the MT cells in Sugars et al. (2004). In conjunction with the finding of nuclear N-terminal htt in the HEK 293 model in the current study, this suggested that between 171aa and 548aa of htt, there may be an important nuclear export sequence (NES) that has not been described. This region contains a known HEAT repeat sequence and some of the known calpain and caspase cleavage sites but not a recognised NES.

In support of the hypothesis that FL htt has to be processed to N-terminal htt fragments in order for htt to stay in the nucleus, EYFP FL WT and MT htt SH-SY5Y models did not express nuclear fluorescence. This suggested the absence of significant amounts of nuclear FL htt which is in agreement with an inducible FL htt cell model (Sugars et al. 2004). However, htt antibody studies in SH-SY5Y cells (see below) demonstrated Ab7667-positive granular staining in the nucleus suggesting that htt up to at least aa1844-2131 can physiologically enter the nucleus.

Nuclear localisation of fluorescence in two of four EYFP WT htt clones investigated, following 2 days differentiation, suggested that WT htt was processed in some clones to a

fragment which could enter the nucleus or that the nuclear membrane became more porous to FL WT htt. Nuclear localisation of FL WT htt has been described by Bessert et al. (1995) but not subsequently. Localisation of FL MT htt was not observed in any of the four MT EYFP clones following differentiation. The immunocytochemical studies using the htt panel of antibodies on the differentiated clones with EYFP nuclear fluorescence, demonstrated that the WT htt nuclear staining was positive for all htt antibodies, which argued against truncation of the htt product entering the nucleus. It is, however, possible that C-terminal cleavage products were also entering the nucleus and being detected, in addition to N-terminal htt products. There is no clear explanation for the localisation of FL WT MT EYFP htt in two out of four WT clones. A specific effect of the integration of the EYFP construct into genomic DNA can not be excluded.

The Abcam (Cambridge, UK) htt antibodies Ab7667 and Ab7668 and to a lesser extent Ab7666 demonstrated nuclear punctate staining, which was especially visible in the mitotic pcDNA 3.1 clones but also in the mitotic EYFP WT and MT FL htt clones. Ab7666, 7667 and 7668 also demonstrated prominent perinuclear accumulations of htt which were also more pronounced in pcDNA3.1 than WT or MT htt EYFP clones (Figs. 4.3. and 4.12-4). This suggested that the Abcam antibodies recognised endogenous htt and that endogenous htt localised physiologically to nuclear and perinuclear locations as described previously (Bessert et al. 1995, De Rooij et al. 1996, Sapp et al. 1997). The relative absence of nuclear staining and strong perinuclear staining in pcDNA 3.1 clones developed with Ab7666 suggested that C-terminal region of endogenous htt may be processed before htt can enter the nucleus. It also suggested that EYFP may inhibit nuclear translocation of htt. The antibodies from Chemicon (EM48, Ab2166 and Ab2168) stained endogenous htt poorly in the pcDNA 3.1 clones, including the perinuclear and

nuclear staining recognised by the Abcam antibodies. The Chemicon antibodies preferentially stained EYFP WT and MT htt (Figs. 4.3 and 4.12-4).

It remains uncertain why only the Abcam antibodies, and not the Chemicon antibodies, should recognise endogenous perinuclear and nuclear htt. The three antibodies used from each manufacturer were raised to epitopes across the whole length of htt and therefore this effect is unlikely to be due to differences in the site of the antigen. All of the antibodies were monoclonal and the same secondary antibody was used throughout all experiments. It remains possible that some of the staining with the Abcam antibodies was cross-reactivity to non-htt proteins, although this would be unlikely with three unrelated antibodies.

In summary, this study demonstrated that N-terminal WT and MT htt can localise to the nucleus and that this process is not associated with increased cell death or dysfunction. The similar localisation of WT and MT N-terminal htt to the nucleus in the HEK 293 model suggested that a difference in localisation of N-terminal was unlikely to account for the molecular changes described in the MT N-terminal HEK 293 cells. The molecular abnormalities in the MT htt EYFP model, such as reduction in complex IV, aconitase and proteasomal activities occurred in the absence of nuclear translocation of htt which suggested that not all MT htt toxicity is mediated by nuclear localisation. The striking nuclear staining of all SH-SY5Y cells by two antibodies to internal epitopes (Ab7668 and Ab7667) but not to a C-terminal htt antibody (Ab7666) suggested that WT htt probably has a physiological role in the nucleus and that it may be cleaved distal to aa2131 at the C-terminus before it enters the nucleus.

6.10. Differentiation and the role of post-mitotic cells in HD

The cells predominantly affected in HD are post-mitotic neurons (Section 1.4.). Eventhough other groups of post-mitotic neurons are relatively spared, such as in the cerebellum, there is no evidence that mitotic cells are severely affected in HD which suggests that a post-mitotic state is one of the factors important in mediating MT htt toxicity. In order to recapitulate the features of post-mitotic neurons, SH-SY5Y cells were used to express FL htt in the EYFP model and retinoic acid was used to differentiate the SH-SY5Y cells Preis et al. (1998). This enabled the investigation of potential changes in subcellular localisation (Section 6.9.3), cellular morphology, possible inclusion formation and processing of htt following differentiation.

Morphology of SH-SY5Y cells following differentiation

Following differentiation for between 2 and 14 days, the SH-SY5Y MT FL htt model demonstrated decreased neuritic process formation, less complex neurite patterns of development and qualitatively reduced cell numbers compared to WT FL htt cells (Fig. 4.9-11). MT htt may alter the function of VAMP and other proteins involved in axonal transport and neurite formation, such as Hap-1 (Rong, J et al. 2006). It has been shown that htt interacts directly, as well as via its binding partner Hap-1, with the dynein/dynactin microtubule-based motor complex responsible for retrograde cellular trafficking. Hap-1 may also bind another molecular motor, kinesin, and thus could play a role (independently or as part of a complex with htt) in anterograde axonal transport (Gauthier et al. 2004 and Caviston et al 2007). This may explain the impaired differentiation observed in the EYFP MT htt compared to EYFP WT htt clones as early as 2 days following treatment with retinoic acid. Decreased neurite formation following differentiation and MT htt expression was also observed in the cell models described by

Wytttenbach et al (2001) and Ye et al (2008) (Table 1.5). In the cell model described by Ye et al (2008), both transiently and stably transfected MT cells developed shorter neurite formation following differentiation with 10 μ M retinoic acid for 48 hours or serum deprivation for 24 hours. In summary, MT htt may inhibit neurite formation during differentiation of neurons by affecting axonal transport and vesicle trafficking (Yang et al 2002 and Section 6.9.1.).

Inclusion formation

There was no evidence of inclusion formation on fluorescence microscopy up to two weeks post-differentiation in any of the four WT and MT htt EYFP clones or up to four weeks in one representative WT and MT clone on fluorescence microscopy and Western blotting. A constitutively expressing FL MT htt neuronal cell model has not been described previously. However, Ye et al. (2008) published a differentiated N2a transiently and stably constitutively expressing N-terminal htt cell model (Table 1.5) which demonstrated predominantly cytoplasmic inclusions in the MT (exon1-150Q) cells transiently transfected but not the stably transfected cells. This would be in agreement with the EYFP MT htt model and suggested that stable constitutive expression of MT htt could have prevented htt inclusion formation. It is speculated that transfected cells which formed inclusions may be die during constitutive expression and a population of htt expressing cells remained that would not form inclusions.

Several differentiated and inducible neuronal cell models of HD have demonstrated htt inclusion formation (Table 1.5). Lunkes et al. (1998) differentiated NG105-15 cells with 1% FCS (from 10% in mitotic cells), 10 mM forskolin and 100 mM IBMX (isobutylmethylxanthine) which expressed 80aa, 502aa and FL htt with 73 or 116polyQ.

Wang et al (1999) and Jana et al. (2001) differentiated mouse N2a cells expressing exon 1 htt with 60 or 150 polyQ with 5mM dcAMP (N6,29-O-dibutyryl adenosine-39:59-cyclic monophosphate sodium salt). All of these models were associated with htt inclusions in differentiated MT cells but the authors did not comment on inclusions in the mitotic cells. The only inducible cell model to compare mitotic with differentiated cells was Wytttenbach et al (2001) using a PC12 cell model. The cells were differentiated for 6 days with 1% horse serum and nerve growth factor (NGF) and the authors described increased cell death and more htt inclusions following differentiation of MT cells compared to mitotic MT cells. It therefore appears that differentiated cells more readily form htt inclusions than mitotic cells and that constitutive expression of MT htt prevents survival of cells with inclusions or prevents inclusion formation. The mechanism by which differentiation promotes htt inclusion formation is not clear but may explain the propensity for greater pathological changes to occur in post-mitotic cells in HD brain and HD transgenic mice (Becher et al 1998, Davies et al 1997, Sathasivam et al. 1999, Orth et al. 2003, Ciammola et al 2006). It is postulated that post-mitotic cells either have reduced capacity to remove abnormal or misfolded MT htt, or that processing of MT htt occurs more readily to a pathological N-terminal fragment.

Huntingtin processing

Following 4 weeks differentiation, a Western blot of WT htt EYFP clone 23 1 1 demonstrated a discrete additional band which migrated at approximately 90kDa. This was not present in a MT clone (88 1 3) or a pcDNA3.1 clone (Fig. 4.16). This additional band would be predicted to be an N-terminal htt fragment of 590 aa. The presence of this N-terminal htt truncated cleavage product could have caused the EYFP nuclear fluorescence observed in clone 23 1 1 following differentiation. The putative caspase 6

cleavage site is at aa.586 in htt. Caspase 6 cleavage of htt has been found to be necessary for neuronal dysfunction and degeneration in an HD mouse model (Graham et al. 2006). The absence of a 590aa N-terminal fragment in the MT clone investigated may have been due to toxicity of the 590aa N-terminal fragment when it contained MT CAG repeats. Alternatively, the failure of the cleavage of the MT htt EYFP clone 88 1 3 to form a 590 aa fragment may have represented an isolated feature of the clone and further studies would assess Western blots of other WT and MT clones.

6.11. Conclusions

6.11.1. Investigating the molecular pathogenesis of HD

The HEK 293 cell model used an inducible system which allowed the analysis of the earliest molecular events in response to WT and MT N-terminal htt with undetectable background expression of the constructs. The SH-SY5Y model used a constitutive system which enabled the investigation of the effects of the FL WT and MT htt expression on a neuronal background and the processing of FL htt. Both the HEK 293 and SH-SY5Y cell models expressed htt with relatively small pathological CAG expansions in the MT clones which was more representative of HD patients. The assessment of the effects of the differences between the cell models, such as cell background, size of the htt fragment and constitutive compared to inducible expression, enabled comparison of data generated in the two cell models, such as mitochondrial and aconitase function. There were drawbacks to the cell models. The relatively small sizes of the CAGs may have limited the pathology associated with MT htt expression. The inducing agent ponA may have inhibited cell division and DMSO caused clumping of the HEK 293 cells. In the SH-SY5Y model, the

N-terminal EYFP tag may have inhibited htt from entering the nucleus and prevented spontaneous inclusion formation.

In comparison to the cell models, the biochemical analysis of 12 muscle biopsies from HD patients and the assessment of the UHDRS in these patients enabled the correlation of clinical parameters and CAG repeats with mitochondrial function in a tissue that was relatively easier to study compared to brain.

6.11.2. FL MT htt cleavage at the polyglutamine/polyproline junction

The cleavage of FL htt to an N-terminal fragment has been identified in HD brains and variably in HD mouse and cell models. The generation of an N-terminal htt fragment may have an important role in the pathogenesis of HD although the exact size of the N-terminal htt fragment, the mechanism of truncation of FL htt and the molecular role of N-terminal htt remain uncertain. Using the SH-SY5Y model, there was no evidence of WT or MT FL htt cleavage under normal growth conditions. A novel N-terminal MT htt fragment of approximately 11kDa was described in the majority of EYFP FL MT htt expressing clones following treatment with lactacystin. This suggested that the formation of the novel MT N-terminal fragment was not a result of processing by chymotrypsin and trypsin-like activities of the proteasome which were inhibited by lactacystin. It is unclear if the cleaved protein accumulated because it was normally degraded by the proteasome, or if lactacystin induced other protease activities which cleaved htt. The absence of the 11kDa band in the WT clones was consistent with a difference in the processing of WT and MT FL htt. The 11kDa fragment was predicted to terminate at the junction between the polyglutamines and the first polyproline region. The consensus sequence does not

predict a known proteolytic site at this junction and suggested a novel mechanism for altered processing of MT htt into a potentially toxic N-terminal fragment.

In order to assess whether the 11kDa fragment caused cellular dysfunction, future work would compare cell death, htt inclusion formation, excess free radicals and mitochondrial dysfunction in the MT clones producing the 11kDa fragment with MT and WT clones not producing the 11kDa fragment following treatment with lactacystin. Protease inhibitors could be used to assess which proteases cleaved MT FL htt to the 11kDa fragment and further analysis of the 11kDa band using mass spectroscopy may identify the size of the fragment and enable its expression in a cell culture system.

The formation of htt inclusions in lactacystin-treated EYFP FL WT and MT clones demonstrated that the breakdown of FL WT and MT htt was dependent on the lactacystin-sensitive components of the proteasome. The inclusions were also found to contain FL htt as evidenced by detection of epitopes across the whole length of htt. Therefore an initial important step in the processing of FL htt may be proteasomal cleavage. Htt may be cleaved by other proteases as evidenced by the formation of the 11kDa fragment in the majority of the MT clones. This suggested a possible mechanism of MT htt toxicity in which MT htt impaired proteasome function causing accumulation of FL MT htt. FL MT htt subsequently could be cleaved by non-proteasomal proteases which may form toxic N-terminal products. In support of this was the finding of reduced trypsin-like activity in the MT EYFP FL htt clones. The further analysis of proteasomal components for evidence of free radical damage, abnormal assembly and co-localisation with MT FL htt would be important in the assessment of the mechanism of MT htt inhibition of the proteasome.

6.11.3. The physiological and pathological location of htt

Using the SH-SY5Y model, endogenous FL htt was found in a predominantly granular cytoplasmic location but there were also accumulations of endogenous htt in a perinuclear and nuclear distribution, and was in agreement with previous data. A novel finding was the reduced nuclear staining with the more C-terminal antibody Ab7666 in comparison to the more N-terminal antibodies Ab7667 and Ab 7668 which suggested physiological cleavage of FL endogenous htt prior to translocation to the nucleus. These findings also supported previous evidence that endogenous htt may have a role in regulating transcription and be involved in nucleo-cytoplasmic trafficking. This location was not affected by WT or MT FL htt expression in the SH-SY5Y model.

The perinuclear inclusions formed in the WT and MT FL htt EYFP clones following treatment with lactacystin were “aggresome-like” and formed in a similar location to the perinuclear accumulation of endogenous htt. Aggresomes form around the microtubule organising centre (MTOC) which suggested that endogenous htt may have a role in MTOC/centrosomal function including vesicular transport. MT N-terminal htt expression in the HEK 293 cell model was associated with increased synaptophysin staining which suggested that MT N-terminal htt may affect vesicular trafficking. Further work would investigate the distribution of other proteins involved in vesicular transport, such as dynein, to assess if there was a more generalised disruption of vesicle trafficking in response to MT htt. N-terminal MT and WT htt expression was mostly cytoplasmic but also nuclear. This suggested that expanded CAGs do not cause preferential nuclear translocation in comparison to WT CAG repeats. However, physiological processing of WT htt to an N-terminal fragment may not occur *in vivo* but is well established in MT htt. Therefore preferential processing of FL MT htt, *in vivo*, to an N-terminal htt fragment

which translocates to the nucleus can not be ruled out as a potential mechanism of MT htt toxicity.

6.11.4. The determinants of mitochondrial dysfunction in HD

There was no evidence of a reduction in MRC activities following N-terminal htt expression in the HEK 293 cell model in comparison to several published cell models. Comparison of published cell models with the HEK 293 model suggested that MT N-terminal htt may cause a reduction in complex II/III activity with greater than 72 CAG repeats and that the size of the N-terminal fragment is less important. The finding of reduced complex IV activity in the SH-SY5Y model and not in the HEK 293 model initially suggested that FL htt was required to inhibit complex IV. This would be consistent with the data from HD post-mortem brain but is in contrast to the reduction in complex IV in the R6/2 mouse. It was therefore postulated that complex IV inhibition occurred following prolonged expression of MT htt, as has been found in the SH-SY5Y model, HD brain and R6/2 mouse and not by the size of the htt fragment. It is possible that cleavage of MT FL htt to a toxic MT N-terminal htt fragment causes complex II/III dysfunction possibly in association with cytoplasmic htt inclusions. This would provide an explanation for prominent complex II/III defects in HD post-mortem brain and N-terminal cell models but not in the R6/2 mouse and the SH-SY5Y model where cytoplasmic htt inclusions are less common or do not occur.

MRC dysfunction may be caused by a direct effect of htt on the MRC, altered mitochondrial biogenesis by MT htt-induced transcriptional dysregulation or due to disrupted mitochondrial trafficking by htt inclusions or transcriptional dysregulation. The temporal relation of mitochondrial dysfunction and excess free radical formation in HD

remains unanswered. Future work would include treatment of the EYFP clones with anti-oxidants to determine if this protected the MT clones from complex IV dysfunction.

6.11.5. Cellular Dysfunction in the absence of htt inclusion formation

The EYFP model is the first stably-transfected constitutively expressing FL htt cell model to be characterised. MT FL htt expression was associated with mitochondrial dysfunction, free radical production and proteasomal dysfunction in the absence of inclusion formation. The N-terminal htt HEK 293 cell model demonstrated increased sensitivity to lactacystin, malonate and paraquat in association with MT N-terminal htt expression also in the absence of inclusion formation or cell death. Htt inclusions may independently be toxic however data from the current thesis suggested that early molecular defects in response to MT htt can occur prior to inclusion formation. It remains possible that if inclusion formation had occurred, the toxic effects of MT htt expression may have been greater. This study does not definitively answer the question of the role of htt aggregates in the pathogenesis of HD. However, htt inclusions are not a prominent early pathological feature in presymptomatic HD brain and the EYFP FL htt model would mimic these conditions more closely than most HD cell models and transgenic mice. The finding of molecular abnormalities described above would favour significant MT htt-induced cellular dysfunction prior to inclusion formation.

6.11.6. A molecular cascade leading to cell death and dysfunction in HD

A hypothesis is postulated using data from the current thesis and previous studies for the sequence of molecular events leading to cell dysfunction and death in HD. This hypothesis suggests that an early event in the pathogenesis of HD is inhibition of complex

IV and/or increased free radical production which leads to a chronic reduction in ATP causing a reduction in proteasome activity, inhibition of vesicular transport, impairment of transcriptional activity and excitotoxicity. Abnormal processing and accumulation of MT htt, possibly in association with impaired proteasomal function, would cause the formation of toxic N-terminal MT htt fragments. The N-terminal fragments and increased free radicals may cause inhibition of complex II/III, leading to further reductions in ATP levels. N-terminal htt aggregation may occur as a later event and cause cellular toxicity by sequestration of key cellular proteins, proteasomal dysfunction and inhibition of intracellular transport mechanisms. The relative roles of FL MT htt compared to N-terminal MT htt in causing toxicity has not been substantiated. HD transgenic mice expressing MT N-terminal htt have a phenotype similar to HD which has been suggested to imply that N-terminal htt may be more important for cellular toxicity than FL MT htt. However, the phenotype of these transgenic models differ from human HD and a neurological phenotype similar to HD has been demonstrated in transgenic mice expressing expanded CAGs in the hprt gene (Ordway et al 1997). It is postulated that eventhough MT N-terminal htt may form aggregates and be independently neurotoxic, it may not represent the initial toxic species in vivo. Fig. 6.1. summarises the molecular mechanisms in the pathogenesis of HD related to the findings in the current thesis. In the 16 years since the discovery of the HD gene, major advances have been made in our understanding of the neurobiology of HD. In spite of this, HD remains an incurable disease with a grave prognosis. Symptomatic and supportive treatments remain the mainstay of current management of HD. A greater understanding of the molecular pathogenesis of HD will enable the development of better rational therapeutic strategies in the future.

Fig. 6.1.

References

Adams, J, Palombella, V-J, Sausville, E.A, Johnson, J, Destree, A, Lazarus, D.D. et al. (1999). Proteasome inhibitors: a novel class of potent and effective antitumor agents. *Cancer. Res.* **59**(11),2615–22.

Alam ZI, Halliwell B, Jenner P. (2000). No evidence for increased oxidative damage to lipids, proteins, or DNA in Huntington's disease. *J Neurochem.* **75**,840-846.

Albin, R.L, Young, A.B, Penney, J.B, Handelin, B, Balfour, R, Anderson, K.D et al. (1990). Abnormalities of striatal projection neurons and N-methyl-D-aspartate receptors in presymptomatic Huntington's disease. *N Engl J Med.* **3322**(18),1293-1298.

Albin, R.L. and Greenamyre , J.T. (1992). Alternative excitotoxic hypothesis. *Neurology.* **42**(4),733-738.

Alexi, T, Hughes, P.E, Faull, R.L, Williams, C.E. (1998a). 3-nitropropionic acid's lethal triplet: cooperative pathways of neurodegeneration. *Neuroreport* **9**,R57-64.

Alexi, T, Hughes, P.E, Knusel, B, Tobin, A.J. (1998b). Metabolic compromise with systemic 3-nitropropionic acid produces striatal apoptosis in Sprague-Dawley rats but not in BALB/c ByJ mice. *Exp. Neurol.* **153**,74-93.

Allan, V. (1996). Motor proteins: a dynamic duo. *Curr. Biol.* **6**(6),630-633.

Ambrose, C.M, Duyao M.P, Barnes G, Bates, G.P, Lin, C.S, Srinidhi, J et al. (1994). Structure and expression of the Huntington's disease gene: evidence against simple inactivation due to an expanded CAG repeat. *Somat. Cell Mol Genet* **20** (1),27-38.

Anderson, S, Bankier, A.T, Barrell, B.G, de Bruijn, M.H, Coulson, A.R, Drouin, J, (1981). Sequence and organisation of the human mitochondrial genome. *Nature*. **290**,457-465.

Andrade, M. A. and Bork, P. (1995) HEAT repeats in the Huntington's disease protein. *Nature Genet.* **11**,115–116.

Arango, M, Holbert, S, Zala, D, Brouillet, E., Pearson, J, Regulier, E, et al. (2006). CA150 expression delays striatal cell death in overexpression and knock-in conditions for mutant huntingtin neurotoxicity. *J. Neurosci.* **26**,4649-4659.

Ardley, H.C., Hung, C-C, and Robinson, P.A. (2005). The aggravating role of the ubiquitin–proteasome system in neurodegeneration. *FEBS letters.* **579**(3),571-576.

Arenas J, Campos, Y, Ribacoba, R, Martín M.A, Rubio J.C, Ablanedo P, et al. (1998). Complex I defect in muscle from patients with Huntington's disease. *Ann. Neurol.* **43**,397-400.

Arrasate M, Mitra, S, Schweitzer, E.S, Segal, M.R, Finkbeiner, S. (2004). Inclusion body formation reduces the levels of mutant huntingtin and the risk of neuronal death. *Nature.* **431**;805-810.

Arzberger, T, Krampfl, K, Leimgruber, S, Weindl, A. (1997) Changes of NMDA receptor subunit (NR1, NR2B) and glutamate transporter (GLT1), mRNA expression in Huntington's disease- an in situ hybridization study. *J. Neuropathol. Exp. Neurol.* **56**(4), 440-454.

Atwal, R.S, Xia, J, Pinchev, D, Taylor, J, Epanand, R, and Truant, R. (2007). Huntingtin has a membrane association signal that can modulate huntingtin aggregation, nuclear entry and toxicity. *Hum. Mol. Genet.* **16**(21),2600-2615.

Augood, S.J. Faull, R.L.M., Love, D.R. & Emson, P.C. (1996). Reduction in enkephalin and substance P messenger RNA in the striatum of early-grade Huntington's disease: a detailed cellular in situ hybridization study. *Neuroscience* **72**(4),1023-1036.

Augood, S.J. Faull, R. L. & Emson, P. C. (1997). Dopamine D1 and D2 receptor gene expression in the striatum in Huntington's disease. *Ann. Neurol.* **42**(2),215-221.

Beckman, L, Robins-Wahlin, T.B, Lundin, A, Ginovart, N, Farde, L. (1997). Cognitive deficits in Huntington's disease are predicted by dopaminergic PET markers and brain volumes. *Brain* **120**,2207-2217.

Bae, B, Hara, M.R, Cascio, M.B, Wellington, C.L, Hayden,M.R, Ross, C.A et al. (2006). Mutant Huntingtin: Nuclear translocation and cytotoxicity mediated by GAPDH. *PNAS.* **103**(9),3405–3409.

Bains, J.S. and Shaw, C. (1997). Neurodegenerative disorders in humans: the role of glutathione in oxidative stress-mediated neuronal death. *Brain Research Reviews*. **25**(3), 335-358.

Bartzokis G, and Tishler TA. (2000). MRI evaluation of basal ganglia ferritin iron and neurotoxicity in Alzheimer's and Huntington's disease. *Cell Mol Biol*. **46**,821-833.

Beal MF. (1992). Does impairment of energy metabolism result in excitotoxic neuronal death in neurodegenerative illness? *Ann Neurol*. **31**,119-130.

Beal, M.F, Brouillet, E, Jenkins, B.G, Ferrante, R.J, Kowall, N.W, Miller, J.M et al. (1993a). Neurochemical and histological characterisation of striatal excitotoxic lesions produced by the mitochondrial toxin 3-nitropropionic acid. *J Neurosci*. **13**,4181-4192.

Beal MF, Brouillet E, Jenkins BG, Henshaw R, Rosen BR, Hyman BT. (1993b). Age-dependent striatal excitotoxic lesions produced by the endogenous mitochondrial inhibitor malonate. *J Neurochem*. **61**,1147-1150.

Beal MF, Henshaw DR, Jenkins BG, Rosen BR, Schulz JB. (1994). Coenzyme Q10 and nicotinamide block striatal lesions produced by the mitochondrial toxin malonate. *Ann Neurol*. **36**,882-888.

Beal MF, Howell N, and Bodis-Wollner I. (eds.) 1997 *Mitochondria and Free Radicals in Neurodegenerative Diseases*, Wiley-Liss, New York.

- Becher M.W, Kotzuk JA, Sharp AH, Davies SW, Bates GP, Price DL, Ross CA. (1998). Intranuclear neuronal inclusions in Huntington's disease and dentatorubral and pallidoluysian atrophy: correlation between the density of inclusions and IT15 CAG repeat length. *Neurobiology of Disease*. **4**,387-97.
- Bence, N.F, Sampat, R.M, and Kopito, R.R. (2001). Impairment of the ubiquitin-proteasome system by protein aggregation. *Science* **292**(5521),1552-1555.
- Benchoua A, Trioulier Y, Zala D, Gaillard MC, Lefort N, Dufour N et al. (2006). Involvement of mitochondrial complex II defects in neuronal death produced by N-terminus fragment of mutated huntingtin. *Mol Biol Cell*. **17**(4),1652-63.
- Benn C.L, Landles, C, Li, H, Strand, A.D, Woodman, B, Sathasivam, K, et al. (2005). Contribution of nuclear and extranuclear polyQ to neurological phenotypes in mouse models of Huntington's disease. *Hum. Mol. Genet*. **14**,3065–3078.
- Bennett, E. J., Bence, N. F., Jayakumar, R. and Kopito, R. R. (2005) Global impairment of the ubiquitin–proteasome system by nuclear or cytoplasmic protein aggregates precedes inclusion body formation. *Mol. Cell* **17**, 351–365.
- Berger, Z., Ravikumar, B., Menzies, F. M., Oroz, L. G., Underwood, B. R., Pangalos, M. N. et al. (2006). Rapamycin alleviates toxicity of different aggregate-prone proteins. *Hum. Mol. Genet*. **15**,433–442.

Bessert, D.A, Gutridge, K.L, Dunbar, J.C, and Carlock, L.R. (1995). The identification of a functional nuclear localization signal in the Huntington disease protein. *Mol. Brain. Res.* **33**(1),165-173.

Bett JS, Goellner GM, Woodman B, Pratt G, Rechsteiner M, Bates GP. (2006) Proteasome impairment does not contribute to pathogenesis in R6/2 Huntington's disease mice: exclusion of proteasome activator REG γ as a therapeutic target. *Hum. Mol. Gen.* **15**(1):33–44.

Bhide, P.G, Day, M, Sapp, E, Schwarz, C, Sheth, A, Kim, J, Young, A.B, et al. (1995). Expression of normal and mutant huntingtin in the developing brain. *J. Neurosci.* **16**(17), 5523-5535.

Bhutani, N., Venkatraman, P. and Goldberg, A. L. (2007) Puromycin-sensitive aminopeptidase is the major peptidase responsible for digesting polyglutamine sequences released by proteasomes during protein degradation. *EMBO J.* **26**,1385–1396.

Bibb JA, Yan Z, Svenningsson P, Snyder GL, Pieribone VA, Horiuchi A et al. (2000). Severe deficiencies in dopamine signaling in presymptomatic Huntington's disease mice. *Proc. Natl. Acad. Sci. USA.* **97**,6809-14.

Biedler, J.L, Roffler-Tarloy, S, Schachner, M and Freedman, L.S. (1978). Multiple neurotransmitter synthesis by human neuroblastoma cell lines and clones. *Cancer Res.* **38**,3751-3757.

Bizat, N, Hermel, J-M, Boyer, F, Jacquard, C, Creminon, C, Ouary, S et al. (2003).

Calpain is a major cell death effector in selective striatal degeneration induced in vivo by 3-nitropropionate: implications for Huntington's disease. *J. Neurosci.* **23**,5020-30.

Block-Galarza, J, Chase, K, Sapp, E, Vaughn, K, Vallee, R.B, DiFiglia, M et al. (1997).

Fast transport and retrograde movement of huntingtin and HAP1 in axons. *NeuroReport.* **8**(9-10),2247-2251.

Bodner, R.A, Outeiro, T.F, Altmann, S, Maxwell, M.M, Cho, S.H, Hyman, B.T. et al

(2006). Pharmacological promotion of inclusion formation: a therapeutic approach for Huntington's disease and Parkinson's disease. *Proc. Natl. Acad. Sci. USA.*

103,4246-4251.

Bogdanov M, Ferrante RJ, Kuemmerle S, Klivenyi P, Beal M.F. (1998). Increased

vulnerability to 3-nitropropionic acid in an animal model of Huntington's disease. *J Neurochem* **71**,2642-4.

Bonini, N.M. (2002). Chaperoning brain degeneration. *Proc. Natl. Acad. Sci. USA.*

99(Supple4),16407-16411.

Boutell, J.M, Thomas, P, Neal, J.W, Weston, V.J, Duce, J, Harper, P.S, Jones A.L.

(1999). Aberrant interactions of transcriptional repressor proteins with the Huntington's disease gene product, huntingtin. *Hun Mol Genet* **8**,1647-1655.

Bowman, A. B., Yoo, S. Y., Dantuma, N. P. and Zoghbi, H. Y. (2005). Neuronal

dysfunction in a polyglutamine disease model occurs in the absence of ubiquitin-

proteasome system impairment and inversely correlates with the degree of nuclear inclusion formation. *Hum. Mol. Genet.* **14**,679–691.

Brandt, J, Bylsma, F.W, Gross, R, Stine, O.C, Ranen, N, and Ross, R.A. (1996). Trinucleotide repeat length and clinical progression in Huntington's disease. *Neurology.* **46**,527-531.

Brennan, W.A, Bird, E.D, Aprille, J.R. (1985). Regional mitochondrial respiratory activity in Huntington's disease brain. *J Neurochem.* **44**,1948-50.

Brinkman, R.R, Mezei, M,M, Theilmann, J, Almqvist, E, Hayden, M.R. (1997). The likelihood of being affected with Huntington disease by a particular age, for a specific CAG size. *Am.J.Hum.Genet.* **60**,1202-1210.

Brouillet, E, Hantraye, P, Ferrante, R.J, Dolan, R, Leroy-Willig, A, Kowall, N.W, Beal, MF. (1995). Chronic mitochondrial energy impairment produces selective striatal degeneration and abnormal choreiform movements in primates. *Proc. Natl. Acad. Sci. USA.* **92**,7105-7109.

Browne SE, Bowling AC, MacGarvey U, Baik, M.J, Berger, S.C, Muqit, M.M. et al. (1997). Oxidative damage and metabolic dysfunction in Huntington's disease: selective vulnerability of the basal ganglia. *Ann. Neurol.* **41**,646-53.

Browne SE, Ferrante RJ, Beal MF. (1999). Oxidative Stress in Huntington's Disease. *Brain Pathol.* **9**,147-163.

Bruyn, G.W. (1968). Huntington's chorea. Historical, clinical and laboratory synopsis. In: Diseases of the Basal Ganglia. Handbook of clinical neurology. (Ed. PJ Vincken and GW Bruyn). 6:298-378.

Bulteau, A-L, Lundberg, K.C, Humphries, K.M, Sadek, H.A, Szweda, P.A. Friguet, B et al. (2001). Oxidative Modification and Inactivation of the Proteasome during Coronary Occlusion/Reperfusion. J. Biol. Chem. **276**(32),30057-30063.

Butterworth J, Yates CM, Reynolds GP. (1985). Distribution of phosphate-activated glutaminase, succinic dehydrogenase, pyruvate dehydrogenase, and α -glutamyl transpeptidase in post-mortem brain from Huntington's disease and agonal cases. J Neurol. Sci. **67**,161-71.

Butterworth NJ, Williams L, Bullock JY, Love DR, Faull RL, Dragunow M (1998). Trinucleotide (CAG) repeat length is positively correlated with the degree of DNA fragmentation in Huntington's disease striatum. Neuroscience. **87**,49-53.

Cairns, B.E, Svensson, P, Wang, K, Hupfeld, S, Graven-Nielsen, T, Sessle, B.J. et al. (2003). Activation of Peripheral NMDA Receptors Contributes to Human Pain and Rat Afferent Discharges Evoked by Injection of Glutamate into the Masseter Muscle. J. Neurophysiol. **90**,2098–2105.

Cairns, B.E. and Dong, X. (2008). The Role of Peripheral Glutamate and Glutamate Receptors in Muscle Pain. Journal of Musculoskeletal Pain. **16**(1/2),85-91.

Canals, J.M, Checa, N, Marco, S, Akerud, P, Michels, A, Perez-Navarro ,E et al. (2001). Expression of brain-derived neurotrophic factor in cortical neurons is regulated by striatal target area. *J. Neurosci.* **21**(1),117-124.

Carmichael, J, Chatellier, J, Woolfson, A, Milstein, C, Fersht, A.R. and Rubinsztein, D.C et al. (2000) Bacterial and yeast chaperones reduce both aggregate formation and cell death in mammalian cell models of Huntington's disease. *Proc. Natl. Acad. Sci.* **97**,9701-9705.

Carter, R.J. Lione, L, Humby, T, Mangiarini, L, Mahal, A, Bates, G.P. et al. (1999). Characterisation of motor deficits in mice transgenic for the human Huntington's disease mutation. *J. Neurosci.* **21**(1),117-124.

Cattaneo E, Rigamonti D, Goffredo D, Zuccato C, Squitieri F, Sipione S. (2001). Loss of normal huntingtin function: new developments in Huntington's disease research. *Trends Neurosci.* **24**(3),182-8.

Caviston, J. P., Ross, J. L., Antony, S. M., Tokito, M. and Holzbaur, E. L. F. (2007). Huntingtin facilitates dynein/dynactin-mediated vesicle transport. *Proc. Natl. Acad. Sci. U.S.A.* **104**,10045–10050.

Cha, J.H. Frey, A.S, Alsdorf, S.A, Kerner, J.A, Kosinski, C.M, Mangiarini, L. et al. (1999). Altered neurotransmitter receptor expression in transgenic mouse models of Huntington's disease. *Philos. Trans. R. Soc. Lond. Biol. Sci.* **354**(1386),981-989.

Chang, D.T.W, Rintoul, G.L. Pandipati, S and Reynolds, I. (2006). Mutant huntingtin aggregates impair mitochondrial movement and trafficking in cortical neurons. *Neurobiol. Dis.* **22**,388-400.

Charles, V, Mezey, E, Reddy, P.H, Dehejia, A Young, T.A, Polymeropoulos, M.H. et al. (2000). Alpha-synuclein immunoreactivity of huntingtin polyglutamine aggregates in striatum and cortex of Huntington's disease patients and transgenic mouse models. *Neuroscience Letters.* **289**,29-32.

Chen, M, Ona, V.O, Li, M, Ferrante, R.J, Fink, K.B, Zhu,S. et al. (2000). Minocycline inhibits caspase-1 and cspase-3 expression and delays mortality in a transgenic mouse model of Huntington's disease. *Nat. Med.* **6**,797-801.

Chinnery PF, Howell N, Andrews RA. (1999). Clinical mitochondrial genetics *J Med Genet.* **36**,425-436.

Chitambar, C. (2005). Cellular iron metabolism: mitochondria in the spotlight. *Blood.* **105**,1844-1845.

Choo Y.S, Johnson, G.V.W, MacDonald, M, Detloff, P.J, and Lesort, M. (2004). Mutant huntingtin directly increases susceptibility of mitochondria to calcium-induced permeability transition and cytochrome c release. *Hum. Mol. Genet.* **13**,1407-1420.

Choo YS, Mao Z, Johnson GV, Lesort M. (2005). Increased glutathione levels in cortical and striatal mitochondria of the R6/2 Huntington's disease mouse model. *Neurosci Lett.* **386**(1),63-8.

Chun, W, Lesort, M, Tucholski, J, Ross, C.A, and Johnson, G.V.W. (2001). Tissue transglutaminase does not contribute to the formation of mutant huntingtin aggregates J. Cell Biol. **153**(1),25-34.

Chun, W, Lesort, M, Lee, M and Johnson, G.V.W. (2002). Mutant huntingtin aggregates do not sensitize cells to apoptotic stressors, FEBS Lett. **515**,61–65.

Chyi T, Chang C. (1999). Temporal evolution of 3-nitropropionic acid-induced neurodegeneration in the rat brain by T2-weighted, diffusion-weighted, and perfusion resonance imaging. Neurosci. **92**,1035-41.

Ciammola, A, Sassone, J, Alberti, L, Meola, G, Mancinelli, E, Russo, M.A. et al. (2006). Increased apoptosis, huntingtin inclusions and altered differentiation in muscle cell cultures from Huntington's disease subjects. Cell Death and Differentiation. **13**,2068–2078.

Ciechanover A, Orian, A and Schwartz, A.L. (2000) .The ubiquitin-mediated proteolytic pathway: mode of action and clinical implications. J Cell Biochem Suppl. 2000;**34**,40-51.

Ciechanover, A. (2006) The ubiquitin proteolytic system: from a vague idea, through basic mechanisms, and onto human diseases and drug targeting. Neurology. **66**, S7–S19.

Clabough, E. B. D. and Zeitlin, S. O. (2006) Deletion of the triplet repeat encoding polyglutamine within the mouse Huntington's disease gene results in subtle

behavioral/motor phenotypes in vivo and elevated levels of ATP with cellular senescence in vitro. *Hum. Mol. Genet.* **15**,607–623.

Coggan AR, Spina RJ, King DS, Rogers MA, Brown M, Nemeth PM, Holloszy J. (1992). Histochemical and enzymatic comparison of the gastrocnemius muscle of young and elderly men and women. *J. Gerontol.* **47**,B71-B76.

Colomer, V, Engelender, S, Sharp, A.H, Duan, K, Cooper, J.K. Lanahan, A et al. (1997). Huntingtin-associated protein 1 (HAP1) binds to a Trio-like polypeptide, with a rac1 guanine nucleotide exchange factor domain. *Hum. Mol. Genet.* **6**(9),1519-1525.

Conconi, M and Friguier, B. (2004). Proteasome inactivation upon aging and on oxidation-effect of HSP 90. *Mol. Biol. Rep.* **24**(1-2),45-50.

Cooper, J.K, Schilling, G, Peters, M.F, Herring, W.J, Sharp, A.H, Kaminsky, Z. et al. (1998). Truncated N-terminal fragments of huntingtin with expanded glutamine repeats form nuclear and cytoplasmic aggregates in cell culture. *Hum. Mol. Genet.* **7**(5),783-790.

Coore, H.G, Denton, R.M, Martin, B.R, and P. J. Randle. (1971). Regulation of adipose tissue pyruvate dehydrogenase by insulin and other hormones. *Biochem. J.* **125**,115-127.

Cornett, J, Cao, F, Wang, C.E, Ross, C.A, Bates, G.P, Li, S.H. et al. (2005). Expansion of huntingtin impairs its nuclear export. *Nat. Genet.* **37**,198–204.

Cubellis, M.V, Caillez, F, Blundell, T.L, and Lovell, S.C. (2005). Properties of polyproline II, a secondary structure element implicated in protein-protein interactions. *Proteins: Structure, Function and Bioinformatics*. **58**(4), 880-892.

Cui, L, Jeong, H, Borovecki, F, Parkhurst, C.N, Tanese, N and Krainc, D. (2006). Transcriptional repression of PGC-1alpha by mutant huntingtin leads to mitochondrial dysfunction and neurodegeneration. *Cell*. **127**(1),59-69.

Cull-Candy S, Brickley S, Farrant M. (2001). NMDA receptor subunits: diversity, development and disease. *Curr Opin Neurobiol*. **11**,327-335.

Cummings, C..J, Mancini, M.A, Antalffy, B, DeFranco, D.B, Orr, H.T, Zoghbi, H.Y et al. (1998). Chaperone suppression of aggregation and altered subcellular proteasome localization imply protein misfolding in SCA 1. *Nat. Genet*. **19**(2),148-154.

Dautry C, Conde F, Brouillet E, Mittoux, V, Beal, M.F, Bloch, G et al. (1999). Serial 1H-NMR spectroscopy study of metabolic impairment in primates chronically treated with the succinate dehydrogenase inhibitor 3-nitropropionic acid. *Neurobiol. Dis*. **6**,259-68.

Davenport, C.B. (1911). *Heredity in relation to eugenics*. New York: (republished by Arno press 1972)

Davie, C.A, Barker, G.C, Quinn, N, Tofts, P.S, and Miller, D.H. (1994). Proton MRS in Huntington's disease. *Lancet* **343**,1580.

Davies, S.W, Turmaine, M, Cozens, B.A, DiFiglia, M, Sharp, A.H, Ross, C.A. et al. (1997). Formation of neuronal intranuclear inclusions underlies the neurological dysfunction in mice transgenic for the HD mutation. *Cell*. **90**(3),537-548.

Deckel A.W, Volmer, P, Weiner, R, Gary, K.A, Covault, J, Sasso, D. et al. (2000). Dietary arginine alters time of symptom onset in Huntington's disease transgenic mice. *Brain Res*. **875**,187-95.

Deckel AW. (2001). Nitric oxide and nitric oxide synthase in Huntington's disease. *J Neurosci Res*. **64**(2),99-107.

Dedeoglu, A, Kubilus, J.K, Jeitner, T.M, Matson, S.A, Bogdanov, M, Kowall, N.W. et al. (2002). Therapeutic effects of cystamine in a murine model of Huntington's disease. *J Neurosci*. **22**(20),8942-8950.

Dejean,L.M, Martinez-Caballero, S, and Kinnally, K.W. (2006). "Is MAC the knife that cuts cytochrome c from mitochondria during apoptosis?". *Cell Death and Differentiation*. **13**,1387–1395.

Dela Cruz, F.E, Kirsch, D.R, Heinrich, J.N. (2000). Transcriptional activity of *Drosophila melanogaster* ecdysone receptor isoforms and ultraspiracle in *Saccharomyces cerevisiae*. *J Mol Endo* **24**,183–191.

Denovan-Wright, E.M. and Robertson, H.A. (2000). Cannabinoid receptor messenger RNA levels decrease in a subset of neurons of the lateral striatum, cortex and hippocampus in transgenic Huntington's disease mice. *Neuroscience*. **98**,705-13.

De Rooij, K.E, Dorsman, J,C, Smoor, M.A, Den Dunnen, J.T, Van Ommen, G.J (1996). Subcellular localisation of Huntington's disease gene product in cell lines by immunofluorescence and biochemical subcellular fractionation. *Hum. Mol. Genet.* **5**(8), 1093-1099.

Diaz-Hernandez, M., Hernandez, F., Martin-Aparicio, E., Gomez-Ramos, P., Moran, M. A., Castano, J. G., Ferrer, I., Avila, J. and Lucas, J. J. (2003). Neuronal induction of the immunoproteasome in Huntington's disease. *J. Neurosci.* **23**,11653–11661.

Diaz-Hernandez, M., Valera, A. G., Moran, M. A., Gomez-Ramos, P., Alvarez-Castelao, B., Castano, J. G., Hernandez, F. and Lucas, J. J. (2006). Inhibition of 26S proteasome activity by huntingtin filaments but not inclusion bodies isolated from mouse and human brain. *J. Neurochem.* **98**,1585–1596.

DiFiglia, M, Sapp, E, Chase, K, Schwarz, C, Meloni, A, Young, C, et al. (1995) Huntingtin is a cytoplasmic protein associated with vesicles in human and rat brain neurons. *Neuron.* **14**,1075-81.

DiFiglia, M, Sapp, E, Chase, K.O, Davies, S.W, Bates, G.P, Vonsattel, J.P. (1997). Aggregation of huntingtin in neuronal intranuclear inclusions and dystrophic neurites in brain. *Science.* **277**(5334),1990-1993.

Ding, Q., Lewis, J. J., Strum, K. M., Dimayuga, E., Bruce-Keller, A. J., Dunn, J. C. and Keller, J. N. (2002) Polyglutamine expansion, protein aggregation, proteasome activity, and neural survival. *J. Biol. Chem.* **277**,13935–13942.

Dohmen, R. J. (2004) SUMO protein modification. *Biochim. Biophys. Acta.* **1695**,113–131.

Downey, P.M. Lozza, G, Petro, R, Diodato, E, Foglia, C, Bottazzoli, F, et al. (2005). Ecdysone-based system for controlled inducible expression of metabotropic glutamate receptor subtypes 2, 5, and 8. *J Biomol Screen.* **10**(8),841-8.

Dragatsis, I, Efstratiadis, A and Zeitlin, S. (1998). Mouse mutant embryos lacking huntingtin are rescued from lethality by wild-type extra-embryonic tissues. *Development.* **125**(8),1529-1539.

Dragunow, M, Faull, R.L, Lawlor, P, Beilharz, E.J, Singleton, K, Walker E.B, et al. (1995). In situ evidence for DNA fragmentation in Huntington's disease striatum and Alzheimer's disease temporal lobes. *Neuroreport.* **6**(7),1053-57.

Dugan LL, Sensi SL, Canzoniero LM, Handran SD, Rothman SM, Lin TS, Goldberg MP, Choi DW. (1995). Mitochondrial production of reactive oxygen species in cortical neurons following exposure to N-methyl-D-aspartate. *J. Neurosci.* **15**,6377-6388.

Duman, J.G and Forte, J.G. (2003). What is the role of SNARE proteins in membrane fusion? *Am J Physiol. Cell Physiol.* **285**,237–C249.

Dunah AW, Jeong H, Griffin A, Kim YM, Standaert DG, Hersch SM, Mouradian MM, Young AB, Tanese N, Krainc D. (2002). Sp1 and TAFII130 transcriptional activity disrupted in early Huntington's disease. *Science.* **296**(5576),2238-43.

Dure, L.S, Landwehrmeyer, G.B, Golden, J, McNeil, S.M, Ge P, Aizawa, H. et al. (1994). IT15 gene expression in foetal human brain. *Brain Res.* **659**(1-2),33-41.

Dykens JA. (1994). Isolated cerebral and cerebellar mitochondria produce free radicals when exposed to elevated Ca^{2+} and Na^+ : implications for neurodegeneration. *J Neurochem.* **63**,584-591.

Duyao, M.P, Auerbach, A.B, Ryan, A, Persichetti, F, Barnes, G,T, McNeil, S.M, et al. (1995). Inactivation of the mouse Huntington's disease gene homologue Hdh. *Science.* **269**(5222),407-410.

Engelender, S, Sharp, A.H, Colomer, V, Tokito, M.K, Lanahan, A, Worley, P. et al. (1997). Huntingtin-associated protein 1 (HAP1), interacts with the p150Glued subunit of dynactin. *Hum. Mol. Genet.* **6**(13),2205-2212.

Epler JL, Shugart LR, Barnett WE. (1970). N-formylmethionyl transfer ribonucleic acid in mitochondria from *Neurospora*. *Biochemistry.* **9**,3575-3579.

Fagni, L., Lafon-Cazal, M., Rondouin, G., Manzoni, O., Lerner-Natoli, M. and Bockaert, J. (1994). The role of free radicals in NMDA-dependent neurotoxicity. *Prog. Brain Res.* **103**,381–390.

Foroud, T, Siemers, E, Kleindorfer, D, Bill, D.J, Hodes, M.E, Norton, J.A. et al. (1995). Cognitive scores in carriers of Huntington's disease gene compared to non carriers. *Ann. Neurol.* **37**,657-664.

Favit, A, Nicoletti, F, Scapagnini, U, Canonico, P.L. (1992). Ubiquinone protects cultured neurons against spontaneous and excitotoxin-induced degeneration. *J Cereb Blood Flow Metab.* **12**,638-645.

Fenteany, G and Schreiber, S.L. (1998). Lactacystin, Proteasome Function, and Cell Fate. *J Biol. Chem.* **273**(15),8545–8548.

Ferrante RJ, Kowall NW, Hersch SM, Brown RH, Beal MF. (1996). Immunohistochemical localisation of markers of oxidative injury in Huntington's Disease. *Soc. Neurosci. Abstr.* **22**,227.

Ferrante, R.J, Gutekunst, C.A, Persichetti, F, McNeil, S.M, Kowall, N.W, Gusella, J.F, MacDonald, M.E. et al. (1997). Heterogeneous topographic and cellular distribution of huntingtin expression in the normal human neostriatum. *J. Neurosci.* **17**,3052-63.

Ferrante, R.J, Andreassen, O.A, Jenkins, B.G, Dedeoglu, A, Kuemmerle, S, Kubilus, J.K. et al. (2000). Neuroprotective effects of creatine in a transgenic mouse model of Huntington's disease. *J. Neurosci.* **20**,4389-97.

Ferrante, R.J, Andreassen, O.A, Dedeoglu, A, Ferrante, K.L, Jenkins, B.G, Hersch, S.M, Beal, M.F. (2002). Therapeutic effects of coenzyme Q10 and remacemide in transgenic mouse models of Huntington's disease. *J Neurosci.* **22**,1592-1599.

Fink, A.L. (1999). Chaperone-mediated protein folding. *Physiol Rev* **79**,425-429.

Forster K, Helbl V, Lederer T, Urlinger S, Wittenburg N, and Hillen W. (1999).

Tetracycline-inducible expression systems with reduced basal activity in mammalian cells. *Nucleic. Acids. Res.* **27**,708–710.

Fukui, H. and Moraes C.T. (2007) Extended polyglutamine repeats trigger a feedback loop involving the mitochondrial complex III, the proteasome and huntingtin aggregates. *Hum Mol Gen* **16**(7),783-797.

Gafni, J, and Ellerby, L.M. (2002). Calpain activation in Huntington's disease. *J. Neurosci.* **22**,4842-9.

Gafni, J, Hermel, E, Young, J.E, Wellington, C.L, Hayden, M.R, Ellerby, L.M. (2004). Inhibition of calpain cleavage of huntingtin reduces toxicity, accumulation of calpain/caspase fragments in the nucleus. *J. Biol. Chem.* **279**,20211-20.

Galper JB and Darnell JE. (1969). The presence of N-formyl-methionyl-tRNA in HeLa cell mitochondria. *Biochem. Biophys. Res. Commun.* **34**,205-14.

Gardner PR, Nguyen DH, White CW. (1994). Aconitase is a sensitive and critical target of oxygen poisoning in cultured mammalian cells and in rat lungs. *Proc Natl Acad Sci USA* **91**,12248-52.

Garseth, M, Sonnewald, U, White, L.R, Rod, M, Zwart, J.A, Nygaard, O, et al. (2000). Proton magnetic resonance spectroscopy of cerebrospinal fluid in neurodegenerative disease: indication of glial energy impairment in Huntington's chorea, but not Parkinson's disease. *J Neurosci. Res.* **60**,779-82.

Gauthier, L. R., Charrin, B. C., Borrell-Pages, M., Dompierre, J. P., Rangone, H., Cordelieres, F. P., De Mey, J., MacDonald, M. E., Lessmann, V. et al. (2004) Huntingtin controls neurotrophic support and survival of neurons by enhancing BDNF vesicular transport along microtubules. *Cell*. **118**,127–138.

Georgalis, Y, Starikov, E.B, Hollenbach, B, Lurz, R, Scherzinger, E, Saenger, W, et al. (1998). Huntingtin aggregation monitored by dynamic light scattering. *Proc. Natl. Acad. Sci. USA*. **95**(11),6118-6121.

Georgiou, N, Bradshaw, J.L, Chiu, E, Tudor, A, O'Gorman, L, Phillips, J.G. (1999). Differential clinical and motor control function in a pair of monozygotic twins with Huntington's disease. *Mov. Disord*. **14**,320-5.

Gerber, H.P, Seipel, K, Georgiev, O, Höfferer, M, Hug, M, Rusconi, S. et al. (1994). Transcriptional activation modulated by homopolymeric glutamine and proline stretches. *Science* **263**(5148),808-811.

Gianni, M, Ponzanelli, I, Mologni, L, Reichert, U, Rambaldi, A, Terao, M. et al. (2000). Retinoid-dependent growth inhibition, differentiation and apoptosis in acute promyelocytic leukemia cells. Expression and activation of caspases. *Cell Death and Differentiation*. **7**(5),447-460

Gincel, D and Shoshan-Barmatz, V. (2002). The Synaptic Vesicle Protein Synaptophysin: Purification and Characterization of Its Channel Activity. *Biophys. J*. **83**(6),3223-3229.

Giunti, P, Stevanin, G, Worth, P.F, David, G, Brice, A, Wood, N.W. (1999). Molecular and clinical study of 18 families with ADCA type II: evidence for genetic heterogeneity and de novo mutations. *Am. J. Hum. Genet.* **64**,1594-603.

Glass M, Dragunow M, and Faull R.L. (2000). The pattern of neurodegeneration in Huntington's disease: A comparative study of cannabinoid, dopamine, adenosine and GABA(A) receptor alterations in the human basal ganglia in Huntington's disease. *Neuroscience.* **97**,505-519.

Goehler, H, Lalowski, M, Stelzl, U, Waelter, S, Stroedicke, M, Worm, U. et al. (2004). A protein interaction network links GIT1, an enhancer of huntingtin aggregation, to Huntington's disease. *Mol. Cell.* **15**,853–865.

Goffredo, D, Rigamonti, D, Tartari, M, De Micheli, A, Verderio, C, Matteoli, M, Goffredo, G. et al.(2002). Calcium-dependent cleavage of wild-type endogenous huntingtin in primary cortical neurons. *J. Biol. Chem.* **277**,39594-8.

Goldberg, Y.P, Nicholson, D.W, Rasper, D.M, Kalchman, M.A, Koide, H.B, Graham, R.K. et al. (1996). Cleavage of huntingtin by apopain, a proapoptotic cysteine protease, is modulated by the polyglutamine tract. *Nat. Genet.* **13**(4),442-449.

Goldring CEP, Kitteringham NR, Jenkins R, Lovatt CA, Randle LE, Abdullah A, Owen A, Liu X, Butler PJ, Williams DP, Metcalfe P, Berens C, Hillen W, Foster B, Simpson A, McLellan L, and Park BK. (2006). Development of a transactivator in hepatoma cells that allows expression of phase I, phase II, and chemical defense genes. *Am J Physiol Cell. Physiol.* **290**,C104–C115.

Gómez-Tortosa, E, MacDonald, M.E, Friend, J.C, Taylor, S.A, Weiler, L.J, Cupples, L.A. (2001). Quantitative neuropathological changes in presymptomatic Huntington's disease. *Ann. Neurol.* **49**,29-34.

Goswami A, Dikshit P, Mishra A, Mulherkar S, Nukina N, Jana NR. (2006). Oxidative stress promotes mutant huntingtin aggregation and mutant huntingtin-dependent cell death by mimicking proteasomal malfunction. *Biochem Biophys Res Commun.* **342(1)**: 184-90.

Graham, R,K, Deng, Y, Slow, E,J, Haigh, B, Bissada, N, Lu, G. et al. (2006). Cleavage at the Caspase-6 Site Is Required for Neuronal Dysfunction and Degeneration Due to Mutant Huntingtin. *Cell.* **125**,1179-1191.

Grafton ST, Mazziotta JC, Pahl JJ, St George-Hyslop P, Haines, J.L, Gusella, J. et al. (1990). A comparison of neurological, metabolic, structural and genetic evaluations in persons at risk for Huntington's disease. *Ann. Neurol.* **5**,614-21.

Grafton, S.T, Mazziotta, J.C, Pahl, J.J, St George-Hyslop, P, Haines, J.L, Gusella, J. et al. (1992). Serial changes of cerebral glucose metabolism and caudate size in persons at risk for Huntington's disease. *Arch. Neurol.* **11**,1161-7.

Gray, M.W. (1992). The endosymbiont hypothesis revisited. *Int. Rev. Cytol.* **141**,233-357.

Greco A, Minghetti L, Levi G. (2000). Isoprostanes, novel markers of oxidative injury, help understanding the pathogenesis of neurodegenerative diseases. *Neurochem Res.* **25**,1357-1364.

Greenberg, C.S. Birckbichler, P.J, Rice, R.H. (1991). Transglutaminases-multifunctional cross-linking enzymes that stabilise tissues. *FASEB Journal.* **5**(15),3071-7.

Greene JG and Greenamyre JT. (1995). Characterization of the excitotoxic potential of the reversible succinate dehydrogenase inhibitor malonate. *J. Neurochem.* **64**,430-436.

Gu M, Gash MT, Mann VM, Javoy-Agid F, Cooper JM, Schapira AHV. (1996). Mitochondrial defect in Huntington's disease caudate nucleus. *Ann Neurol* **39**:385-9.

Gusella, J.F. and MacDonald, M.E. (1998). Huntingtin: a single bait hooks many species. *Curr. Opin. Neurobiol.* **8**(3),425-430.

Gusella, J.F. and MacDonald, M.E. (2000). Molecular genetics: unmasking polyglutamine triggers in neurodegenerative disease. *Nature Rev. Neurosci.* **1**,109-115.

Gutkunst, C.A, Levey, A.I. Heilman, C,J. Whaley, W,L. Yi, H, Nash, N.R. et al. (1995). Identification and localisation of huntingtin in brain and lymphoblasts with anti-fusion protein antibodies. *Proc. Natl. Acad. Sci. USA.* **92**,8710-14.

Gutkunst, C.A, Li, S.H, Yi, H, Ferrante, R.J, Li, X.J, Hersch, S.M. (1998). The Cellular and Subcellular Localization of Huntingtin-Associated Protein 1 (HAP1): Comparison with Huntingtin in Rat and Human. *J. Neurosci.* **18**(19),7674-7686.

- Gutekunst, C.A, Li, S.H, Yi, H, Mulroy, J.S, Kuemmerle, S, Jones, R. et al. (1999). Nuclear and neuropil aggregates in Huntington's disease: relationship to neuropathology. *J. Neurosci.* **19**,2522-34.
- Hackam, A.S, Singaraja, R, Wellington, CL, Metzler, M, McCutcheon, K, Zhang, T, et al. (1998). The influence of huntingtin protein size on nuclear localisation and cellular toxicity. *J. Cell. Biol.* **141**(5),1097-1105.
- Hackam, A.S, Singaraja, R, Zhang, T, Gan, L, Hayden, M.R. (1999). *In vitro* evidence of both the nucleus and cytoplasm as subcellular sites of pathogenesis in Huntington's disease. *Hum Mol Gen.* **8**(1),25-33.
- Hackam, A.S, Yassa, A.S, Singaraja, R, Metzler, M, Gutekunst, C.A, Gan, L. et al. (2000). Huntingtin interacting protein 1 induces apoptosis via a novel caspase-dependent death effector domain. *J. Biol. Chem.* **275**(52),41299-41308.
- Hantraye P, Riche D, Maziere M, Isacson O. (1990). A primate model of Huntington's disease: behavioral and anatomical studies of unilateral excitotoxic lesions of the caudate-putamen in the baboon. *Exp Neurol.* **108**(2),91-104.
- Hargreaves, I.P, Duncan, A.J, Wu, L, Agrawal, A, Land, J.M, Heales, S.J. et al. (2007). Inhibition of mitochondrial complex IV leads to secondary loss complex II-III activity: implications for the pathogenesis and treatment of mitochondrial encephalomyopathies. *Mitochondrion.* **7**(4),284-7.

Harjes, P, and Wanker, E. (2003). The hunt for huntingtin function: interaction partners tell many different stories. *Trends Biochem. Sci.* **28**,425–433.

Harms L, Meierkord H, Timm G, Pfeiffer L, Ludolph AC. (1997). Decreased N-acetyl-aspartate/choline ratio and increased lactate in the frontal lobes of patients with Huntington's disease: a proton magnetic resonance spectroscopy study. *J. Neurol. Neurosurg. Psych.* **62**,27-30.

Harper PS and Jones L. (2002). Huntington's disease: genetic and molecular studies. Chapter 5. 113-158. In *Huntington's Disease*, Oxford Medical Publications.

Harris ZL, Klomp LW, Gitlin JD. (1998). Aceruloplasminemia: an inherited neurodegenerative disease with impairment of iron homeostasis. *Am. J. Clin. Nutr.* **67**(5 Suppl),972S-977S.

Hartl, F.U. and Hayer-Hartl, M. (2002). Molecular chaperones in the cytosol: from nascent chain to folded protein. *Science.* **295**,1852-1858.

Haskins, B.A. and Harrison M.B. (2000). Huntington's Disease. *Curr. Treatment Opt. Neurol.* **2**:243-262.

Hattori A, Luo Y, Umegaki H, Munoz J, Roth GS. (1998). Intrastratial injection of dopamine results in DNA damage and apoptosis in rats. *Neuroreport.* **9**,2569-2572.

Hattula, K and Peranen, J. (2000). FIP-2, a coiled-coil protein, links huntingtin to Rab8 and modulates cellular morphogenesis. *Curr. Biol.* **10**(24),1603-1606.

Hausladen A and Fridovich I. (1994). Superoxide and peroxynitrite inactivate aconitases, but nitric oxide does not. *J. Biol. Chem.* **269**,29405-8.

Hay, D.G, Sathasivam, K, Tobaben, S, Stahl, B, Marber, M, Mestril, R. et al. (2004). Progressive decrease in chaperone protein levels in a mouse model of Huntingtin's disease and induction of stress proteins as a therapeutic approach. *Hum. Mol. Genet.* **13**,1389-1405.

Heiser, V, Scherzinger, E, Boeddrich, A, Nordhoff, E, Lurz, R, Schugardt, N et al. (2000). Inhibition of huntingtin fibrillogenesis by specific antibodies and small molecules: implications for Huntington's disease therapy. *Proc. Natl. Acad. Sci. USA.* **97**(12), 6739-44.

Hickey, M.A and Chesselet, M-F. (2003). Apoptosis in Huntington's disease
Prog Neuropsychopharmacol. Biol. Psychiatry. **2**,255-65.

Hilditch-Maguire, P, Trettel, F, Passani, L.A, Auerbach, A, Persichetti, F, MacDonald, M.E. (2000). Huntingtin: an iron-regulated protein essential for normal nuclear and perinuclear organelles. *Hum. Mol. Genet.* **9**(19),2789-2797.

Ho, L.W, Brown, R, Maxwell, M, Wytttenbach, A, Rubinsztein, D.C. et al. (2001). Wild type huntingtin reduces the cellular toxicity of mutant huntingtin in mammalian cell models of Huntington's disease. *J. Med. Genet.* **38**(7),450-452.

Hoang, T.Q, Bluml, S, Dubowitz, D.J, Moats, R, Kopyov, O, Jacques, D, et al. (1998). Quantitative proton-decoupled ³¹P MRS and ¹H MRS in the evaluation of Huntington's and Parkinson's diseases. *Neurology*. **50**,1033-40.

Hockly, E, Cordery, P.M, Woodman, B, Mahal, A, van Dellen, A, Blakemore, C et al. (2002). Environmental enrichment slows disease progression in R6/2 Huntington's disease mice. *Ann. Neurol*. **51**,235-42.

Hockly E, Richon VM, Woodman B, Smith DL, Zhou X, Rosa E. et al. (2003). Suberoylanilide hydroxamic acid, a histone deacetylase inhibitor, ameliorates motor deficits in a mouse model of Huntington's disease. *Proc Natl Acad Sci U S A*. **100**(4), 2041-6.

Hodgson, J.G, Agopyan, N, Gutekunst, C.A, Leavitt, B.R, LePiane, F, Singaraja, R. et al. (1999). A YAC mouse model for Huntington's disease with full-length mutant huntingtin, cytoplasmic toxicity, and selective striatal neurodegeneration. *Neuron*. **23**,181-192.

Hoffner, G, Kahlem, P and Djian, P. (2002). Perinuclear localization of huntingtin as a consequence of its binding to microtubules through an interaction with β -tubulin: relevance to Huntington's disease. *J. Cell Sci*. **115**,941-948.

Holmberg, C. I., Staniszewski, K. E., Mensah, K. N., Matouschek, A. and Morimoto, R. I. (2004) Inefficient degradation of truncated polyglutamine proteins by the proteasome. *EMBO J*. **23**,4307–4318.

Hoogeveen, A.T, Willemsen, R, Meyer, N, de Rooij, K.E, Roos, R.A, van Ommen, G.J. et al. (1993). Characterization and localization of the Huntington disease gene product. *Hum Mol Gen.* **2**(12),2069-2073.

Huang, C.C, Faber, P.W, Persichetti, F, Mittal, V, Vonsattel, J.P, MacDonald, M.E. et al. (1998). Amyloid formation by mutant huntingtin: threshold, progressivity and recruitment of normal polyglutamine proteins. *Somatic Cell and Molecular Genetics.* **24**,217-233.

Huang, K, Yanai, A, Kang, R, Arstikaitis, P, Singaraja, R.R, Metzler, M et al. (2004) Huntingtin-interacting protein HIP14 is a palmitoyl transferase involved in palmitoylation and trafficking of multiple neuronal proteins. *Neuron.* **44**,977–986.

Humbert, S, Bryson, E.A, Cordelieres, F.P, Connors, N.C, Datta, S.R, Finkbeiner, S et al. (2002). The IGF-1/Akt pathway is neuroprotective in Huntington's disease and involves huntingtin phosphorylation by Akt. *Dev. Cell.* **2**,831–837.

Huntington, G. (1872). On chorea. *Medical and Surgical Reporter.* **26**:320-321.

Huntington's Disease Collaborative Research Group (1993). A novel gene containing a trinucleotide repeat that is expanded and unstable on Huntington's disease chromosomes. The Huntington's Disease Collaborative Research Group. *Cell.* **72**,971-83.

Huntington Study Group. (1996). Unified Huntington's Disease Rating Scale: reliability and consistency. *Mov. Disord.* **11**(2),136-42.

Huntington Study Group. (1998). Safety and tolerability of the free-radical scavenger OPC-14117 in Huntington's disease. *Neurology*. **50**,1366-1373.

Huntington Study Group. (2001). A randomised, placebo-controlled trial of the coenzyme Q₁₀ and remacemide in Huntington's disease. *Neurology*. **57**,397-404.

Huynh D.P, Figueroa, K, Hoang, N, Pulst, S.M. (2000). Nuclear localization or inclusion body formation of ataxin-2 are not necessary for SCA2 pathogenesis in mouse or human. *Nat Genet*. **26**,44-50.

Ikeda, H, Yamaguchi, M, Sugai, S, Aze, Y, Narumiya, S, Kakizuka, A. Ikeda, H. (1996). Expanded polyglutamine in Machado-Joseph disease protein induces cell death in vitro and in vivo. *Nat Gen*. **13**,196-202.

Imarisio, S, Carmichael, J, Korolchuk, V, Chen, C.W, Saiki, S, Rose, C, Imarisio, S. et al. (2008). Huntington's disease: from pathology and genetics to potential therapies. *Biochem. J*. **412**,191–209.

Ishikawa, K, Owada, K, Ishida, K, Fujigasaki, H, Shun Li, M, Tsunemi, T, Ishikawa, K. et al. (2001). Cytoplasmic and nuclear polyglutamine aggregates in SCA6 Purkinje cells. *Neurology*. **56**,1753-1756.

Jackson MJ, Pye D and Palomero J. (2006). The production of reactive oxygen and nitrogen species by skeletal muscle. *J Appl Physiol*. **102**(4),1664-70.

Jana, N.R. Tanaka, M, Wang, G, Nukina, N. (2000). Polyglutamine length-dependent interaction of Hsp40 and Hsp70 family chaperones with truncated N-terminal huntingtin: their role in suppression of aggregation and cellular toxicity. *Hum. Mol. Genet.* **9**,2009-18.

Jana, N.R, Zemskov, E.A, Wang, G, Nukina, N. (2001). Altered proteasomal function due to the expression of polyglutamine-expanded truncated N-terminal huntingtin induces apoptosis by caspase activation through mitochondrial cytochrome c release. *Hum. Mol. Genet.* **10**(10),1049-1059.

Jason, G.W, Suchowersky, O, Pajurkova, E.M, Graham, L, Klimek, M.L, Garber, A.T. et al (1997). Cognitive manifestations of Huntington's disease in relation to genetic structure and clinical onset. *Arch. Neurol.* **54**,1081-1088.

Jenkins BG, Koroshetz WJ, Beal MF, Rosen BR. (1993). Evidence for impairment of energy metabolism in vivo in Huntington's disease using localised ¹H NMR spectroscopy. *Neurology* **43**,2689-95.

Jenkins BG, Rosas HD, Chen YCI, Makabe, T, Myers, R, MacDonald, M, et al. (1998). ¹H NMR spectroscopy studies of Huntington's disease. Correlations with CAG repeat numbers. *Neurology.* **50**,1357-65.

Jenkins BG, Klivenyi P, Kustermann E, Andreassen, O.A, Ferrante, R.J, Rosen, B. et al. (2000). Nonlinear decrease over time in N-acetyl aspartate levels in the absence of neuronal loss and increases in glutamine and glucose in transgenic Huntington's disease mice. *J. Neurochem.* **74**,2108-119.

Johnston JA, Ward CL and Kopito RR. (1998). Aggresomes: a cellular response to misfolded proteins. *J Cell Biol.* **143**,1883–1898.

Kahlem, P. et al. (1996). Peptides containing glutamine repeats as substrates for transglutaminase-catalyzed cross-linking: relevance to diseases of the nervous system. *Proc. Natl. Acad. Sci. USA.* **93**(25),14580-14585.

Kahlem, P, Terre, C, Green, H, Djian, P. (1998). Transglutaminase action imitates Huntington's disease: selective polymerization of huntingtin containing expanded polyglutamine. *Mol. Cell.* **1**(4),595-601.

Kalchman, M.A, Graham, R.K, Xia, G, Koide, H.B, Hodgson, J.G, Graham, K.C et al. (1996). Huntingtin is ubiquitinated and interacts with a specific ubiquitin-conjugating enzyme. *J. Biol. Chem.* **271**(32),19385-19394.

Kalchman, M.A, Koide, H.B, McCutcheon, K, Graham, R.K, Nichol, K, Nishiyama, K, et al. (1997). HIP1, a human homologue of *S. Cerevisiae* S1a2p, interacts with membrane associated huntingtin in the brain. *Nat. Genet.* **16**(1),44-53.

Kaltenbach, L. S., Romero, E., Becklin, R. R., Chettier, R., Bell, R., Phansalkar, A., Strand. et al. (2007) Huntingtin interacting proteins are genetic modifiers of neurodegeneration. *PLoS Genet.* **3**,e82.

Karpuj, M.V. Garren, H, Slunt, H, Price, D.L, Gusella, J, Becher, M.W. et al. (1999). Transglutaminase aggregates huntingtin into nonamyloidogenic polymers, and its

enzymatic activity increases in Huntington's disease brain nuclei. *Proc. Nat. Acad. Sci. USA.* **96**,7388-7393.

Karpuj, M.V, Becher, M.W, Springer, J.E, Chabas, D, Youssef, S, Pedotti, R. et al. (2002). Prolonged survival and decreased abnormal movements in transgenic model of Huntington disease, with administration of the transglutaminase inhibitor cystamine. *Nat Med* **8**,143-149.

Kazantsev, A, Preisinger, E, Dranovsky, A, Goldgaber, D, Housman, D. et al. (1999). Insoluble detergent-resistant aggregates form between pathological and non-pathological lengths of polyglutamine in mammalian cells. *Proc. Natl. Acad. Sci. USA.* **96**(20),11404-11409.

Kegel, K.B, Kim, M, Sapp, E, McIntyre, C, Castano, J.G, Aronin, N. et al. (2000). Huntingtin expression stimulates endosomal-lysosomal activity, endosome tabulation and autophagy. *J. Neurosci.* **20**(19),7268-7278.

Kegel, K.B, Meloni, A.R, Yi, Y, Kim, Y.J, Doyle, E, Cuiffo, B.G. et al. (2002). Huntingtin is present in the nucleus, interacts with the transcriptional corepressor C-terminal binding protein, and represses transcription. *J. Biol. Chem.* **277**,7466–7746.

Kim, M, Lee, H.S, LaForet, G, McIntyre, C, Martin, E.J, Chang, P, Kim. et al. (1999). Mutant huntingtin expression in clonal striatal cells: dissociation of inclusion formation and neuronal survival by caspase inhibition. *J. Neurosci.* **19**(3),964-973.

Kim, M, Roh, J.K, Yoon, B.W, Kang, L, Kim, Y.J, Aronin, N. et al. (2003). Huntingtin is degraded to small fragments by calpain after ischaemic injury. *Exp. Neurol.* **183**,109-15.

Kim, Y.J, Yi, Y, Sapp, E, Wang, Y, Cuiffo, B, Kegel, K.B. et al (2001) Caspase 3-cleaved N-terminal fragments of wild-type and mutant huntingtin are present in normal and Huntington's disease brains, associate with membranes, and undergo calpain dependent proteolysis. *Proc. Natl. Acad. Sci.* **98**(22),12784-12789.

Kim Y.J, Sapp E, Cuiffo BG, Sobin, L, Yoder, J, Kegel, K.B. et al. (2006). Lysosomal proteases are involved in generation of N-terminal huntingtin fragments. *Neurobiol. Dis.* **22**,346-356.

King, T.E. (1967). Preparation of succinate cytochrome c reductase and the cytochrome b-c1 particle and reconstitution of succinate cytochrome c reductase. *Meth. Enzymol.* **10**,216-225.

Kirkwood, S.C, Siemers, E, Hodes, M.E, Conneally, P.M, Christian, J.C, Foroud, T. et al. (2000). Subtle changes among presymptomatic carriers of the Huntington's disease gene. *J. Neurol. Neurosurg. Psych.* **69**(6),773-9.

Koponen JK, Kankkonen H, Kannasto J, Wirth T, Hillen W, Bujard H, et al. (2003). Doxycycline-regulated lentiviral vector system with a novel reverse transactivator rtTA2S-M2 shows a tight control of gene expression in vitro and in vivo. *Gen. Ther.* **10**,459-466.

Koroshetz WJ, Jenkins BG, Rosen BR and Beal MF. (1997). Energy metabolism defects in Huntington's disease and effects of coenzyme Q₁₀. *Ann. Neurol.* **41**,160-5.

Kosinski, C.M, Cha, J.H, Young, A.B, Persichetti, F, MacDonald, M, Gusella, J.F, Penney, J.B.Jr. et al. (1997). Huntingtin immunoreactivity in the rat striatum: differential accumulation in projection and interneurons. *Exp. Neurol.* **144**(2),239-247.

Kremer, B. (2002). Clinical Neurology of Huntington's disease. Chapter 2. p29-61 in 3rd Edition Huntington's Disease, Oxford Medical Publications.

Kuhl, D.E, Phelps, M.E, Markham, C.H, Metter, E.J, Riege, W.H, Winter, J. (1982). Cerebral metabolism and atrophy in Huntington's disease determined by 18FDG and computed tomographic scan. *Ann. Neurol.* **12**,425-34.

Kuwert, T, Lange, H.W, Langen, K-J, Herzog, H, Albrecht, A, Feinendegen, .L.E. (1990). Cortical and subcortical glucose consumption measured by PET in patients with Huntington's disease. *Brain.* **113**,1405-23.

Kuwert T, Lange HW, Boecker H, Titz, H, Herzog, H, Aulich, A. et al. (1993). Striatal glucose consumption in chorea-free subjects at risk of Huntington's disease. *J. Neurol.* **241**,31-6.

Laforet, G.A, Sapp, E, Chase, K, McIntyre, C, Boyce, F.M, Campbell, M. et al. (2001). Changes in cortical and striatal neurons predict behavioural and electrophysiological abnormalities in a transgenic murine model of Huntington's disease. *J. Neurosci.* **21**,9112-23.

La Fontaine MA, Geddes JW, Banks A and Butterfield DA. (2000) 3-nitropropionic acid induced in vivo protein oxidation in striatal and cortical synaptosomes: insights into Huntington's disease. *Brain Res.* **858**,356-362.

Lagouge M, Argmann C, Gerhart-Hines Z, Meziane, H, Lerin, C, Daussin, F et al. (2006). Resveratrol improves mitochondrial function and protects against metabolic disease by activating SIRT1 and PGC-1 α . *Cell.* **127**(6),1109–22.

Larsen, N.B, Rasmussen, M, Rasmussen L.J. (2005). Nuclear and mitochondrial DNA repair: similar pathways? *Mitochondrion.* **5**(2),89-108.

La Spada, A.R. Wilson, E.A., Lubahn, D.B., Harding, A.E. and Fishbeck, K.H. (1991). Androgen receptor gene mutations in X-linked spinal and bulbar muscular atrophy. *Nature.* **36**,443-7.

Lawrence, A.D, Weeks, R.A, Brooks, D.J, Andrews, T.C, Watkins, L.H, Harding, A.E. et al. (1998). The relationship between striatal dopamine receptor binding and cognitive performance in Huntington's disease. *Brain.* **121**,1343-1355.

Leavitt, B.R, Guttman, J.A, Hodgson, J.G, Kimel, G.H, Singaraja, R, Vogl, A.W. et al (2001). Wild-type huntingtin reduces the cellular toxicity of mutant huntingtin in vivo. *Am J Hum Genet.* **68**(2),313-24.

Leenders KL, Frackowiak RSJ, Quinn N, Marsden CD. (1986). Brain energy metabolism and dopaminergic function in Huntington's disease measured in vivo using positron emission tomography. *Mov. Disord.* **1**,69-77.

Leonard JV and Schapira AHV. (2000a). Mitochondrial respiratory chain disorders I: mitochondrial DNA defects. *Lancet.* **355**,299-304.

Leonard JV, Schapira AHV. (2000b). Mitochondrial respiratory chain disorders II: neurodegenerative disorders and nuclear gene defects. *Lancet.* **355**,389-394.

Lesort, M. Lee, M, Tucholski, J, Johnson, G.V. (2003). Cystamine inhibits caspase activity: implications for the treatment of polyglutamine disorders. *J Biol. Chem.* **278**(6), 3825-3830.

Levine, M.S, Klapstein, G.J, Koppel, A, Gruen, E, Cepeda, C, Vargas, M.E. et al. (1999). Enhanced sensitivity to N-methyl-D-aspartate receptor activation in transgenic and knock-in mouse models of Huntington's disease. *J. Neurosci. Res.* **58**,515-32.

Leone, T.C, Lehman, J.J, Finck, B.N, Schaeffer, P.J, Wende, A.R, Boudina, S. et al. (2005) PGC-1 α deficiency causes multi-system energy metabolic derangements: muscle dysfunction, abnormal weight control and hepatic steatosis. *PLoS Biol.* **3**,e101.

Li, H, Li, SH, Johnston, H, Shelbourne, PF, Li, XJ. (2000). Amino-terminal fragments of mutant huntingtin show selective accumulation in striatal neurons and synaptic toxicity. *Nat. Genet.* **25**,385-9.

Li, H, Wyman, T, Yu, Z.X, Li, S.H, Li, X.J. (2003) Abnormal association of mutant huntingtin with synaptic vesicles inhibits glutamate release. *Hum. Mol. Genet.*, **12**,2021–2030.

Li, J.Y, Plomann, M, Brundin, P. (2003). Huntington's disease: a synaptopathy? *Trends Mol. Med.* **9**,414–420.

Li SH, Schilling G, Young WS 3rd, Li XJ, Margolis RL, Stine OC. et al. (1993). Huntington's disease gene (IT15) is widely expressed in human and rat tissues. *Neuron.* **11**(5),985-93.

Li, S.H, Gutekunst, C.A, Hersch, S.M, Li, X.J. (1998). Interaction of huntingtin-associated protein with dynactin P150Glued. *J. Neurosci.* **18**(4),1261-1269.

Li, S.H, Cheng, A.L, Li, H, Li, X.J. (1999). Cellular Defects and Altered Gene Expression in PC12 Cells Stably Expressing Mutant Huntingtin. *J Neurosci.* **19**(13),5159–5172.

Li, S.H, Lam, S, Cheng, A.L and Li, X.J. (2000). Intranuclear huntingtin increases the expression of caspase-1 and induces apoptosis. *Hum. Mol. Genet.* **9**(19),2859-2867.

Li, S.H. and Li XJ. (2004). Huntingtin-protein interactions and the pathogenesis of Huntington's disease. *Trends Genet.* **20**,146-154.

Li X.J, Li S.H, Sharp A.H, Nucifora F.C Jr, Schilling G, Lanahan A Li. et al. (1995). A huntingtin-associated protein enriched in brain with implications for pathology. *Nature.* **378**(6555),398-402.

Lieberman A.P. and Fischbeck K.H. (2000). Triplet repeat expansion in neuromuscular disease. *Muscle Nerve*. **23**,843-50.

Lightowers, R.N, Chinnery, P.F, Turnbull, D.M and Howell, N. (1997). Mammalian mitochondrial genetics: heredity, heteroplasmy and disease *Trends Genet*.**13**,450-455.

Lin, C.H, Tallaksen-Greene, S, Chien, W.M, Cearley, J.A, Jackson, W.S, Crouse, A.B. et al. (2001). Neurological abnormalities in a knock-in mouse model of Huntington's disease. *Hum. Mol. Genet*. **10**,137-144.

Lin, J, Wu, H, Tarr, P.T, Zhang, C.Y, Wu, Z, Boss, O. et al. (2002) Transcriptional co-activator PGC-1 α drives the formation of slow-twitch muscle fibres. *Nature*. **418**,797–801.

Lione, L.A, Carter, R.J, Hunt, M.J, Bates, G.P, Morton, A.J, Dunnett, S.B (1999). Selective discrimination learning impairments in mice expressing the human Huntington's disease mutation. *J. Neurosci*. **19**(23),10428-10437.

Liu, Y.F, Deth, R.C, Devys, D. (1997). SH3 domain-dependent association of huntingtin with epidermal growth factor receptor signaling complexes. *J. Biol. Chem*. **272**(13), 8121-8124.

Liu YF, Dorow D and Marshall J. (2000). Activation of MLK2-mediated signaling cascades by polyglutamine-expanded huntingtin. *J. Biol. Chem*. **275**(25),19035-19040.

Lodi, R, Schapira, A.H, Manners, D, Styles, P, Wood, N.W, Taylor, D.J. et al. (2000). Abnormal in vivo skeletal muscle energy metabolism in Huntington's disease and dentatorubropallidoluysian atrophy. *Ann. Neurol.* **48**,72-6.

Loeffler, D.A, LeWitt, P.A, Juneau, P.L, Sima, A.A, Nguyen, H.U, DeMaggio, A.J, et al. (1996). Increased regional brain concentrations of ceruloplasmin in neurodegenerative disorders. *Brain Res.* **738**,265-274.

Lonergan, T, Brenner, C, Bavister, B. (2006). Differentiation-related changes in mitochondrial properties as indicators of stem cell competence. *J Cell Phys.* **208**(1),149–153.

Ludolph, A.C, He, F, Spencer, P.S, Hammerstad, J, and Sabri, M. (1991). 3-nitropropionic acid-exogenous animal neurotoxin and possible human striatal toxin. *Can. J. Neurol. Sci.* **18**,492-8.

Lunkes, A and Mandel, J.L. (1998). A cellular model that recapitulates major pathogenic steps of Huntington's disease. *Hum. Mol. Genet.* **7**(9),1355-61.

Lunkes, A, Lindenberg, K.S, Ben-Haïem, L, Weber, C, Devys, D, Landwehrmeyer, G.B. (2002). Proteases acting on mutant huntingtin generate cleaved products that differentially build up in cytoplasmic and nuclear inclusions. *Mol. Cell.* **10**,259-69.

Luo, S, Vacher, C, Davies, J.E, Rubinsztein, D.C. (2005). Cdk5 phosphorylation of huntingtin reduces its cleavage by caspases: implications for mutant huntingtin toxicity. *J. Cell Biol.* **169**,647–656.

Luthi-Carter, R, Strand, A, Peters, N.L, Solano, S.M, Hollingsworth, Z.R, Menon, A.S. et al. (2000). Decreased expression of striatal signaling genes in a mouse model of Huntington's disease. *Hum. Mol. Genet.* **9**(9),1259-1271.

Luthi-Carter, R, Hanson, S.A, Strand, A.D, Bergstrom, D.A, Chun, W, Peters, N.L. et al. (2002). Dysregulation of gene expression in the R6/2 model of polyglutamine disease: parallel changes in muscle and brain. *Hum. Mol. Genet.* **11**,1911–1926.

MacDonald, M.E, Vonsattel, J.P, Shrinidhi, J, Couropmitree, N.N, Cupples, L.A, Bird, E.D et al. (1999). Evidence for the GluR6 gene associated with younger onset age in Huntington's disease. *Neurology.* **53**,1330-1332.

Maglione, V., Cannella, M., Gradini, R., Cislighi, G. and Squitieri, F. (2006). Huntingtin fragmentation and increased caspase 3, 8 and 9 activities in lymphoblasts with heterozygous and homozygous Huntington's disease mutation. *Mech. Ageing Dev.* **127**,213–216.

Mangiarini, L, Sathasivam K, Sellar M, Cozens B, Harper A, Hetherington C, et al. (1996). Exon 1 of the HD Gene with an expanded CAG Repeat Is Sufficient to Cause a Progressive Neurological Phenotype in Transgenic Mice. *Cell.* **87**,493-506.

Mann V, Cooper JM, Javoy-Agid F, Agid Y, Jenner P, Schapira AHV. (1990). Mitochondrial function and parental sex effect in Huntington's disease. *Lancet* **336**,749.

Mantamadiotis, T, Lemberger, T, Bleckmann, S.C, Kern, H, Kretz, O, Martin, et al. (2002) Disruption of CREB function in brain leads to neurodegeneration. *Nat. Genet.* **31**,47-54.

Marsh, J.L, Walker, H, Theisen, H, Zhu, Y.Z, Fielder, T, Purcell, J, et al. (2000). Expanded polyglutamine peptides alone are intrinsically cytotoxic and cause neurodegeneration in drosophila. *Hum. Mol. Genet.* **9**(1),13-25.

Martin, W.R.W, Clark, C, Ammann, W, Stoessl, A.J, Shtybel, W and Hayden, M.R. (1992). Cortical glucose metabolism in Huntington's disease. *Neurology* **42**,223-9.

Martin, W.R.W, Hanstock, C, Hodder, J, and Allen, J.S. (1996). Brain energy metabolism in Huntington's disease measured with in vivo proton magnetic resonance spectroscopy. *Ann. Neurol.* **40**,538.

Martín-Aparicio, E, Yamamoto, A, Hernández, F, Hen, R, Avila, J and Lucas, J.J. (2001). Proteasomal-dependent aggregate reversal and absence of cell death in a conditional model of Huntington's disease. *J. Neurosci.* **21**(22),8772-8781.

Martinez-Arca, S, Alberts, P, Zahraoui, A, Louvard, D and Galli, T. (2000). Role of Tetanus Neurotoxin Insensitive Vesicle-Associated Membrane Protein (Ti-Vamp) in Vesicular Transport Mediating Neurite Outgrowth. *Cell Biol.* **149**(4),889–900.

Martindale, D, Hackam, A, Wieczorek, A, Ellerby, L, Wellington, C, McCutcheon, K. et al. (1998). Length of huntingtin and its polyglutamine tract influences localisation and frequency of intracellular aggregates. *Nat. Genet.* **18**(2),150-154.

Matthews, R.T, Yang, L, Jenkins, B.G, Ferrante, R.J, Rosen, B.R, Kaddurah-Daouk, R, et al. (1998). Neuroprotective effects of creatine and cyclocreatine in animal models of Huntington's disease. *J Neurosci.* **18**,156-163

Mazziotta, J.C, Phelps, M.E, Pahl, J.J, Huang, S.C, Baxter, L.R, Riege, W.H, et al. (1987). Reduced cerebral glucose metabolism in asymptomatic subjects at risk for Huntington's disease. *N. Engl. J. Med.* **316**,357-62.

McBride, H.M, Neuspiel, M and Wasiak, S. (2006). Mitochondria: More Than Just a Powerhouse. *Curr. Biol.* **16**(14),R551-R560.

McCampbell, A et al. (2001). Histone deacetylase inhibitors reduce polyglutamine toxicity. *PNAS.* **98** (26):15179–15184.

McGill J.K. and Beal, F. (2006). PGC-1 α , a New Therapeutic Target in Huntington's disease?. *Cell.* **127**,465-468.

McGuire, J.R., Rong, J, Li, S-H, and Li, X-J. (2006). Interaction of huntingtin-associated protein-1 with kinesin light chain: implications in intracellular trafficking in neurons. *J. Biol. Chem.* **281**,3552–3559

McKee, E.E, Ferguson, M, Bentley, A.T and Marks, T.A. (2006). Inhibition of mammalian mitochondrial protein synthesis by oxazolidinones. *Antimicrob Agents Chemother.* **50**(6),2042-9.

- McLaughlin, B.A, Nelson, D, Erecinska, M and Chesselet MF. (1998). Toxicity of dopamine to striatal neurons in vitro and potentiation of cell death by a mitochondrial inhibitor. *J. Neurochem.* **70**,2406-2415.
- Mende-Mueller, L.M, Toneff, T, Hwang, S.R, Chesselet, M.F and Hook, V.Y. (2001). Tissue-specific proteolysis of Huntingtin (htt) in human brain: evidence of enhanced levels of N- and C-terminal htt fragments in Huntington's disease striatum. *J. Neurosci.* **21**,1830–1837.
- Menei, P, Pean, J.M, Nerriere-Daguin, V, Jollivet, C, Brachet and P, Benoit, J.P. (2000). Intracerebral implantation of NGF-releasing biodegradable microspheres protects striatum against excitotoxic damage. *Exp. Neurol.* **161**,259-272.
- Meriin, A.B, Mabuchi, K, Gabai, V.L, Yaglom, J.A, Kazantsev, A, Sherman, M.Y. (2001). Intracellular aggregation of polypeptides with expanded polyglutamine domain is stimulated by stress-activated kinase MEKK1. *J. Cell Biol.* **153**(4),851-864.
- Metzler, M, Chen, N, Helgason, C.D, Graham, R.K, Nichol, K, McCutcheon, K, et al. (1999). Life without huntingtin:normal differentiation into functional neurons. *J. Neurochem.* **72**(3),1009-1018.
- Metzler, M, Legendre-Guillemain, V, Gan, L, Chopra, V, Kwok, A, McPherson, P.S, et al. (2001). HIP1 functions in clathrin-mediated endocytosis through binding to clathrin and adaptor protein 2. *J. Biol. Chem.* **276**(42),39271-39276.

Milakovic, T, and Johnson, G.V. (2005). Mitochondrial respiration and ATP production are significantly impaired in striatal cells expressing mutant huntingtin. *J. Biol. Chem.* **280**(35),30773-82.

Milner, D.J, Mavroidis, M, Weisleder, N, Capetanaki, Y, Milner, D.J. (2000). Desmin cytoskeleton linked to muscle mitochondrial distribution and respiratory function. *J. Cell. Biol.* **150**,1283-1298.

McC Campbell, A, Taye, A.A, Whitty, L, Penney, E, Steffan, J.S, Fischbeck, K.H. (2001). Histone deacetylase inhibitors reduce polyglutamine toxicity. *Proc. Natl. Acad. Sci. U.S.A.* **98**(26),15179-84.

Morton, A.J, Lagan, M.A, Skepper, J.N, Dunnett, S.B. (2000). Progressive formation of inclusions in the striatum and hippocampus of mice transgenic for the human Huntington's disease mutation. *J. Neurocytol.* **29**,679-702.

Morton, A.J and Edwardson, J.M. (2001). Progressive depletion of complexin II in a transgenic mouse model of Huntington's disease. *J. Neurochem.* **76**,166-72.

Muchowski, P.J, Schaffar, G, Sittler, A, Wanker, E.E, Hayer-Hartl, M.K and Hartl, F.U. (2000) HSP 70 and HSP 40 chaperones can inhibit self-assembly of polyglutamine proteins into amyloid-like fibrils. *Proc. Natl. Acad. Sci. USA.* **97**(14),7841-7846.

Murphy, K.P, Carter, R.J, Lione, L.A, Mangiarini, L, Mahal, A, Bates, G.P et al. (2000). Abnormal synaptic plasticity and impaired spatial cognition in mice transgenic for exon 1 of the Huntington's disease mutation. *J. Neurosci.* **20**(13),5115-5123.

Myers, R.H, Sax, D.S, Koroshetz, W.J, Mastromauro, C, Cupples, L.A, Kiely, D.K. et al. (1991). Factors associated with slow progression in Huntington's disease. *Arch. Neurol.* **48**,800-4.

Myers, R.H. (2004). Huntington's disease genetics. *NeuroRx.* **1**,255–262.

Nagai, Y, Onodera, O, Chun, J, Strittmatter, W.J, and Burke JR. (1999). Expanded polyglutamine domain proteins bind neurofilament and alter the neurofilament network. *Exp. Neurol.* **155**(2),195-203.

Nakanishi, K. (1992). Past and Present Studies with Ponasterones, the First Insect Molting Hormones from Plants. *Steroids.* **57**,649-657.

Nasir, J, Floresco, S.B, O'Kusky, J.R, Diewert, V.M, Richman, J.M, Zeisler, J. et al. (1995). Targeted disruption of the Huntington's disease gene results in embryonic lethality and behavioral and morphological changes in heterozygotes. *Cell.* **81**(5), 811-823.

Nellemann, C, Abell, K, Norremolle, A, Lokkegaard, T, Naver B, Ropke, C, Nellemann, C. et al. (2000). Inhibition of huntingtin synthesis by antisense oligodeoxynucleotides. *Mol. Cell. Neurosci.* **16**(4),313-323.

Neuwald, A. F. and Hirano, T. (2000) HEAT repeats associated with condensins, cohesins, and other complexes involved in chromosome-related functions. *Genome Res.* **10**,1445–1452.

No, D, Yao, T.P, Evans, R.M. (1996). Ecdysone-inducible gene expression in mammalian cells and transgenic mice. *Proc. Natl. Acad. Sci. USA.* **93**,3346-3351.

Nollen, E.A, Garcia, S.M, van Haften, G, Kim, S, Chavez, A, Morimoto, R.I. et al. (2004). Genome-wide RNA interference screen identifies previously undescribed regulators of polyglutamine aggregation. *Proc. Natl. Acad. Sci. USA.* **101**,6403-6406.

Novelli, A, Reilly, J.A, Lysko, P.G, Henneberry, R.C. (1988). Glutamate becomes neurotoxic via the N-methyl-D-aspartate receptor when intracellular energy levels are reduced. *Brain. Res.* **451**,205-212.

Nucifora, F.C. Jr, Sasaki, M, Peters, M.F, Huang, H, Cooper, J.K, Yamada, M et al. (2001). Interference by huntingtin and atrophin-1 with CBP-mediated transcription leading to cellular toxicity. *Science.* **291**,2432-8.

Obrietan, K. and Hoyt, K.R. (2004) CRE-mediated transcription is increased in Huntington's disease transgenic mice. *J. Neurosci.* **24**,791-796.

Ona, V.O, Li, M, Vonsattel, J.P, Andrews, L.J, Khan, S.Q, Chung, W.M. et al. (1999). Inhibition of caspase-1 slows disease progression in a mouse model of Huntington's disease. *Nature.* **399**,263-7.

Ordway, J.M, Tallaksen-Greene, S, Gutekunst, C.A, Bernstein, E.M, Cearley, J.A, Wiener. et al. (1997). Ectopically expressed CAG repeat cause intranuclear inclusions and a late-onset neurological phenotype in the mouse. *Cell.* **91**,753-763.

Orr, A.L, Li, S, Wang, C.E, Li, H, Wang, J, Rong, J, Xu, X. et al. (2008). N-terminal mutant huntingtin associates with mitochondria and impairs mitochondrial trafficking. *J Neurosci.* **28**(11),2783-92.

Orth, M, Cooper, J.M, Bates, G.P and Schapira, A.H. (2003). Inclusion formation in Huntington's disease R6/2 mouse muscle cultures. *J.Neurochem.* **87**,1-6.

Pang Z and Geddes JW. (1997). Mechanisms of cell death induced by the mitochondrial toxin 3-nitropropionic acid: acute excitotoxic necrosis and delayed apoptosis. *J Neurosci.* **17**,3064-3073.

Panov, A.V, Gutekunst, C.A, Leavitt, B.R, Hayden, M.R, Burke, J.R, Strittmatter, W.J. et al. (2002) Early mitochondrial calcium defects in Huntington's disease are a direct effect of polyglutamines. *Nat. Neurosci.* **5**(8),731-736.

Parker, W.D, Boyson, S.J, Luder, A.S and Parks, J.K. (1990). Evidence for a defect in NADH:ubiquinone oxidoreductase (complex I) in Huntington's disease. *Neurology.* **40**,1231-4.

Patel, M, Day, B.J, Crapo, J.D, Fridowich, I, McNamara, J.O. (1996). Requirement for superoxide in excitotoxic cell death. *Neuron* **16**,345-55.

Paulsen, J.S, Zhao, H, Stout, J.C, Brinkman, R.R, Guttman, M, Ross, C.A, et al. Huntington Study Group. (2001). Clinical markers of early disease in persons near onset of Huntington's disease. *Neurology.* **57**(4),658-62.

Penney, J.B. Jr, Vonsattel, J.P, MacDonald, M.E, Gusella, J.F, Myers, R.H. (1997). CAG repeat number governs the development rate of pathology in Huntington's Disease. *Ann. Neurol.* **41**,689-692.

Perez, M.K, Paulson, H.L. and Pittman, R.N. (1999). Ataxin-3 with an altered conformation that exposes the polyglutamine domain is associated with the nuclear matrix. *Hum Mol Genet.* **8**(13),2377-85.

Perez-Severiano, F, Rios, C, and Segovia, J. (2000). Striatal oxidative damage parallels the expression of a neurological phenotype in mice transgenic for the mutation of Huntington's disease. *Brain Res.* **862**,234-237.

Perutz, M.F, Johnson, T, Suzuki, M, Finch, J.T. (1994). Glutamine repeats as polar zippers: their possible role in inherited neurodegenerative diseases. *Proc. Natl. Acad. Sci. USA.* **91**,5355–5358.

Perutz, M.F. (1996). Glutamine repeats and inherited neurodegenerative diseases: molecular aspects. *Curr. Op. Struct. Biol.* **6**,848-858.

Peters, M.F, Nucifora, F.C. Jr, Kushi, J, Seaman, H.C, Cooper, J.K, Herring, W.J, et al. (1999). Nuclear targeting of mutant huntingtin increases toxicity. *Mol. Cell. Neurosci.* **14**(2),121-128.

Petersen, A, Mani, K and Brundin, P. (1999). Recent advances on the pathogenesis of Huntington's disease. *Exp. Neurol.* **157**,1-18.

Petersen, A, Larsen, K.E, Behr, G.G, Romero, N, Przedborski, S, Brundin, P. et al. (2001). Expanded CAG repeats in exon 1 of the Huntington's disease gene stimulate dopamine-mediated striatal neuron autophagy and degeneration. *Hum. Mol. Genet.* **10**(12),1243-1254.

Petrasch-Parwez, E, Nguyen, H.P, Lobbecke-Schumacher, M, Habbes, H.W, Wiczorek, S, Riess, O, et al. (2007). Cellular and subcellular localization of huntingtin aggregates in the brain of a rat transgenic for Huntington's disease. *J. Comp. Neurol.* **501**(5),716-30.

Pfeiffer, J.A.F. (1913). A contribution to the pathology of chronic progressive chorea. *Brain.* 35,276-292.

Pratley, R.E, Salbe, A.D, Ravussin, E, Caviness, J.N. (2000). Higher sedentary energy expenditure in patients with Huntington's disease. *Ann. Neurol.* **47**,64-70.

Preis, P.N, Saya, H, Nadasdi, L, Hochhaus, G, Levin, V, Sadee, W. (1988). Neuronal Cell Differentiation of Human Neuroblastoma Cells by Retinoic Acid plus Herbimycin A, *Cancer Res.* **48**,6530-6534.

Puranam, K.L, Wu, G, Strittmatter, W.J, Burke, J.R. Polyglutamine expansion inhibits respiration by increasing reactive oxygen species in isolated mitochondria. *Biochem. Biophys. Res. Commun.* **341**,607-613.

Qiu, Z, Norflus, F, Singh, B, Swindell, M. K, Buzescu, R, Bejarano, M., et al. (2006) Sp1 is up-regulated in cellular and transgenic models of Huntington disease, and its reduction is neuroprotective. *J. Biol. Chem.* **281**,16672–16680.

Quarrell, O.W.J, Tyler, A, Cole, G et al. (1988). Population studies of Huntington's Disease in Wales. *Clin. Genet.* **33**:189-195.

Ragan, C.I, Wilson, M.T, Darley-Usmar, V.M and Lowe, P.N. (1987). Subfractionation of mitochondria, and isolation of the proteins of oxidative phosphorylation. In: Darley-Usmar, V.M. Rickwood, D, Wilson, M.T. (eds). *Mitochondria, a Practical Approach*. London IRL Press, pp79-112.

Raths, S, Rohrer, J, Crausaz, F and Riezman. (1993). End3 and end4: two mutants defective in receptor-mediated and fluid-phase endocytosis in *Saccharomyces cerevisiae*. *J. Cell Biol.* **120**(1),55-65.

Ravikumar, B, Duden, R, and Rubinsztein, D.C. (2002) Aggregate-prone proteins with polyglutamine and polyalanine expansions are degraded by autophagy. *Hum. Mol. Genet.* **11**,1107–1117.

Ravikumar, B, Vacher, C, Berger, Z, Davies, J.E, Luo, S, Oroz, L.G, et al. (2004). Inhibition of mTOR induces autophagy and reduces toxicity of polyglutamine expansions in fly and mouse models of Huntington's disease. *Nat. Genet.* **36**,585-595.

Raymond, L. (2003). Excitotoxicity in Huntington disease. *Clin. Neurosci. Res.* **3**(3), 121-128.

Reddy, P.H, Williams, M, Charles, V, Garrett, L, Pike-Buchanan, L, Whetsell, W.O.Jr et al. (1998). Behavioural abnormalities and selective neuronal loss in HD transgenic mice expressing mutated full-length HD cDNA. *Nat. Genet.* **20**,198-202.

Redfearn, E.R. (1967). Isolation and determination of ubiquinone. *Meth. Enzymol.* **10**,381-384.

Reilly, C.A. and Aust, S.D. (1997). Stimulation of the ferroxidase activity of caeruloplasmin during iron loading into ferritin. *Arch Biochem Biophys.* **347**,242-248.

Reiner, A, Del Mar, N, Meade, C.A, Yang, H, Dragatsis, I, Zeitlin, S, et al. (2001). Neurons lacking huntingtin differentially colonize brain and survive in chimeric mice. *J. Neurosci.* **21**,7608-19.

Reiner, A, Dragatsis, I, Zeitlin, S, Goldowitz, D. (2003). Wild type huntingtin plays a role in brain development and neuronal survival. *Mol. Neurobiol.* **28**,259–273.

Richfield, E.K. and Herkenham, M. (1994). Selective vulnerability in Huntington's disease: preferential loss of cannabinoid receptors in the lateral globus pallidus. *Ann. Neurol.* **36**(4),577-584.

Riesbeck, K, Bredberg, A, Forsgren, A. (1990). Ciprofloxacin does not inhibit mitochondrial functions but other antibiotics do. *Antimicrob. Agents. Chemother.* **34**,167-169.

Rigamonti, D, Sipione, S, Goffredo, D, Zuccato, C, Fossale, E, Cattaneo, E. (2001).

Huntingtin's neuroprotective activity occurs via inhibition of procaspase-9 processing. *J. Biol. Chem.* **276**(18),14545-14548.

Rizzuto, R. (2001) Intracellular Ca²⁺ pools in neuronal signalling. *Curr. Op. Neurobiol.* **11**,306-311.

Rockabrand, E, Slepko, N, Pantalone, A, Nukala, V.N, Kazantsev, A, Marsh, J.L. et al. (2007) The first 17 amino acids of Huntingtin modulate its sub-cellular localization, aggregation and effects on calcium homeostasis. *Hum. Mol. Genet.* **16**(1),61 - 77.

Roizin, L, Stellar, S, Liu, J. (1979). Neuronal nuclear-cytoplasmic inclusions in Huntington's disease: electron microscopic investigations. *Adv. Neurol.* **23**,95-122.

Rong, J, McGuire, J.R, Fang, Z.H, Sheng, G, Shin, J.Y, Li, S,H et al.(2006). Regulation of Intracellular Trafficking of Huntingtin-Associated Protein-1 Is Critical for TrkA Protein Levels and Neurite Outgrowth. *J. Neuro.* **26**(22),6019–6030.

Ross, C.A. (1995) When more is less: pathogenesis of glutamine repeat neurodegenerative diseases. *Neuron.* **15**,493–496.

Ross, C.A. and Poirier, M.A. (2004). Protein aggregation and neurodegenerative disease. *Nat. Med.* **10**, (Suppl.),S10–S17.

Ross, R.A, Biedler, J.L, Spengler, B.A and Reis, D.J. (1981). Neurotransmitter-Synthesizing Enzymes in 14 Human Neuroblastoma Cell Lines. *Cell. Mol. Neurobiol.* **1**(3).

Rubinsztein, D.C, Leggo, J, Coles, R, Almqvist, E, Biancalana, V, Cassiman, J.J. et al. (1996). Phenotypic characterisation of individuals with 30-40 CAG repeats in the Huntington's disease (HD) gene reveals HD cases with 36 repeats and apparently normal elderly individuals with 36-39 repeats. *Am. J. Hum. Genet.* **59**,16-22.

Rubinsztein, D.C, Leggo, J, Chiano, M, Dodge, A, Norbury, G, Rosser, E. et al. (1997). Genotypes at the GluR6 kainate receptor locus are associated with variation in the age of onset of Huntington's disease. *Proc. Natl. Acad. Sci. USA.* **94**,3872-3876.

Sakahira, H, Breuer, P, Hayer-Hartl, M.K, Hartl, F.U. (2002). Molecular chaperones as modulators of polyglutamine protein aggregation and toxicity. *Proc. Natl. Acad. Sci. USA.* **99**(Suppl 4),16412-16418.

Sanchez I, Xu, C.J, Juo, P, Kakizaka, A, Blenis, J and Yuan, J. (1999). Caspase-8 is required for cell death induced by expanded polyglutamine repeats. *Neuron.* **22**(3), 623-33.

Sanchez-Pernaute, R, Garcia-Segura, J.M, del Barrio Alba, A, Viano, J, de Yébenes, J.G. (1999). Clinical correlation of ¹H MRS changes in Huntington's disease. *Neurology.* **53**,806.

Sapp, E, Schwarz, C, Chase, K, Bhide, P.G, Young, A.B, Penney, J, Sapp, E. (1997).
Huntingtin localization in brains of normal and Huntington's disease patients. *Ann.
Neurol.* **42**(4),604-612.

Sapp, E, Penney, J, Young, A, Aronin, N, Vonsattel, J.P, DiFiglia, M. (1999). Axonal
transport of N-terminal huntingtin suggests early pathology of corticostriatal projections
in Huntington's disease. *J. Neuropathol. Exp. Neurol.* **58**(2),165-173.

Sathasivam, K, Hobbs, C, Turmaine, M, Mangiarini, L, Mahal, A, Bertaux, F et al.
(1999). Formation of polyglutamine inclusions in non-CNS tissue. *Hum. Mol. Genet.*
8,813-22.

Saudou, F, Finkbeiner, S, Devys, D, Greenberg, M.E. (1998). Huntingtin acts in the
nucleus to induce apoptosis but death does not correlate with formation of intranuclear
inclusions. *Cell.* **95**(1),55-66.

Sawa, A, Wiegand, G.W, Cooper, J, Margolis, R.L, Sharp, A.H, Lawler, J.F Jr, et al.
(1999). Increased apoptosis of Huntington disease lymphoblasts associated with repeat-
length dependent mitochondrial depolarisation. *Nat. Med* **5**,1194-8.

Sawa, A, Tomoda, T, and Bae, B.I. (2003). Mechanisms of neuronal cell death in
Huntington's disease. *Cytogenet Genome Res.* **100**(1-4),287-95.

Sawa, A, Nagata, E, Sutcliffe, S, Dulloor, P, Cascio, M.B, Ozeki, Y. et al. (2005).
Huntingtin is cleaved by caspases in the cytoplasm and translocated to the nucleus via

perinuclear sites in Huntington's disease patient lymphoblasts. *Neurobiol. Dis.* **20**(2), 267-274.

Sayre, L.M, Perry, G and Smith, M.A. (1999). Redox metals and neurodegenerative disease. *Curr. Opin. Chem. Biol.* **3**,220-225.

Schaffar, G, Breuer, P, Boteva, R, Behrends, C, Tzvetkov, N, Strippel, N et al. (2004) Cellular Toxicity of Polyglutamine Expansion Proteins: Mechanism of Transcription Factor Deactivation. *Mol. Cell.* **15**,95-105.

Scherzinger, E, Sittler, A, Schweiger, K, Heiser, V, Lurz, R, Hasenbank, R. et al (1999). Self-assembly of polyglutamine-containing huntingtin fragments into amyloid-like fibrils: implications for Huntington's disease pathology. *Proc. Natl. Acad. Sci. (USA)*. **96**(8), 4604-4609.

Schilling, G, Becher, M.W, Sharp, A.H, Jinnah, H.A, Duan, K, Kotzuk, J.A. et al. (1999). Intranuclear inclusions and neuritic aggregates in transgenic mice expressing a mutant N-terminal fragment of huntingtin. *Hum. Mol. Genet.* **8**,97-407.

Schilling, G, Savonenko, A.V, Coonfield, M.L, Morton, J.L, Vorovich, E, Gale, A, et al. (2004).Environmental, pharmacological, and genetic modulation of the HD phenotype in transgenic mice. *Exp. Neurol.* **187**,137–149.

Schilling, G, Savonenko, A.V, Klevytska, A, Morton, J.L, Tucker, S.M, Poirier, M. et al. (2004) Nuclear-targeting of mutant huntingtin fragments produces Huntington's disease-like phenotypes in transgenic mice. *Hum. Mol. Genet.* **13**,1599–1610.

Schilling, G, Klevytska, A, Tebbenkamp, A.T, Juenemann, K, Cooper, J, Gonzales, V. et al. (2007). Characterization of Huntingtin Pathologic Fragments in Human Huntington Disease, Transgenic Mice, and Cell Models. *J. Neuropathol. Exp. Neurol.* **66**(4),313-320.

Schmitt, I, Bachner, D, Megow, D, Henklein, P, Hameister, H, Epplen, J.T. et al. (1995). Expression of the Huntington disease gene in rodents: cloning the rat homologue and evidence for downregulation in non-neuronal tissues during development. *Hum. Mol. Genet.* **4**(7),1619-1624.

Schulz, J.B, Henshaw, D.R, MacGarvey, U, Beal, M.F. (1996). Involvement of oxidative stress in 3-nitropropionic acid neurotoxicity. *Neurochem Int.* **29**,167-171.

Sharp, A.H, Love, S.J, Schilling, G, Li, S.H, Li, X.J, Bao, J. et al. (1995). Widespread expression of Huntington's disease gene (IT15) protein product. *Neuron* **14**(5), 1065-1074.

Shelbourne, P.F, Killeen, N, Hevner, R.F, Johnston, H.M, Tecott, L, Lewandoski, M. et al. (1999). A Huntington's disease CAG expansion at the murine *Hdh* locus is unstable and is associated with behavioural abnormalities in mice. *Hum. Mol. Genet.* **8**,763-74.

Sheline CT and Choi DW. (1998). Neuronal death in cultured murine cortical cells is induced by inhibition of GAPDH and triosephosphate isomerase. *Neurobiol Dis* **5**,47-54.

Seo, H, Sonntag, K.C, Isacson, O. (2004). Generalised Brain and Skin Proteasome Inhibition in Huntington's Disease. *Ann. Neurol.* **56**(3),319-328.

Seo, H, Sonntag, K.C, Kim, W, Cattaneo, E, Isacson, O. Seo. (2007). Proteasome Activator Enhances Survival of Huntington's Disease. Neuronal Model Cells. PLoS ONE **2**(e238):1-8.

Seong, I.S, Ivanova, E, Lee, J.M, Choo, Y.S, Fossale, E, Anderson, M. et al (2005). HD CAG repeat implicates a dominant property of huntingtin in mitochondrial energy metabolism. Hum. Mol. Genet. **14**,2871–2880.

Servadio, A, Koshy, B, Armstrong, D, Antalffy, B, Orr, H.T, Zoghbi, H.Y. (1995). Expression analysis of the ataxin-1 protein in tissues from normal and spinocerebellar ataxia type 1 individuals. Nat Genet. **10**(1),94-8.

Shelbourne, P.F, Killeen, N, Hevner, R.F, Johnston, H.M, Tecott, L, Lewandoski, M. Et al. (1999). A Huntington's disease CAG expansion at the murine Hdh locus is unstable and associated with behavioural abnormalities in mice. Hum. Mol. Genet. **8**(5),763-774.

Shin, J-Y, Fang, Z-H, Yu, Z, et al. (2005). Expression of mutant huntingtin in glial cells contributes to neuronal excitotoxicity. J. Cell Biol. **171**(6): 1001-1012.

Siemers, E, Foroud, T, Bill, D.J, Sorbel, J, Norton, J.A. Jr, Hodes, M.E. et al (1996). Motor changes in presymptomatic Huntington's disease gene carriers. Arch. Neurol. **53**,487-492.

Sieradzan, K.A, Mehan, A.O, Jones, L, Wanker, E.E, Nukina, N, Mann, D.M. (1999). Huntington's disease nuclear inclusions contain truncated, ubiquitinated huntingtin protein. *156*,92-99.

Simmons, D.A, Casale, M, Alcon, B, Pham, N, Narayan, N, Lynch, G. (2007). Ferritin accumulation in dystrophic microglia is an early event in the development of Huntington's disease. *Glia*. **55**(10),1074-1084.

Sipione, S, Rigamonti, D, Valenza, M, Zuccato, C, Conti, L, Pritchard, J. et al. (2002) Early transcriptional profiles in huntingtin-inducible striatal cells by microarray analyses. *Hum. Mol. Genet.* **11**,1953–1965.

Sittler, A, Walter, S, Wedemeyer, N, Hasenbank, R, Scherzinger, E, Eickhoff, et al. (1998). SH3GL3 associates with the Huntingtin exon 1 protein and promotes the formation of polyglu-containing protein aggregates. *Mol. Cell.* **2**(4),427-436.

Slow, E.J, Graham, R.K, Osmand, A.P, Devon, R.S, Lu, G, Deng, Y, Slow, E.J. et al. (2005). Absence of behavioral abnormalities and neurodegeneration in vivo despite widespread neuronal huntingtin inclusions. *Proc. Natl. Acad. Sci. (USA)*. **102**,11402-7.

Smith, D.L, Portier, R, Woodman, B, Hockly, E, Mahal, A, Klunk, W.E. et al. (2001). Inhibition of polyglutamine aggregation in R6/2 HD brain slices-complex dose response profiles. *Neurobiol. Dis.* **8**(6),1017-1026.

Snider, B.J, Moss, J.L, Revilla, F.J, Lee, C.S, Wheeler, V.C, Macdonald, M.E. et al. (2003). Neocortical neurons cultured from mice with expanded cag repeats in the

huntingtin gene: unaltered vulnerability to excitotoxins and other insults. *Neuroscience*. **120**(3),617-625.

Solans, A, Zambrano, A, Rodríguez, M, Barrientos, A. (2006). Cytotoxicity of a mutant huntingtin fragment in yeast involves early alterations in mitochondrial OXPHOS complexes II and III. *Hum. Mol. Genet.* **15**(20),3063-3081.

Sorensen, S.A, Fenger, K and Olsen, J.H. (1999). Significantly lower incidence of cancer among patients with Huntington's disease: an apoptotic effect of an expanded polyglutamine tract? *Cancer*. **86**(7),1342-1346.

Squitieri, F, Sabbadini, G, Mandich, P, Gellera, C, Di Maria, E, Bellone, E. et al. (2000). Family and molecular data for a fine analysis of age at onset in Huntington's disease. *Am. J. Med. Genet.* **95**,366-373

Squitieri, F, Gellera, C, Cannella, M, Mariotti, C, Cislighi, G, Rubinsztein, D. C. et al. (2003). Homozygosity for CAG mutation in Huntington disease is associated with a more severe clinical course. *Brain*. **126**,946–955.

Stack, E.C, Matson, W.R and Ferrante, R.J. (2008). Evidence of oxidant damage in Huntington's disease: translational strategies using antioxidants. *Ann. N.Y. Acad. Sci.* **1147**,79-92.

Stahl, W, and Swanson, P.D. (1974). Biochemical abnormalities in Huntington's chorea brains. *Neurology*. **24**,813-9.

Steffan, J.S, Kazantsev, A, Spasic-Boskovic, O, Greenwald, M, Zhu, Y.Z, Gohler, H. et al. (2000). The Huntington's disease protein interacts with p53 and CREB-binding protein and represses transcription. *Proc. Natl. Acad. Sci., USA* **97**(12),6763-6768.

Steffan, J.S, Bodai, L, Pallos, J, Poelman, M, McCampbell, A, Apostol, B.L. et al. (2001). Histone deacetylase inhibitors arrest polyglutamine-dependent neurodegeneration in *Drosophila*. *Nature*. **413**(6857),739-43.

Steffan, J.S, Agrawal, N, Pallos, J, Rockabrand, E, Trotman, L.C, Slepko, N. et al. (2004). SUMO modification of huntingtin and Huntington's disease pathology. *Science* **304**,100–104.

Stevanin, G, Fujigasaki, H, Lebre, A.S, Camuzat, A, Jeannequin, C, Dode, C. et al. (2003). Huntington's disease-like phenotype due to trinucleotide repeat expansions in the TBP and JPH3 genes. *Brain*. **126**,29-36.

St-Pierre, J, Drori, S, Uldry, M, Silvaggi, JM, Rhee, J, Jäger, S. et al. (2006). Suppression of reactive oxygen species and neurodegeneration by the PGC-1 transcription co-activators. *Cell*. **127**,397-408.

Strand, A.D, Aragaki, A.K, Shaw, D, Bird, T, Holton, J, Turner, C, Tapscott, S.J, Tabrizi, S.J, Schapira, A.H, Kooperberg, C, Olson, J.M. (2005). Gene expression in Huntington's disease skeletal muscle: a potential biomarker. *Hum.Mol.Genet*. **14**,1863-1876.

- Strehlow, A.N, Li, J.Z, Myers, R.M. (2007). Wild-type huntingtin participates in protein trafficking between the Golgi and the extracellular space *Hum Mol Genet.* **16**(4),391–409.
- Strong, T.V, Tagle, D.A, Valdes, J.M, Elmer, L.W, Boehm, K, Swaroop, M. et al. (1993). Widespread expression of the human and rat Huntington's disease gene in brain and non-neural tissues. *Nat. Genet.* **5**(3),259-265.
- Suhr, S.T, Senut, M.C, Whitelegge, J.P, Faull, K.F, Cuizon, D.B, Gage, F.H. et al. (2001). Identities of sequestered proteins in aggregates from cells with induced polyglutamine expression. *J. Cell Biol.* **153**(2),283-294.
- Sun, B, Fan, W, Balciunas, A, Cooper, J.K, Bitan, G, Steavenson, S. et al. (2002) Polyglutamine repeat length dependent proteolysis of huntingtin. *Neurobiol. Dis.* **11**,111-122
- Sun, Y, Savanenin, A, Reddy, P.H and Li, Y.F. (2001). Polyglutamine-expanded huntingtin promotes sensitization of N-methyl-D-aspartate receptors via post-synaptic density 95. *J Biol Chem.* **276**,24713-24718.
- Taanman, J.W. (1999). The human mitochondrial genome: structure, transcription, translation and replication. *Biochim. Biophys. Acta.* **1410**,103-123.
- Tabrizi, S.J, Cleeter, M.W.J, Xuereb, J, Taanman, J.W, Cooper, J.M and Schapira, A.H.V. (1999). Biochemical abnormalities and excitotoxicity in Huntington's disease brain. *Ann. Neurol.* **45**,25-32.

Tabrizi, S.J, Workman, J, Hart, P.E, Mangiarini, L, Mahal, A, Bates, G. et al. (2000). Mitochondrial dysfunction and free radical damage in the huntington R6/2 transgenic mouse. *Ann. Neurol.* **47**,80-6.

Tabrizi, S.J, Orth, M, Wilkinson, J.M, Taanman, J.W, Warner, T.T, Cooper, J.M. et al. (2000). Expression of mutant alpha-synuclein causes increased susceptibility to dopamine toxicity. *Hum Mol Genet.* **18**,2683-9.

Tabrizi, S.J, Blamire, A.M, Manners, D.N, Rajagopalan, B, Styles, P, Schapira, A.H. et al. High-dose creatine therapy for Huntington disease: a 2-year clinical and MRS study. (2005). *Neurology.* **64**(9),1655-6

Takano, H, and Gusella, J. F. (2002). The predominantly HEAT-like motif structure of huntingtin and its association and coincident nuclear entry with dorsal, an NF- κ B/Rel/dorsal family transcription factor. *BMC Neurosci.* **3**,15.

Tanaka, Y, Igarashi, S, Nakamura, M, Gafni, J, Torcassi, C, Schilling, G. et al. (2006). Progressive phenotype and nuclear accumulation of an amino-terminal cleavage fragment in a transgenic mouse model with inducible expression of full-length mutant huntingtin. *Neurobiol. Dis.* **21**,381-91.

Tawil, R, and Van Der Maarel, S.M. (2006). Facioscapulohumeral muscular dystrophy. *Muscle Nerve.* **1**,1-15.

- Telenius, H, Kremer, H.P, Theilmann, J, Andrew, S.E, Almqvist, E, Anvret, M. et al. (1993). Molecular analysis of juvenile Huntington's disease: the major influence of (CAG)_n repeat length is the sex of the affected patient. *Hum Mol. Genet.* **2**,1535-1540.
- Tellez-Nagel, I, Johnson, A.B and Terry, R.D. (1974). Studies on brain biopsies of patients with Huntington's chorea. *J. Neuropathol. Exp. Neurol.* **33**(2),308-332.
- Thomas, L.B, Gates, D.J, Richfield, E.K, O'Brien, T.F, Schweitzer, J.B, Steindler, D.A. et al. (1995). DNA end labeling (TUNEL) in Huntington's disease and other neuropathological conditions. *Exp. Neurol.* **133**(2),265-272.
- Trifunovic, A, Wredenberg, A, Falkenberg, M, Spelbrink, J.N, Rovio, A.T, Bruder, C.E. et al. (2004). Premature ageing in mice expressing defective mitochondrial DNA polymerase. *Nature.* **429**,417-423.
- Trojanowski, J.Q. and Lee, V.M. (2000). "Fatal attractions" of proteins. A comprehensive hypothetical mechanism underlying Alzheimer's disease and other neurodegenerative disorders. *Ann. NY. Acad. Sci.* **924**,62-67.
- Truant, R, Atwal, R.S and Burtnik, A. (2007). Nucleocytoplasmic trafficking and transcription effects of huntingtin in Huntington's disease. *Prog. Neurobiol.* **83**,211-227.
- Trushina, E, Dyer, R.B, Badger, J.D, Ure, D, Eide, L, Tran, D.D. et al. (2004). Mutant huntingtin impairs axonal trafficking in mammalian neurons in vivo and in vitro. *Mol. Cell. Biol.* **24**,8195-8209.

Tsai, Y.C, Fishman, P.S, Thakor, N.V, and Oyler, G.A. (2003) Parkin facilitates the elimination of expanded polyglutamine proteins and leads to preservation of proteasome function. *J. Biol. Chem.* **278**,22044–22055.

Tsuang, D, DiGiacomo, L, Lipe, H, Bird, T.D. (1998). Familial aggregation of psychotic symptoms in Huntington's disease. *Am. J. Med Genet.* **81**,323-327.

Tsuji, S. (2000). Dentatorubral-pallidoluysian atrophy (DRPLA). *J Neurol. Transm. Suppl.* **58**,167-80.

Tukamoto, T, Nukina, N, Ide, K and Kanazawa, I. (1997). Huntington's disease gene product, huntingtin, associates with microtubules *in vitro*. *Brain Res. Mol. Brain Res.* **51**(1-2),8-14.

Turmaine, M, Raza, A, Mahal, A, Mangiarini, L, Bates, G.P, Davies, S.W. (2000). Nonapoptotic neurodegeneration in a transgenic mouse model of Huntington's disease. *Proc. Natl. Acad. Sci. USA.* **97**,8093-97.

Turner, C, Cooper, J.M, Schapira, A.H. Turner. (2007). Clinical correlates of mitochondrial function in Huntington's disease muscle. *Mov. Disord.* **22**(12),1715-21.

Urlinger, S, Baron, U, Thellmann, M, Hasan, M.T, Bujard, H, and Hillen, W. (2000). Exploring the sequence space for tetracycline-dependent transcriptional activators: novel mutations yield expanded range and sensitivity. *Proc. Natl. Acad. Sci. USA.* **97**,7963–7968.

Usdin, M.T, Shelbourne, P.F, Myers, R.M, Madison, D.V. (1999). Impaired synaptic plasticity in mice carrying the Huntington's disease mutation. *Hum. Mol. Genet.* **8**,839–846.

Van Dellen, A, Welch, J, Dixon, R.M, Cordery, P, York, D, Styles, P. et al. (2000). N-Acetylaspartate and DARPP-32 levels decrease in the corpus striatum of Huntington's disease mice. *Neuroreport.* **11**,3751-7.

Van Dellen, A, Blakemore, C, Deacon, R, York, D, Hannan, A.J. (2000b). Delaying the onset of Huntington's in mice. *Nature.* **404**,721-2.

Van Raamsdonk, J.M, Pearson, J, Rogers, D.A, Bissada, N, Vogl, A.W, Hayden, M.R. et al. (2005). Loss of wild type huntingtin influences motor dysfunction and survival in the YAC128 mouse model of Huntington disease. *Hum. Mol. Genet.* **14**,1379-1392.

Van Roon-Mom, W.M, Pepers, B.A, Hoen, P.A, Verwijmeren, C.A, den Dunnen, J.T, Dorsman, J.C et al. (2008). Mutant huntingtin activates Nrf2-responsive genes and impairs dopamine synthesis in a PC12 model of Huntington's disease. *BMC Mol. Biol.* **9**(1),84 Epub.

Velier, J, Kim, M, Schwarz, C, Kim, T.W, Sapp, E, Chase, K, et al. (1998). Wild-type and mutant huntingtins function in vesicle trafficking in the secretory and endocytic pathways. *Exp. Neurol.* **152**(1),34-40.

Venkatraman, P, Wetzel, R, Tanaka, M, Nukina, N, Goldberg, A.L. (2004). Eukaryotic proteasomes can not digest polyglutamine sequences and release them during degradation of polyglutamine-containing proteins. *Mol. Cell.* **14**,95-104.

Vila, M and Przedborski, S (2003). Targeting Programmed Cell Death in Neurodegenerative Diseases. *Neuroscience.* **4**,1–11.

Voges, D, Zwickl, P and Baumeister, W. (1999). The 26S proteasome: a molecular machine designed for controlled proteolysis. *Annu. Rev. Biochem.* **68**,1015-1068.

Vonsattel, J-P, Myers, R.H, Stevens, T.J, Ferrante, R.J, Bird, E.D, Richardson, E.P. (1985). Neuropathological classification of Huntington's disease. *J. Neuropath. Exp. Neurol.* **44**,559-577.

Vonsattel, J-P and DiFiglia, M. Huntington Disease. (1998). *J. Neuropathol. Exp. Neurol.* **57**,369-384.

Waelter, S, Boeddrich, A, Lurz, R, Scherzinger, E, Lueder, G, Lehrach, H. et al. (2001a). Accumulation of mutant huntingtin fragments in aggresome-like inclusion bodies as a result of insufficient protein degradation. *Mol. Biol. Cell.* **12**,1393-1407.

Waelter, S, Scherzinger, E, Hasenbank, R, Nordhoff, E, Lurz, R, Goehler, H, Waelter, S. et al. (2001b). The huntingtin interacting protein 1 (HIP1) is a clathrin and alpha-adaptin-binding protein involved in receptor-mediated endocytosis. *Hum. Mol. Genet.* **10**(17), 1807-1817.

Wang, G.H, Mitsui, K, Kotliarova, S, Yamashita, A, Nagao, Y, Tokuhira, S. et al. (1999). Caspase activation during apoptotic cell death induced by polyglutamine in N2a cells. *NeuroReport*. **10**,2435-8.

Wang, X, Sarkar, A, Cicchetti, F, Yu, M, Zhu, A, Jokivarsi, K. et al. (2005). Cerebral PET imaging and histological evidence of transglutaminase inhibitor cystamine induced neuroprotection in transgenic R6/2 mouse model of Huntington's disease. *J Neurol. Sci*. **231**(1-2),57-66.

Wanker, E.E, Rovira, C, Scherzinger, E, Hasenbank, R, Walter, S, Tait, D. et al. (1997). HIP-1: a huntingtin interacting protein isolated by the yeast two-hybrid system. *Hum. Mol. Genet*. **6**(3),487-495.

Wanker, E.E. and Dröge, A. Chapter 12. In *Huntington's disease* Eds. Bates, Harper and Jones. Oxford University Press (2002).

Wang, G.H, Mitsui, K, Kotliarova, S, Yamashita, A, Nagao, Y, Tokuhira, S. et al. (1999). Caspase activation during apoptotic cell death induced by expanded polyglutamine in N2a cells. *Neuroreport*. **10**(12),2435-8.

Wang, X. (2001). The expanding role of mitochondria in apoptosis. *Genes and Development*. **15**(22),2922-2933.

Warby, S.C, Chan, E.Y, Metzler, M, Gan, L, Singaraja, R.R, Crocker, S.F. et al. (2005). Huntingtin phosphorylation on serine 421 is significantly reduced in the striatum and by polyglutamine expansion in vivo. *Hum. Mol. Genet*. **14**,1569-1577.

Warner, D.S, Sheng, H and Batinic-Haberle, I. (2004). Oxidants, antioxidants and the ischemic brain. *J Exp Biol.* **207**,3221-3231

Weeks, R.A, Piccini, P, Harding, A.E and Brooks, D,J. (1996). Striatal D1 and D2 dopamine receptor loss in asymptomatic mutation carriers of Huntington's disease. *Ann. Neurol.* **40**,49-54.

Weigell-Weber Schmid, W and Spiegel, R. (1996). Psychiatric symptoms and CAG expansion in Huntington's disease. *Am. J. Med. Genet.* **67**,53-57.

Weinberger, D.R, Berman, K.F, Iadarola, M, Driesen, N and Zec, R.F. (1998). Prefrontal cortical blood flow and cognitive function in Huntington's disease. *J. Neurol. Neurosurg. Psychiatry.* **51**,94-104.

Wellington, C.L, Ellerby, L.M, Hackam, A.S, Margolis, R.L, Trifiro, M.A, Singaraja, R, et al. (1998). Caspase cleavage of gene products associated with triplet expansion disorders generates truncated fragments containing the polyglutamine tract. *J. Biol. Chem.* **273**(15),9158-9167.

Wellington, C.L, Singaraja, R, Ellerby, L, Savill, J, Roy, S, Leavitt, B. et al. (2000). Inhibiting caspase cleavage of huntingtin reduces toxicity and aggregate formation in neuronal and non-neuronal cells. *J. Biol. Chem.* **275**(26),19831-38.

Wellington, C.L, Ellerby, L.M, Gutekunst, C.A, Rogers, D, Warby, S, Graham, R.K. et al. (2002). Caspase cleavage of mutant huntingtin precedes neurodegeneration in Huntington's disease. *J. Neurosci.* **22**,7862-72.

Wexler, N.S, Young, A.B, Tanzi, R.E, Travers, H, Starosta-Rubinstein, S, Penney, J.B, et al. (1987). Homozygotes for Huntington's disease. *Nature.* **326**,194-197.

Wharton, D.C. and Tzagoloff, A. (1967). Cytochrome oxidase from beef heart mitochondria. *Meth. Enzymol.* **10**,245-257.

Wheeler, V.C, White, J.K, Gutekunst, C.A, Vrbanac, V, Weaver, M, Li, X.J. et al. (2000). Long glutamine tracts cause nuclear localisation of a novel form of huntingtin in medium spiny striatal neurons in HdhQ92 and HdhQ111 knock-in mice. *Hum. Mol. Genet.* **9**,503-13.

White, J.K, Auerbach, W, Duyao, M.P, Vonsattel, J.P, Gusella, J.F, Joyner, A.L. et al. (1997). Huntingtin is required for neurogenesis and is not impaired by the Huntington's Disease CAG expansion. *Nat. Genet.* **17**(4),404-410.

Wigley, W.C, Fabunmi, R.P, Lee, M.G, Marino, C.R, Muallem, S, DeMartino, G.N. et al. (1999). Dynamic association of proteasomal machinery with the centrosome. *J. Cell Biol.* **145**,481-490.

Wild, E.J. and Tabrizi, S.J. (2007). Huntington's disease phenocopy syndromes. *Curr Opin Neurol.* **6**,681-7.

Wilkinson, F.L, Nguyen, T.M, Manliak, S.B, Thomas, P, Neal, J.W, Harper, P.S. et al. (1999). Localization of rabbit huntingtin using a new panel of monoclonal antibodies. *Brain Res Mol Brain Res.* **69(1)**:10-20.

Wood, J.D, MacMillan, J.C, Harper, P.S, Lowenstein, P.R, Jones, A.L. (1996). Partial characterisation of murine huntingtin and apparent variations in the subcellular localisation of huntingtin in human, mouse and rat brain. *Hum. Mol. Genet.* **5(4)**,481-487.

Wytttenbach, A, Carmichael, J, Swartz, J, Furlong, R.A, Narain, Y, Rankin, J. et al. (2000). Effects of heat shock, heat shock protein 40 (HDJ-2), and proteasome inhibition on protein aggregation in cellular models off Huntington's disease. *Proc. Natl. Acad. Sci. USA.* **97(6)**,2898-2903.

Wytttenbach, A, Swartz, J, Kita, H, Thykjaer, T, Carmichael, J, Bradley, J et al. (2001). Polyglutamine expansions cause decreased CRE-mediated transcription and early gene expression changes prior to cell death in an inducible cell model of Huntington's disease. *Hum Mol Genet.* **10(17)**,1829-45.

Xia, J, Lee, D.H, Taylor, J, Vandelft, M and Truant, R. (2003). Huntingtin contains a highly conserved nuclear export signal. *Hum. Mol. Genet.* **12**,1393–1403.

Yamamoto, A, Lucas, J.J and Hen, R. (2000). Reversal of neuropathology and motor dysfunction in a conditional model of Huntington's disease. *Cell.* **101**,57-66.

- Yanai, A, Huang, K, Kang, R, Singaraja, R.R, Arstikaitis, P, Gan, L, et al. (2006) Palmitoylation of huntingtin by HIP14 is essential for its trafficking and function. *J. Biol. Chem.* **281**,824–831.
- Yang, H, Standifer, K.M and Sherry, D.M. (2002). Synaptic protein expression by regenerating adult photoreceptors. *J. Comp. Neurol.* **443**(3),275-88.
- Ye, C, Zhang, Y, Wang, W, Wang, J and Li, H. (2008). Inhibition of neurite outgrowth and promotion of cell death by cytoplasmic soluble mutant huntingtin stably transfected in mouse neuroblastoma cells. *Neurosci Lett.* **442**(1),63-8.
- Young, A.B. (1998) In *Molecular Neurology* (ed. J.B.Martin), pp.35-54. Scientific American Inc., New York.
- Yu, Z.X, Li, S.H, Nguyen, H.P and Li, X.J. (2002). Huntingtin inclusions do not deplete polyglutamine containing transcription factors in HD mice. *Hum. Mol. Genet.* **11**(8),905–914.
- Zeitlin, S, Liu, J.P, Chapman, D.L, Papaioannou, V.E and Efstratiadis, A. (1995). Increased apoptosis and early embryonic lethality in mice Nullizygous for the Huntington's disease homologue. *Nat. Genet.* **11**(2),155-163.
- Zeron, M.M, Chen, N, Moshaver, A, Lee, A.T, Wellington, C.L, Hayden, M.R, et al. (2001). Mutant huntingtin enhances excitotoxic cell death. *Mol. Cell. Neurosci.* **17**,41-53.

Zeron, M.M, Hansson, O, Chen, N, Wellington, C.L, Leavitt, B.R, Brundin, P. et al.

(2002). Increased sensitivity to N-methyl-D-aspartate receptor-mediated excitotoxicity in a mouse model of Huntington's disease. *Neuron*. **33**,849–860.

Zeron, M.M, Fernandes, H.B, Krebs, C, Shehadeh, J, Wellington, C.L, Leavitt, B.R. et al.

(2004) Potentiation of NMDA receptor-mediated excitotoxicity linked with intrinsic apoptotic pathway in YAC transgenic mouse model of Huntington's disease. *Mol. Cell. Neurosci.* **25**,469–479.

Zhou, H, Cao, F, Wang, Z, Yu, Z.X, Nguyen, H.P, Evans, J. et al. (2003). Huntingtin forms toxic NH₂-terminal fragment complexes that are promoted by the age-dependent decrease in proteasome activity. **163**,109-18.

Zuccato, C, Ciammola, A, Rigamonti, D, Leavitt, B.R, Goffredo, D, Conti, L. et al.

(2001). Loss of huntingtin-mediated BDNF gene transcription in Huntington's disease. *Science*. **293**(5529),493-498.

Zuccato, C, Tartari, M, Crotti, A, Goffredo, D, Valenza, M, Conti, L. et al. (2003).

Huntingtin interacts with REST/NRSF to modulate the transcription of NRSE-controlled neuronal genes. *Nat. Genet.* **35**,76-83.

Appendix

1.1. The standard PCR reaction conditions using G49 and G50:

“Denaturation”	94 ⁰ C	4min	1 cycle	
“Denaturation”	94 ⁰ C	1min	} 25 cycles	
“Primer annealing”	54 ⁰ C	1min		
“Primer extension”	72 ⁰ C	1min		
“Extension”	72 ⁰ C	10 min	1 cycle	

1.2. Sequencing the 5' junction

The standard conditions for sequencing the 5' junction between the EYFP sequence and the 5' end of full-length huntingtin sequence in SHSY5Y cells, using the EYFPfor and RS2:

“Denaturation”	94 ⁰ C	2min	1 cycle	
“Denaturation”	94 ⁰ C	30 secs	} 35 cycles	
“Primer annealing”	64 ⁰ C	45 secs		
“Primer extension”	72 ⁰ C	60 secs		
“Extension”	72 ⁰ C	10 min	1 cycle	

1.3. Sequencing the 3' junction

The standard conditions for sequencing the 3' junction between EYFP-C1 plasmid and the 3' end of full-length huntingtin sequence in SHSY5Y cells, using the R2 and F3:

“Denaturation”	94 ⁰ C	2min	1cycle	
“Denaturation”	94 ⁰ C	30 secs	} 35 cycles	
“Primer annealing”	58 ⁰ C	45 secs		
“Primer extension”	72 ⁰ C	60 secs		
“Extension”	72 ⁰ C	10 min	1 cycle	

1.4. Buffers

TE

For one litre

10mM Tris. Cl (pH8.0)(1.2114g)

1mM EDTA (pH8.0) (2mls from the 0.5M stock)

Make up to 1 litre.

0.5M EDTA (pH8.0)

186.1gdisodium ehtylenediaminetetra-acetate.2H₂O

Make up to 800ml with H₂O

Adjust pH with NaOH (approx. 20g of pellets)

Make up to 1 litre.

50XTAE

For one litre

242g Tris Base

57.1ml Glacial Acetic Acid

100ml 0.5M EDTA pH8.0

Homogenisation buffer (pH 7.4) made up as below;

<u>Reagent</u>	<u>500ml</u>
ddH ₂ O	made up to 500ml
10mM Tris (MW 121.1)	0.606g
1mM K ₂ EDTA (MW 404.5)	0.202g
0.25M Sucrose (MW342.3)	42.79g

Dissociation Buffer for Western blotting

- 1) 0.1% SDS
- 2) 62.5 mM Tris HCl pH6.9
- 3) Protease inhibitors (pepstatin A 1mg/ml, leupeptin 1mg/ml, aprotinin 1mg/ml, PMSF 2µg/ml)

4x NuPAGE Sample buffer (pH 8.5)

Glycerol (40%)	4g
Tris Base (564mM)	0.682g
Tris HCl (424mM)	0.666g
LDS (8%)	0.8g
EDTA (2.04mM)	0.006g
Serva Blue G250 (0.88mM)	0.0075g
Phenol Red (0.7mM)	0.0025g

Made up to 10ml with ddH₂O

NuPAGE Running Buffer x20 500ml (TRIS-Acetate SDS) pH 8.25

Tricine (1M) 89.5g

Tris Base (1M)60.5g

SDS (2%) 10g

Made up to 500ml with ddH₂O

NuPAGE Running Buffer (MOPS pH 7.7/MES pH7.3)

MOPS (1M) 104.6g

or MES (1M) 97.6g

Tris Base (1M)60.6g

SDS (69.3mM) 10g

EDTA (20.5mM) 3g

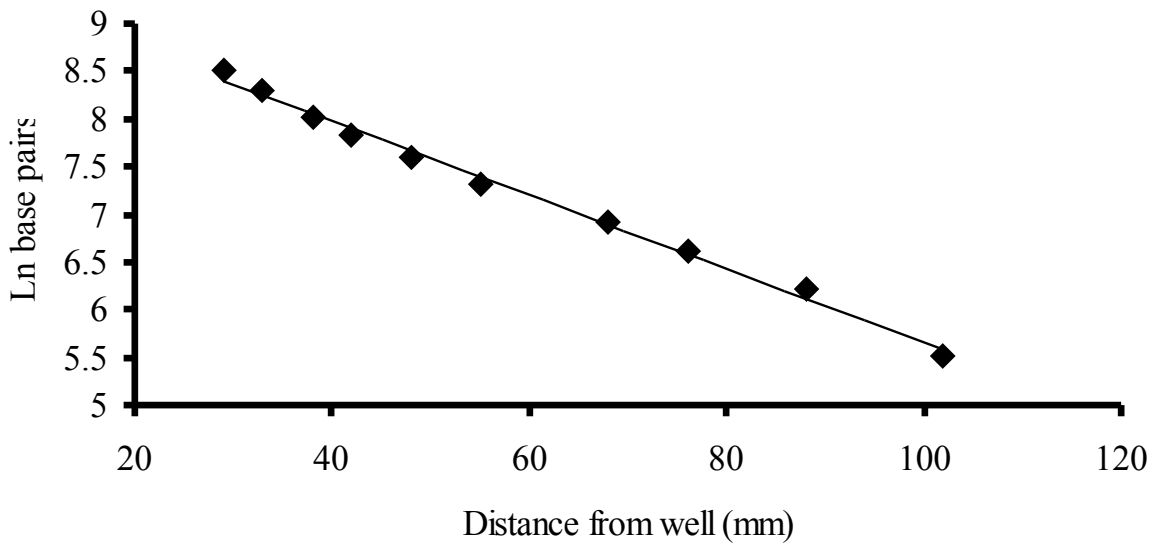
Made up to 500ml with ddH₂O

1.5. HEK 293 clone sequencing: Standard Curve

Standard curve for known DNA markers and distance from well.

Base pairs	ln base pair	Distance from well (mm)
250	5.52	102
500	6.21	88
750	6.62	76
1000	6.91	68
1500	7.31	55
2000	7.60	48
2500	7.82	42
3000	8.00	38
4000	8.29	33
5000	8.52	29

Normal curve for DNA ladder relating ln (base pair) versus distance from well



1.6. Unified Huntington's Disease Rating Scale (UHDRS)

1) MOTOR ASSESSMENT

OCULAR PURSUIT (horizontal and vertical)

0=complete (normal) 1=jerky movement 2=interrupted pursuits/full range 3=incomplete range 4=cannot pursue

SACCADE INITIATION (horizontal and vertical)

0=normal 1=increased latency only 2=suppressible blinks or head movements 3=insuppressible head movements 4=cannot initiate saccades

SACCADE VELOCITY (horizontal and vertical)

0=normal 1=mild slowing 2=moderate slowing 3=severely slow, full range 4=incomplete range

DYSARTHRIA

0=normal

1=unclear, no need to repeat 2=must repeat to be understood 3=mostly incomprehensible 4=mute

TONGUE PROTRUSION

0=can hold tongue fully protruded for 10 seconds 1=cannot keep fully protruded for 10 seconds 2=cannot keep fully protruded for 5 seconds 3=cannot fully protrude tongue 4=cannot protrude tongue beyond lips

MAXIMAL DYSTONIA (trunk and extremities)

0=absent

1=slight/intermittent 2=mild/common or moderate/intermittent 3=moderate/common 4=marked/prolonged

MAXIMAL CHOREA (face, mouth, trunk and extremities)

0=absent

1=slight/intermittent 2=mild/common or moderate/intermittent 3=moderate/common 4=marked/prolonged

RETROPULSION PULL TEST

0=normal 1=recovers spontaneously 2=would fall if not caught 3=tends to fall spontaneously 4=cannot stand

FINGER TAPS (right and left)

0=Normal

1=Mild slowing and or reduction in amplitude 2=Moderately impaired. Definite and early amplitude fatiguing
May have occasional arrests in movement 3=Severely impaired. Frequent hesitation in initiating movements or
arrests in ongoing movements 4=Can barely perform the task.

PRONATE/SUPINATE-HANDS (right and left)

0=normal

1=mild slowing and/or irregular 2=moderate slowing and irregular 3=severe slowing and irregular 4=cannot perform

LURIA (fist-hand-palm test)

0=3 4 in 10 seconds, no cue 1=<4 in 10 seconds, no cue 2=2 4 in 10 seconds, with cues 3=<4 in 10 seconds with cues 4=cannot perform

RIGIDITY -ARMS (right and left)

0=absent 1 = slight or present only with activation 2=mild to moderate 3=severe, full range of motion 4=severe with limited range

BRADY KINESIA-BODY

0=normal

1=minimally slow 2=mildly but clearly slow 3=moderately slow, some hesitation 4=markedly slow, long delays in initiation

GAIT

0=normal gait, narrow base 1=wide base and/or slow 2=wide base and walks with difficulty 3=walks only with assistance 4=cannot attempt

TANDEM WALKING

0=normal for 10 steps 1=1 to 3 deviations from straight line 2=>3 deviations 3=cannot complete 4=cannot attempt

2) COGNITIVE ASSESSMENT

VERBAL FLUENCY TEST (raw score)

SYMBOL DIGIT MODALITIES TEST (raw score)

STROOP INTERFERENCE TEST Color Naming (number correct) Word Reading (number correct)

Interference (number correct)

3) BEHAVIORAL ASSESSMENT

Rate the severity and frequency of the following using the scale below:

Severity 0=absent 1=slight, questionable 2=mild 3=moderate 4=severe

Frequency 0=almost never 1=seldom 2=sometimes 3=frequently 4=almost always

Sad/Mood: feeling sad, sad voice/expression, tearfulness, inability to enjoy anything.

Low Self-Esteem/Guilt: self blame, self deprecation including feelings of being a bad or unworthy person, feelings of failure.

Anxiety: worries, anticipation of the worst, fearful anticipation.

Suicidal Thoughts: feels life not worth living, has suicidal thoughts, active suicidal intent, preparation for the act. behavior, physical violence, verbal outbursts, threatening, foul, or abusive language.

Disruptive or Aggressive Behavior: threatening behavior, physical violence, verbal outbursts, threatening, foul, or abusive language.

Irritable Behavior: impatient, demanding, inflexible, driven and impulsive, uncooperative.

Obsessions: recurrent and persistent ideas, thoughts or images

Compulsions: repetitive, purposeful, and intentional behaviors.

Delusions: Fixed false beliefs, not culturally shared

Hallucinations: a perception without physical stimulus:

Auditory, Visual, Tactile, Gustatory and Olfactory

Does the investigator believe the subject is confused? Yes or No

Does the investigator believe the subject is demented? Yes or No

Does the investigator believe the subject is depressed? Yes or No

Does the subject require pharmacotherapy for depression? Yes or No

4) FUNCTIONAL ASSESSMENT Yes or No

Could subject engage in gainful employment in his/her accustomed work?

Could subject engage in any kind of gainful employment?

Could subject engage in any kind of volunteer or non-gainful work?

Could subject manage his/her finances (monthly) without help?

Could subject shop for groceries without help?

Could subject handle money as a purchaser in a simple cash transaction?

Could subject supervise children without help?

Could subject operate an automobile safely and independently?

Could subject do his/her own housework without help?

Could subject do his/her own laundry (wash/dry) without help?

Could subject prepare his/her own meals without help?

Could subject use the telephone without help?

Could subject take his/her own medications without help?

Could subject feed himself/herself without help?

Could subject dress himself/herself without help?

Could subject bathe himself/herself without help?

Could subject use public transportation to get places without help?

Could subject walk to places in his/her neighborhood without help?

Could subject walk without falling?

- Could subject walk without help?
- Could subject comb hair without help?
- Could subject transfer between chairs without help?
- Could subject get in and out of bed without help?
- Could subject use toilet/commode without help?
- Could subject's care still be provided at home?

5) INDEPENDENCE SCALE

Please indicate the most accurate current level of subject's independence (only 0 or 5 selections are acceptable)

- 100: No special care needed
- 090: No physical care needed if difficult tasks are avoided
- 080: Pre-disease level of employment changes or ends; cannot perform household chores to pre-disease level, may need help with finances
- 070: Self-care maintained for bathing, limited household duties (cooking and use of knives), driving terminates; unable to manage finances
- 060: Needs minor assistance in dressing, toileting, bathing; food must be cut for patient
- 050: 24-hour supervision appropriate; assistance required for bathing; eating, toileting
- 040: Chronic care facility needed; limited self feeding, liquefied diet
- 030: Patient provides minimal assistance in own feeding, bathing, toileting
- 020: No speech, must be fed
- 010: Tube fed, total bed care

6) FUNCTIONAL CAPACITY

OCCUPATION

0=unable 1=marginal work only 2=reduced capacity for usual job 3=normal

FINANCES

0=unable 1=major assistance 2=slight assistance 3=normal

DOMESTIC CHORES

0=unable 1=impaired 2=normal

ADL

0=total care 1=gross tasks only 2=minimal impairment 3=normal

CARE LEVEL

0=full time skilled nursing 1=home or chronic care 2=home